U. S. DEPARTMENT OF THE INTERIOR
U. S. GEOLOGICAL SURVEY

Materials Provided at the Workshop "Geophysical Map Interpretation on the PC", Convened April 21-22, 1993

by

V. J. S. Grauch, Jeffrey D. Phillips, Donald B. Hoover, James A. Pitkin,
K. Eric Livo, and Anne McCafferty*

1993

Open-File Report 93-560

93-560A	Text (Paper Copy)
93-560B	Version 2.11 update to potential-field software (4 diskettes)
93-560C	Version 1.03 REMAPP Software (2 diskettes)
93-560D	Getchell grids and image files (8 diskettes)

*U. S. Geological Survey, Box 24006, M/S 964, Federal Center, Denver, CO 80225-0046

Preface

Open-file report 93-560 represents material provided to participants of the workshop "Geophysical Map Interpretation on the PC" that was convened April 21-22, 1993, in Denver in conjunction with the Society of Economic Geologists meeting "Integrated Methods in Exploration and Discovery". The meeting was sponsored in part by the U. S. Geological Survey (USGS), and the workshop was prepared and presented by USGS scientists using USGS facilities. In order to make the workshop information more widely available, we are releasing the handout materials as text and diskettes, comprising Open-File Report 93-560A through D.

The text portion of the material provided at the workshop, which primarily consolidated information already published, was intended to supplement oral presentations and exercises on the personal computer (PC), and provide a reference for participants after the workshop. In addition, the material was submitted by the six different instructors without much review for consistency of style. For publication purposes of Open-File Report 93-560A, we have made some additions and modifications to provide more coherency. However, **this report is still not intended to stand alone and should be used only as a source of information and reference** to more complete, explanatory material. Selected bibliographies are provided at the end of each major section.

In addition, software was provided on diskettes that represented slight modifications or updates to published software. These software updates are hereby provided to the public as an interim measure before the full complement of updates on the software has been completed. Open-file report 93-560B updates the potential-field software, version 2.1 (Phillips and others, 1993, USGS Digital Data Series DDS-9), and *requires previous installation of version 2.0* (Open-file report 92-18). Open-file report 93-560C is version 1.03 of the REMAPP software, which is modified from version 1.00 (Open-file report 90-88). Installation of version 1.03 does *not* require any previous installation of REMAPP software. However, no test data sets are provided and the documentation text is included only as an ASCII file on the diskette.

Data from the Getchell area presently available to the public on magnetic tape were also provided to the participants as binary grid and image files on diskettes and are being released as 93-560D. Chapter 12 includes a complete description of these files. In order to view the image files, installation of the updated potential-field software (Open-File Reports 93-560B and 92-18) is required.

The workshop participants also had access to several additional demonstration grids and images from the Getchell data set during the workshop, including digital overlays of geology and deposit locations. The additional images are included in Open-File 93-560D. Instructions to create the demonstration grids from the grids provided in 93-560D have been added to the text where these grids are required by the software demonstrations and exercises. Color figures of some of these images were given to workshop participants and

are included in this report also. These figures illustrate the techniques and procedures used with geophysical mapping software and do not constitute interpretations.

Because this document was prepared by authors who have different style preferences and word processing systems, some differences in format are to be expected. However, for demonstrations of program runs, we generally follow some conventions, as illustrated by the following example and explained afterwards:

```
C:>addgrd
 first input file :
 gcond9.cgd
title=getchell log10 900 hz conductivity (log of resist. inver
 nc X nr          =         194          249
 xo, yo, dx, dy =      -46.000000     4525.000000     2.000000E-01
  2.000000E-01
 operator  h(elp), + - * / m %    :
 +                                                  << addition operator
 second input file [constant] :
 <CR>
```

Entering a carriage return here will take the default answer in brackets.

```
 the 2nd grid will be replaced by a constant value
 enter constant:
 3.5
 output file :
 gcond9b.cgd
 output title [ same as file 1 ]
 Getchell log10 900 hz conductivity + 3.5

Stop - Program terminated.
```

C:> indicates a DOS prompt. Alternatively, **the programs can be run from a menu, which is what we recommend unless otherwise noted.** A map of the menu structure is provided in Chapter 6 so that programs can be easily found by name. Underlined text indicates responses by the user; all other text is generated by the program until the FORTRAN end-of-program message "Stop - Program terminated". Anotations are indicated by "<<", or by intervening text lines having a different font or different indentation than the program demonstration text. <CR> represents carriage return, accomplished by pressing the ENTER key.

Many of the examples in the chapter text are explained more fully as part of independent exercises located at the end of major sections. These exercises are included to provide practice with the software and illustrate some of the methods discussed in the text. **They require acquisition of the full Open-File Report 93-560 (parts A-D), a PC with a math co-processor** (see hardware requirements in Chapter 6), **and either Open-File Report 92-18 or CD-ROM DDS-9.**

Workshop participants were also provided copies of several published reports and software not duplicated in this open-file report; they are the following:

Bankey, Viki, and Anderson, W. L., 1989, Some geophysical programs, data bases, and maps from the U. S. Geological Survey, 1971-1989: U. S. Geological Survey Open-File Report 89-659, 18 p.

Cordell, Lindrith, Phillips, J. D., and Godson, R. H., 1992, U. S. Geological Survey potential-field geophysical software, version 2.0: U. S. Geological Survey Open-File Report 92-18: 92-18A is 16 p. of documentation; 92-18B through G are five MS-DOS diskettes containing software and test data sets.

Livo, K. E., 1990, REMAPP - PC: Remote sensing image processing software for MS-DOS personal computers, version 1.00: U. S. Geological Survey Open-File Report 90-88: 90-88A is 62 p. of documentation; 90-88B through E are four MS-DOS diskettes containing software and test data sets.

Pitkin, J. A., and Duval, J. S., 1980, Design parameters for aerial gamma-ray surveys: Geophysics, v. 45, no. 9, p. 1427-1439.

Table of Contents

Page

Preface i

Table of Contents iv

List of Figures x

List of Tables xi

Introductory Materials for Workshop

Announcement xii

Brief Description xiii

Outline and Schedule xiv

List Of Instructors and Workshop Staff xviii

Chapter 1. Principles Of Potential-Field Methods 1-1

Introduction 1-1

Gravity Method 1-1

Aeromagnetic Method 1-4

Bibliography 1-8

Chapter 2. Principles Of Electrical Methods 2-1

Electrical Methods 2-1
- Self potential 2-1
- Induced polarization 2-1
- Mise-à-la-masse 2-1
- Galvanic resistivity 2-4
- Electromagnetic 2-4

Electrical Properties 2-5

References 2-13

Table of Contents--Continued

Page

Chapter 3. Principles Of Airborne Radioactivity Measurements 3-1

Primary Topics of the Selected References 3-4

Selected References 3-4

Chapter 4. Geophysical Deposit Models 4-1

Geophysical Model of Diamond Pipes 4-2

Geophysical Model of Carbonate-hosted Au-Ag 4-6

Geophysical Model of Homestake Au 4-11

Chapter 5. Overview of the Getchell Study Area and Airborne Demonstration Project 5-1

Introduction 5-1

Geologic Setting 5-2
- Lithology 5-6
- Structures 5-6
- Mineral deposits 5-6

Data Descriptions 5-7
- Topographic data 5-7
- Radioelement data 5-7
- Aeromagnetic data 5-7
- Airborne electromagnetic data 5-8

Acknowledgments 5-8

References 5-8

Table of Contents--Continued

Page

Chapter 6. Getting Started with the Software 6-1

Grids 6-1
Common grid problems 6-1
Bibliography 6-2

Description of File Formats
Description of USGS grid format 6-3
Description of USGS post file format
Generic post file 6-4
Gravity post file 6-4
Manipulate airborne data (MAD) post files 6-5
Description of USGS xyz file format 6-6
Description of image formats 6-6

Introduction to USGS Potential-Field Software 6-7
History 6-7
Disclaimer 6-8
References 6-8
Hardware requirements 6-8
Installation 6-8
Organization 6-9
Online help and documentation 6-12
General program operation 6-12
General program conventions
Command files 6-13
Questions that contain items in brackets 6-13
Geographic conventions 6-14
Rules of thumb when in doubt 6-14

Basic Grid Utility Programs 6-15

Introduction to REMAPP Image-Processing Software 6-18
Introduction 6-18
History 6-18
Future 6-19
Disclaimer 6-19
Hardware requirements 6-19
Installation 6-20
Use with potential-fields software 6-21

Independent PC Exercises I 6-22

Table of Contents--Continued

Page

Chapter 7. Displaying Grids 7-1

Display Types 7-1

Contour Plots 7-5
CONTOUR program help file 7-5
Example - running CONTOUR 7-16
DETOUR and DETOURG 7-17
GRAFEDIT 7-17

REMAPP Display Programs 7-18
Basic REMAPP Programs 7-18
DISPLAY functions 7-21
Clarification of mapping pairs (STRETCH) 7-21

IMVIS Image Viewing System 7-22
IMVIS program information 7-22
Viewing a single image 7-22
Viewing an image set 7-27
Label files 7-28
REDUCE program information 7-35
REORDER program information 7-36

Generating IMVIS images from grid files 7-38
HISTNORM 7-38
GRD2IMG 7-38
RAINPAL 7-39
ADDPAL 7-39
CSR 7-39
CEDGE 7-41

Independent PC Exercises II 7-42

Chapter 8. Map Enhancement Techniques for Gravity and Magnetic Data 8-1

Introduction to Map Enhancement Techniques 8-1

Common Operations
Reduction-to-pole transformation 8-2
Pseudogravity transformation 8-2
Vertical derivatives 8-3
References 8-3

Table of Contents--Continued

Page

Chapter 8. Map Enhancement Techniques for Gravity and Magnetic Data--Continued

Spectral Analysis and the FFT
- General background 8-5
- References 8-6
- FFTFIL program information 8-7
  - FFTFIL program help file 8-7
  - FFTFIL program demonstration and exercise 8-10

Independent PC Exercises III 8-16

Horizontal-Gradient Method
- Applied to gravity data 8-17
- Applied to magnetic data 8-17
- References 8-23
- BOUNDARY program demonstration and exercise 8-24

Terrace Method 8-28
- General background 8-28
- Demonstration I - Terrace operation on Getchell pseudogravity 8-28
- Demonstration II- Terrace operation with density scaling 8-30
- References 8-36

Independent PC Exercises IV 8-37

Chapter 9. Map Enhancement Techniques for Resistivity Data 9-1

Horizontal-Gradient Method 9-1

Resistivity Ratio Data 9-1

Buried-Conductor Enhancement 9-4

References 9-5

ADDGRD Program Demonstration 9-7

Table of Contents--Continued

Page

Chapter 10. Map Enhancement Techniques For Radioactivity Data 10-1

Introduction to Color Composites 10-1

Demonstration of DISPLAY to make Getchell radioelement composites 10-6
Construction of REMAPP image files 10-6
U, K, Th color composite 10-6
Individual element color composites 10-7

Chapter 11. Data Integration 11-1

Integrating Data Sets Using Composite Images 11-1
Introduction 11-1
Reference 11-1
Constructing IMVIS color composites 11-1

Integrating Data Sets Through Multiplication 11-6
Reference 11-7

Independent PC exercises V 11-10

Chapter 12. Sources Of Information 12-1

Gravity and Magnetic Data Sources 12-1

Airborne Geophysics Contractors 12-2

Digital Getchell Data
National Geophysical Data Center announcement 12-5
Description of data files contained in 93-560D 12-7
Common parameters for Getchell data 12-7
Explanation of file extensions for Getchell data 12-7
Description of images contained in 93-560D 12-10

PC Software 12-13
Background 12-13
References 12-13

List of Figures

Figure	Description	Page
1-1	Ranges and averages of densities and magnetic susceptibilities for various rock types	1-3
2-1	Diagram illustrating the five principal electrical methods and their source phenomena	2-2
2-2	Tree diagram showing a classification of electromagnetic methods	2-3
2-3	Distribution diagrams of resistivity values for several types of rocks	2-6
2-4	Diagram showing variation of resistivity as a function of age for various rock types	2-9
2-5	Ranges of resistivities for selected sedimentary rocks	2-11
2-6	Ranges of resistivities for selected crystalline rocks	2-12
3-1	Radioelement contents reported for a variety of lithologies	3-6
5-1	Location of Getchell trend and Osgood Mountains	5-3
5-2	Geological map of the Osgood Mountains area	5-4
6-1	PFMENU index	6-10
8-1	Color-shaded relief image of the 1st-vertical derivative of the reduced-to-pole magnetic field data	8-4
8-2	Various fields over a dense/magnetic body with a near-vertical edge	8-18
8-3	Magnetic profiles over hypothetical thick and thin prisms	8-20
8-4	Comparison of horizontal-gradient method applied to reduced-to-pole magnetic data versus pseudogravity	8-21
8-5	Color-shaded relief image of horizontal-gradient magnitudes of pseudogravity	8-22
8-6	TERRACE-magnetization map of pseudogravity residual	8-31
9-1	Color shaded-relief image of the horizontal-gradient magnitude of the log of the 900-Hz apparent resistivity	9-2
9-2	Color shaded-relief image of the log10 of the ratio of 7200-Hz apparent resistivity to 900-Hz apparent resistivity	9-3
9-3	Color shaded-relief image of a data combination to enhance buried conductive material	9-6

List of Figures--Continued

		Page
10-1	Potassium contour map	10-2
10-2	Uranium contour map	10-3
10-3	Thorium contour map	10-4
11-1	Color shaded-relief image of a data combination to enhance physical-property boundaries	11-8
11-2	Color shaded-relief image of a data combination to enhance lithologic variations	11-9

List of Tables

Table	Description	Page
1-1	Magnetic units	1-6
2-1	Connate water average resistivities from various regions and lithologies	2-8
7-1	Comparison of display techniques	7-2
7-2	Sequence of programs to follow for application of various display techniques to grids	7-3
12-1	Diskette index and specification of grid files	12-8
12-2	Description of data files	12-9
12-3	Diskette index and image file descriptions	12-11
12-4	PLOT menu overlay file descriptions	12-12

WORKSHOP:

GEOPHYSICAL MAP INTERPRETATION ON THE PC

A workshop convened
in conjunction with the Conference

INTEGRATED METHODS IN EXPLORATION AND DISCOVERY

Denver, Colorado
April 21-22, 1993

Sponsored by
Society of Economic Geologists

Co-sponsored by
Society of Exploration Geophysicists
Association of Exploration Geochemists
and
U.S. Geological Survey

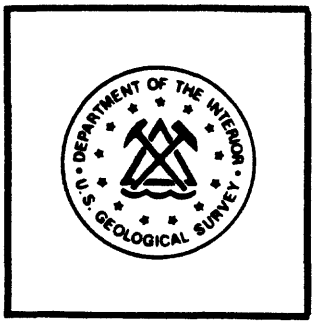

GEOPHYSICAL MAP INTERPRETATION ON THE PC

April 21-22, 1993

OBJECTIVE/GOALS: To introduce geologists and young geophysicists to the use of geophysical data as an aid in geologic mapping. The use of gravity, magnetic, airborne EM and radiometrics in tracing lithologic units and structural features important in mineral exploration will be a key focus.

VENUE AND NUMBER OF DAYS: Short lectures followed by hands-on excercises on the PC. Classes will be held at the USGS computing center, Federal Center, Lakewood, Colorado. Size limited to 20 people.

DESCRIPTION: Introductory lectures on the principles of mapping with gravity, airborne EM, magnetic, and radiometric data for mineral exploration problems on district scale followed by exercises in interpretation of gridded geophysical data in terms of geologic structures and lithologies related to mineral deposits. Data from the Getchell gold trend area, Nevada will be used for illustrative examples and exercises. Topics will include (1) physical-property parameters available from geophysics and their relationships to geology, (2) characteristics and limitations of geophysical data, (3) display methods used for areal geophysical data, (4) techniques of data enhancement and (5) methods of integration and correlation among various data types. The workshop will include use of PC-based software and data bases for analyzing 2-D geophysical data (depth, the third dimension, will *not* be the focus of this course). The basic data are assumed to be gridded geophysical data.

PREREQUISITES/SUPPLIES: Participants should have a basic knowledge of geological and geophysical exploration techniques and a working knowledge of MS-DOS and Intel 80386-based (PC) microcomputers. Software, instruction materials, Getchell data, and the use of a PC for each participant will be supplied. Participants may bring their own data sets provided they are in USGS Branch of Geophysics grid format.

INSTRUCTORS (all from USGS, Denver):

V. J. S. (Tien) Grauch
Donald Hoover
James Pitkin
K. Eric Livo
Anne McCafferty
Jeffrey Phillips

KEY CONTACTS:

Tien Grauch, USGS, Denver
Doug Klein, USGS, Denver

Workshop: Geophysical Map Interpretation on the PC

WEDNESDAY, APRIL 21, 1993

I. Introduction

0830 A. Outline of course--Tien Grauch

1. Nongeophysical audience

2. Focus on geophysical *map* interpretation--start with a grid

3. Geophysical methods covered: gravity, magnetics, airborne EM, airborne radioactivity (gamma-ray). *Not* covered: remote-sensing methods

4. Goals
   a. familiarity with geophysical map methods
   b. familiarity with USGS software

5. Getchell trend data used for demonstration

0845 B. Logistics--Doug Klein

II. Principles of Geophysical-Map Methods

(Each subtopic includes discussion of associated physical property, physical property vs. lithology, depth of investigation, ambiguities, geologic/mineral-deposit features that are resolved, typical data acquisition problems, recognition of cultural features, data acquisition specifications for mapping at a district scale, and common sources of data.)

0900 A. Gravity--Tien Grauch

0930 B. Magnetics--Tien Grauch

1000 COFFEE BREAK

1015 C. Airborne EM--Don Hoover

1100 D. Airborne radioactivity--Jim Pitkin

III. Geophysical Data and Mineral Deposits

1130 A. Geophysical characteristics of mineral deposits--Don Hoover

1200 LUNCH BREAK

WEDNESDAY, Continued

1300 B. Introduction to the Getchell trend study--Don Hoover

1. Background
2. Geologic/mineral deposit setting
3. Airborne geophysical surveys
4. Some interpretative results and publications available

IV. Working with Grids

1330 A. About grids--Tien Grauch

1. grids and gridding limitations
2. common grid problems to watch for
   a. sampling limitations (beading, pockmarks)
   b. processing problems (herring-bone)
   c. overfiltering

1345 B. Introduction to the potential-field software--Jeff Phillips and Tien Grauch

1. History
2. Installation, hardware requirements, and directory organization
3. Online help and documentation (PFHELP)*
4. USGS grid format and "dvals"
5. General program operation (command files, data types, etc.)
6. Grids available for this workshop
7. Basic grid utility programs (ID, GHIST, REGRID)*

C. Displaying gridded data

1415 1. Display types--Tien Grauch

1430 COFFEE BREAK

---

*Includes a PC program demonstration

WEDNESDAY, Continued

1445 2. contour plots (CONTOUR, DETOUR, DETOURG)*--Jeff Phillips

1500 3. raster images--Eric Livo
   a. imaging non-remote-sensing data
   b. REMAPP demonstration*

1530 4. color, color-shaded relief (IMVIS system)*--Jeff Phillips

1600 - 1700 Independent PC exercise

THURSDAY, APRIL 22, 1993

V. Map Enhancement Techniques

A. Gravity and magnetics

0830 1. Features of the Getchell magnetic (and gravity) data--Tien Grauch

0845 2. Transformations--Tien Grauch
   a. reduction-to-pole
   b. pseudogravity
   c. first vertical derivative
   d. comparisons using Getchell magnetic data*

0915 3. Spectral analysis using FFT--Tien Grauch and Jeff Phillips
   a. terminology
   b. FFT uses
      i. facilitate computations
      ii. isolate components of the data (bandpass)
   c. cautions on and misuses of FFT
   d. FFTFIL program demonstration*

0945 Independent PC Exercise

1000 4. horizontal-gradient method (BOUNDARY)*--Tien Grauch

1030 COFFEE BREAK

1045 5. terrace method (TERRACE)*--Anne McCafferty and Jeff Phillips

1100 Independent PC Exercise

---

*Includes a PC program demonstration

THURSDAY, Continued

1130 LUNCH

1300 B. Airborne EM--Don Hoover and Tien Grauch

1. features of the Getchell resistivity maps
2. horizontal-gradient magnitude
3. ratio map
4. buried conductive material map

1330 C. Airborne radioactivity--Jim Pitkin

1. features of the Getchell gamma-ray data
2. ratio maps
3. composite maps (DISPLAY)*

VI. Integration of Data Sets

1400 A. nontraditional composites--Jeff Phillips

1415 Independent PC Exercise

1430 COFFEE BREAK

1445 B. multiplication (ADDGRD)*--Tien Grauch

1515 **VII. Wrap-up**

A. Geophysical contractors--Don Hoover

B. Future software updates--Jeff Phillips

C. Acknowledgments--Doug Klein

1530-1700 Independent PC Exercise

---

*Includes a PC program demonstration

GEOPHYSICAL MAP INTERPRETATION ON THE PC

LIST OF USGS INSTRUCTORS AND WORKSHOP STAFF

Branch of Geophysics
U.S. Geological Survey
Denver Federal Center, Mail Stop 964
Denver, Colorado 80225

Phone (303) 236-1212, FAX (303) 236-1425

Gravity and Magnetic methods

Tien Grauch: Workshop Chairman and co-organizer (potential-field geophysics, Getchell study team member)
Jeff Phillips: Instructor (potential-field geophysics, geophysical software developement)
Anne McCafferty: Instructor (potential-field geophysics)

Airborne Electromagnetic methods

Don Hoover: Instructor (electrical geophysics, Getchell study team member)

Aeroradioactivity methods

Jim Pitkin: Instructor (gamma-ray geophysics, Getchell study team member)

Remote Sensing

Eric Livo: Instructor (remote sensing geophysics, geophysical software development)

PC software assistant

Bob Kucks: Software assistant (potential-field geophysics)

Workshop co-organizer and logistical coordinator

Doug Klein: (electrical geophysics)

Chapter 1. Principles of Potential-Field Methods

INTRODUCTION

Potential-field methods include gravity and magnetic methods, two of the oldest geophysical techniques in use. Although these two methods reflect two completely different physical properties of rocks, they are usually considered together because of their mathematical similarities. Both gravity and magnetic fields are vectors. Under certain conditions valid for most geophysical surveys, both gravity and magnetic fields can be expressed as the gradient of a scalar Φ, called a potential, that satisfies Laplace's equation,

$$\frac{\partial^2\phi}{\partial x^2} + \frac{\partial^2\phi}{\partial y^2} + \frac{\partial^2\phi}{\partial z^2} = 0. \qquad (1\text{-}1)$$

This very important result is the backbone of all potential-field methods and leads to some useful and unique mathematical properties.

Only one component of the gravity or magnetic vector field is measured in most geophysical surveys. Fortunately any component of the field also satisifies Laplace's equation, and consequently many of the important properties associated with the potential also are applicable to the gravity or magnetic quantities actually measured. These properties are the focus of subsequent discussions in this and following chapters.

GRAVITY METHOD

Gravity anomalies represent variations in the earth's gravitational field caused by variations in crustal density. Although these variations are normally measured at stations on the ground, data collection is fast, economical, and commonly can be supplemented by previously collected data that is publicly available from government agencies (Chapter 12). Thus, data coverage in most parts of the U.S. is often adequate for constructing and interpreting maps. However, not all the gravity stations in archived files are accurate. Commonly, one must remove "bad stations", or ones with obviously erroneous values, before interpreting the data.

Gravity meters measure the vertical attraction of the whole earth in units of acceleration, approximately 9.8 m/sec^2 (980,000 mgal) at the equator. The exploration geophysicist, however, is interested only in that small part of each measurement caused by density variations in the crust, and measurements commonly are reduced in order to remove all other contributions to the gravity field. These contributions include the field of an average earth with no topography above sea level plus the effects of the earth's rotation, lunar and solar tides, sensor altitude and motion, and all rocks of "average" density above sea level. The quantity that remains is called the complete Bouguer anomaly (CBA), or Bouguer anomaly for short. The adjective "complete" distinguishes the CBA from the so-called simple Bouguer anomaly, which does not take into account the effects of

surrounding terrain. The reduction of observed gravity to CBA requires an assumption of average crustal density, called the reduction density, and typically taken to be 2.67 g/cm^3 (2670 kg/m^3 in SI units). The various reduction equations used by the USGS are described by Cordell and others (1982).

Bouguer anomalies are produced by volumes of rock having densities that contrast with the surrounding country rock. Anomalies of most interest to exploration geophysicists commonly give closed contours on contour maps, although anomalous values are not confined to areas of closed contours. In general, positive anomalies (highs) occur over volumes of rock that are denser than the surrounding rocks, and negative anomalies (lows) occur over bodies of rock that are less dense than the surrounding rocks. Layered rocks of essentially homogeneous density in each layer, such as some sedimentary units, by themselves produce only a constant shift in gravity values. However, lithologic changes that disrupt the layers, such as an intrusion, can produce an associated gravity anomaly. Similarily, layers that have been disrupted by structures such as folds and block faulting also produce gravity anomalies. Terrain composed of rocks having a density other than the reduction density also produces anomalies that correspond to the shape of topography.

At regional scales, Bouguer anomalies are inversely proportional to topography because topographic loads are compensated by mass depletions at depth, following the principles of isostasy. At these scales and in mountainous terrain, it is useful to remove the effects of an isostatic model so that variations within the upper crust are enhanced (Simpson and others, 1986). At more local scales, such as district scales, it may be useful to remove a regional field that is based on a least-squares fit of a polynomial surface to the data. This serves to help isolate smaller anomalies of interest.

The shape and magnitude of a Bouguer anomaly produced by one body of rock is complexly related to the body's shape and bulk density. Bulk density is a measure of the average density of a volume of rock that incorporates the effects of porosity and other voids in the rocks, such as those produced by joints, fractures, and brecciation. Bulk density is given by

$$\rho_{bulk} = \rho_{grain}(1 - \phi) + \phi\rho_{fill}, \qquad (1\text{-}2)$$

where ρ_{grain} is the density of the individual grains in the rock, ϕ is the porosity, and ρ_{fill} is the density of the material filling the pores. In most cases, bulk density as reflected in gravity measurements at the Earth's surface are assumed to be close to bulk density of rock samples measured in the laboratory. Densities of rocks rarely vary outside of the range 1.0 to 3.0 g/cm^3 (1000 to 3000 kg/m^3), and commonly vary even less (Nettleton, 1971). Figure 1-1 shows average density values for various rock types. More extensive data are presented in Daly and others (1966). In general, low densities are expected for sedimentary rocks, especially unconsolidated sediments. Notable exceptions are carbonate rocks, especially those containing dolomite. High densities are expected for igneous and

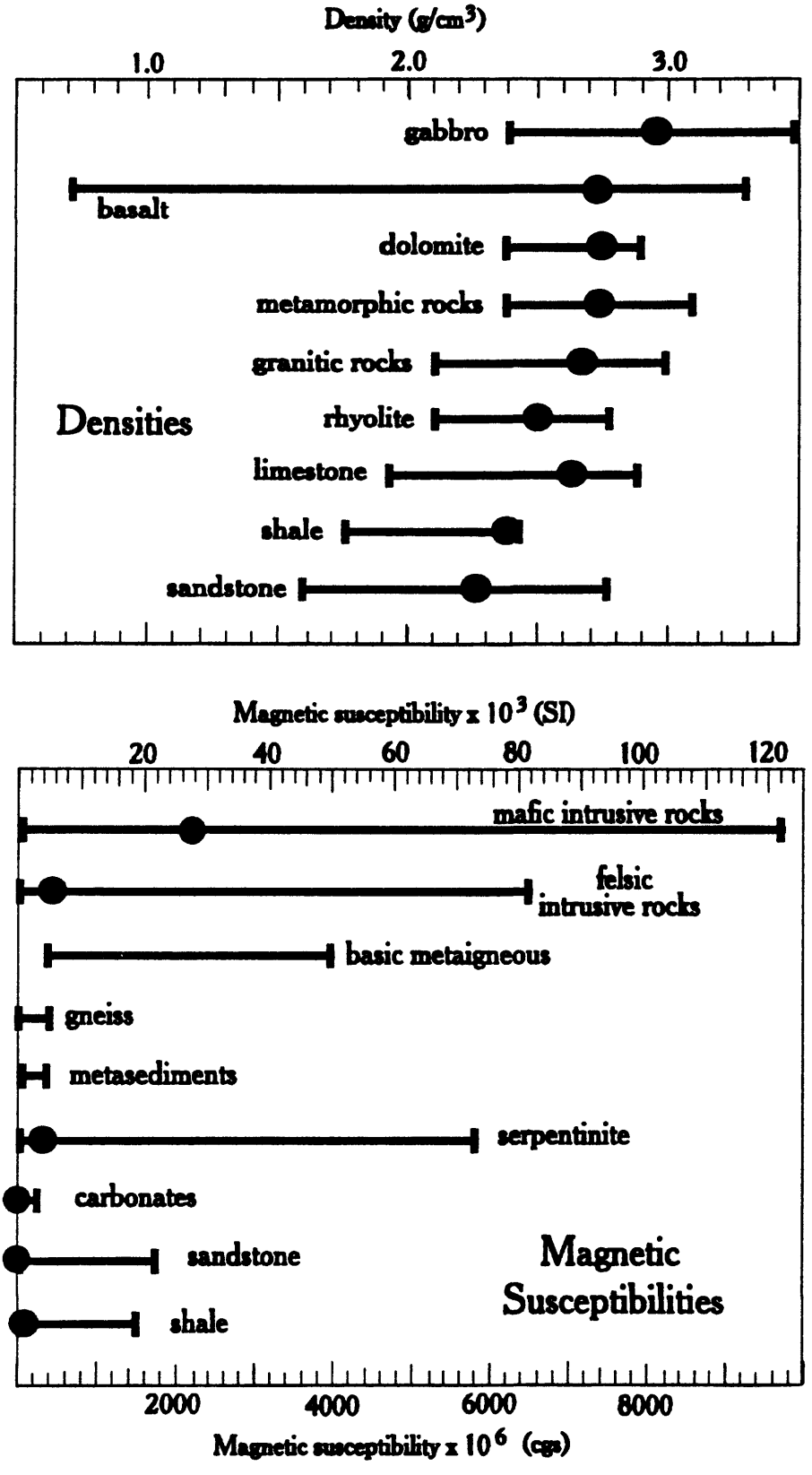

Figure 1-1. Ranges (bars) and averages (solid circles) of densities and magnetic susceptibilities for various rock types. Data from Daly and others (1966), Dobrin (1976), Johnson and Olhoeft (1984), and Carmichael (1982). The range for metasediments may be much larger than indicated.

metamorphic rocks, and are generally higher the more mafic material they contain. In the absence of available density measurements, densities are commonly estimated on the basis of rock type. Unlike other estimates of physical properties of rocks, such estimates are usually reliable.

The size (amplitude) and shape of an anomaly are related to the depth, density contrast, and shape of its source. Generally, gravity anomalies are located directly over their respective sources, and are broader and lower in magnitude the deeper the source. As *a rule of thumb*, one can consider anomaly amplitude to decrease as the square of the distance from the source, although the relation is actually very complicated. The steepest slopes of anomalies tend to occur over abrupt, lateral changes in density, such as at lithologic contacts or faults.

The interpretation of gravity anomalies is inherently ambiguous, because theoretically there are an infinite number of sources with different shapes and depths that can produce the same anomaly. For example, anomalies may be due to lithologic variations, structural relief, or both, at a variety of depths. The number of solutions can be reduced significantly by adding geologic and other geophysical constraints and comparison to other data sets.

Design of a gravity survey depends on the goal of the survey. If the goal is regional reconnaissance, the gravity spacing should be as close to equi-spaced as possible, although the actual spacing and location of stations are usually determined by practicalities. If certain targets are to be located, such as near-vertical faults, one could produce a likely model of the feature and from that determine the spacing that would adequately resolve such features.

Gravity data are fairly immune to cultural features (manmade structures or objects) in common exploration situations. Gravity surveys in urban areas must consider the gravitational effects of surrounding buildings.

AEROMAGNETIC METHOD

Magnetic methods measure variations in the strength of the earth's magnetic field produced by the magnetization of rocks containing significant amounts of magnetic minerals (commonly magnetite). Magnetic measurements taken to aid geologic interpretation of the subsurface are most effectively and efficiently acquired by aircraft. Geophysical contractors are available to acquire new data; older data are available from government agencies (Chapter 12).

Magnetometers commonly measure the total field, the intensity of the magnetic field in the direction of the earth's main field. Removal of variations of the field due to aircraft position and movement, atmospheric and solar effects, and the field produced by the earth's core gives the total-intensity residual field, commonly called total-field residual or aeromagnetic anomaly data. The first two sources of variation are removed during data

reduction of the airborne survey based on field measurements taken during the survey. Removal of the Earth's main field may be done subsequently, using the International Geomagnetic Reference Field (IGRF; Langel, 1992). The IGRF, which now is updated every five years, is a model of the earth's main field which predicts the configuration of the field from the date of the IGRF to five years hence. However, because temporal variations in the earth's main field cannot be completely predicted, the IGRF models become somewhat inaccurate, especially nearing the end of each five-year update period. By international agreement, Definitive Geomagnetic Reference Fields (DGRF; Langel, 1992) are issued on a periodic basis which describe the actual configuration of the earth's field at times in the past. Thus, although aeromagnetic surveys are reduced with an appropriate IGRF, the errors introduced by the IGRF cannot be evaluated until the release of the appropriate DGRF some time later.

The shape and magnitude of a magnetic anomaly produced by one body of rock is complexly related to the body's shape and total magnetization. Total magnetization **M** is a vector quantity described as a vector sum of the induced and remanent components of magnetization:

$$\mathbf{M} = \mathbf{M_r} + \mathbf{M_i}. \tag{1-3}$$

Induced magnetization aligns with the direction of the Earth's magnetic field **H** and is proportional to the magnetic susceptibility κ of the rock so that

$$\mathbf{M_i} = \kappa\, \mathbf{H}. \tag{1-4}$$

Remanent magnetization $\mathbf{M_r}$, the subject of paleomagnetic studies, is the vector sum of all permanent magnetizations acquired since the formation of the rock. It is usually described in terms of its intensity, declination measured from north, and inclination measured down from horizontal. The types, strengths, and directions of permanent magnetizations are determined by a variety of factors, including initial rock chemistry, emplacement and cooling history, later hydrothermal alteration, and the behavior of the earth's field during the rock's history. If the direction of the remanent magnetization is roughly the same as the present earth's field, the rocks are said to be normally magnetized; if the magnetization has the opposite direction, the rocks are said to be reversely magnetized.

Table 1-1 lists units in the cgs and SI system commonly attributed to the parameters used in magnetic interpretation. Magnetic interpreters have historically preferred cgs units, even though SI units are now standard in the literature. Thus, magnetic units are a common source of confusion in practice.

TABLE 1-1. MAGNETIC UNITS

$$M = M_r + \kappa H,$$

Symbol	Explanation	cgs Units	Conversion Factor*	SI Units
M	Total Magnetization	emu/cm^3	10^3	A/m
M_r	Remanent Magnetization	emu/cm^3	10^3	A/m
κ	Magnetic Susceptibility	dimensionless	4π	dimensionless
H	Earth's Magnetic Field	oersted	10^{-4}	A/m

*Multiply the conversion factor by the value in cgs units to convert to SI units.

Notes:

1) Earth magnetic field values are commonly given in gammas (cgs) or nanoTeslas (SI), but must be converted to the units on this table before using the above equation:
   1 oersted $\approx$ 1 gauss $\approx$ 1 emu/cm^3 $\approx 10^5$ gamma $\approx 10^5$ nanoTesla $= 10^{-4}$ Tesla
2) Although κ is dimensionless, it is commonly given in units of emu/cm^3 or emu/g in the cgs system to distinguish between susceptibility per unit volume and susceptibility per unit mass.
3) For more information see Shive (1986).

Magnetic interpreters often assume that M_r is negligible, so that susceptibility is the only parameter considered. It is a good assumption on regional scales and where anomalies are generally caused by intrusive and crystalline basement rocks; we will deal with this situation first. As *a rule of thumb*, the magnetic susceptibility κ (in the cgs system) roughly corresponds to the concentration of magnetic minerals as

$$\kappa \sim 0.25\ p, \qquad (1\text{-}5)$$

where p is the fraction of magnetite per volume (e.g., one volume percent magnetite gives $p=.01$ and $\kappa \sim 2500 \times 10^{-6}$), except for high fractions ($p > 0.10$). Magnetic susceptibilities of rocks are quite variable, even within the same rock unit. Generally, sedimentary rocks are so weakly magnetic that they are virtually invisible to regional aeromagnetic surveys. On the other hand, crystalline rocks generally have high susceptibilities, increasing in value the more mafic the rock. Average susceptibilities for several rock types are shown in Figure 1-1. Exceptions to these generalities are common; this table should be used for general guidance only. More extensive measurements of magnetic properties can be found in Carmichael (1982).

Where rocks have significant remanent magnetization, one can sometimes assume that the remanent component is collinear with the earth's field. This assumption is reasonable at regional scales and for relatively undisturbed rocks that have remanent directions roughly collinear with the present earth's field direction. As *a rule of thumb* for aeromagnetic interpretation, the fields are considered to be collinear when they are within 25^{o} of each other (Bath, 1968). This simplifies equations (1-3) and (1-4) to

$$M = (M_r + \kappa H) = \kappa_a H, \qquad (1\text{-}6)$$

where only intensities of the vectors are now considered. Equation (1-6) simplifies interpretation by considering the remanent intensity and susceptibility together as the scalar κ_a, or apparent susceptibility. Strong negative aeromagnetic anomalies are often indicative of rocks with a dominant reversely magnetized remanent component (having a negative apparent susceptibility), although such anomalies can be associated with other effects as well.

Significant exceptions to these assumptions about remanent magnetization can occur in volcanic rocks (Grauch, 1987) and in rock bodies containing a high percentage of magnetite, such as iron formations. Many standard map enhancement techniques are not applicable in these areas, and interpretation becomes more difficult. However, laboratory measurements may help determine parameters required for modeling.

Typically, an isolated rock body in the northern hemisphere having a total magnetization with positive inclination produces a magnetic anomaly shifted southward from the center of the body and a weak low on the northern side, called a polarity low. The size (amplitude) and shape of an anomaly are related to the depth, magnetization, and

shape of its source. As *a rule of thumb*, one can consider anomaly amplitude to decrease as the cube of the distance from the source, although the relation is actually very complicated. The interpretation of magnetic anomalies is inherently ambiguous, because theoretically there are an infinite number of sources with different shapes and depths that can produce the same anomaly. The number of solutions can be reduced significantly by adding geologic and other geophysical constraints.

In practice, anomalies are not isolated from each other. Groups of overlapping anomalies are commonly viewed as patterns, where differences between patterns generally express structural, topographic, and lithologic variations. Discrimination of individual magnetic sources from the patterns can be very difficult because the signals of all the sources may interfere with each other. In these cases, interpreters emphasize the character and changes in anomaly patterns and their correlation to mapped geology to resolve variations in lithology, and (or) depth to magnetic sources. Abrupt changes in anomaly patterns or the presence of gradient trends are commonly associated with near-vertical lithologic contacts or faults. The absence of anomalies over exposed rocks that produce anomalies elsewhere may indicate hydrothermal alteration that has destroyed magnetic minerals. General correlation of anomaly shapes with topographic shapes indicates that magnetic rocks compose the topography.

The resolving power of an aeromagnetic survey is determined primarily by flight-line spacing and height above magnetic sources. The closer the flight lines are to the ground, the better is the resolution of magnetic sources directly below, especially if the sources are near the surface. The closer the flight lines are together, the better is the resolution of magnetic sources between lines. A survey with flight lines spaced twice as wide as their height above ground samples the effects of magnetic sources between and below the flight lines equally, giving the most reliable contour maps (Reid, 1980). Most surveys, including ones for the Getchell trend area, have flight lines spaced wider than twice the height above ground to cut costs or to accommodate the requirements of other geophysical instruments on board. In addition, magnetic sources with linear strikes, such as dikes and faults, are best resolved by flying perpendicular to strike.

Anomalies caused by cultural features (manmade structures or objects) can be expected in high-resolution surveys, depending on the size of the feature. Cultural features can best be recognized by comparison of anomalies of very limited lateral extent with the known location of metal objects, such as (in order of decreasing significance) buildings, junkyards, large metal equipment (such as drill rigs, vehicles), and steel-cased drill holes.

BIBLIOGRAPHY

Bath, G. D., 1968, Aeromagnetic anomalies related to remanent magnetism in volcanic rock, Nevada Test Site: Geol. Soc. America Memoir 110, p. 135-146.

Blakely, R. J., in press, Potential theory in solid-earth gravity and magnetic studies: Cambridge University Press.

Blakely, R. J., and Connard, G. G., 1989, Crustal studies using magnetic data: Geological Society of America Memoir 172, p. 45-60.

Carmichael, R. S., 1982, Magnetic properties of rocks and minerals *in* Carmichael, R. S., Ed., Handbook of Physical Properties of Rocks, V. II: CRC Press, Boca Raton, Florida, p. 229-288.

Cordell, Lindrith, Keller, G. R., and Hildenbrand, T. G., 1982, Bouguer gravity map of the Rio Grande Rift: U. S. Geol. Survey Geophysical Investigations Map GP-949, scale 1:1,000,000. [contains gravity reduction equations]

Daly, R. A., Manger, G. E., and Clark, S. P., Jr., 1966, Density of rocks *in* Clark, S. P., Jr., Ed., Handbook of Physical Constants, revised edition: Geological Society of America Memoir 97, p. 20-26.

Dobrin, M. B., 1976, Introduction to geophysical prospecting, third edition, McGraw-Hill, 630 p.

Grant, F. S., and West, G. F., 1965, Interpretation theory in applied geophysics: McGraw-Hill, 584 p.

Grauch, V. J. S., 1987, The importance of total magnetization in aeromagnetic interpretation of volcanic areas; An illustration from the San Juan Mountains, Colorado: Expanded abstracts with biographies, 57th Annual International Society of Exploration Geophysicists meeting, Oct. 11-15, 1987, p. 109-110.

Johnson, G. R., and Olhoeft, G. R., 1984, Density of rocks and minerals *in* Carmichael, R. S., Ed., Handbook of Physical Properties of Rocks, V. III: CRC Press, Boca Raton, Florida, p. 1-38.

Kellogg, O. D., 1953, Foundations of Potential Theory: Dover Publications, Inc., New York, 384 p.

Langel, R. A., 1992, International Geomagnetic Reference Field, 1991 revision: Eos, Transactions, American Geophysical Union, v. 73, no. 16, p. 182.

Nettleton, L. L., 1971, Elementary gravity and magnetics for geologists and seismologists: Society of Exploration Geophysicists, Tulsa, Okla., 121 p.

Parasnis, D. S., 1966, Mining geophysics: Elsevier, 356 p.

Reynolds, R. L., Rosenbaum, J. G., Hudson, M. R., and Fishman, N. S., 1990, Rock magnetism, the distribution of magnetic minerals in the earth's crust, and aeromagnetic anomalies: U. S. Geological Survey Bulletin 1924, p. 24-45.

Shive, P. N., Suggestions for the use of SI units in magnetism: Eos, v. 67, no. 3, January 21, 1986, p. 25.

Simpson, R. W., and Jachens, R. C., 1989, Gravity methods in regional studies: Geological Society of America Memoir 172, p. 35-44.

Simpson, R. W., Jachens, R. C., Blakely, R. J., and Saltus, R. W., 1986, A new isostatic residual gravity map of the conterminous United States with a discussion on the significance of isostatic residual anomalies: Journal of Geophysical Research, v. 91, no. B8, p. 8348-8372.

Telford, W. M., Geldart, L. P., Sheriff, R. E., and Keys, D. A., 1976, Applied geophysics: Cambridge, 860 p.

Vacquier, V., Steenland, N. C., Henderson, R. G., and Zietz, Isidore, 1951, Interpretation of aeromagnetic maps: Geological Soc. of America Memoir 47, 155 p.

Van Blaricom, Richard, 1980, Practical geophysics: Northwest Mining Association, 303 p.

Chapter 2

PRINCIPLES OF ELECTRICAL METHODS

This chapter directly adapts an overview on electrical methods, and earth resistivity variations with lithologies from Hoover and others (1992). This provides a summary of electrical methods needed to understand the fundamentals of interpreting electrical geophysical maps.

Electrical methods

In contrast to other geophysical methods, electrical methods comprise a multiplicity of separate techniques that measure distinct geophysical attributes of the earth, using differing instruments and procedures, having variable exploration depth and lateral resolution, and with a large and confusing list of names and acronyms describing techniques and variants of techniques. We have divided the electrical methods into five distinct classes: (A) the self potential, (B) the induced polarization method, (C) the mise-à-la-masse, (D) the galvanic resistivity, and (E) the electromagnetic resistivity. These are shown in figure 2-1, where the three distinct source phenomena are identified and some variations of each method listed. In the case of electromagnetic methods there are so many variations, and differing acronyms and trade names that the variations are detailed in figure 2-2. In spite of all the variants of the electromagnetic method, measurements fundamentally are of the earth's electrical impedance or relates to changes in impedance. Some of the electromagnetic methods listed in figure 2-2 are hybrid techniques because source fields may be generated through galvanic contact to the earth (TURAIR, CSAMT, etc.), or receiver electric fields may be measured through galvanic contact to the earth (CSAMT, AMT-MT, VLF, telluric, etc.). However, for convenience these have been classified with the electromagnetic methods.

A. Self Potential

The self potential method has several possible sources giving rise to a dc or quasi-dc natural electrical field. For mineral deposits the most important is the Sato and Mooney (1960) type source established when an electronic conductor, such as a massive sulfide or graphite body, extends between an oxidizing and reducing zone or over a range in pH. Other self potential sources are due to flux of water or heat through the earth.

B. Induced polarization

The induced polarization method provides a measure of polarizable minerals within the water-bearing pore spaces of rocks. These minerals are metallic-luster sulfides, clays, and zeolites. The above mineral groups, in order to be detected, must present an active surface to the water in the pore space. Sulfide mineral grains completely enclosed by a nonconducting matrix such as silica will not be detected by the IP method. Since the IP response relates to the presence of active surface areas within the rock, disseminated sulfides provide a much better target than massive sulfides for this technique. This method has found its greatest application in exploration for disseminated sulfide ores where its good sensitivity (as low as 0.5% total metallic luster sulfide may be detected, according to Sumner, 1976) makes it a primary tool.

C. Mise-à-la-masse

The mise-à-la-masse method is a little-used technique that is applied to conductive ore deposits that have a large resistivity contrast with the host rock. Under these conditions, electrical contact is made to the ore body, either at the surface or through a drillhole, with a source of direct or low

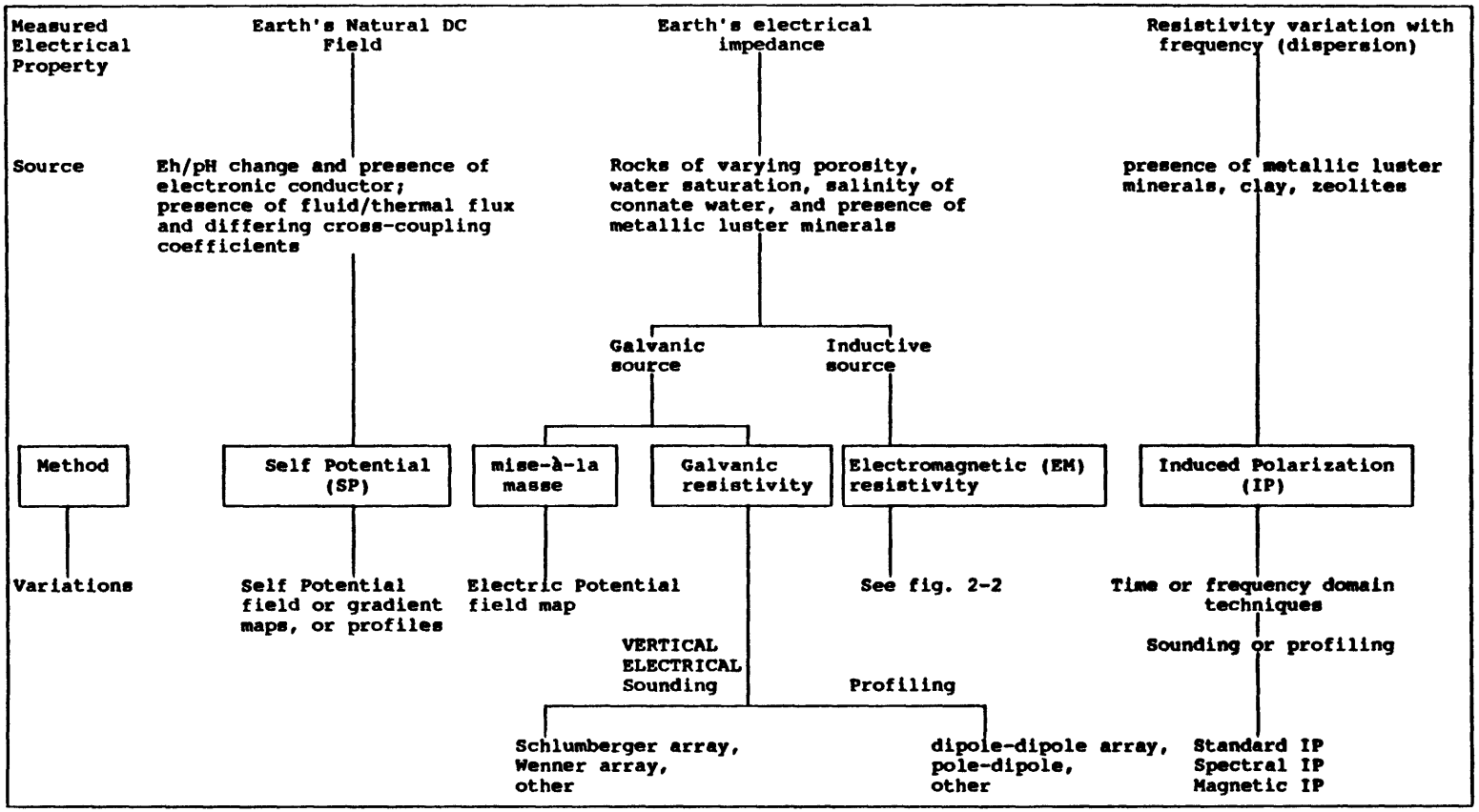

Figure 2-1. Diagram illustrating the five principal electrical methods and their source phenomena.

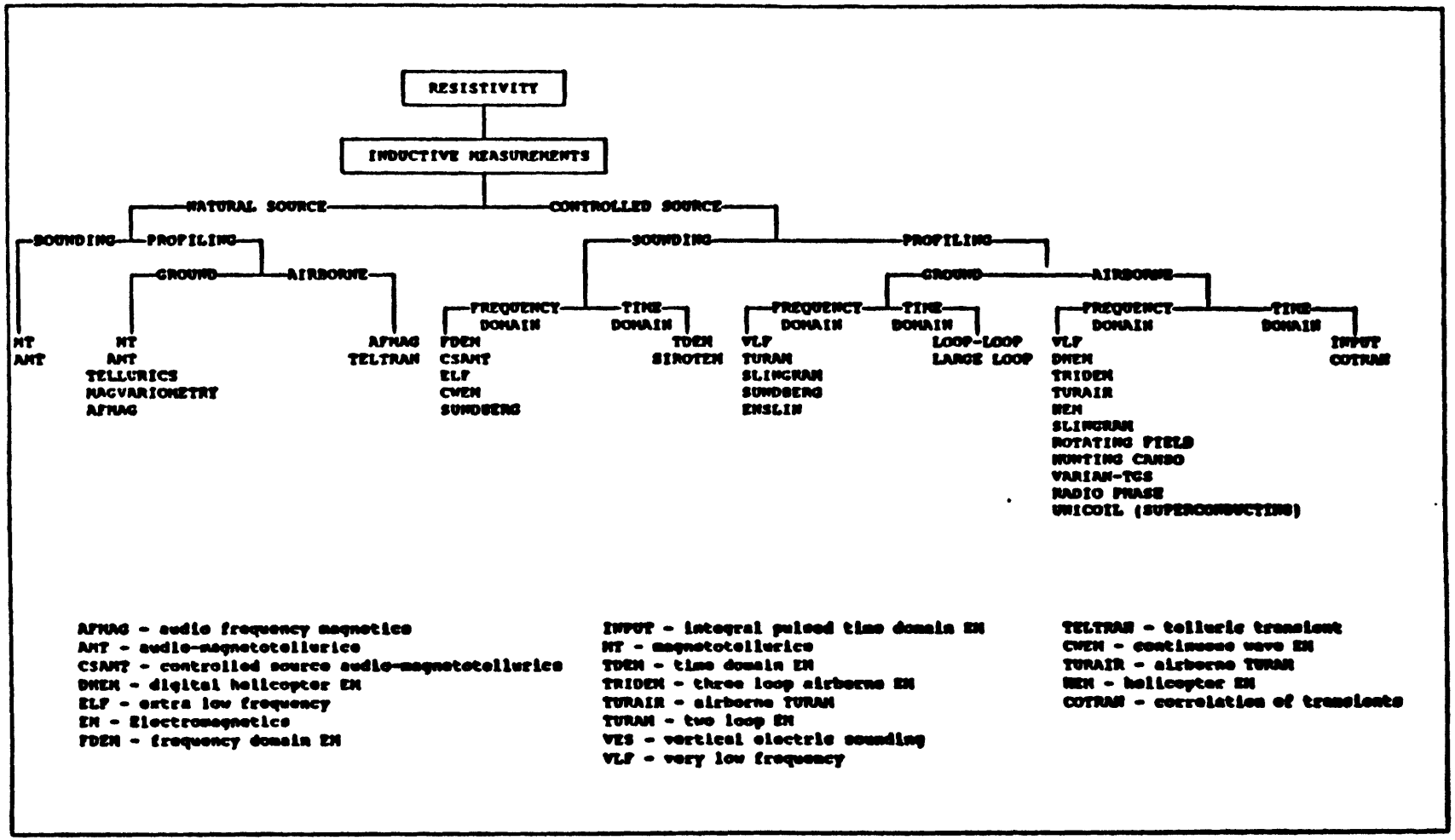

Figure 2-2. Tree diagram showing a classification of electromagnetic methods, and some of the techniques belonging to each branch.

frequency current. The other electrical pole is placed some distance away. When energized, the ore body becomes essentially an equipotential surface. The field from this body can then be mapped at the surface revealing the position of ore below the surface. An excellent example of this method is given by Mansinha and Mwenifumbo (1983). Application of this method is principally for massive sulfides.

D. Galvanic resistivity

Galvanic resistivity methods, often referred to as "dc" resistivity methods, provide a measure of earth resistivity using a dc or low frequency ac current source. Source current is introduced into the earth, and the electric field is measured, through electrodes in galvanic contact with the earth. Resistivity in earth materials is primarily a function of porosity and water content, high porosity giving low resistivity in water saturated rocks. Resistivity values may range over five orders of magnitude in normal near-surface environments. Electrical conduction in rocks at dc and low frequencies occurs through ionic migration in the water of the pore spaces and more rarely, partially by electronic conduction through metallic luster minerals. Because metallic luster minerals typically do not provide long continuous circuit paths for conduction in the host rock, bulk rock resistivity almost always is controlled by the water content and dissolved ionic species present.

In contrast to potential field methods dealing with natural fields such as gravity, magnetic, and self potential methods, the galvanic resistivity techniques use an applied field and are thus able to control the depth of exploration by the spacing of the current and potential electrodes. If one is looking for lateral resistivity changes within a given depth range, then a fixed electrode array may be used to profile across an area of interest. On the other hand, if information on variations of resistivity with depth are desired, then an array may be expanded about a fixed point (a vertical electrical sounding, VES). The variations between profiling and sounding and between electrode arrays leads to differing names being applied to each variant, i.e., Schlumberger (array), vertical electrical sounding (VES), etc.

The galvanic techniques have application to a wide variety of ore deposit exploration. Massive sulfides can provide a direct very low resistivity target, or alteration products within and around hydrothermal deposits often provide a clear low resistivity target. The wide range of resistivities of earth materials also makes the method applicable to identification of lithologies and structures that may control mineralization.

E. Electromagnetic

Electromagnetic methods are probably the most confusing to the non-practitioner because of the many variants, and acronyms, or trade names used to describe them. Figure 2-2 presents one scheme for classification of EM methods in a tree form. The first branch is based on whether the energy source is natural or artificial. For each of these the next level of branching is based on whether the method is a profiling technique or a sounding technique. The third level of branching is based on whether it is an airborne or ground method, and the last branch based on time domain or frequency domain techniques. At the ends of these 9 resultant branches are given the names and acronyms of some of the electromagnetic methods that apply. In all, thirty-one different terms are shown, and this is not an exhaustive list.

The practical exploration depth of each system is quite variable and depends on the operating frequencies, the rock resistivity, structure, and the source-to-receiver distance. For controlled source airborne methods the maximum exploration depth is on the order of 100 meters. The natural source

airborne methods have greater depth potential, but unfortunately none have been used for many years. As in galvanic resistivity techniques, soundings can be made by changing the source-to-receiver separation. In practice such soundings are normally used in shallow exploration. However, electromagnetic methods also permit sounding by variation of the operating frequency or time, for time domain systems, and this procedure is becoming of greater importance in exploration, especially where definition of deep features are desired. In the compilation of deposit characteristics no attempt is made to distinguish among the numerous EM methods, nor in many cases between EM and galvanic resistivity methods. For all of these various techniques, they either provide a measure of resistivity or impedance or respond to changes in resistivity or impedance, and this is the important attribute for the model.

The most common application of EM methods to minerals exploration has probably been in the search for massive sulfides. Normally airborne methods are used to screen large areas providing a multitude of targets for further screening by ground methods. Airborne EM methods are now beginning to find increasing use in mapping applications where lithologic and structural features can be identified in areas of difficult access or where cover exists (Palacky, 1986; Hoover and others, 1991).

Hohmann and Ward (1981) provide an excellent review of electrical methods that are used in minerals exploration.

ELECTRICAL PROPERTIES

In the upper kilometer or so where most minerals exploration takes place the resistivity of earth materials is even less representative of lithologic type than are seismic velocities. In this environment earth resistivity is generally determined entirely by rock porosity and the conductivity of the fluid filling the pore space. Because porosity and fluid conductivity are not parameters closely related to lithologic type, especially for igneous and metamorphic rocks, empirical relationships between resistivity and lithologic type show a wide variation. The picture is further complicated by problems related to laboratory measurements on hand or core samples of in-situ resistivities. Samples may dry prior to measurement requiring rehydration with water that may not be representative of the original connate water, and small samples may not be representative of the effect of fractures in the bulk. In part because of these problems, several authorities do not even provide summary results of resistivities of wet igneous or metamorphic rocks as a function of specific lithologic types (Keller, 1966, Keller and Frischknecht, 1966, Keller, 1982, and Olhoeft, 1981). Sedimentary rocks because of their importance to the petroleum industry are more extensively studied.

Illustrative of the broad range of resistivities measured on rocks and the lumping of major lithologic types are figures given by Grant and West (1965) and similar illustrations from Sumner (1976), that were reproduced by Hallof (1980). These are shown in figure 2-3 redrafted to the same scale for comparison. The figure shows resistivities covering a span of ten orders of magnitude, 10^{-1} to 10^{9} ohm-meters. The upper four decades represent measurements on laboratory samples of low porosity or very dry samples, and are not representative of in-situ bulk resistivities which will rarely exceed 10^{5} ohm-m. Again, this emphasizes the need for caution when applying laboratory results to the field situation.

Below the water table, and in rocks where electronic conduction processes due to metallic luster sulfide minerals can be neglected, conduction is controlled by migration of charged ions in the pore water. The charged ions can be considered to be particles moving under the force of an applied electric field in a viscous fluid. The current then is proportional to the

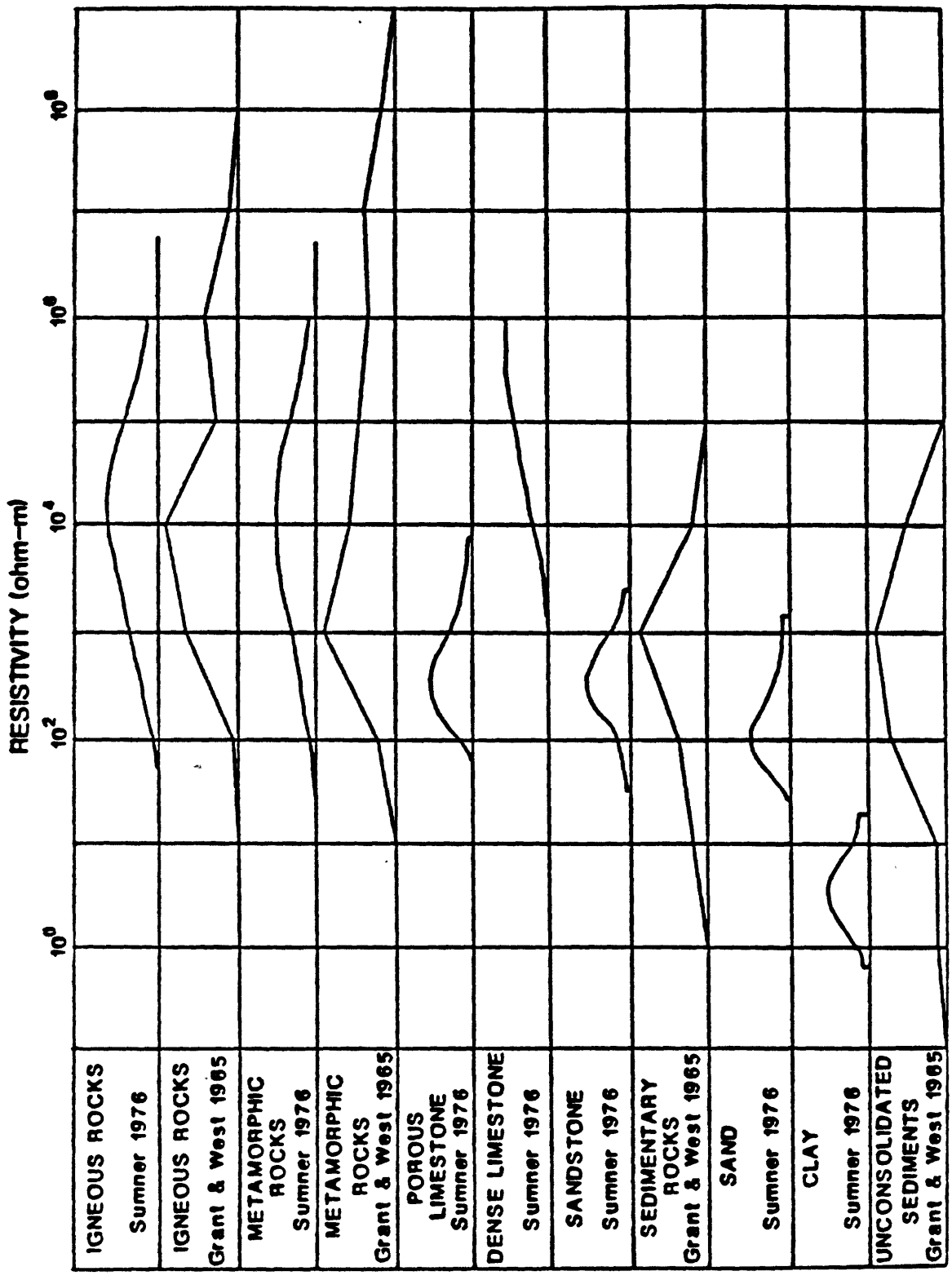

Figure 2-3. Distribution diagrams of resistivity values for several types of rocks from Sumner (1976) and Grant and West (1965).

number of ions, ion size, water viscosity, and electric field. Rock resistivity then is related principally to the concentration of dissolved and ionized species in solution, and water viscosity since ion size does not vary appreciably. Viscosity is a factor when the pore water temperature changes. Increasing temperature decreases both viscosity and resistivity.

Although the connate water resistivity and porosity control the resistivity of most rocks, connate water resistivity typically does not vary over a wide range. Table 2-1 from Keller and Frischknecht (1966) gives average values of connate water resistivity observed for a number of regions and lithologies. In general, shallow waters and waters from crystalline rocks have the highest resistivities, while deeper waters, or those from sediments, show the lowest resistivities. The average resistivity range is seen to be a little over two orders of magnitude.

The more extensive studies of sedimentary rocks have resulted in an empirical relationship for sediments called Archie's law that relates resistivity (ρ) to porosity (ϕ) and the connate water resistivity (ρ_w). The relationship is:

$$\rho = A\rho_w\phi^{-m} \tag{2-1}$$

where A and m are empirical constants dependent on the type of sediment. Keller and Frischknecht (1966) give values of A and m for a number of sediments in which A varies from 0.47 to 2.3 and m from 1.64 to 0.23. Where reasonable estimates of sedimentary host or cover rock porosity and connate water resistivity can be made, Archie's law can be used to provide resistivities for modeling.

In the vadose (unsaturated) zone, rock resistivities do not increase in direct proportion to the degree of undersaturation. Nonlinear effects result from the presence of a continuous film of water between grains at larger values of partial saturation, and from surface conduction effects. Keller and Frischknecht (1966) provide further details on these effects.

Desert soils and alluvium exhibit an interesting paradox in the vadose zone where the dryness might be expected to result in increased resistivity over that of soils in moister regions. However, most desert soils show resistivities in the range of 10-100 ohm-m, about an order of magnitude lower than soils from regions with average rainfall. This is due to the compensating effect of increased salt content in the residual moisture held by the soils.

For a given rock type the resistivity normally increases with age and depth of burial, principally because of the associated decrease in porosity. Keller and Frischknecht (1966) give a table of resistivity ranges for rocks of various ages and types that shows a typical change of 1.5 to 2 orders of magnitude increase from Quaternary to Precambrian for the same type of rock. These results are shown graphically in figure 2-4. The five orders of magnitude range shown here is more representative of in-situ values measured in the earth.

Table 2-1. Connate water average resistivities from various regions and lithologies (from Keller and Frischknecht, 1966).

Water Source	Average Resistivity (ohm-m)
European igneous rocks	7.6
South African igneous rocks	11.0
South African metamorphic rocks	7.6
Precambrian Australian metamorphic rocks	3.6
Pleistocene to recent European sedimentary rocks	3.9
Pleistocene to recent Australian sedimentary rocks	3.2
Tertiary European sedimentary rocks	1.4
Tertiary Australian sedimentary rocks	3.2
Mesozoic European sedimentary rocks	2.5
Paleozoic European sedimentary rocks	0.93
Oil field chloride waters	0.16
Oil field sulfate waters	1.2
Oil field bicarbonate waters	0.98
Jurassic Colorado-Utah USA waters	1.8
Cisco series Texas, USA. waters	0.061
Pennsylvanian, Oklahoma, USA waters	0.062

The presence of electronic conductors, such as graphite and the metallic luster sulfides, do not normally contribute to the lowering of host and cover rock resistivities. Their presence as ore or in association with ore often makes an ore body detectable by electrical methods. These situations are covered in the individual models under properties of the deposit itself. Occasionally, sulfides or graphite may be deposited as thin continuous films in a network along the fracture planes of rocks as may occur in stockwork deposits. When this happens, a few percent of these electronic conductors can cause a dramatic lowering of resistivity suggestive of much greater mineral content. Graphite is particularly notable for its ability to reduce rock resistivity when present in small quantities along fracture planes (Grant and West, 1965).

Although the above discussion identifies many problems that complicate the application of resistivity methods to minerals exploration, in practice there are many straightforward uses of this technique. Mafic rocks are found to weather to colluvial material with lower resistivity than felsic rocks. This permits mapping of such units by airborne electromagnetic methods as demonstrated by Palacky (1986) in Brazil, and to exploration for kimberlite pipes (Gerryts, 1967). Hydrothermal ore deposits often have large alteration haloes extending for some distance into various host rocks. Alteration processes often increase the porosity of the host rock during argillization and propylitization, whereas silicification can decrease porosity. Either of these processes can provide detectable resistivity contrasts. Deposits often are controlled by fracturing and faulting which causes increased host rock porosity that can be detected by the associated lower resistivity. However,

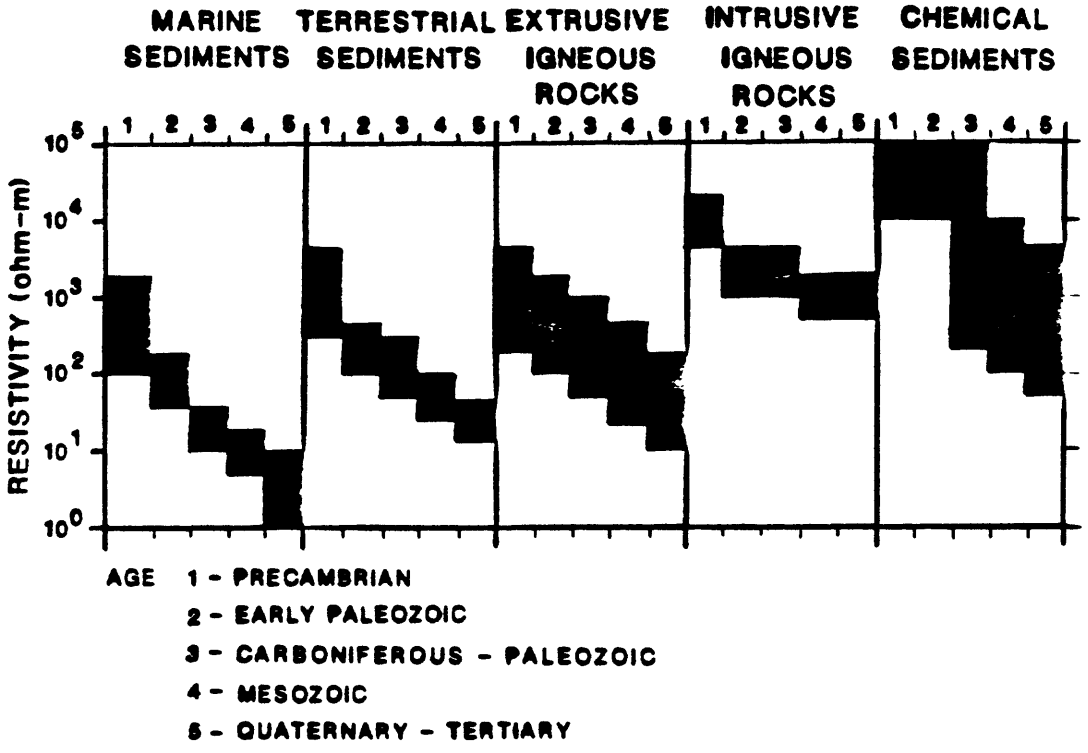

Figure 2-4. Diagram showing variation of resistivity as a function of age for marine and terrestrial sediments, extrusive and intrusive igneous rocks and for chemical sediments (from Keller and Frischknecht, 1966).

in practice, within given districts, lithologic units often will have uniform electrical properties that do permit them to be mapped.

Sedimentary and metasedimentary rocks, especially those that show a strong orientation of pore spaces, or that contain interbedded units, may exhibit significant resistivity anistropy. Keller and Frischknecht (1966) give values of coefficients of anisotropy for various rock types, some of which show resistivity differences exceeding a factor of 10. Crystalline rocks in which a preferred fracture orientation exists also may show significant anisotropy.

Figure 2-5 shows ranges of resistivities for nine types of sedimentary rocks given by Fedynskiy (1967) and Telford and others (1976). Figure 2-6 shows resistivity ranges for twelve types of igneous and metamorphic rocks also taken from Fedynskiy (1967) and Telford and others (1976). On average, these rock types show a wide range of overlap in values. Telford and others (1976) also give a listing of resistivities observed on a variety of metallic ores, to which the interested reader is referred.

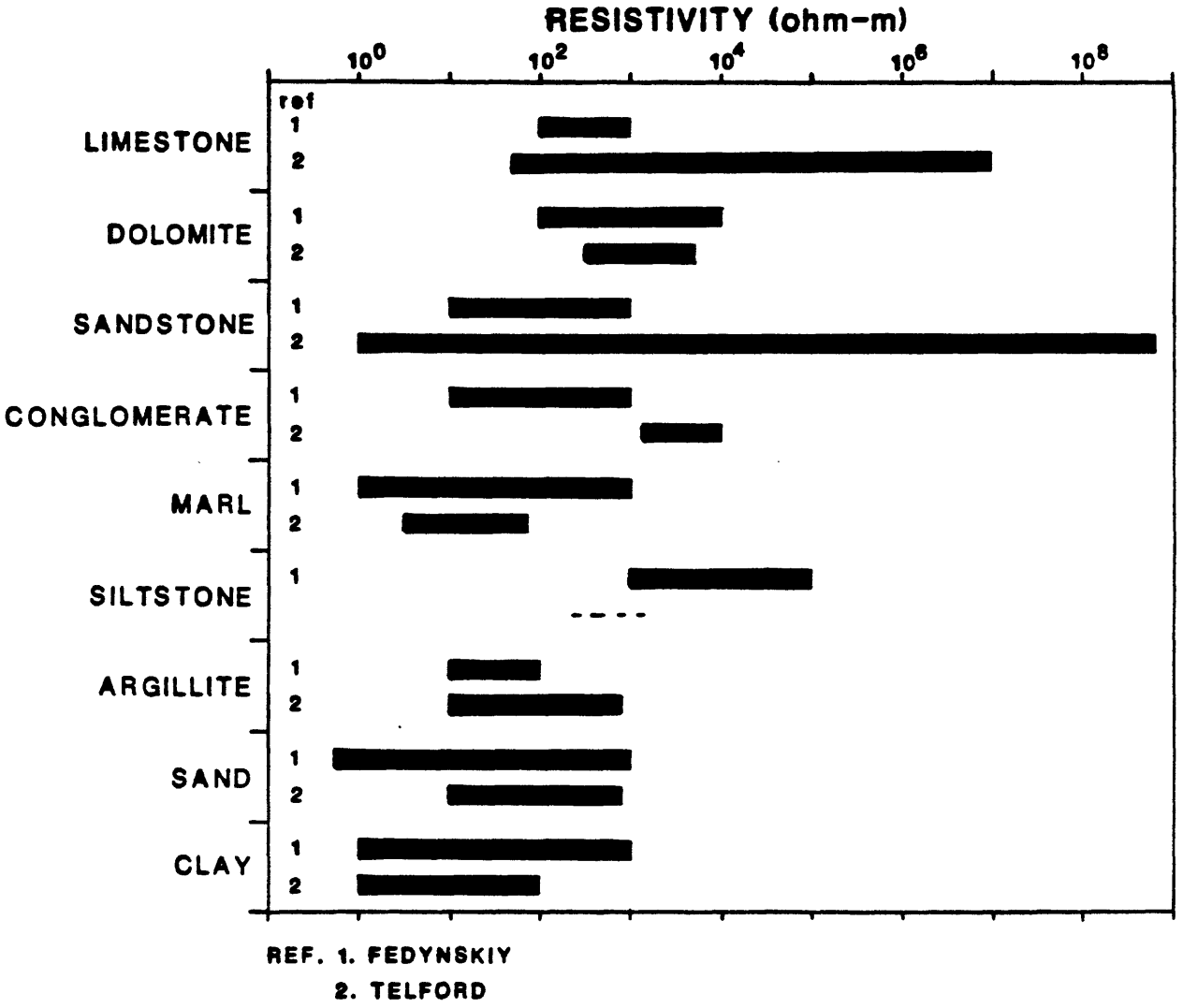

Figure 2-5. Ranges of resistivities for selected sedimentary rocks from Fedynskiy (1967) and Telford and others (1976).

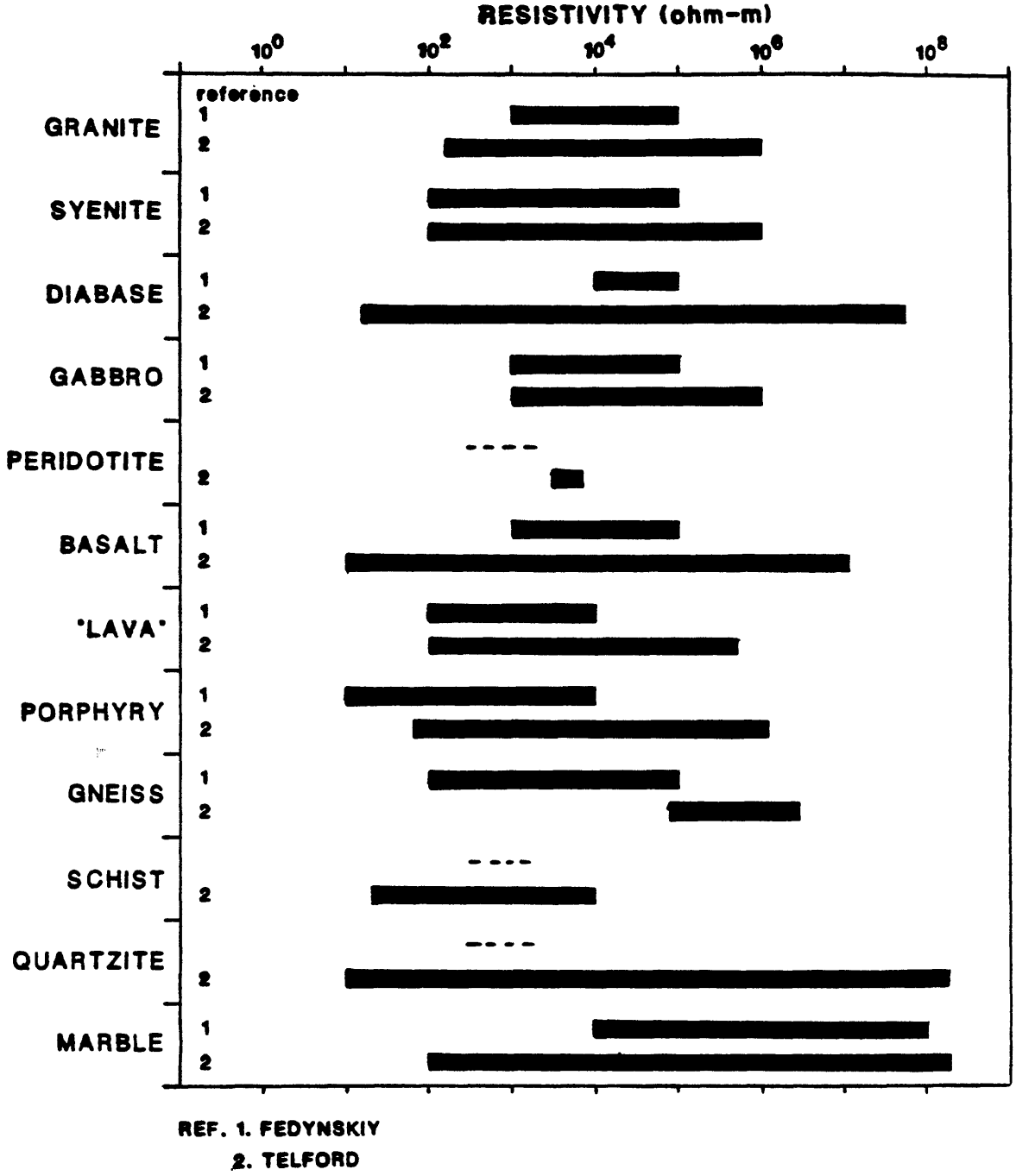

Figure 2-6. Ranges of resistivities for selected crystalline rocks from Fedynskiy (1967) and Telford and others (1976).

References

Fedynskiy, V.V., 1967, Razvedochnaya geofizika (reconnaissance geophysics): Nedra, Moscow, 672 p. (in Russian).

Gerryts, E., 1967, Diamond prospecting by geophysical methods - a review of current practice, in *Mining and Ground Water Geophysics 1967*: Canadian Geological Survey, p. 439-446.

Grant, F.S., and West, G.F., 1965, Interpretation theory in applied geophysics: McGraw-Hill, 584 p.

Hallof, P.G., 1980, Grounded electrical methods in geophysical exploration, in *Practical geophysics*, Blaricom, R.V., ed.: Northwest Mining Association, p. 39-151.

Hammond, W.R., and Sprenke, K.F., 1991, Radar detection of subglacial sulfides: Geophysics, v. 56, no. 6, p. 870-873.

Hohmann, G.W., and Ward, S.H., 1981, Electrical methods in mining geophysics: Economic Geology 75th Anniversary Volume, p. 806-828.

Hoover, D.B., Grauch, V.J.S., Pitkin, J.A., Krohn, D., and Pierce, H.A., 1991, Getchell trend airborne geophysics - an integrated airborne geophysical study along the Getchell trend of gold deposits, North-Central Nevada: in Geology and Ore Deposits of the Great Basin, G.L. Raines, R.E. Lisk, R.W. Schafer, and W.H. Wilkinson, eds.: Geological Society of Nevada, v. 2, p. 739-758.

Hoover, D.B., Heran, W.D., and Hill, P.L., 1992, The geophysical expression of selected mineral deposit models: U.S. Geological Survey Open-File Report 92-557, 129 p.

Keller, G.V., 1966, Electrical properties of rocks and minerals, in *Handbook of physical constants*, Clark, S.P., Jr., ed.: Geological Society America Memoir 97, p. 553-577.

Keller, G.V., 1982, Electrical properties of rocks and minerals, in *Handbook of physical properties of rocks*, V.I., Carmichael, R.S., ed.: CRC Press, p. 217-294.

Keller, G.V., and Frischknecht, F.C., 1966, Electrical methods in geophysical prospecting: Pergamon Press, 523 p.

Mansinha, L., and Mwenifumbo, C.J., 1983, A mise-a-la-masse study of the Cavendish geophysical test site: Geophysics v. 48, no. 9, p. 1252-1257.

Olhoeft, G.R., 1981, Electrical properties of rocks, in *Physical properties of rocks and minerals*, Touloukian, Y.S., Judd, W.R., and Roy, R.F., eds.: McGraw Hill, p. 257-330.

Palacky, G.J., 1986, Airborne resistivity mapping: Geological Survey of Canada, paper 86-22, G.J. Palacky ed., 195 p.

Sato, M., and Mooney, H.M., 1960, The electrochemical mechanism of sulfide self-potentials: Geophysics v. 25, no. 1, p. 226-249.

Sumner, J.S., 1976, Principles of induced polarization for geophysical exploration: Elsevier, 277 p.

Telford, W.M., Geldart, L.P., Sheriff, R.E., and Keys, D.A., 1976, Applied geophysics: Cambridge, 860 p.

Chapter 3. Principles Of Airborne Radioactivity Measurements

The following text is a brief review of the basic parameters of aerial gamma-ray surveying. The selected references which follow are a source of further information.

Airborne radioactivity surveys map the surface distribution of the natural radioelements potassium (K), uranium (U), and thorium (Th) by measuring gamma-rays emitted during radioelement decay. Gamma-rays are electromagnetic radiation which can penetrate a few hundred meters of air, thereby enabling their measurement by instruments operated in low-flying aircraft. Those detected originate in the uppermost 50 cm of rock and soil.

K, U, and Th concentration and distribution are controlled by petrologic conditions during rock- and mineral-forming processes. Geology and soil chemistry are prime factors in controlling the surface distribution of the radioelements. Consequently, measurements of radioelement distribution are useful in geologic mapping, mineral exploration, and in understanding the geologic processes that controlled the distribution.

Gamma-rays are detected with scintillation crystals (normally thallium-activated sodium iodide), which emit a flash of light (scintillation) when impacted by gamma-rays. The intensity of the flash of light is proportional to the energy of the incident gamma-ray. A photomultiplier (PM) tube, optically coupled with a scintillation crystal in a light-tight container, produces a voltage proportional to the energy of the gamma ray. PM output pulses are fed to pulse-height sorting and counting (multi-channel analyzer) systems in order to produce a "spectrum" of natural gamma-rays. This is the geophysical method "gamma-ray spectrometry."

Aerial gamma-ray spectrometers are calibrated to monitor the 1.46 MeV (million electron volts) photopeak of the isotope K-40 for K distribution, the 1.76 MeV photopeak of the isotope Bi-214 in the U-238 decay series for U distribution, and the 2.62 MeV photopeak of the isotope Tl-208 in the Th-232 decay series for Th distribution. Regions or windows monitored per photopeak are 0.2 MeV wide for K-40 and Bi-214 and 0.4 MeV wide for Tl-208. K-40 produces one photopeak at 1.46 MeV and is 0.0119 percent of total K. U-238 has a complex decay series which includes the isotopes Th-230, Ra-226, and Rn-222; all occur prior to the 1.76 MeV Bi-214 photopeak in the decay series, and all can behave differently geochemically. Consequently, disequilibrium - all members of a decay series not present in their proper proportions - is a problem with Bi-214 based determinations of U, and must be considered during interpretation. The Th-232 decay series is not as complex as U-238, and disequilibrium is normally not a problem. Spectrometer systems also monitor a total count or total gamma-ray activity window, most commonly from 0.4 to 3.0 MeV. Spectrometers should be operated in a gain and/or high voltage stabilization mode, to assure that the photopeaks of interest are located in the proper channels of the multi-channel analyzer.

Gamma-rays that originate at ground surface are absorbed in air at an exponential rate; the half-thicknesses in air (distance at which half the ground level intensity occurs) are 102 m for 1.46 MeV, 112 m for 1.76 MeV, and 137 m for 2.62 MeV. These parameters plus safety and economic considerations have resulted in most geologic-based aerial gamma-ray spectrometry surveys being flown at a nominal 122 m above ground level. A rule of thumb is that flight line spacing should be no greater than twice the survey altitude to obtain complete ground coverage for an aerial gamma-ray survey (Pitkin and Duval, 1980). All aerial gamma-ray data must be normalized to the survey altitude using coefficients derived during test flying of the specific spectrometer system.

In addition to the terrestrial contribution, aerial gamma-ray measurements detect radioactivity from at least three other sources. These include Rn-222, which occurs in the atmosphere as part of the U-238 decay series, cosmic (or extraterrestrial) sources, and material of and within the aircraft. The contribution of Rn-222 in air, together with the cosmic contribution, is monitored while surveying, and the aircraft contribution is determined by test flights prior to surveying. All quantities are removed from the aerial measurements prior to data processing and reduction so that the terrestrial contribution remains as an enhanced data product. Quantitative calibration of spectrometer systems at sites of known radioelement concentrations (Geodata International Inc., 1977; Ward, 1978) permits conversion of fully corrected counts per unit time for the K, U, and Th windows to percent K and parts per million U and Th. The correction coefficients for the Compton backscatter effect, the phenomenon that results from incompletely absorbed gamma-rays in scintillation crystals, are most accurately determined at sites of known concentrations.

Spectrometric surveys use sodium iodide crystals packaged in multi-crystal arrays to detect gamma-rays. While right cylinder crystals are available in varied dimensions, the common detector is a 10.16 cm X 10.16 cm X 40.64 cm "log" (volume 4.2 liters) mounted with a 10.16 cm PM at one end. Logs are packaged in fours for a total volume of 16.8 liters. Helicopter surveys can utilize two packages of logs, one package per skid, for a total volume of 33.6 liters. Fixed-wing surveys can utilize three packages for a total of 50.4 liters. The advisability of the larger volume for geologic-based spectrometer surveys is demonstrated by these numbers for several 50.4 liter aerial systems: 75 to 85 counts per second per percent K, 12 to 13 counts per second per part per million U, 5 to 6 counts per second per part per million Th. Proportionate numbers for smaller volumes are obtained by simple arithmetic.

Separate sodium iodide detectors are used for Rn-222 in air monitoring systems. These detectors consist of one or two logs mounted on a 1.25 cm Pb sheet placed on top of one of the 16.8 liter packages discussed in the previous paragraph. The Rn-222 in air detector commonly is referred as the 2-pi detector because it detects gamma-rays originating from the solid angle above the horizontal plane of the aircraft. The 16.8 liter detectors are referred to as 4-pi detectors because they detect gamma-rays from all

sources. The 2-pi detector has its own sorting and counting electronics and the data from this system is used to calculate the Rn-222 in air correction for the 4-pi spectrometer.

Modern digital spectrometer systems record all data on magnetic tape, commonly at 1-second intervals, which translates to 30 to 60 m of ground coverage per sample interval at the speeds normally used for aerial gamma-ray surveys. A convenient concept to use when planning an aerial survey uses the ratio of the (primary) detector volume (V) to the ground velocity (v) of the aircraft. The minimum acceptable value for V/v has been determined empirically at 0.2. For example, V= 16.8 liters and v = 120 km/hr gives 0.14 and V = 33.6 liters and v= 120 km/hr results in 0.28. For the latter example, the larger detector volume permits increasing the ground velocity to 160 km/hr (V/v = 0.21) and still acquiring acceptable data.

Flight parameters for the Getchell helicopter aerial gamma-ray survey (TerraSense Inc., 1989):

- flight lines oriented N58 W and 400 m apart;
- flight altitude 122 m above ground level;
- survey area totaled 466 km^2, included two tie lines flown normal to survey lines;
- minimum detector volume 24.6 liters;
- minimum V/v = 0.2;
- contractor used detector of 33.6 liters with separate Rn-222 monitor of 8.4 liters;
- spectrometer data corrected for background radioactivity, spectral backscatter, Rn-222 in air, and were altitude normalized;
- spectrometer system quantitatively calibrated at ground and aerial sites, and an altitude curve was flown over Utah Lake near Provo, Utah;
- fully corrected K, U, Th data converted to quantitative units of semi-quantitative ground concentrations of percent and parts per million (assuming equilibrium for U and Th);
- contractor computed 0.2 km grids and prepared K, U, and Th contour maps (black-&-white) at 1:24,000-scale.

USGS open-file report (TerraSense, 1989) included the contour maps and a brief text. The 0.2 km digital grid files supplied by the contractor to the USGS are available for purchase from:

Ron Buhmann, Tape Librarian, MCG
National Oceanic and Atmospheric Administration U.S. Department of Commerce
Mountain Administrative Support Center
325 Broadway
Boulder, CO 80303-3328
telephone 303/497-6128

(the 0.2-km grids on Open-File 93-XXD are those supplied by the contractor).

PRIMARY TOPICS OF THE SELECTED REFERENCES

Calibration procedures: Grasty (1976), Grasty and Darnley (1971);

Color compositing: Duval (1983);

Gamma-rays and gold, includes Russian citations: Hoover and Pierce (1990);

Geophysical attributes, mineral deposit models: Hoover, Heran, and Hill (1992);

Getchell gold trend: Pitkin (1991) and TerraSense (1989);

Handbook on gamma-ray surveying: International Atomic Energy Agency (1979);

How to plan an aerial survey: Pitkin and Duval (1980).

Quantitative calibration: Geodata (1978), Ward (1977);

Review of gamma-ray methods: Darnley (1972), Duval (1990), and Killeen (1979).

SELECTED REFERENCES

Darnley, A.G., 1972, Airborne gamma-ray survey techniques, *in* Bowie, S.H.U., and others, (eds), Uranium prospecting handbook: The Institution of Mining and Metallurgy, p. 174-211.

Duval, J.S., 1983, Composite color images of aerial gamma-ray spectrometric data: Geophysics, v. 48, no. 6, p. 722-735.

Duval, J.S., 1990, Radioactivity and some of its applications in geology, *in* Symposium on the application of geophysics to engineering and environmental problems: Society of Engineering and Mineral Exploration Geophysics, p. 1-61.

Geodata International Inc, 1977, Lake Mead dynamic test range for calibration of airborne gamma radiation measuring systems: U.S. Department of Energy Open-File Report GJBX-46(77), 83 p.

Grasty, R.L., 1976, A calibration procedure for an airborne gamma-ray spectrometer: Geological Survey of Canada Paper 76-16, 9 p.

Grasty, R.L., and Darnley, A.G., 1971, The calibration of gamma-ray spectrometers for ground and airborne use: Geological Survey of Canada Paper 71-17, 27p.

Hoover, D.B., and Pierce, H.A., 1990, Annotated bibliography of gamma-ray methods applied to gold exploration: U.S. Geological Survey Open-File Report 90-203, 23 p.

Hoover, D.B., Heran, W.D., and Hill, P.L., eds, 1992, The geophysical expression of selected mineral deposit models: U.S. Geological Survey Open-File Report 92-557, 129 p.

International Atomic Energy Agency, 1979, Gamma-ray surveys in uranium exploration: International Atomic Energy Agency Technical Report Series no. 186, 90 p.

Killeen, P.G., 1979, Gamma ray spectrometric methods in uranium exploration - application and interpretation, *in* Hood, P.J., ed., Geophysics and geochemistry in the search for metallic ores: Geological Survey of Canada, Economic Geology Report 31, p. 163-229.

Pitkin, J.A., 1991, Preliminary results of geochemical analyses of selected aerial gamma-ray anomalies, Getchell trend of gold deposits, Humboldt County, Nevada, in Good, E.E., and others, eds., USGS research on mineral resources-1991 program and abstracts: U.S. Geological Survey Circular 1062, p. 60-61.

Pitkin, J.A., 1991, Radioelement data for the Getchell trend, Humboldt County, Nevada: geologic discussion and possible significance for gold mineralization, in Raines, G.L., and others, eds., Geology and ore deposits of the Great Basin, symposium proceedings: Geological Society of Nevada, v. II, p. 759-770.

Pitkin, J.A., and Duval, J.S., 1980, Design parameters for aerial gamma-ray surveys: Geophysics, v. 45, no. 9, p. 1427-1439.

TerraSense Inc., with an introduction by J.A. Pitkin and P.L. Hill, 1989, Uranium, potassium, and thorium contour maps derived from a helicopter gamma-ray spectrometer survey of the Getchell Trend, Humboldt County, Nevada: U.S. Geological Survey Open-File Report 89-287, 9 p., 12 sheets, scale 1:24,000.

Ward, D.L., 1978, Construction of calibration pads facility, Walker Field, Grand Junction, Colorado: U.S. Department of Energy Open-File Report GJBX-37(78), 57 p.

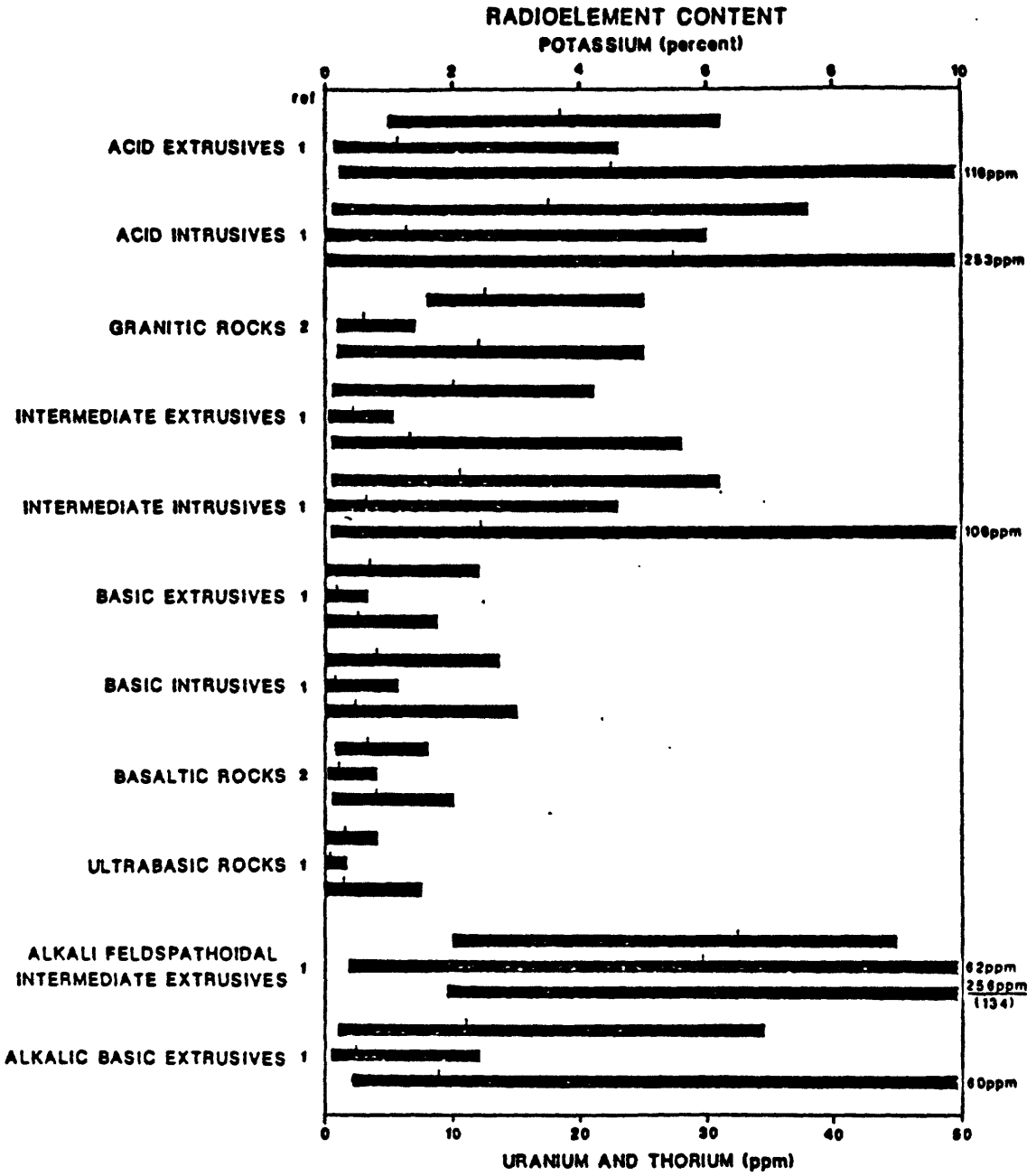

Figure 3-1.
Radioelement contents reported for a variety of lithologies from 1. Wollenberg and Smith (1982) and 2. Hansen (1980). For each type of lithology the elements are in the order top to bottom, K, U, Th. The small vertical bar indicates the mean value. Modified from Hoover, Heran, and Smith (1992).

Hansen, D.A., 1980, Radiometrics, in Van Blaricom, Richard, ed.: Practical geophysics for the exploration geologist, p. 1-38.

Hoover, D.B., Heran, W.D., and Hill, P.L., eds, 1992, The geophysical expression of selected mineral deposit models: U.S. Geological Survey Open-File Report 92-557, 129 p.

Wollenberg, H.A., and Smith, A.R., 1982, Radiogenic heat production of crustal rocks - an assessment based on geochemical data: Geophysical Research Letters, v. 14, no. 3, p. 295-298.

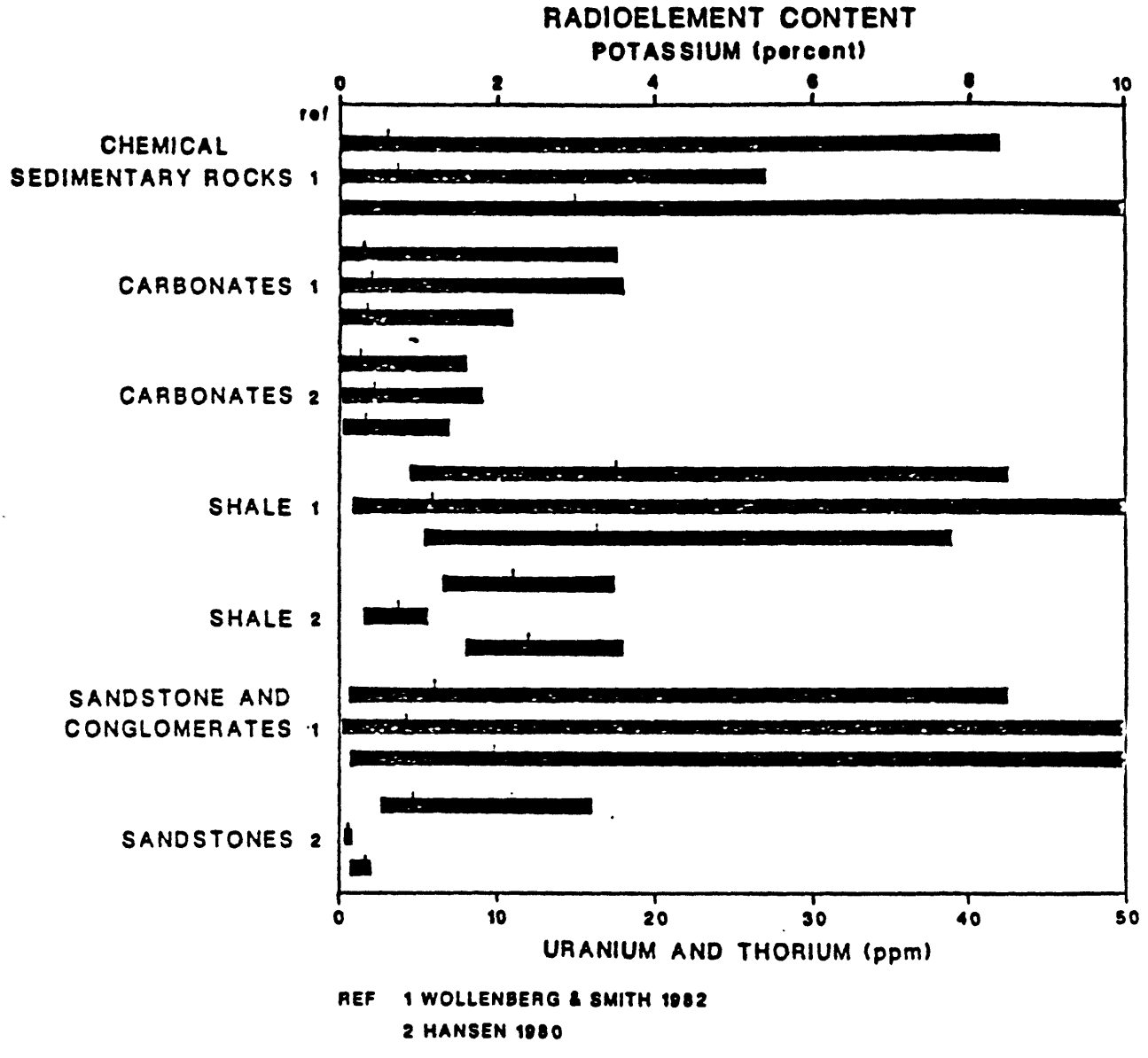

Figure 3-1 continued

Chapter 4

GEOPHYSICAL DEPOSIT MODELS

The final product of an interpretation of a geophysical map is a derivative map that translates the geophysical data to interpreted structures, lithologies, alteration haloes, etc. The interpretive geophysical maps and other geological information can then be used to further understand earth processes, and often directly aid assessment and exploration for mineral resources. But, exploration requires knowledge about the geophysical signatures of typical deposit types. Unfortunately, there are too few summary reports giving average characteristics and ranges of responses for most types of mineral deposits.

The USGS has recently compiled geophysical characteristics of several important types of deposits. The work is presented by Hoover and others (1992) in a report entitled *The Geophysical Expression of Selected Mineral Deposit Models*. Three individual deposit models from this compilation are shown here: 1. Diamond Pipes, 2. Carbonate-hosted Au-Ag (Carlin type), and 3. Homestake Au (Greenstone belt Au). These three models indicate the types of geophysical data typically acquired in exploration for each type of deposit, and the kinds of geophysical responses observed. This will give the student an idea of what to look for in interpreting geophysical maps in the search for mineral deposits.

The airborne data sets provided in the course are of the Getchell area, north-central Nevada. At present gold is the principal commodity mined there, and all deposits are of the sediment-hosted or Carlin type. The student can compare the summary results given in the geophysical model with the images he/she creates and his/her interpretation.

Hoover, D.B., Heran, W.D., and Hill, P.L., 1992, The geophysical expression of selected mineral deposit models: U.S. Geological Survey Open-File Report 92-557.

GEOPHYSICAL MODEL OF DIAMOND PIPES

COX AND SINGER Model No. 12 — Compilers - D.B. Hoover, D.L. Campbell

Geophysically similar models-No. 10 Carbonatites; No. 29b, Olympic Dam

A. Geologic Setting

- Kimberlite or lamproite diatremes emplaced along zones of basement weakness within or on the margins of stable cratons; (Dawson, 1971) often in groups of three or more.
- Often spatially related to carbonatites, but not normally occurring along same zones of crustal weakness (Dawson, 1967; Garson, 1984). A genetic relationship is open to question.

B. Geologic Environment Definition

Regional magnetic, gravity, and remote sensing surveys may identify deep-seated fracture systems and related anteclises or syneclises that define zones of weak crust favorable for emplacement (de Boarder, 1982; Tsyganov, and others, 1988).

C. Deposit Definition

Individual diatremes generally appear as circular to elliptical bodies in remote sensing images, and on magnetic, gravity, or resistivity maps. The diatremes may show as distinct magnetic highs (Yakutia, West Africa) of hundreds to a few thousand nT, but high remanence or magnetic host rocks can result in negative or no anomalies. Gravity (order of 1 mgal), resistivity, and seismic velocity anomalies generally show as lows over the diatremes related to serpentization and weathering of the mafic rocks. Radioelement surveys have generally not been effective, although in Yakutia Fedynsky and others (1967) report that they have been used to differentiate between diamond-bearing basaltic kimberlite from barren micaceous kimberlite and carbonatites (da Costa, 1989; Kamara, 1981; Gerryts, 1970; Macnae, 1979; Guptasarma and others, 1989).

D. Size and Shape of

	Shape	Average Size/Range
Deposit	Vertical cone, carrot-like	0.1 to 5 km diameter; generally 0.4 to 1 km depth to about 2 km
Alteration haloe	Irregular about pipe	thin, not geophy. significant
Cap	Elliptical cylinder	0.1 to 5 km, 0-10's m thick

E. Physical Properties (units)	Deposit	Alteration	Cap	Host
	kimberlite or lamproite pipe	Si, CO_2, K metasomatism	clay-rich weathering zone-blue and yellow ground	any cratonic unit
1. Density (gm/cm^3)	2.75[5] 2.64-3.12[2,5,11] 2.35-2.55[8]	?	2.35?[13] 2.5-2.62[2]	*
2. Porosity	low-moderate	low?	high[2]	*
3. Susceptibility (cgs)	$1x10^{-4}$-$1x10^{-2}$[8] to $2.3x10^{-3}$[6]	?	$1x10^{-5}$-$1x10^{-3}$[8] to $2x10^{-5}$[6]	*
4. Remanence	variable 0-0.8-2.0[13]	?	variable	*
5. Resistivity (ohm-m)	100-2000[2,8,11,13]	medium-high	2-100[2,8,11,13]	*
6. IP Effect (msec.)	low	low?	low, 0-4[10]	*
7. Seismic Velocity (km/sec)	2.6-3.3[2]	high?	1.5[2]	*
8. Radioelements				
K (%)	2.6 average 0.07-6.7[1]	medium	medium?	*
U (ppm)	0.26, average 0.07-0.8[1]	low	very low	*
Th (ppm)	0.44, average 0.17-0.9[1]	low	low	*

F. Remote Sensing Characteristics

Visible and near IR-lineaments may reflect zones of crustal weakness along which pipes were emplaced. Lineament intersections may be favored locations (Tsyganov and others, 1988). Vegetation anomalies related to drainage and lithologies can be used for location. Alteration products of kimberlite, such as serpentine, chlorite, and vermiculite show distinct spectral absorption features that can be detected (Kingston, 1989).

G. Comments

The relatively small size, 0.4-1.km, of most pipes requires detailed coverage for identification. Signature differs from carbonatites in reduced amplitude of magnetic anomaly, and by a small negative gravity anomaly in contrast to the large positive anomaly of carbonatites. A combination of magnetic, gravity, and resistivity methods is most used in exploration. No single method is universally applicable. Radioelement methods have had relatively little use, although they should have some application in differentiating varieties of kimberlites and lamproite. Some Russian literature (Ratnikov, 1970) gives very low values of density for kimberlites. These probably refer to serpentinized or weathered samples and are not representative of unaltered rock. Gerryts (1967) gives a rule-of-thumb of 1 mgal/183 meters (200 yards) of pipe diameter for the gravity low. A broad

gravity high ring about the central low, and due to dense, deeper, kimberlite has not been observed. Guptasarma and others (1989) report both positive and negative gravity and magnetic responses over kimberlites in India.

H. References

1. Clark, S.P., Jr., Peterman, Z.E., and Keier, K.S., 1966, Abundances of uranium, thorium, and potassium, in Clark, S.P., Jr., ed., Handbook of Physical Constants: G.S.A. Memoir 97, p. 521-542.
2. da Costa, Alberto, J.M., 1989, Paimietfontein kimberlite pipe, South Africa--A case history: Geophysics, v. 54, no. 6, p. 689-700.
3. de Boarder, H., 1982, Deep-reaching fracture zones in the crystalline basement surrounding the West Congo System and their control of mineralization in Angola and Gabon: Geoexploration, v. 20, p. 259-273.
4. Fedynsky, V.V., Brodovoi, V.V., and Gelamkov, V.A., 1967, Geophysics in prospecting and exploration for mineral deposits in the USSR, in Morley, L.W., ed., Mining and Ground Water Geophysics: Geological Survey of Canada, p. 667-687.
5. Gerryts, E., 1967, Diamond prospecting by geophysical methods--A review of current practice, in Morley, L.W., ed., Mining and Ground Water Geophysics: Geological Survey of Canada, p. 439-446.
6. Guptasarma, D., Chetty, T.R.K., Murthy, D.S.N., Ramana Rao, A.V., Venkatanarayana, B., Babu Roo, V., Shanker Reddy B., and Singh, B., 1989, Case history of a kimberlite discovery, Wajrakarur area, A.P., South India, in G.P. Garland, ed., Proceedings of Exploration 87, Ontario Geological Survey Special Volume 3, p. 888-897.
7. Kailasam, L.N., 1967, Mining geophysics in India and the role of government in this field, in Morley, L.W., ed., Mining and Ground Water Geophysics: Geological Survey of Canada, p. 439-446.
8. Kamara, A.Y.S., 1981, Review-geophysical methods for kimberlite prospecting: Australian Bulletin of Society of Exploration Geophysics, v. 12, p. 43-51. [Best overview in english]
9. Kingston, M., 1989, Spectral reflectance features of kimberlites and carbonatites: GSA Special Pub. No. 14 Kimberlites and Related Rocks.
10. Litinskii, V.A., 1963, Measurement of magnetic susceptibility in prospecting for kimberlite pipes: The Mining Magazine, v. 109, p. 137-146.
11. Macnae, J.C., 1979, Kimberlites and exploration geophysics: Geophysics, v. 44, p. 1395-1416.
12. Norman, J.W., Price, N.J., and Peters, E.R., 1977, Photogeological fracture trace study of controls of kimberlite intrusion in Lesotho basalts: Trans. Institute Mining and Metall., v. 868, p. 78-90.
13. Ratnikov, V.N., 1970, Diamond deposits of Yakutla, in Klichnikov, V.A., Brodovoy, V.V., Morozov, M.D., and Solovov, A.P., eds., Geophysical Exploration of Ore Deposits, Kazakstan Branch All Union Science Research Institute for Reconnaissance Geophysics, p. 566-575.
14. Romanov, N.N., and Manakov, A.V., 1987, Possibilities of magnetic surveying in prospecting for kimberlite pipes: Geologiya i Geofizika, v. 28, no. 12, p. 73-78.
15. Tsyganov, V.A., Mikoyev, I.I., and Chernyy, S.D., 1988, Local criteria for the structural control of kimberlite magmatism in Western Yakutla: International Geol. Review, v. 30, p. 657-667.

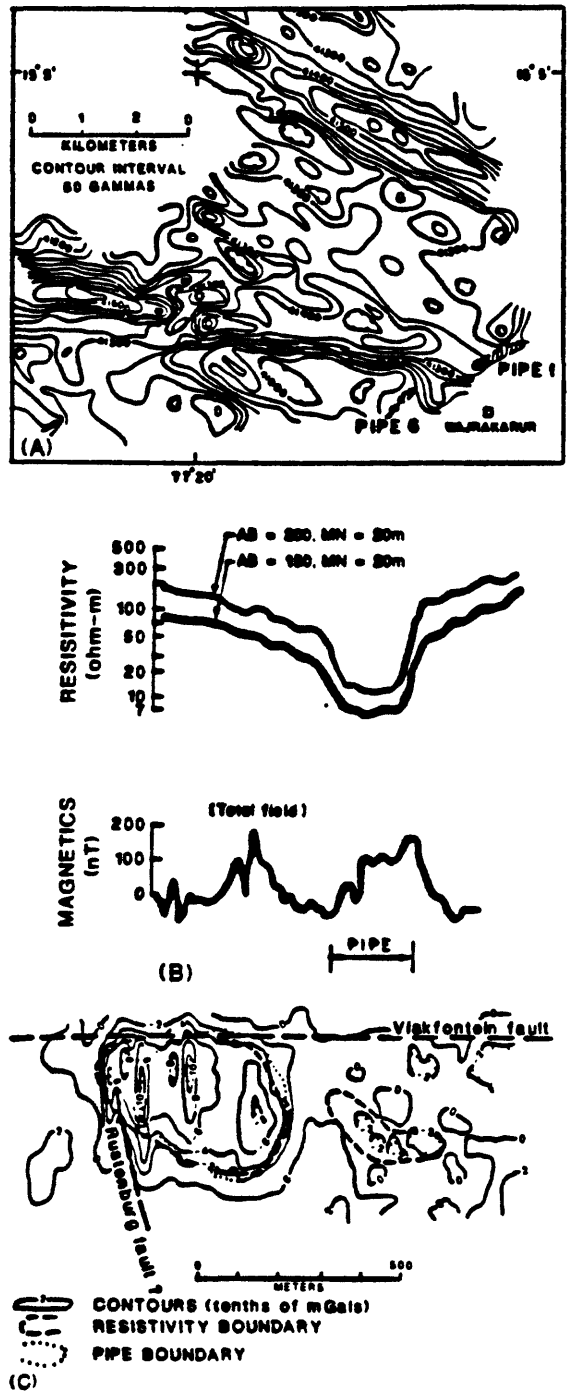

Figures A. Strong regional magnetic linear adjacent to two kimberlite pipes in the Wajrakarur area, Andhra Pradesh, India adapted from Guptasarma and others (1989). Contour interval is 50 gamma. B. Resistivity and ground magnetic traverse across the Palmietfontein pipe South Africa adapted from da Costa (1989). C. A residual gravity map of the Palmietfontein pipe also showing its emplacement at the junction of the Vlakfontein and Rustenburg faults, after da Costa (1989).

COX AND SINGER MODEL No. 26a

Compilers - W.D. Heran
D.B. Hoover

A. Geologic Setting

- Regionally adjacent to or along high-angle normal fault zones related to continental margin rifting, or regional thrust faults or bedding.
- Selective hydrothermal replacement of carbonaceous limestones or dolomite where these are intruded by igneous rocks.
- Very fine grain native gold and/or silver, pyrite and arsenic sulfide disseminated in host rocks and associated silica replacement.

B. Geologic Environment Definition

Remote sensing data can define major lineaments and tectonic structural zones and their intersection with major fault systems (Rowan and Wetlaufer, 1981). Remotely sensed data can define major lithologic boundaries and areas of alteration (Kruse and others, 1988). Aeromagnetic and gravity methods have been used to delineate the margins of intrusions in the near subsurface and determine major faults beneath sedimentary cover (Grauch, 1988, Grauch and Bankey, 1991). Radioelement data have possibilities for defining zones of hydrothermal alteration associated with faulting (Pitkin, 1991). Airborne electromagnetic resistivity data have been used to map lithology and detect alteration in addition to delineating structure at the surface and under shallow cover (Taylor, 1990; Pierce and Hoover, 1991; Hoover and others, 1991; and Wojniak and Hoover, 1991).

C. Deposit Definition

High angle fault zones and shear zones can be mapped by a variety of electromagnetic methods as conductive anomalies within sediments or crystalline rocks (Hoekstra and others, 1989; Hoover and others, 1984; Heran and Smith, 1984; Heran and McCafferty, 1986). Detailed magnetic and gravity surveys can be employed to delineate pluton margins, map major fault zones, lithologic boundaries and determine depth of alluvial cover (Grauch, 1988). Electrical resistivity methods are able to map hydrothermal alteration and faulting as a resistivity low and silicification caps as a high (Hallof, 1989; Corbett, 1990; and Hoekstra and others, 1989). Seismic methods have been used to delineate high angle faults, lithologic contacts and hydrothermal alteration (Cooksley and Kendrick, 1990). Gold bearing structures containing clay or carbonaceous (graphite) material can be mapped using the induced polarization method. Radiometric surveys have possibilities for mapping alteration along faults (Porter, 1984).

D. Size and Shape of	Shape	Average Size/Range
Deposit	Tabular to highly irregular	3.9,0.4-20x10^6 m^3
Alteration Haloe/s	Variable, irregular	?
Cap	Irregular blanket	?

E. Physical Properties	Deposit	Alteration	Cap	Host
Description	Hydrothermal replacement of calcareous rock	-	Siliceous replacement	calcareous rocks
1. density (gm/cc)	2.6	-	?	2.65-1.9-2.9[1]
2. porosity	?	?	?	
3. susceptibility (10^{-6}cgs)	0.0-?	-	low	20-0-280[1]
4. remanence	low	-	low	?
5. resistivity (ohm-m)	20,10-50	-	variable	1500-350-6000[1]
6. chargeability (mv-sec/v)	30,20-40[1]	-	?	5.2-20[1]
7. seismic vel. (km/sec)	2.5[2]	-	?	4.3-6[2]
8. radioelements				
K%	variable up to 4.5	-	?	0.27
U-ppm	variable up to 10	-	?	2.2,0.1-9.0
Th-ppm	variable up to 16	-	?	1.7,0.1-7
9. Other (specific)				

F. Remote Sensing Characteristics

Visible and Near IR - Regionally, landsat images have been used to delineate lineaments and major structural zones in Nevada (Rowan and Wetlaufer, 1981). Distinctive signitures can be detected from hydrothermal alteration products exposed at the surface (ie., illite, kaolinite, montmorillonite, jarosite and alunite).

Thermal IR - Emissivity-ratio images prepared from data acquired by the Thermal Infrared Mapping System (TIMS) have been used to detect and map previously unrecognized silicified carbonate host rocks at the Carlin deposit, Nevada (Watson and others, 1990).

G. Comments

Intense exploration for this deposit type in the 80's has generated a variety of geophysical applications many of which are helpful in areas of cover. Regional exploration can be greatly aided by remote sensing and airborne EM. Ground EM profiling is the best bet for locating faults. Electrical or EM techniques can define areas of alteration.

H. References

1. Ballantyne, E., 1989, Advisory systems for selecting the proper geophysical techniques for mining exploration: Univ. of Missouri, Rolla, unpublished PhD. thesis, 121 p.
2. Cooksley, J.W., and Kendrick, P.H., 1990, Use of seismic geophysics in the detection of epithermal precious metal deposits in the western U.S.: Explore - The Association of Exploration Geochemists Newsletter, no. 67, p. 1-4.
3. Corbett, J.D., 1990, Overview of geophysical methods applied to precious metal exploration in Nevada, in Seminar: Geophysics in Gold Exploration, sponsored by Geological Society of Nevada and SEG mining committee, p. 1-21.
4. Grauch, V.J.S., 1988, Geophysical tools for defining covered features: significance for disseminated gold deposits in Nevada, USA [ext. abs.]: Geological Society of Australia, Bicentennial Gold 88.
5. Grauch, V.J.S., and Bankey, Viki, 1991, Preliminary results of aeromagnetic studies of the Getchell Disseminated Gold Deposit Trend, Osgood Mountains, north-central Nevada, in Raines, G.L., Lisk, R.E., Schafer, R.W., and Wilkinson, W.H., eds., Geology and Ore Deposits of the Great Basin, Volume 2: Geological Society of Nevada, p. 781-791.
6. Hallof, P.G., 1989, The use of the CSAMT method to map subsurface resistivity structures in gold exploration in Nevada [abs.]: Abstract to poster at SEG Annual Meeting, Dallas.
7. Heran, W.D., and McCafferty, A.M., 1986, Geophysical surveys in the vicinity of Pinson and Getchell mines, Humboldt Cuonty, Nevada: U.S. Geological Survey Open-File Report 86-432.
8. Heran, W.D., and Smith, B.D., 1984, Geophysical surveys at the Getchell and Preble disseminated gold deposits, Humboldt County, Nevada: U.S. Geological Survey Open-File Report 84-795.
9. Hoekstra, P., Hild, J., and Blohm, M., 1989, Geophysical surveys for precious metal exploration in the basin and range, Nevada, in Bhappo, R.B., and Harden, R.J., eds., Gold Forum on Technology and Practices -- World Gold '89: Society of Mining Engineering, Proceedings, p. 69-75.

10. Hoover, D.B., Grauch, V.J.S., Pitkin, J.A., Krohn, M.D., and Pierce, H.A., 1991, Getchell trend airborne geophysics--An integrated airborne geophysical study along the Getchell Trend of Gold Deposits, north-central Nevada, in Raines, G.L., Lisk, R.E., Schafer, R.W., and Wilkinson, W.H., eds., Geology and Ore Deposits of the Great Basin, Volume 2: Geological Society of Nevada, p. 739-758.
11. Hoover, D.B., Pierce, H.A., and Merkel, D.C., 1986, Telluric traverse and self potential data release in the vicinity of the Pinson Mine, Humbolt County, Nevada: U.S. Geological Survey Open File Report 86-341.
12. Kruse, F.A., Hummer-Miller, Susanne, and Watson, Ken, 1988, Thermal infrared remote sensing of the Carlin disseminated gold deposit, Eureka County, Nevada, in Bulk Mineable Precious Metal Deposits of the Western United States: Symposium Proceedings of the Geological Society of Nevada, p. 734.
13. Pierce, H.A., and Hoover, D.B., 1991, Airborne electromagnetic applications--Mapping structure and electrical boundaries beneath cover along the Getchell Trend, Nevada, in Raines, G.L., Lisk, R.E., Schaefer, R.W., and Wilkinson, W.H., eds., Geology and Ore Deposits of the Great Basin, Volume 2: Geological Society of Nevada, p. 771-780.
14. Pitkin, J.A., 1991, Radioelement data of the Getchell Trend, Humboldt County, Nevada--Geologic discussion and possible significance for gold exploration, in Raines, G.L., Lisk, R.E., Schafer, R.W., and Wilkinson, W.H., eds., Geology and Ore Deposits of the Great Basin, Volume 2: Geological Society of Nevada, p. 759-770.
15. Porter, E.W., 1984, Radioactivity as a tool for gold exploration [abs.]: Geological Society of America, v. 16, no. 6, p. 625.
16. Rowan, L.C., and Wetlaufer, P.H., 1981, Relation between regional lineament systems and structural zones in Nevada: AAPG Bulletin, v. 65, no. 8, p. 1414-1432.
17. Taylor, R.S., 1990, Airborne EM resistivity applied to exploration for disseminated precious metal deposits: Geophysics--The Leading Edge of Exploration, February 1990, p. 34-41.
18. Watson, Ken, Kruse, F.A., and Hummer-Miller, Susanne, 1990, Thermal infrared exploration in the Carlin trend, northern Nevada: Geophysics. v. 55, no. 1, p. 70-79.
19. Wojniak, W.S., and Hoover, D.B., 1991, The Getchell Gold Trend, northwestern Nevada--Geologic structure delineated by further exploration of electromagnetic data collected during a helicopter survey [abs.]: U.S. Geological Survey Circular 1062, 7th Annual McKelvey Forum, p. 77.

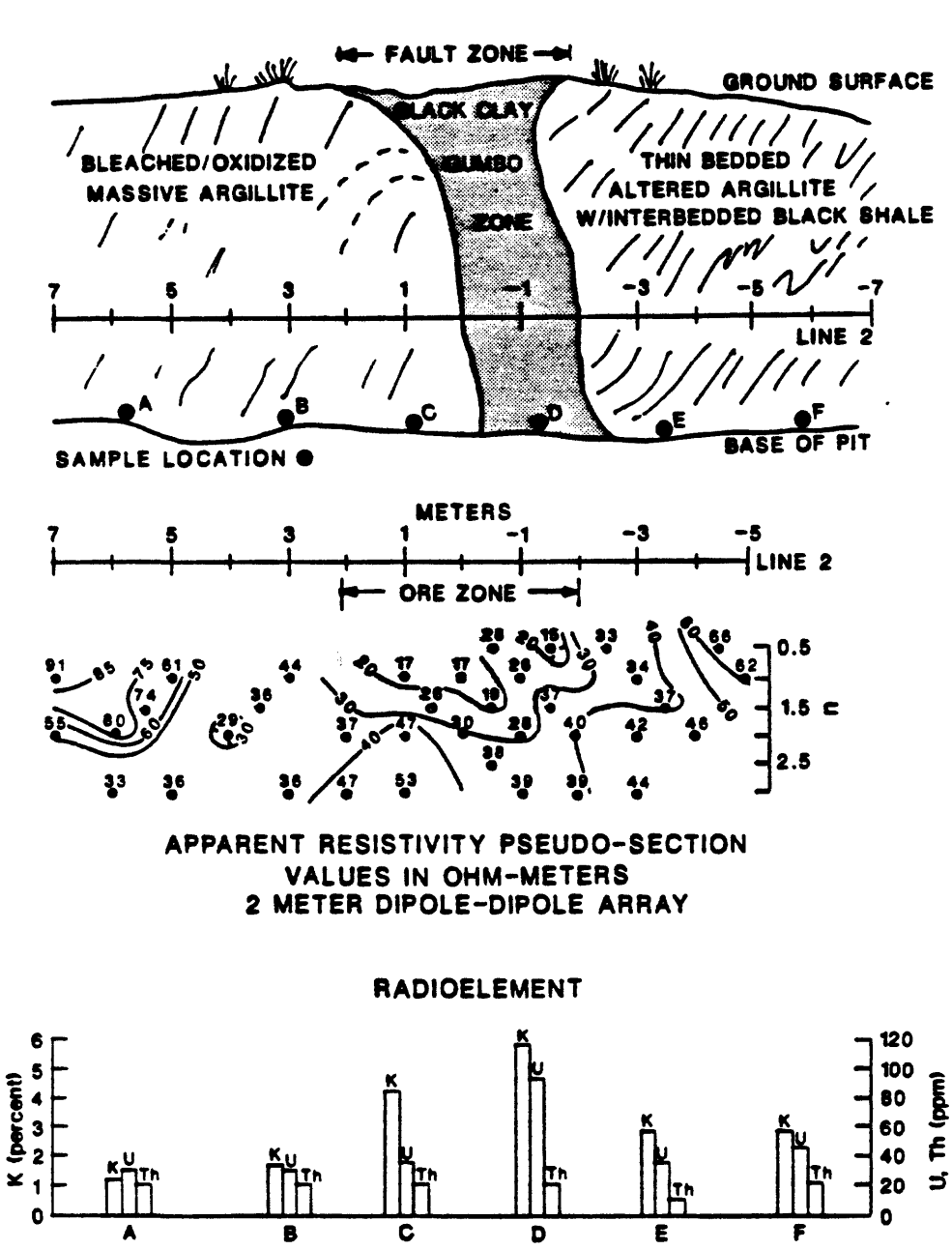

Figure 1. Apparent resistivity and radioelement data obtained in the South Pit at the Getchell Mine, Humbolt County, Nevada. Short-dipole in-situ electrical measurements taken across a mineralized structure, show low resistivities correlated with the ore zone. Radioelement data show significant increases in K and U in the ore zone (Heran and Smith, 1984).

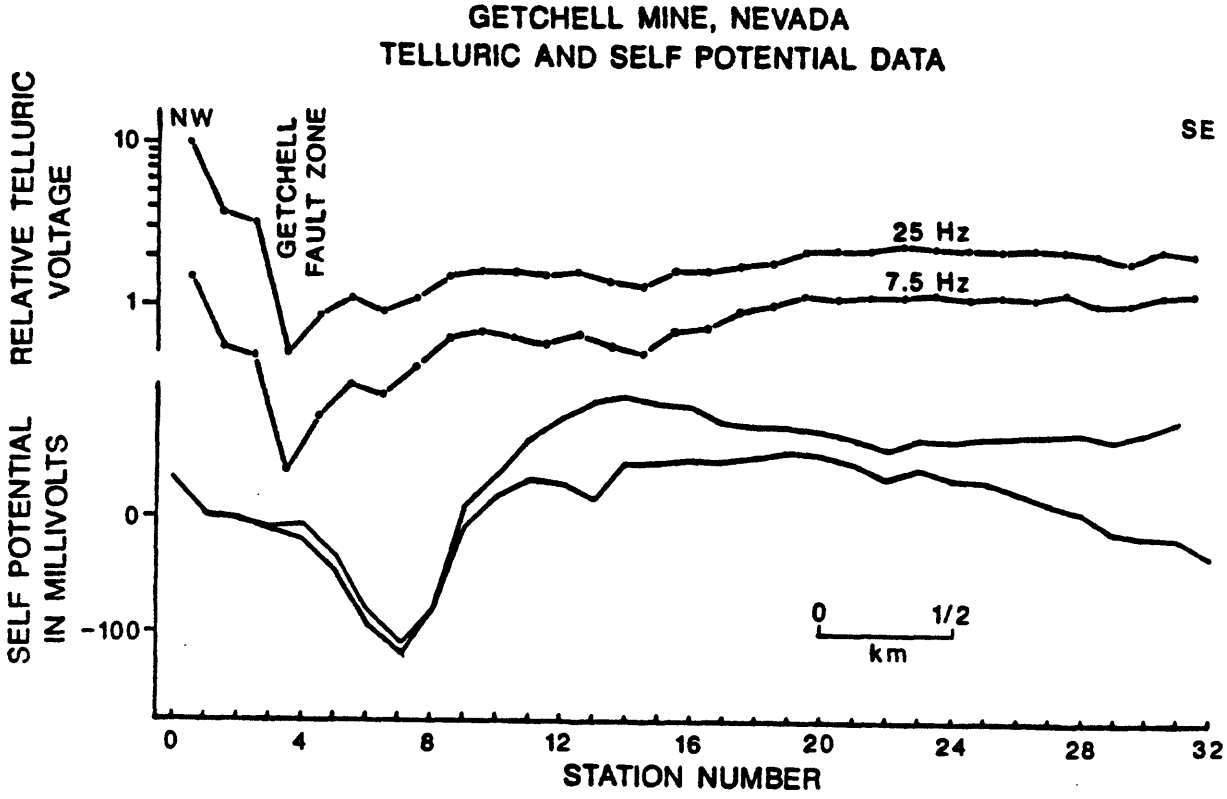

Figure 2. Telluric and self potential data across the northern end of First Miss Gold's Summer Camp deposit prior to mining. The Getchell fault zone shows as a pronounced low in relative telluric voltage, indicating that the fault zone at 25 and 7.5 Hz has much lower resistivity than the surrounding rocks. A broad self potential low is observed east of the main fault zone which is inferred to be related to graphitic material along a parallel fault (from Hoover and others, 1986).

COX AND SINGER Model No. 36b Compiler - W.D. Heran
Geophysically similar models - No. 36a Low Sulfide Au-Quartz Veins

A. Geologic Setting

- Mainly within Archean age regionally metamorphosed (greenschist-facies) mafic and felsic metavolcanic rocks, komatiites, and volcaniclastic sediments interlayered with banded iron-formation. Greenstone units typically intruded by felsic plutons and locally by quartz and/or syenite porphyry.
- Deposits are common near regional division between predominantly metavolcanic and metasedimentary rocks in greenstone belt.
- Stratabound to stratiform deposit consisting of bedded ores of native gold with various sulfides in Fe-rich siliceous or carbonate-rich chemical sediments overlying vein and stockwork feeder zones, often interlayered with flow rocks. Beds may be cut by quartz-carbonate veins containing gold. Deposits are commonly structurally controlled.

B. Geologic Environment Definition

Remote sensing data can delineate regional lineaments, major structural zones, lithologic boundaries and areas of hydrothermal alteration (Honey and Daniels, 1985; Crosta and Moore, 1989; Yatabe and others, 1984; Longman, 1984). Greenstone belts can be outlined by aeromagnetic surveys, which may reflect a regional magnetic low if the belt is magnetite-deficient, in other cases a high if it is magnetite-rich (Grant, 1985). Aeromagnetic surveys are used to define regional structures and locate iron rich metasediments and mafic and ultramafic volcanic rock, within the greenstone belt (Lindeman, 1984; Boyd, 1984). Airborne magnetic data may also define intrusives at the edges or within greenstone belts which may be magnetite deficient compared to normal granitoid rocks (Grant, 1984). Combined airborne EM/magnetic surveys have been used in mapping structure within greenstone belts (Boa Hora, 1986). Airborne radioelement surveys can delineate high potassium zones related to sericite alteration and help define lithologic boundaries (Cunneen and Wellman, 1987). Gravity can be utilized to help determine the depth of belt rocks, define shear zones and folded structures or locate buried intrusives (Costa and Byron, 1988). Electrical soundings and gravity data have been used to model maximum depths of greenstone sequences (DeBeer, 1982).

C. Deposit Definition

Detailed magnetic surveys have been used to map banded iron formations; predict strike extensions, bedding thickness and dip of magnetic zones within the stratigraphic sequence (Lindeman, 1984) and help unravel structure that controls mineralization (Pemberton and others, 1985). Also, detailed magnetic data are employed to map intrusives and dikes associated with ore zones (Koulomzine and Brossard, 1947) and identify alteration which involves both the formation and destruction of magnetic minerals (Fuchter and others, 1991). The strong association of gold with sulfides has permitted the use of a variety of electromagnetic methods to map these zones as conductors (Lindeman, 1984; Valliant, 1985; Costa and Byron, 1988. EM techniques are also used to help map stratigraphy and structure (Pemberton and Carriere, 1985). The induced polarization method is effective in mapping sulfides as resistivity lows and as positive zones of increased polarization (Mathisrud and Sumner, 1967; Sheehan and Valliant, 1985; Hallof, 1985). The IP method can be used to distinguish between mineralized and non-mineralized conductive (EM) anomalies (Costa, and Byron, 1988). IP has been used successfully underground to map pencil-like ore shoots (Mathisrud, and Sumner, 1967). The Mise-a-la-masse electrical technique has been used to delineate the size, shape, and position of individual mineralized units within a sequence (Polomé, 1989). Radiometric surveys can also be used to define areas of hydrothermal alteration (Costa and Byron, 1988).

D. Size and Shape of	Shape	Average Size/Range
Deposit	layered sheet or lens	$0.3x10^6m^3$, $.03-3.9x10^6m^3$
Alteration	irregular	

E. Physical Properties	Deposit	Alteration	Host
1. Density (gm/cc)	3.1[1]; average 2.9-3.4[1]	?	*
2. Porosity	?	?	*
3. Susceptibility (10^{-6} cgs)	500[1] average 0-5000[1]		*
4. Remanence	?	?	*
5. Resistivity (ohm-m)	1[1] average .1-10[1]	?	*
6. IP Effect			
chargeability (mv-sec/v)	50[1] average 20-200[1]	?	*
percent freq. effect (PFE)	12.5[1] ave 5-50[1]	?	*
7. Seismic Velocity (km/sec)	?	?	*
8. Radiometric			
K (%)	moderate-high	moderate-high	*
U (ppm)	moderate-very high	variable	*
Th (ppm)	variable	variable	*

F. Remote Sensing Characteristics

Remote sensing applications to exploration are based on identifying indirect indicators of potential host rocks including spectral, albedo, and textural characteristics. Potential host rocks composed of iron oxides and carbonate minerals can be uniquely identified with high spectral resolution instruments (imaging spectrometers) in the visible and near-infrared (Rowan and others, 1983; Clark and others, 1990). More importantly, imaging spectrometer data can be used to identify and map the distribution of specific iron oxide species (Taranik and others, 1991). Broad-band data in the visible and near-infrared, such as Landsat Thematic Mapper, are effective for separating carbonate- and iron oxide-bearing potential host rocks from other lithologies on regional and local scales (Knepper, 1989). Enhanced Landsat data have been used to define lineaments, fracture patterns and major structures (Longman, 1984). Airborne MSS data can delineate faults, joints and stratigraphic units (Honey and Daniels, 1985).

G. Comments

Regional exploration for and within greenstone terranes has commonly employed aeromagnetic data and more recenty radioelement and remotely sensed data, in Australia, Canada, and Brazil. In general, greenstone terranes have a *low and rough* magnetic character, meaning a low background level with numerous intense short-wavelength anomalies (Grant, 1985).

H. References

1. Ballantyne, E., 1989, Advisory systems for selecting the proper geophysical techniques for mining exploration: unpublished Ph.D. thesis, Univ. of Missouri, Rolla, 121 p.
2. Boyd, D.M., 1984, Aeromagnetic surveys and gold, in Doyle, H.A., ed., Geophysical exploration for Precambrian gold deposits: University of Western Australia Publication No. 10, p. 81-96.
3. Clark, R.N., Gallagher, A.J., and Swayze, G.A., 1990, Material absorption band depth mapping of imaging spectrometer data using a complete band shape least-squares fit with library reference spectra: Proceedings of the Second Airborne Visible/Infrared Imaging Spectrometer (AVIRIS) Workshop, JPL Publication 90-54, p. 176-186.
4. Crosta, A.P., and Moore, J.M., 1989, Enhancement of landsat thematic mapper imagery for residual soil mapping in SW Minas Gerais State, Brazil; a prospecting case history in greenstone belt terrain, in Proceedings of the Seventh Thematic Conference on Remote Sensing for Exploration Geology; methods, integration, solutions: Proceedings of the Thematic Conference on Remote Sensing for Exploration Geology, no. 7, p. 1173-1187.
5. Cunneen, J.P., and Wellman, P., 1987, The use of airborne geophysics and ground gravity surveys in understanding the geology of the eastern goldfields of western Australia: Exploration Geophysics, v. 18, no. 2, p. 22-25.
6. da Boa Hora, M.P.P., 1986, Applied Geophysics in Brazil: Geophysics, The Leading Edge of Exploration, July, p. 39-41.
7. da Costa, A.J.M., and Byron, C.L.,1988, Evolution of geophysical techniques over various types of archean gold occurrences on the farms Roodepoort and Eersteling, Pietersburg greenstone belt, South Africa [ext. abs.]: Geological Society of Australia, Bicentennial Gold 88, extended abstracts, p. 518-520.
8. De Beer, J.H., 1982, A geophysical study of the Murchison greenstone belt, South Africa: International symposium on Archean and early Proterozoic geologic evolution and metallogenesis. Salvador, Bahia, Brazil 1982. Revista-Brasileira-de-Geociencias. 12(1-3), p. 105-112.
9. Fuchter, W.H.A., Hodgson, C.J., and Watts, A.H., 1991, Magnetic mapping of cryptic wall rock alteration associated with gold mineralization at the Blanket mine and its environs in Zimbabwe, South Africa: Brazil Gold '91, Ladeira, E.A., ed., The Economics, Geology, Geochemistry and Genesis of Gold Deposits.
10. Grant, F.S., 1985, Aeromagnetics, geology, and ore environments, II. Magnetite and ore environments: Elsevier Science, Geoexploration, v. 24, p. 335-362.
11. Hallof, P.G., and Yamashita, M., 1985, The use of the induced-polarization method to locate gold-bearing sulfide mineralization [abs.]: Geophysics, v. 50, no. 2, p. 304.
12. Honey, F.R., and Daniels, J.L., 1985, Application of Carr Boyd Minerals Limited Airborne Multispectral Scanner to Spectral Discrimination of Hydrothermally altered areas: Proceedings of the International Symposium on Remote Sensing of Environment, Fourth Thematic Conference, Remote Sensing for Exploration Geology, v. 1, p. 227-231.
13. Knepper, D.H., Jr., 1989, Mapping hydrothermal alteration with Landsat thematic mapper data, in Lee, Keenan, ed., Remote sensing in exploration geology--A combined short course and field trip: 28th International Geological Congress Guidebook T182, p. 13-21.

14. Koulomzine, T., and Brossard, L., 1947, The use of geophysics in prospecting for gold and base metals in Canada: Geophysics, 12, p. 651-662.
15. Lindeman, F.W., 1984, Geophysical case history of Water Tank Hill--Mt. Magnet, W.A., in Doyle, H.A., ed., Geophysical exploration for Precambrian gold deposits: University of Western Australia, 10, p. 97-112.
16. Longman, M.J., 1984, Location of gold deposits by digital processing of landsat data, in Doyle, H.A., ed., Geophysical exploration for Precambrian Gold deposits: University of Western Australia Pub. No. 10, p. 65-80.
17. Mathisrud, G.C., and Sumner, J.S., 1967, Underground induced polarization surveying at the Homestake Mine: Mining Congress Journal No. 3.
18. Pemberton, R.H., and Carriere, 1985, Hemlo Gold Camp Geophysics [abs]: Geophysics, v. 50, no. 2, p. 304.
19. Polomé, L.G.B.T., 1989, The application of the mise-a-la-masse electrical technique in greenstone belt gold exploration: Exploration Geophysics, v. 20, p. 113-116.
20. Rowan, L.C., Goetz, A.F.H., Crowley, J.K., and Kingston, M.J., 1983, Identification of hydrothermal mineralization in Baja California, Mexico, from orbit using the shuttle multispectral infrared radiometer: IEEE Digest, v. 1, p. 3.1-3.9.
21. Sheehan, D.G., and Valliant, R., 1985, Exploration, discovery, and description of an Archean, stratiform pyritic gold orebody, Hemlo, Ontario: Program and Abstracts, CHIM Bulletin, v. 76, no. 881, p. 86-87.
22. Taranik, D.L., Kruse, F.A., Goetz, A.F.H., and Atkinson, W.W., 1991, Remote sensing of ferric iron minerals as guides for gold exploration: Proceedings of the Eighth Thematic Conference on Geologic Remote Sensing, Environmental Research Institute of Michigan, ann Arbor, Michigan, v. 1, p. 197-205.
23. Valliant, R., 1985, The Lac discoveries; the geology of the Hemlo pyritic gold deposit in light of the Bousquet and Dayon examples: Canadian Mining Journal, v. 106, no. 5, p. 39-47.
24. Yatabe, S.M., Howarth, P.J., Hogg, W.A., and Bruce, W.D., 1984, Airborne MSS and MEIS II data for lineament enhancement in northern Ontario: Proceedings Canadian Symposium on Remote Sensing, no. 9, p. 375-385.

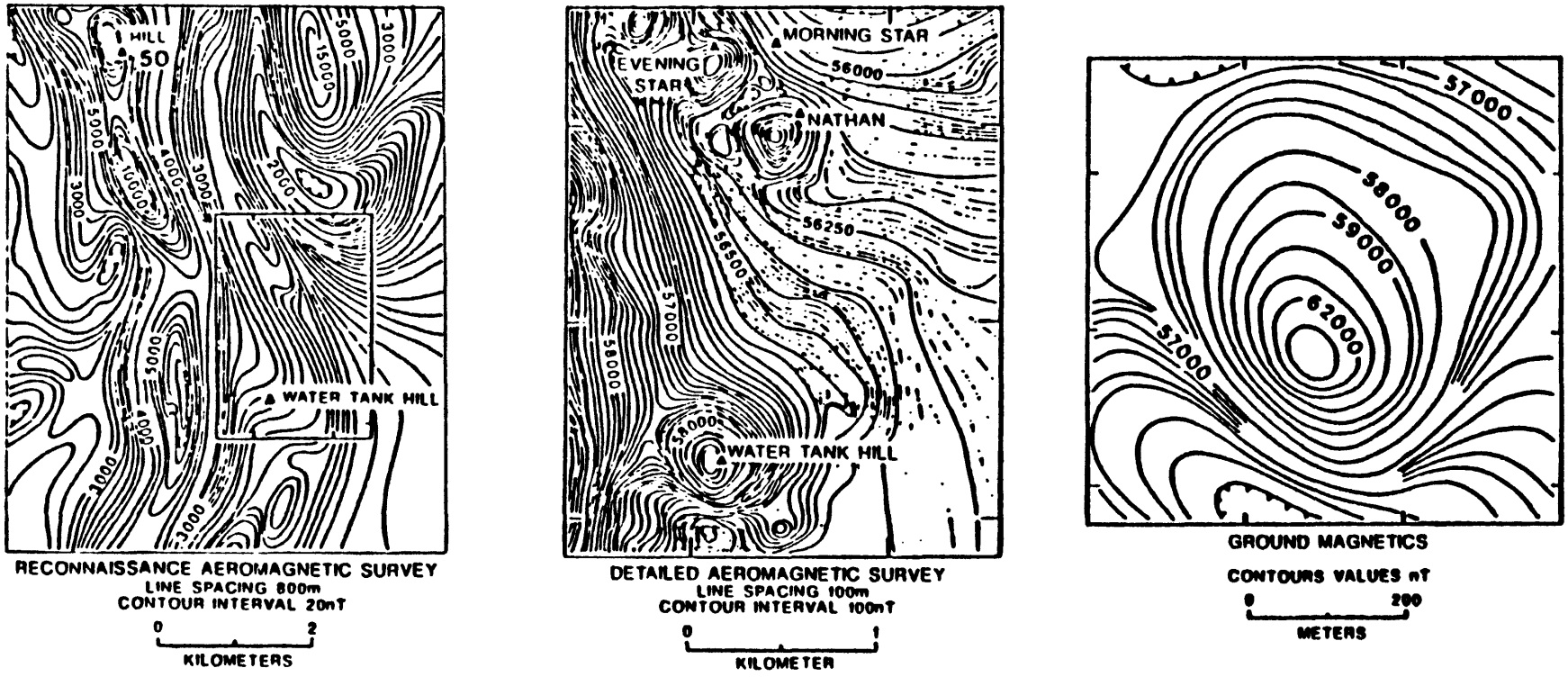

Figure 1. Magnetic data from Water Tank Hill, Mt. Magnet area, Western Australia. The recon aeromagnetic data (800 m) does not define the deposit well, but the detailed (100 m) data show an obvious oval response. Detailed ground magnetics further define its signiture. (peak response is 7000 nT above background) (after Lindeman, 1984)

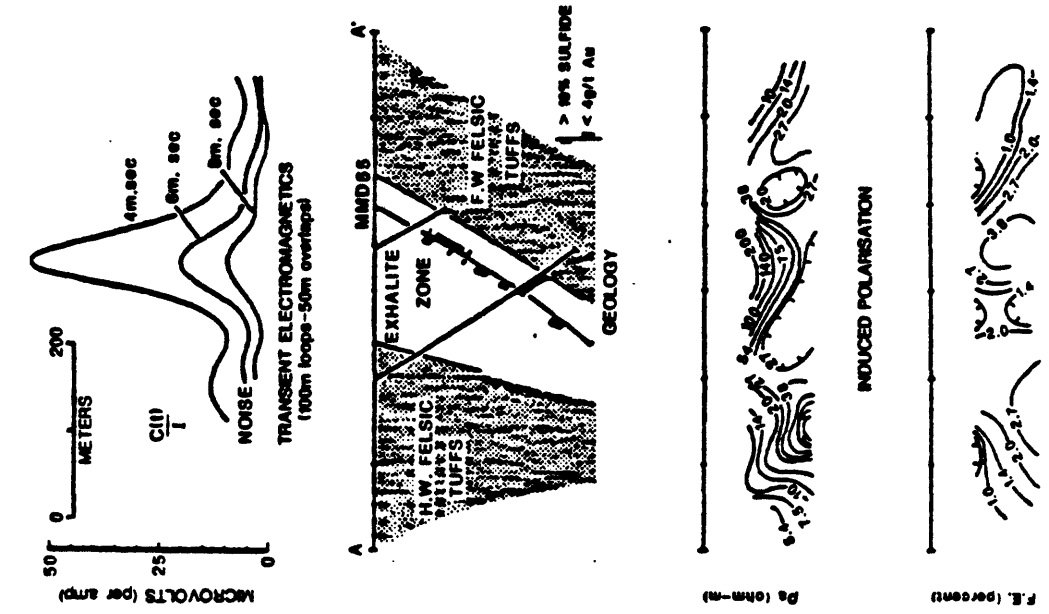

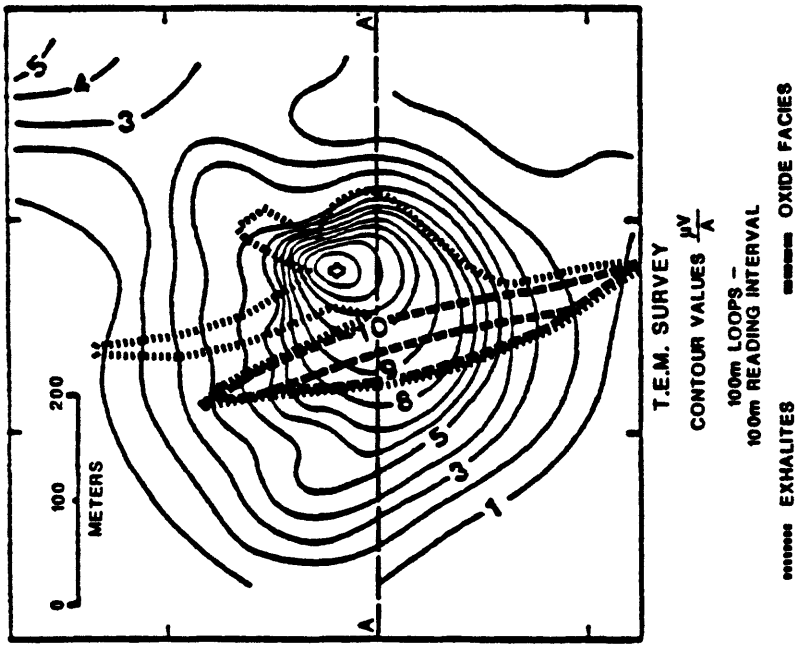

Figure 2. Geology, Transient EM and IP data from Water Tank Hill, Mt. Magnet area, Western Australia. The discovery hole MMD 55 was drilled to test the TEM and IP anomalies. The apparent resistivity high appears to relate to BIF (exhalite zone). (after Lindeman, 1984)

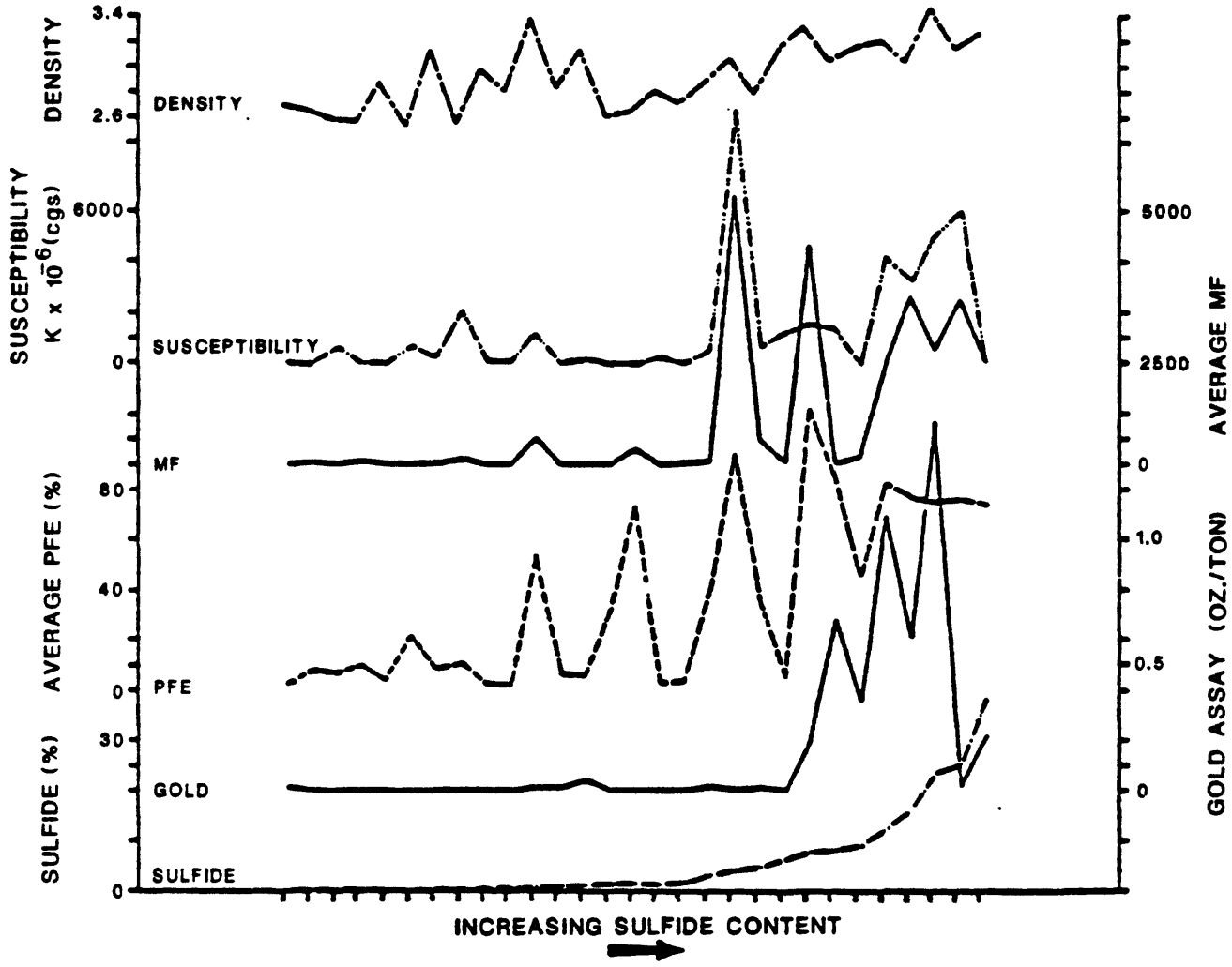

Figure 3. Laboratory physical property measurements on core samples from the Homestake Mine (from Mathisrud and Sumner, 1967).

Chapter 5. OVERVIEW OF THE GETCHELL STUDY AREA AND AIRBORNE DEMONSTRATION PROJECT

INTRODUCTION

The quest for minerals, particularly in developed nations, is increasingly focusing on exploration in covered terranes as the probability of new discoveries in exposed areas diminishes. The problems posed by cover require more sophistication in the application of existing technology and the development of new techniques. Improvements may involve better ways of looking through cover rocks or better methods for identifying subtle differences within the cover arising from buried structures or mineralized rocks at depth. Geophysical methods will play an increasingly important role in integrated exploration programs in the future because of their ability to directly address the problems presented by covered deposits.

The U.S. Geological Survey (USGS), in its minerals assessment programs is facing the same problems as industry in the evaluation of the potential of covered areas for mineral commodities. In 1988 funding was made available for several airborne geophysical demonstration programs that were intended to show the application of multi-sensor surveys. An integrated airborne program along the Getchell trend, Humboldt County, Nevada, was proposed as part of ongoing research on assessment methods that was already underway in the area. Funding became available in April; flying began in August and was completed in early November 1988.

The Getchell Trend Airborne Demonstration Program was designed to illustrate the potential of an integrated and comprehensive airborne geophysical surveying program for exploration or assessment in covered terranes. Additionally, it would provide data on the geophysical signatures, and their variability for a variety of different types of deposits that were known in the area. Four distinct geophysical methods were employed: infrared and visible multispectral imaging (remote sensing), gamma-ray spectrometry, magnetics, and electromagnetics. Each technique measures distinctly different physical properties of the earth that are useful for constraining interpretations based on only one method. The remote sensing and gamma-ray methods map properties of very-near-surface materials, that reflect surficial lithologies and subtle mineralogical or chemical variations within and between units. Electromagnetic methods provide information on electrical resistivity to depths of about 100 m with commercially available instrumentation, whereas magnetic methods respond to magnetic sources at any depth. Hoover and others (1991) review preliminary results of the airborne surveys, concentrating on the areas where multiple methods complement each other to improve the interpretation of the geologic setting. Companion papers in the same volume discuss the individual airborne techniques that were used (Pitkin, 1991, gamma-ray data; Grauch and Bankey, 1991, magnetic data; and Pierce and Hoover, 1991, electromagnetic data).

The Getchell trend was chosen for this study because of the presence of a variety of known types of mineral deposits, including bedded barite, skarn tungsten, tungsten-bearing manganese, silver, and disseminated gold. Active gold mines include those at the Preble, Pinson, Mag, Getchell, Rabbit Creek, and Chimney deposits. These known deposits provide a means for testing methods and models. The Rabbit Creek deposit was of particular interest. At the time of the flying, it was a blind deposit with over 100 m alluvial of cover; it was being drilled, but stripping of the cover had not yet begun.

This provided a unique opportunity to test a combination of methods. The cooperation of most of the mining companies in providing access to their properties for ground studies also was an important factor in selecting this study area.

The area surveyed lies principally on the eastern flank of the Osgood Mountains (Fig. 5-1), and covers an area of about 450 km^2. In general, the northern margin is at the Chimney deposit, and the southern boundary lies along Interstate Highway 80. The western boundary is the crest of the Osgood Mountains. From the crest of the range the survey area extends east about 12 km to where the cover rocks are believed too thick for present exploitation. For practical reasons, the coverage of individual airborne surveys varied.

Two strips of 63-channel airborne imaging spectrometer data in the near infrared and visible region were acquired specifically for this project, by Geophysical Environmental Research Corporation (GER). Previously acquired remote sensing data from the Landsat Thematic Mapper (TM) satellite and the Thermal Infrared Multispectral Scanner (TIMS) system of the Stennis Space Center at NASA were also available. The TIMS system was reflown for this project, but extensive cloud cover made the data unusable. Gamma-ray data were acquired by TerraSense, Inc. using a complete calibrated system for quantitative measurement of the radioelements, uranium, thorium, and potassium, using a helicopter platform. Combined magnetic and electromagnetic data were contracted from DIGHEM, Inc., again using a helicopter. To supplement the magnetic data acquired by DIGHEM, the USGS flew additional areas using its in-house system and a fixed-wing platform. The magnetic, gamma-ray, and electromagnetic data were acquired with a maximum flightline spacing of 400 m (1/4 mile).

The digital data in both flight-line and gridded form, have been released through the National Oceanic and Atmospheric Administration's Geophysical Data Center, Boulder, Colorado. Color shaded-relief maps of these data at 1:100,000 scale also can be seen at the Nevada Bureau of Mines in Reno, and at USGS offices in Menlo Park, California, Tucson, Arizona, Spokane, Washington, Denver, Colorado, Salt Lake City, Utah, and Reston, Virginia. U.S. Geological Survey geophysical maps of the magnetic and electromagnetic data are also in press (Grauch and Bankey, in press; Wojniak and others, in press).

GEOLOGIC SETTING

The Osgood and Edna Mountains region has undergone repeated episodes of structural deformation particularly during the Paleozoic. Mesozoic and Cenozoic extrusive and intrusive rocks further complicated or masked relationships. The following geological summary is based on mapping by Hotz and Willden (1964), Willden (1964), and Erickson and Marsh (1974a, 1974b), and unpublished mapping by A.R. Wallace and D.M. McGuire, both of the USGS.

Extensive new mapping is currently being conducted by mining companies in the region. As additional information becomes available, changes in the interpretation of the geological, geochemical, and geophysical data can be expected.

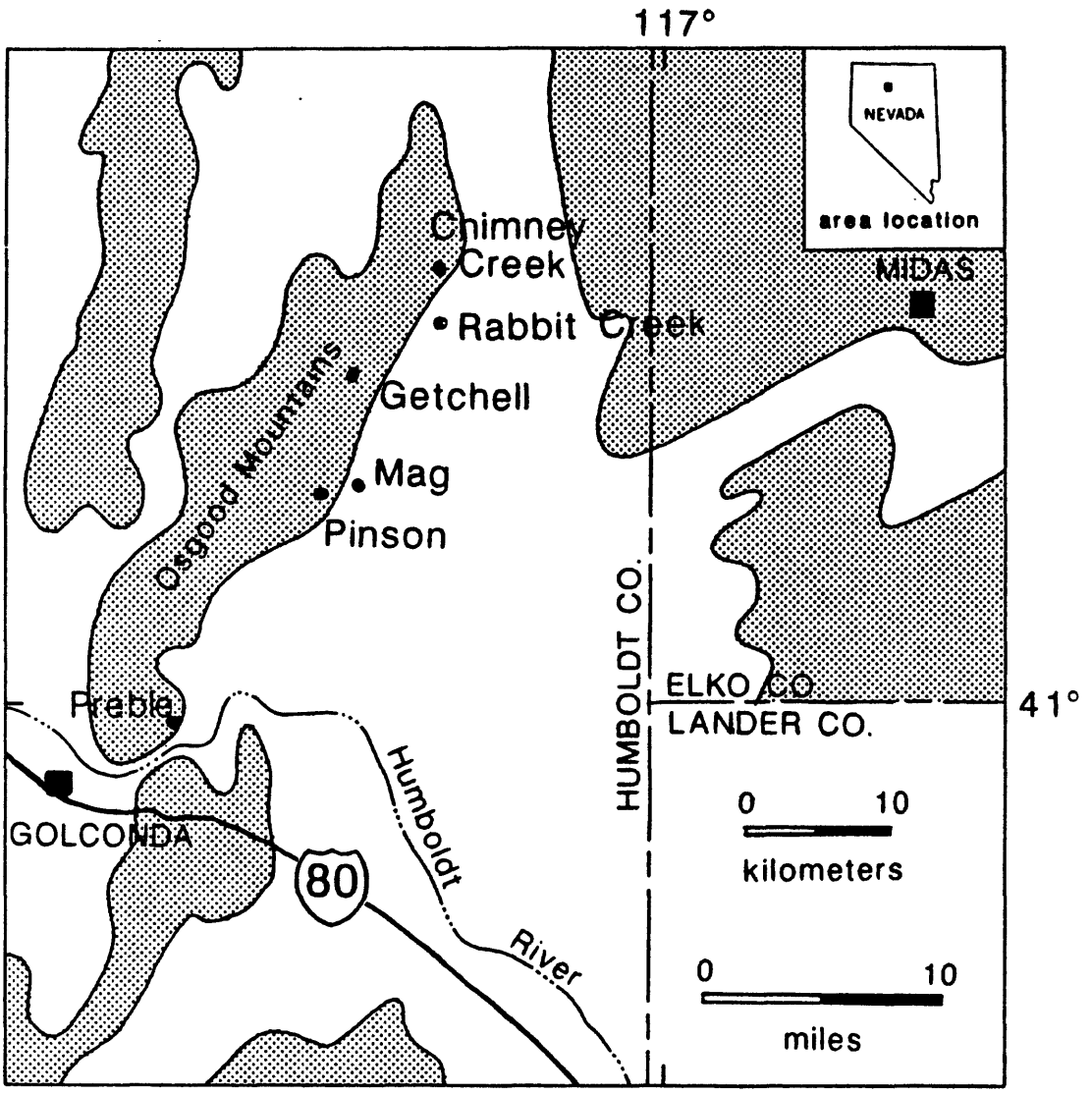

Figure 5-1--Location of Getchell trend and Osgood Mountains.

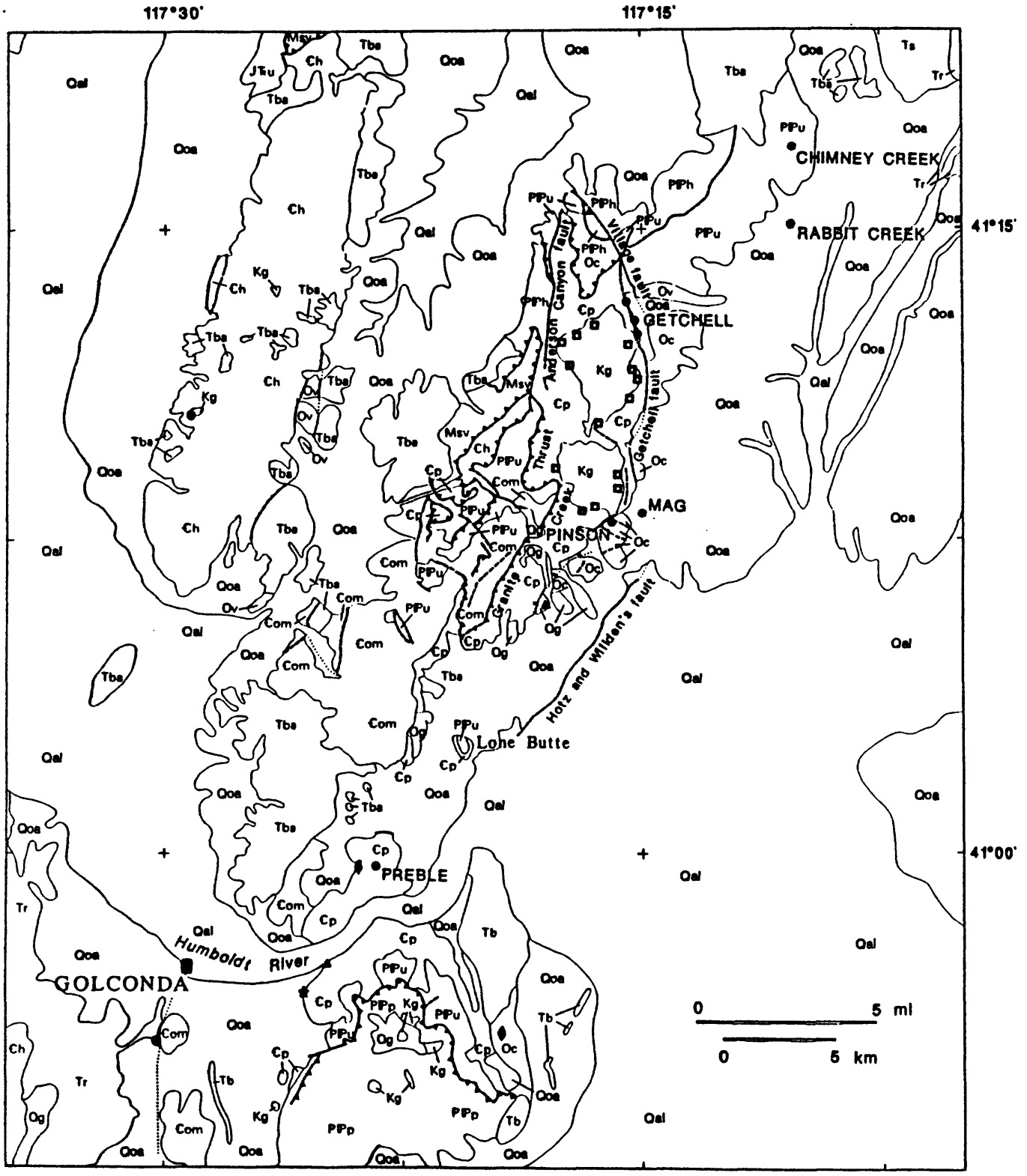

Fig. 5-2 Geological map of the Osgood Mountain area, Humboldt County, Nevada adopted from Willden (1964), Hotz and Willden (1964), and Erickson and Marsh (1974a, 1974b).

DESCRIPTION OF MAP UNITS
(Listed in approximate stratigraphic order)

Qal - Quaternary alluvium

Qoa - Older Quaternary alluvium

Qg - Quaternary gravel

Tb - Pliocene basalt

Tr - Miocene rhyolite flows and tuffs

Ts - Miocene clastic rocks and tuffs

Tba - Miocene basalt and basaltic andesite

Kg - Cretaceous granodiorite (about 90 Ma)

JTRu - Jurassic and Triassic metaclastic rocks, undivided

PPu - Permian and Pennsylvanian clastic and carbonate rocks, undivided. Includes Edna Mountain Formation (Permian), Antler Peak Limestone (Pennsylvanian and Permian), Highway Limestone (Pennsylvanian), and Battle Formation (Pennsylvanian). In the Osgood Mountains, includes the Etchart Limestone (Pennsylvanian and Permian) and the Adam Peak Formation (Pennsylvanian and Permian).

PPp - Pumpernickel Formation (Pennsylvanian and Permian)--siliceous sedimentary and volcanic rocks

PPh - Pennsylvanian and Permian siliceous sedimentary and volcanic rocks, undivided. Includes the Havallah Formation (Pennsylvanian and Permian), rocks similar to the Havallah and Pumpernickel Formations in the Hot Springs range, and the Farrel Canyon Formation (Pennsylvanian and Permian) in the Osgood Mountains.

Msv - Mississippian siliceous sedimentary and volcanic rocks. In the Osgood Mountains includes the Goughs Canyon Formation.

Ov - Valmy Formation (Ordovician)--Chert and greenstone

Oc - Comus Formation (Ordovician)--Carbonate rocks and sandstone

Ch - Harmony Formation (Cambrian)--Sandstone and shale. Includes small exposures of Paradise Valley Chert (Cambrian) on the west side of the Hot Springs Range.

Cp - Preble Formation (Cambrian)--Shale and limestone

Com - Osgood Mountain Quartzite (Cambrian)

Contact

Fault, dashed where approximately located, dotted where concealed

Thrust fault, sawteeth on upper plate

MAG Gold deposit; names indicate operational or developing mines

Tungsten deposit

Silver deposit

Barite deposit

Manganese deposit

Lithology

The oldest units shown on the geologic map (Fig. 5-2) are Paleozoic quartzite, shale, limestone, and sandstone deposited in shallow shelf to eugeosynclinal environments. The Osgood Mountain Quartzite (Ɛom), of Early Cambrian(?) age, is the oldest of these units and is overlain by Middle and Upper Cambrian shales and limestones of the Preble Formation (Ɛp). Middle and Upper Ordovician Comus Formation (Oc) carbonates and shales were deposited directly on the Preble Formation. Overlying these are Ordovician cherts, greenstones, and argillites of the Valmy Formation (Ov). Only minor exposures of the latter unit occur in the area studied. Silurian to Early Mississippian units are missing in this area as a result of disturbances of the Early Mississippian Antler orogeny, but a return to shelf-type sedimentation resulted in the deposition of the Antler-age sequence, which in the study area includes limestone, shale, and sandstone of Pennsylvanian to Permian age. The only known Mesozoic units in the area are intrusive rocks of granodiorite composition, which were responsible for tungsten mineralization, and possibly for gold mineralization (Silberman et al., 1974). The most prominent exposure is the Osgood Mountains pluton in the northern part of the Osgood Mountains. In outcrop the pluton appears as two ovoid bodies joined by a narrow septum to form an hour glass-shaped body. This body appears prominently in all the geophysical data. A smaller granodiorite pluton is present in the Edna Mountains east of Golconda, with most exposures north of the interstate highway. Skarns and hornfels developed in carbonate rocks on the margins of the plutons host all but one of the tungsten deposits.

Cenozoic rocks of the region consist principally of basalt and basaltic andesite flow and Neogene to Quaternary fanglomerates. Rhyolites and tuffs are present to the east and southwest of the survey area and they are source rocks for some of the alluvial material in the area. Only minor amounts of rhyolites and tuffs are known in the study area.

Structures

The Paleozoic rocks in this area were extensively deformed during three pre-Tertiary tectonic events. Thrusting during the Antler and Sonoma orogenies brought western facies deep-water units over or interleaved them with, eastern facies, shallow-water units in a complex assemblage. This can be seen in the Osgood and Edna Mountains (Fig. 5-2) where exposures are good.

These thrusts are generally north or northeast striking. The Paleozoic units are tilted and folded, often isclinally, and steeply dipping. Bedding strikes generally north or northeast and dips generally east to southeast.

Mesozoic faults have been identified only adjacent to the Osgood Mountains pluton. These are normal, north to northeast striking faults, and include the Anderson Canyon, Getchell, and Village faults (Fig. 5-2).

Cenozoic Basin-and-Range extension reactivated north-striking normal faulting and produced the Osgood and Edna Mountains horst blocks. During the Basin-and-Range extension, mafic and felsic dikes were intruded along many of these reactivated zones. The high angle faults in these zones were important ore controls for most sediment hosted gold deposits at both regional and deposit scales (Percival and others, 1988).

Mineral Deposits

A variety of types of mineral deposits are present in the survey area (Fig. 5-2). Gold is of primary interest today and is being actively mined at the Preble, Pinson, Mag, Getchell, Rabbit Creek, and Chimney deposits (Fig. 5-2). During the period 1939-1941, the Getchell mine was the leading gold producer in Nevada. Exploration in the area now is entirely focused on gold, with private industry having extensive exploration programs on all available land.

Bedded barite has been mined from four deposits in the Preble and Comus Formations in the southern half of the study area. None of these are presently active. Scheelite was mined from numerous skarn deposits surrounding the Osgood Mountains pluton from 1942-1962. Humboldt County ranks second in the state for production of tungsten, with the bulk of that production coming from deposits in this area (Stager and Tingley, 1988). No commercial tungsten mineralization has been found adjacent to the intrusive in the Edna Mountains.

Silver has been produced from the Silver Lode claims just west of the Preble mine and from the Silver Coin and adjacent mines in the southeast part of the survey region.

A unique tungsten-bearing manganese deposit at the Golconda mine on the west flank of the Edna Mountains was mined from 1941-1945 (Stager and Tingley, 1988). This is a Quaternary, hot-spring manganese deposit formed on steeply dipping Preble Formation and overlain by tufa (Kerr, 1940). Mineralization extends only a short distance into the underlying rocks. The spring is weakly active today.

DATA DESCRIPTIONS

Release of the Getchell digital data was made through the U.S. Department of Commerce's National Geophysical Data Center, and announced February 17, 1989. Further information on the digital data is contained in Chapter 12.

Topographic Data

The digital topographic data base was obtained from the Defense Mapping Agency and based on 1^{o} x 2^{o} topographic quadrangles. The data were projected into UTM coordinates (base latitude 0^{o}; central meridian 117^{o}w) and interpolated onto grids having equally spaced intervals of 0.1 km. These data are also available from the National Geophysical Data Center.

Radioelement Data

The USGS contracted with TerraSense, Inc., of Sunnyvale, California for a helicopter gamma-ray spectrometer survey of the Getchell area (TerraSense, 1989). The survey was flown in October 1988 on 400-m (1/4 mi) spaced flight lines oriented northwest-southeast at a nominal 122-m (400 feet) above ground level. The spectrometer system used 33 liters (2048 cubic inches) of sodium iodide crystals to detect near surface terrestrial gamma-rays and a 8 liter (512 cubic inches) detector to monitor radon in air. The gamma-ray data were corrected for background radioactivity, spectral backscatter, radon in air, were altitude normalized, and were converted to concentration units of parts per million for uranium (U) and thorium (Th) and percent for potassium (K). Equilibrium in the uranium and thorium decay series was assumed. The data were projected into UTM coordinates (base latitude 0^{o}; central meridian 117^{o}W) and interpolated onto grids having equally spaced intervals of 0.2 km.

Aeromagnetic Data

Three aeromagnetic data sets are available for the Getchell trend (Grauch and Bankey, 1991; in press). Only one survey, which was acquired for the USGS by DIGHEM, Inc. in October 1988, will be used for demonstration at this workshop. The DIGHEM survey was flown by helicopter with a cesium-vapor magnetometer nominally 40 m (130 feet) above ground. The flight lines were directed northwest-southeast and spaced 400 m (1/4 mile) apart except over the vicinity of known gold deposits where they were spaced 200 m (1/8 mile) apart. Three extra long flights across the area are for magnetic modeling purposes.

The data were projected into UTM coordinates (base latitude 0^{o}; central meridian 117^{o}W) and interpolated onto a grid having equally spaced intervals of 0.1 km. Diurnal variations and the standard International Geomagnetic Field model were removed from the grid.

Airborne Electromagnetic Data

Airborne electromagnetic (AEM) data were acquired over the Getchell Trend in October, 1988 using the DIGHEM IV system (Fraser, 1979). The horizontal coplaner coil pairs used in the DIGHEM IV system were operated at 56,000 Hz, 7200 Hz and 900 Hz. The survey was flown by helicopter with the sensor at a nominal 30 m (100 feet) above ground. Flight lines were oriented northwest-southeast and spaced 400 m (1/4 mile) apart except in the vicinity of known gold deposits where the spacing was 200 m (1/8 mile) apart. Apparent resistivity data were derived from the AEM data using algorithms described by Fraser (1986) and form the data sets presented in this workshop. The data were projected into UTM coordinates (base latitude 0^{o}; central meridian 117^{o}W) and interpolated onto a grid having equally spaced intervals of 0.1 km.

ACKNOWLEDGMENTS

The USGS studies along the Getchell Trend, both ground and airborne, have been done in cooperation with First Miss Gold Corp., Santa Fe Pacific Minerals, Pinson Mining, and Battle Mountain Exploration who provided access to their lands. The ability to obtain complementary ground data was an important factor in determining where the airborne surveys would be flown. In particular we wish to thank Mr. Richard Nanna of First Miss Gold, Mr. Roy Owen of Santa Fe Pacific Minerals, Mr. Edward Kretchmer of Pinson Mining, and Mr. Kurt Payne of Battle Mountain Exploration for all the help given and for many hours of lively discussion.

REFERENCES

Erickson, R.L., and Marsh, S.P., 1974a, Geologic map of the Golconda quadrangle, Humboldt County, Nevada: U.S. Geological Survey Geologic Quadrangle Map GQ-1174, scale 1:24,000.

Erickson, R.L., and Marsh, S.P., 1974b, Geologic map of the Iron Point quadrangle, Humboldt County, Nevada: U.S. Geological Survey Geologic Quadrangle Map GQ-1175, scale 1:24,000.

Fraser, D.C., 1979, The multicoil II airborne electromagnetic system: Geophysics v. 44, p. 1367-1394.

Fraser, D.C., 1986, DIGHEM resistivity techniques in airborne electromagnetic mapping, in Palacky, G.J., ed., Airborne resistivity mapping: Geological Survey of Canada, paper 86-22, p. 45-54.

Grauch, V.J.S., and Bankey, Viki, 1991, Preliminary results of aeromagnetic studies of the Getchell disseminated gold deposit trend, Osgood Mountains, north-central Nevada, in Raines, G.L., Lisle, R.E., Schafer, R.W., and Wilkinson, W.H., eds., Geology and Ore Deposits of the Great Basin, Symposium Proceedings: Geological Society of Nevada, Reno, NV, p. 781-792.

Grauch, V.J.S., and Bankey, Viki, in press, Aeromagnetic and related maps of the Getchell gold trend area, Osgood Mountains, north-central Nevada: U.S. Geological Survey Geophysical Map GP-1003-B, scale 1:100,000.

Hoover, D.B., Grauch, V.J.S., Pitkin, J.A., Krohn, M.D., and Pierce, H.A., 1991, An integrated airborne geophysical study along the Getchell trend of gold deposits, north-central Nevada, in Raines, G.L., Lisle, R.E., Schafer, R.W., and Wilkinson, W.H., eds., Geology and Ore Deposits of the Great Basin, Symposium Proceedings: Geological Society of Nevada, Reno, NV, p. 739-758.

Hotz, P.E., and Willden, Ronald, 1964, Geology and mineral deposits of the Osgood Mountains quadrangle, Humboldt County, Nevada: U.S. Geological Survey Professional Paper 431, 128 p.

Kerr, P.F., 1940, Tungsten-bearing manganese deposit at Golconda, Nevada: Geological Society of America Bulletin, v. 51, p. 1359-1390.

Percival, T.J., Bagby, W.C., and Radtke, A.S., 1988, Physical and chemical features of precious metal deposits hosted by sedimentary rocks in the western United States, in Schafer, R.W., Cooper, J.J., and Vikre, P.G., eds., Bulk minable precious metal deposits of the western United States: Geological Society of Nevada, Reno, p. 11-34.

Pierce, H.A., and Hoover, D.B., 1991, Airborne electromagnetic applications - mapping structure and electrical boundaries beneath cover along the Getchell trend, Nevada, in Raines, G.L., Lisle, R.E., Schafer, R.W., and Wilkinson, W.H., eds., Geology and Ore Deposits of the great Basin, Symposium Proceedings: Geological Society of Nevada, Reno, NV, p. 771-780.

Pitkin, J.A., 1991, Radioelement data of the Getchell trend, Humboldt County, Nevada - Geological discussion and possible significance for gold exploration, in Raines, G.L., Lisle, R.E., Schafer, R.W., and Wilkinson, W.H., eds., Geology and Ore Deposits of the Great Basin, Symposium Proceedings: Geological Society of Nevada, Reno, NV, p. 759-770.

Silberman, M.L., Berger, B.R., and Koski, R.A., 1974, K/Ar relations of granodiorite emplacement and tungsten and gold mineralization near the Getchell mine, Humboldt County, Nevada: Economic Geology v. 69, p. 646-656.

Stager, H.K., and Tingley, J.V., 1988, Tungsten deposits in Nevada: Nevada Bureau of Mines and Geology Bulletin 105, 205 p.

TerraSense, Inc., with an introduction by J.A. Pitkin and P.L. Hill, 1989, Uranium, potassium, and thorium contour maps derived from a helicopter gamma-ray spectrometer survey of the Getchell trend, Humboldt County, Nevada: U.S. Geological Survey Open-File Report 89-287, 9 p., 12 sheets, scale 1:24,000.

Willden, Ronald, 1964, Geology and mineral deposits of Humboldt County, Nevada: Nevada Bureau of Mines and Geology Bulletin 59, 154 p.

Wojniak, W.S., Hoover, D.B., and Grauch, V.J.S., in press, Electromagnetic survey maps showing apparent resistivities of the Getchell gold trend, Osgood Mountains, north-central Nevada: U.S. Geological Survey Geophysical Map GP-1003-A, 3 plates, scale 1:100,000.

Chapter 6. Getting Started with the Software

GRIDS

This workshop starts at the point of having a gridded data set, which is usually supplied by the airborne geophysical contractor. Ideally, geophysical data should be collected at equally spaced points on a two-dimensional grid, but in most cases this is impractical. Therefore, the values at grid points must be interpolated from irregularly spaced data. When the spacing between data points is highly variable, the reliability of the grid is also highly variable. For example, samples are densely spaced along flight lines, but are widely spaced perpendicular to flight lines, common in airborne surveys. Gravity stations are usually placed where practical, resulting in parts of the area that are well covered and parts that are not. Thus, grid points in the areas of dense sampling are fairly representative of the data but may lose the original data resolution if spaced wider than the data points. Grid points in sparsely sampled areas involve more interpolation of the gridding algorithm and may be inaccurate. In addition, data points collected at variable elevations are usually gridded as though they were all at one elevation, reducing the reliability of the data representation depending on the severity of the elevation differences (Cordell, 1992).

Many geophysical grids are constructed using a minimum curvature algorithm (Briggs, 1974), in common use at the USGS as program MINC (Webring, 1981). Other methods are discussed by Crain (1970). None of these methods can overcome the fundamental problems of gridding irregularly spaced sample points (Cordell, 1992), but this is a subject of current research and will not be addressed further here. Discussion of the minimum curvature algorithm and the parameters of MINC are found in Webring (1981).

In order to use the USGS software presented at this workshop, grids should be in USGS standard grid format. A description of this format and an example of FORTRAN code for writing USGS grid files are included on a following page.

Common Grid Problems

Although we do not address fundamental problems of gridding, there are several common grid problems that have easily identifiable characteristics: (1) pockmarks, (2) herring-bone pattern, (3) beading, and (4) elongation perpendicular to flight lines. Pockmarks are common in gravity maps and are very local anomalies associated with some of the station locations. They look like pockmarks or pimples in graytone or shaded displays, but may not be noticeable on contour maps. They are produced by small errors in gravity measurements and undersampling of local gravity features (Cordell, 1992). The undersampling is a consequence of measuring the gravity field directly on gravity sources and the impracticality of densely spaced stations. Eventually gridding algorithms may be able to compensate for these features (Cordell, 1992). Until then, interpretation should concentrate on the smoother, more regional features.

Herring-bone patterns arise in flight-line data where flight lines are not correctly compensated for parameters affected by flight direction. Lack of compensation for changes of aircraft heading as it moves through the earth's magnetic field is one common case. Another occurs when lines are flown ascending over a topographic slope in one direction and descending in the opposite direction

on neighboring lines. Because the aircraft cannot ascend as rapidly as it can descend, the flight paths tend to differ in height above ground where topographic slopes are steepest. These elevation differences lead to systematic variations in the measured values of the magnetic field that alternate from line to line. Gridding of these data produce a herring-bone or zig-zag pattern between flight line locations. Herring-bone problems can be reduced by a filtering procedure applied to grids commonly called decorrugation (Urquhart, 1989), but some resolution is then lost.

When the flight-line spacing of a survey is too wide to adequately sample anomalies that lie between the flight lines, gridding programs tend to produce artifacts that look like "beads" strung along flight lines. This is especially common in aeromagnetic surveys flown at spacings greater than twice the height above shallowest magnetic sources (Reid, 1980). The flight-line specifications of the airborne gamma-ray/magnetic surveys flown for the National Uranium Resource Evaluation (NURE) program in the mid-1970's and early 1980's commonly have this problem. Unfortunately, these are the only publicly available data in many areas of the U.S. In practice, maps with beading can be beautified through upward continuation, a standard analytical technique that suppresses local anomalies and emphasizes regional ones (supported by program FFTFIL in the software package). However, missing information between flight lines can never be regained and resolution of anomalies that *were* properly sampled may be significantly lost. In severe cases, a better alternative is to interpret the data in profile form.

Some gridding algorithms and decorrugation filters are designed to minimize the beading problem, but can sometimes overfilter the data by artificially elongating features perpendicular to the flight line. The problem can be recognized by an overall pattern of linear trends on the map that are perpendicular to the flight direction. Correction of the problem requires regridding the flight-line data with proper parameters (Webring, 1981).

Bibliography

Briggs, I. C., 1974, Machine contouring using minimum curvature: Geophysics, V. 39, no. 1, p. 39-48.

Cordell, Lindrith, 1992, A scattered equivalent-source method for interpolation and gridding of potential-field data in three dimensions: Geophysics, v. 57, no. 4, p. 629-636.

Crain, I. K., 1970, Computer interpolation and contouring of two-dimensional data: a review: Geoexploration, v. 8, p. 71-86.

Reid, A. B., 1980, Aeromagnetic survey design: Geophysics, v. 45, no. 5, p. 973-976.

Urquhart, Ted, 1989, Decorrugation of enhanced magnetic field maps: Society of Exploration Geophysicists expanded abstracts with biographies, 59th Annual International SEG meeting, p. 371-372.

Webring, Michael, 1981, MINC; A gridding program based on minimum curvature: U. S. Geological Survey Open-File Report 81-1224, 41 p.

DESCRIPTION OF USGS GRID FORMAT

The USGS standard grid is a binary file consisting of a header record followed by one record for each row of data. The origin of the grid is the lower left-hand corner. Each row is read from left to right (usually west to east) and rows are read sequentially from bottom to top (usually south to north). Note that parameters xo, dx, yo, and dy must all have the same distance units.

A. Header record (23 4-byte words)

id - 56 ASCII characters of identification (14 words)
pgm - 8 ASCII characters of creation program identification (2 words)
ncol - number of columns of data (integer, 1 word) in each row
nrow - number of rows of data (integer, 1 word)
nz - number of words per data element (integer, 1 word). Most programs require nz=1
xo - position coordinate of first (leftmost) column of data (real, 1 word)
dx - equal spacing interval between columns (real, 1 word). Most programs require a nonzero value.
yo - position coordinate of first (bottom) row of data (real, 1 word)
dy - equal spacing interval between rows (real, 1 word). Most programs require a nonzero value.

B. Data record. Each data record contains one row of real data. The first word should contain the row coordinate, but in most programs this coordinate value is treated as a dummy. Record length is (ncol*nz)+1 words. To flag grid points where there are no data, the values are set to a large number, usually greater than or equal to 1.e+38. These values are called "dvals".

FORTRAN code to access USGS standard grids commonly has the following form (assuming nz=1).

```
      dimension g(maxcol), id(14), pgm(2)

      dum=0.0
      read or write (...) id,pgm,ncol,nrow,nz,xo,dx,yo,dy
      do 10 j=1,nrow
      read or write (...) dum,(g(i), i=1,ncol)
      do 5 i=1,ncol

        [operate on each g(i)]

5     continue
      read or write (...) dum, (g(i), i=1,ncol)
10    continue
```

Alternatively, all the grid data can be read into a two-dimensional array. However, this usually severely restricts the size of grids that can be manipulated because of memory limitations.

DESCRIPTION OF USGS POST FILE FORMAT

Generic Post File

A post file is a binary file in which each record contains a record identification, x and y coordinates, and any number of dependent variables.

Field	Description
id	8 ASCII characters of record identification (character*8).
x	x coordinate of record. This can be longitude in decimal degrees or units of distance from the central meridian for projected data (usually in kilometers) (real*4).
y	y coordinate of record. This can be latitude in decimal degrees or units of distance from the central meridian for projected data (usually in kilometers) (real*4).
z(1,...,N)	N dependent variables (real*4 for each one), where N depends on the program. However, most programs expect 6 dependent variables, following the standard post file formats for magnetic and gravity data, described below.

Gravity Post File

Field	Description
id	8 ASCII characters of gravity station identification.
x	x coordinate of record. This can be longitude in decimal degrees or units of distance from the central meridian for projected data (usually in kilometers).
y	y coordinate of record. This can be latitude in decimal degrees or units of distance from the central meridian for projected data (usually in kilometers).
z(1)	Free-air anomaly in mGal.
z(2)	Complete Bouguer anomaly in mGal, assumed reduction density=2.67 g/cm^3 (2670 kg/m^3).
z(3)	Elevation in feet or meters.
z(4)	Inner-zone terrain correction used to compute the complete Bouguer anomaly, in mGal, assumed reduction density=2.67 g/cm^3 (2670 kg/m^3). Inner zone is usually 0-5 km from station.
z(5)	Outer-zone terrain correction used to computer the complete Bouguer anomaly, in mGal, assumed reduction density=2.67 g/cm^3 (2670 kg/m^3). Outer zone is usually 5-167 km from station.
z(6)	Observed gravity minus 980,000 mGal.

Field	Description
id	8 ASCII characters of flight line identification.
x	x coordinate of record. This can be longitude in decimal degrees or units of distance from the central meridian for projected data (usually in kilometers).
y	y coordinate of record. This can be latitude in decimal degrees or units of distance from the central meridian for projected data (usually in kilometers).
z(1)	Residual magnetic data, i.e. total field intensity minus IGRF or DGRF, in nanoTesla.
z(2)	Total field intensity magnetic data, in nanoTesla.
z(3)	Height above terrain, in meters.
z(4)	Barometric elevation, in meters.
z(5)	Fiducial number.
z(6)	Year and Julian day as YEAR.DAY (e.g., February 3, 1985 would be 1985.034).

DESCRIPTION OF USGS XYZ FILE FORMAT

The xyz file is a binary file containing 3 real*4 words per record. Each record contains the following fields.

Field	Description
x	x coordinate of record. This can be longitude in decimal degrees or units of distance from the central meridian for projected data (usually in kilometers).
y	y coordinate of record. This can be latitude in decimal degrees or units of distance from the central meridian for projected data (usually in kilometers).
z	data value (any type) at the location described by x and y.

DESCRIPTION OF IMAGE FORMATS

Two image display programs are supplied; each uses a different image format. The DISPLAY program uses the REMAPP (REMote sensing Array Processing Procedures) image format (Livo, 1990, USGS Open-File Report 90-88). Grids can be converted to REMAPP images by using the program GRDREM in the REMAPP software package.

The IMVIS display system uses a modified PDS (Planetary Data System) image format. Grids can be converted to PDS graytone images by using the GRD2IMG batch program, to color shaded-relief PDS images by using the CSR batch program, or to color edge-enhanced PDS images by using the CEDGE batch program (Phillips and others, 1993, USGS Digital Data Series DDS-9).

INTRODUCTION TO USGS POTENTIAL-FIELD SOFTWARE

This section describes the three sets of software diskettes given to workshop participants. These are the potential-field software package version 2.0 from Open-File Report 92-18 (Cordell and others, 1992), a set of updated potential-field programs (version 2.11) essentially from CD-ROM DDS-9 (Phillips and others, 1993), and the REMAPP image display software package from Open-File report 90-88 (Livo, 1990).

HISTORY

The USGS (U.S. Geological Survey) began developing software for reduction and interpretation of potential-field geophysical data shortly after we helped to pioneer the airborne magnetometer in the late 1940's. Originally, each scientist wrote his or her own software, following his or her own unique format. In 1971 we established a standardized binary format for grid, line, and point data, thereafter allowing programs developed by many scientists to be shared. The result was a pool of constantly evolving software representing, over time, a combined effort which could not be duplicated without substantial cost in research, development, and mistakes.

Recognizing this software system to be a potentially valuable resource, we provide the system for implementation on personal computers. Personal computers are widely available worldwide and provide a good medium for training and technology transfer, even if the software will eventually be installed on a larger computer or modified. Although most of these programs have been in use for some time on other types of computers, some are new, and few of the programs have been much exercised and tested on a personal computer. Some of the programs have been released in earlier reports (Godson and Mall, 1989, for example). Version 2.0 of the system (Cordell and others, 1992) represented a major consolidation and upgrade. This version (2.11) comprises version 2.0 with updates and additional programs. Some program bugs have been repaired, but others no doubt remain, and new programs are continually being developed. We plan to release upgrades 2.2, 2.3... through USGS Map Distribution in due course. In this spirit, we ask that users please report errors and malfunctions to:

Jeffrey D. Phillips
U.S. Geological Survey
Box 25046
Federal Center MS-964
Denver CO 80225
USA

With the exception of the menu system (WMS.EXE AND WAITER.OVL), the programs are not subject to copyright and can therefore be freely copied, distributed, and modified, although the official version can only be obtained through USGS Map Distribution.

Authorship of the larger programs is indicated in the help files and source code. However, many codes have been subsequently modified by others. Names of authors of well-known algorithms are mentioned here for identification of the algorithm; full citations will be found in the help (.hlp) files, which are accessible through the PFHELP utility.

DISCLAIMER

Although these programs have been used by the U.S. Geological Survey, no warranty, expressed or implied, is made by the USGS as to the accuracy and functioning of the programs and related program material, nor shall the fact of distribution constitute any such warranty, and no responsibility is assumed by the USGS in connection therewith.

REFERENCES

Cordell, Lindrith, Phillips, J.D., Godson, R.H., 1992, U.S. Geological Survey potential-field geophysical software version 2.0: U.S. Geological Survey Open-FIle Report 93-18, 18p., 6 diskettes.

Godson, R.H., and Mall, M.R., 1989, Potential-field geophysical programs for IBM compatible microcomputers version 1.0: U.S. Geological Survey Open-File Report 89-197, 23p., 5 diskettes.

Livo, K. Eric, 1990, REMAPP-PC remote sensing image processing software for MS-DOS personal computers version 1.00: U.S. Geological Survey Open-File Report 90-88A-E, 64 p., 4 diskettes.

Phillips, J.D., Duval, J.S., and Ambrosiak, R.A., 1993, National geophysical data grids: gamma-ray, gravity, magnetic, and topographic data for the conterminous United States: U.S. Geological Survey Digital Data Series DDS-9, 1 CD-ROM.

All publications can be purchased from:

USGS Map Distribution
Box 25286, Building 810
Denver Federal Center
Denver, CO 80225
Phone: (303) 236-7476

HARDWARE REQUIREMENTS

The software distributed through this course is designed for processing of geophysical data on a personal computer running under the DOS operating system. The software requires that the computer have a full 640 kbytes of memory and a math coprocessor. A 386/33 or 486 processor, a VGA or super VGA graphics adaptor, and a large hard disk are recommended.

INSTALLATION

Begin by installing the original potential-field software (version 2.0) from OF 92-18. Insert the INSTALL disk (disk #1) in the floppy drive. Go to the hard drive and create a directory named PF. Make this your default directory. Copy install.bat from the INSTALL disk, and run it. For example, to install from the b: floppy disk drive to the c: hard drive, type the following five commands:

```
c:
cd \
md pf
cd pf
copy b:install.bat
install b
```

Next install the potential-field software updates from the version 2.11 INSTALL diskette. Insert the diskette in the floppy drive; go to the PF directory on the hard drive; copy install.bat from the INSTALL disk, and run it. For example, to install from the b: disk drive, type the following four commands:

```
c:
cd \pf
copy b:install.bat
install b
```

ORGANIZATION

The installation procedure will create the following subdirectories:

\PF\BIN - containing the executable files
\PF\SOURCE - containing the source files
\PF\HELP - containing the help files
\PF\TEST - containing test data files
\PF\PLOT - containing the plot library source files
\PF\CONTOUR - containing the contour program source files

Once C:\PF\BIN is added to your PATH statement in the AUTOEXEC.BAT file and the computer has been rebooted, the potential field software can be accessed from within a menu system by typing the command PFMENU at the DOS prompt. Alternatively, the individual programs can be accessed from the DOS prompt by typing their names.

Within the menu system, the programs are organized into submenus by topic (Fig. 6-1). A short description follows each program name. Some programs appear under more than one topic. A program can be invoked by highlighting it in the menu using the mouse or arrow keys and hitting the Enter key.

Figure 6-1.-- **PFMENU INDEX**

DISPLAY PROGRAMS

CONTOUR	DETOUR	DETOURG	DISPLAY	EXAMPLE	GRDREM
NORMAL	PMASK				

IMAGE GENERATION

CEDGE	CEE	CSHADE	CSR	GRADIENT	GRD2IMG
GRDREM	HISTNORM	IMVIS	MAKELBL	NORMAL	RAINBOW
RAINPAL	RAINZERO	REDUCE	REM2DAT	REG3	SHADE
XYZ2GRF	ZEROPAL				

QUICK IMAGE GENERATION

CEDGE	CSR	HISTNORM	GRD2IMG	ADDPAL	IMVIS
RAINPAL					

FILTERING

AVER2D	CHESS	GRADIENT	MEDIFILT	NORMAL	SURFIT
TAYLOR	TERRACE				

FFT FILTERING

	CK_DIMS	PREP	FFTFIL	DE_PREP	PROFFILT
	PROFFT	PROFSPEC			

F_OPTIONS

	F_ADD	F_AMP	F_A_AMP	F_AZIM	F_DECOMP
	F_DX	F_DY	F_DZ	F_GRAV	F_MAG
	F_POT	F_RTP	F_SRAS	F_STRIP	

MATCHED FILTERING

MFINIT	MFDESIGN	MFFILTER	MFPLOT

GRID MERGING PROGRAMS

ADDGRD	COMPGRD	EMPTY	GMERGE	INSERT	JIGSAW
JMRG	MAGMRG	MEGAPLUG	TILT	UTILITY	

GRID UTILITY PROGRAMS

ADDGRD	ASCII2SF	COMBGR	CORREL	DECIMATE	DVAL
EMPTY	G2XYZ	GHIST	GRAFEDIT	GRDMAX	GRDREM
GRD_STAT	ID	IGRFGRD	INSERT	JIGSAW	LOG
MEDIPLUG	MEDIPLG1	MEGAPLUG	PRJGRD	PRJPT	PROFGRD
REGRID	SCALE	SF2ASCII	SHODVALS	SKIM	STDBNDY
SURFIT	TILT	TRANSPOS	TRIMGRD	UTILITY	

INTERPRETATION & MODELING

BOUNDARY	GI3	GRAVPOLY	IGRFPT	MAGPOLY	PFGRV3D
PFMAG3D	SAKI	TERRACE	VARMAG	WERNER	

MISCELLANEOUS PROGRAMS

EDIT	FORC	MTYPE	RDEL

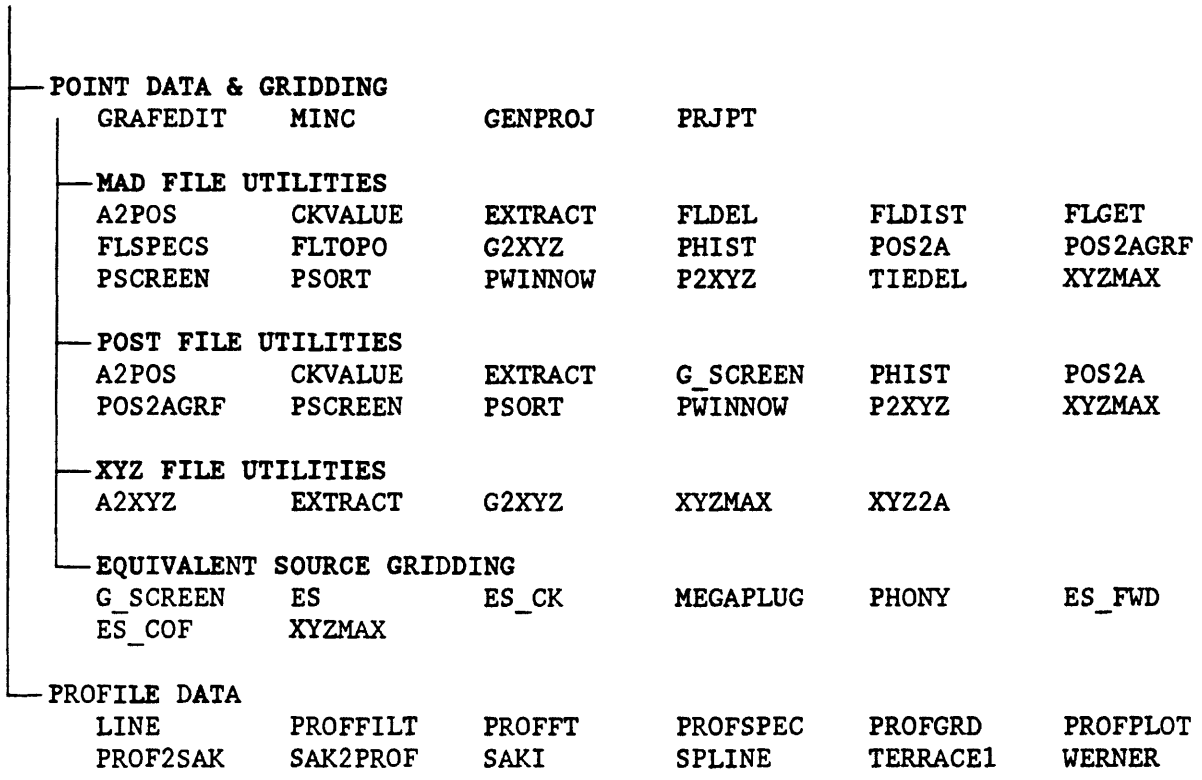

Figure 6-1.--continued

ONLINE HELP AND DOCUMENTATION

Each submenu contains a ** HELP ** entry that can be used to display a somewhat longer description of each program in that catagory. Detailed help on individual programs can be displayed by typing the program name when the 'program name:' prompt is displayed, or by entering the program name in the command line window of the menu. The help facility can also be invoked from the DOS prompt by typing PFHELP or PFHELP 'program_name'. Each submenu also contains a DOS menu entry that invokes a DOS shell for executing DOS commands. To return to the menu from the DOS shell type EXIT and hit the Enter key.

GENERAL PROGRAM OPERATION

A program is started by typing its name on the command line. Parameters and data are communicated to the program either by typing responses to prompts or by means of a namelist-based command file, normally having file-name suffix ".cmd". Command files begin with &parms and end with &. See the examples under general program conventions and the program help (.hlp) files.

New with version 2.1 (Phillips and others, 1993) is a menu system for accessing the potential-field programs. Once the programs are installed, the menu system can be started by typing PFMENU at the command line and pressing the <Enter> key. The menu system assumes that the directory containing the executable programs is in the user's PATH, and it uses the DOS 5.0 editor EDIT to edit command files for programs requiring them. Each level of the menu contains a HELP option for accessing the help files and a DOS option for temporarily exiting to DOS. The menu system can be modified or customized (to add additional programs, for example) by using the <Ins> or <Insert> key. You may find that some of the larger programs, like CONTOUR and DISPLAY, may require too much memory to execute from within the menu system, especially if you have memory-resident software installed.

Command Files

Many programs in the potential-field software package require a command file to input most or all of the parameters for the program. Command files, usually designated with the file extension **.cmd**, start with the delimiter **$parms** (or **&parms**) and end with the delimiter **$** (or **&**). In between the delimiters, the parameter names are given and equated to the input value for that parameter, following the format prescribed in the documentation or help file for the program. For example, if a program requires input of parm1 (a real number), parm2 (a character name), parm3 (an integer), and parm4 (two real numbers), a command file might look like the following.

```
$parms
parm1=1.2, parm2='filename', parm3=5, parm4= -245.2, 305
$
```

The delimiters need not be given on separate lines. Note that all character parameters, such as file names, are enclosed in single quotes. Many programs will ask for required parameters not given by the command file; the documentation usually states which parameters these are. Some programs also require information starting on the line after the end delimiter.

Questions That Contain Items In Brackets

1. If there is only one item inside the brackets, this is the default response and will be used by the program by pressing ENTER. For example, by pressing ENTER in answer to the question that follows, the program will next ask for a constant value instead of a second input file.

```
second input grid [constant]?
```

2. Several items inside the brackets give the preferred form of the answer. In the following example, the program accepts a one-letter answer as listed in the brackets.

```
Want to see histogram, standard dev., both, or none [h,s,b,n]?
```

Geographic Conventions

Longitudes are negative if west of Greenwich and latitudes are negative if south of the equator. Projections are referred to by number according to the following:

1: American polyconic
2: ellipsoidal transverse Mercator (sometimes referred to as UTM)
3: Mercator
4: Lambert. Lower and upper parallels can be specified or default to 33 and 45 degrees.
5: Albers equal area for conterminous U.S. Standard parallels are 29.5 and 45.5 degrees.
6: Albers equal area for Alaska. Standard parallels are 55 and 65 degrees.
7: Albers equal area for Hawaii. Standard parallels are 8 and 18 degrees.
8: reserved
9: spherical transverse Mercator (special for Geological Society of America's "Decade of North American Geology" map series).

Rules Of Thumb When In Doubt

1. If the program is asking for a file name or format, try a carriage return to use the default or bypass the question.

2. If the program is asking for a function or command file and the proper answer is unclear, try typing **h** or **help**. (One notable exception is program UTILITY, which uses **h** for another function. In this case, when asked for a function, type a wild character, such as **?**, and you will get a list of available functions.)

3. If the program is asking for an option that is an integer, try typing **0** or **999** to get a list of options.

Some of the data grids on the data diskettes have been trimmed of some of the exterior rows and columns that are entirely flagged as having no data (files with extension .trm). Thus, these grids do not have the same dimensions as grids of the full Getchell area (files with extension .grd). The coarse grid files (with extension .cgd) have larger grid intervals and different dimensions also. This is a problem if you wish to compare two grids with programs like **ADDGRD** (demonstrated later). The following demonstrates the procedure for getting a trimmed grid to match the specifications of a whole-area grid. This also demonstrates the capabilities of the programs **ID**, **UTILITY**, and **GHIST**, which report on the grid specifications, manipulate aspects of the grid structure and values, and look at the data distribution, respectively. These examples constitute part of the independent exercises presented later in this chapter (p. 6-22). A full description of the files used below are found in Chapter 12.

```
C:>id
Enter input file name:
gboug.grd
* Getchell Bouguer gravity 2.67, UTM 0 117
min-curv
ncol =  387     nrow =  496     nz =  1
x0 = -46.00000      dx =  .1000000       y0 =  4525.000      dy =  .1000000
Stop - Program terminated.


C:>id
Enter input file name:
gres72.trm
* Log10 of Getchell 7200-Hz apparent resist., decorrugated
trimmed
ncol =  341     nrow =  495     nz =  1
x0 = -41.80000      dx =  .1000000       y0 =  4525.000      dy =  .1000000
Stop - Program terminated.
```

Note the different grid specifications of the files. Now we'll use **UTILITY** to match **gres72.trm** to **gboug.grd**.

```
C:>utility

function : 2                                  <<Look at available options first
available operations
r reorder elements
x extract subset
l look at grid values
h change header info
e edit grid points
m merge subset- xo,yo in number of cols,rows offset
c binary xyz coordinate output
s stop
```

```
function : x
input grid : gres72.trm
output grid : gres72.grd
id=Log10 of Getchell 7200-Hz apparent resist., decorrugatedpgm=trimmed
nz=1  size=   341  495
xo,yo = -41.80000      4525.000      dx&dy=    .10000        .10000
output grid title
Getchell log10 of 7200 Hz apparent resistivity
>> new origin
enter either 0 for integer starting location
          or 1 for lower-left coordinate
1
enter lower-left x,y coordinate in data units
-46 4525
>> output size
enter either 0 for ending column and row number
          or 1 for upper-right coordinate
          or 2 for specified ncol, nrow
2
enter new dimensions (integer ncol,nrow)
387 496
output grid ncol,nrow will be         387         496

function :l                                  << the letter l as in "look"
input grid :gres72.grd
id=Getchell log10 of 7200 Hz apparent resistivity          pgm=trimmed
nz=1  size=   387  496
xo,yo = -46.00000      4525.000      dx&dy=    .10000        .10000
row : -1

function :s
Stop - Program terminated.
```

Now if we want to take a quick look at the data distribution of GRES72.GRD, we can use the program **GHIST**.

```
C:>ghist
Enter input file:
gres72.grd
minimum=  .8274294E-01          maximum=  4.033751
mean=  1.912304              max - min =  3.951009
       78315 valid points,    40.80% of grid
Want to see histogram, standard dev., both, or none [h,s,b,n]?  b
I found histogram interval of   .3700000    , giving  10 histogram classes
Want to redefine interval ? y
Enter new interval: .4
Interval of   .4000000     gives   9 histogram classes
Want to see percent or count of values [p or c]?  c

Standard Deviation =   .6145250
```

```
midpoint (interval=     .4000    )   HISTOGRAM

 .8300E-01 |     26
 .4830     |X    585
 .8830     |XXXXXX   3251
 1.283     |XXXXXXXXXXXXXXXXXXXXXXXXXXXX  14650
 1.683     |XXXXXXXXXXXXXXXXXXXXXXXXXXXXXXXXXXXXXXXXXXXXXXXX  25247
 2.083     |XXXXXXXXXXXXXXXXXXXXXXXXXXXX  16140
 2.483     |XXXXXXXXXXXXXXXXX   9583
 2.883     |XXXXXXXX   4171
 3.283     |XXXXX   2865
 3.683     |XXX   1704
 4.083     |     93

REPRINT info, CHANGE histogram, or STOP [r, c, or s]? s

Stop - Program terminated.
```

Matching the coarse-interval grids to the fine-interval grids requires program **REGRID**, which re-interpolates values at new grid points. This procedure is demonstrated next.

```
C:>regrid

file to be interpolated :  gu.cgd

Getchell uranium surface concentration (ppm)              pgm:gdcnv
ncol=  194 nrow=  249
xo,yo=    -46.000         4525.0       dx,dy=     .20000          .20000

output file :  gu.grd
title :
Getchell uranium (ppm)

new dx,dy :  .1 .1
change location or areal coverage ?  y

enter new  x origin, y origin, ncol, nrow :
-46 4525 387 496

Stop - Program terminated.
```

INTRODUCTION TO REMAPP IMAGE-PROCESSING SOFTWARE

Version 1.03 of REMAPP-PC has been modified from version 1.00 for tighter integration with the USGS Potential Fields software Open File (OF 92-18). Several new programs have been added to convert data back and forth from USGS Grid format to USGS REMAPP format.

Introduction

The REMote sensing Array Processing Procedures (REMAPP) is a series of programs for processing satellite and aircraft digital image data, such as Landsat Multispectral Scanner (MSS) and Thematic Mapper (TM), Systeme Probatoire d'Observation de la Terre (SPOT), Airborne Visible and Infrared Imaging Spectrometry (AVIRIS), or other digital data. To use the REMAPP system an IBM-PC compatible computer with Video Graphics Array (VGA) color display and a hard disk are required. No additional software packages are needed to support REMAPP.

The REMAPP package is useful for image display and enhancement, and other more specific uses, such as mineral alteration studies and basic spectral work. Image processing routines include mathematical operations, image statistics, contrast enhancement, spatial and color coordinate transformations, edge enhancement, and masking. Image files are supported with file management, file utility, and file import/export routines. All routines are stand-alone programs.

Image files may contain a maximum of 8192 pixels (picture elements) per scanline as 8 or 16-bits/pixel data, with the number of scanlines restricted only by the amount of hard disk storage capacity. Image file format consists of a REMAPP header record followed by single band or band interleaved by line (BIL) binary image data.

Images are displayed using up to 256 colors or 64 shades of gray, with 8 graphic plane colors available in either mode. Maximum screen resolution is 200 scanlines by 320 pixels; however, larger files may be displayed by windowing or subsetting the data within the display program, yielding larger spatial coverage with degraded resolution. All image processing routines however, retain full eight or 16-bits per pixel DN precision.

History

The 'REMAPP' system was developed over a period of years by the U. S. Geological Survey, Branch of Geophysics, using several mini-computers. Some of the most useful stand-alone subroutines have been converted here to run in the MS-DOS environment. Tying the image processing system together is the display driver program DISPLAY, that enables digital image data to be displayed and analyzed. The driver package includes image buffers, graphics overlays, cursor, histogram stretch and windowing capabilities.

REMAPP-PC Version 1.00 (Open-File Report 90-88) has been published as USGS Open File Report 90-88. Version 1.00 contains a single file - per image data format. This original open file does not integrate with the potential field software.

REMAPP-PC Version 2.00 (Open-File Report. 91-449) the current standard release, but uses a more complicated subdirectory/file structure. This version contains the programs found in version 1.00 plus imaging spectrometry routines and MS-Window pif files.

REMAPP-PC Version 1.00 modified (version 1.03, this release) contains all the version 1.00 programs, plus a modified DISPLAY, and extra programs which are useful with the potential field software. This release includes the most useful programs from version 2.00 and version 3.00.

Future

REMAPP Version 3.00 is in pre-beta test. It compiles on PCs, and the UNIX Sun, HP, and Data General computer systems. PCs will contain both DOS and MS-Windows display versions. UNIX versions use an X-window display program (Pick Works - see future open file). This version also contains potential fields software extensions, as well a selectable variety of file formats. Completion date is probable in early 1994.

Disclaimer

This report is preliminary and has not been reviewed for conformity with the U.S. Geological Survey editorial standards. Use of trade names in this report is for descriptive purposes only and does not imply endorsement by the USGS.

Although this program has been used by the U.S. Geological Survey, no warranty, expressed or implied, is made by the USGS as to the accuracy and functioning of the program and related program material, nor shall the fact of distribution constitute any such warranty, and no responsibility is assumed by the USGS in connection therewith.

Hardware Requirements

This image processing system requires an MS-DOS IBM compatible PC computer with 640 kilobytes of system memory and a VGA graphics display.

Optional equipment is a math coprocessor, which is highly recommended (and is required for the potential-field software). All programs have been compiled to run on the entire family of Intel PC CPU chips, with or without math coprocessor chips. A math coprocessor will automatically be used if present.

The program DISPLAY is the only program requiring specific equipment. All the other programs are non-graphic and will run on PC's with any video display. DISPLAY

requires VGA graphics and 640 kilobytes of system memory, of which something over 530K needs to be free (use MEM or CHKDSK to check). Multiprocessing with these DOS programs is available with 386 class PC's using Microsoft Windows 3.1.

Installation

An install program can be used to copy all files from the distribution disks. To install the software into the default directory \PCREMAPP, log onto the floppy drive (A: or B:) containing the INSTALL disk, then type:

INSTALL <floppy drive> <hard-drive> (e.g., INSTALL A: C:)

where the floppy drive is either A: or B:, and the hard-drive is C: or greater. INSTALL will place all executable programs in the default directory \PCREMAPP under the subdirectory \BIN. For proper program execution, set the PATH environmental variable, in autoexec.bat, to include this subdirectory (i.e., PATH=C:\PCREMAPP\BIN).

At least 530 kilobytes of free memory are required for the DISPLAY and REMROT programs to run properly. To gain this much free memory, memory managers are sometimes required. MS-DOS versions 5.0 and 6.0, and MS-Windows 3.x contain the HIMEM.SYS and EMM386.EXE memory managers. On 386 class machines, place the statements:

```
DEVICE=C:\WINDOWS\HIMEM.SYS
DEVICE=C:\WINDOWS\EMM386.EXE
DOS=HIGH,UMB
```

into the CONFIG.SYS file, and:

SMARTDRV.EXE (into the AUTOEXEC.BAT file)
or
SMARTDRV.SYS (into the CONFIG.SYS file).

Use whatever options for these commands suit your needs (see your DOS or WINDOW manual). HIMEM.SYS maps the computer memory as linear extended memory. EMM386.EXE re-maps this extended memory as expanded memory. DOS=HIGH places most of the DOS resident program into the first 64KB of the second megabyte of memory, while DOS=UMB enables high memory access with DEVICEHIGH and LOADHIGH commands. SMARTDRV is a hard disk caching program which will help prevent disk thrashing and faster throughput.

Use with Potential Fields Software

The Potential Fields software package and the REMAPP-PC image processing software package complement each other. Geophysical reduction of the data may be performed in the GRID format, then graphically enhanced, analyzed, and interpreted visually. Because of the parallel development between GRID and image processing systems, many utility programs will perform the same operations. Histograms, math routines, and data and file maintenance may all be done in either system.

Visualization of the data may utilize imagery, color shaded relief, or contour plots. DISPLAY, IMVIS, and CONTOUR provide these results. Each program has its own strengths. DISPLAY presents, contrast enhances, color composites, and interacts rapidly with image data. It lacks in having a small display area (320 x 200) and coarse color composites. The other programs have similar unique advantages. Consideration of the program goal and thought to data processing and analysis can use the best features of these programs to your advantage.

INDEPENDENT PC EXERCISES I

1. Following the installation directions on page 6-9, install the potential-field software from the diskettes in 93-560B (this assumes you already have available the diskettes from open-file 92-18). Following the installation directions on page 6-20, install the REMAPP software from the diskettes in 93-560C. Be sure to reconfigure your config.sys (if necessary) and autoexec.bat files. Don't forget to edit the PATH statement in the autoexec.bat file and reboot.

2. Invoke the menu system by typing **pfmenu**. Referring to the menu tree on figure 6-1 (p. 6-10), browse through the menu. The items in each menu can be chosen by moving the mouse or arrow key to highlight the desired function then hitting return. If the first letter of the function is unique in the menu, the function can be invoked by typing that letter. Remember that you can use the + key on the numeric pad to move down the menu list if it is too long to fit on one screen, and the - key to get back up the list. The ESC key can be used to quickly get out of a menu and to DOS, if so desired. A function is available in the submenus to temporarily leave the menu and go to the DOS environment. Type **exit** from the DOS prompt to get back to the menu. After running a program, you will automatically return to the menu or you will be asked to hit any key to return.

FROM NOW ON, PROGRAMS WILL BE REFERRED TO BY NAME, NOT BY LOCATION IN THE MENU AND SUBMENUS. WE RECOMMEND YOU USE THE PFMENU SYSTEM AND REFER TO THE MENU MAP ON FIGURE 6-1 TO FIND THE PROGRAM DESIRED.

3. From the DOS environment, make a directory to contain test data sets (such as **c:\workshop**). Full descriptions of data sets available are contained in Chapter 12. Copy the file **gmag.trm** from diskette #1 in 93-560D to this directory. This grid file represents the magnetic data that was flown by DIGHEM. Get into **pfmenu**. Following the demonstration of **UTILITY** (starting on p. 6-15), extract a subset from gmag.trm, called **gmagsub.grd**, that has the following grid specifications:
   Lower left coordinate (xo, yo) = -31 4551
   New dimensions (ncol, nrow) = 128 128
   New title suggestion: Subset over pluton, Getchell DIGHEM mag, UTM 0, -117
   Use the look function to check the grid specifications of your subset.

4. Use **GHIST** to look at a histogram of **gmagsub.grd**. The statistics should look like this:

```
minimum= -1029.969              maximum=  1226.719
mean=  154.0145               max - min =  2256.688
       14340 valid points,     87.52% of grid
```

   Generate a few histograms using different class intervals. If you pick too small an interval you'll have trouble seeing the whole histogram.

Chapter 7. Displaying Grids

DISPLAY TYPES

The way geophysical data are presented on a map is very important because each form of display can bring out different features of the data. Therefore, a variety of forms of display should be examined.

Display techniques have several forms: (1) line-contour maps, where contour lines follow constant values of the data; (2) color-density slice maps, where each data interval is represented by a different color; (3) graytone images, where data intervals are much smaller and are represented by a large range of gray tones; (4) gray-shade images, like graytone images except that the data are treated as though they have relief and are shaded by a sun at a particular angle, (5) color shaded-relief, which combines the colors of the color-density slice map with the shading of the gray-shade map, and (6) color edge-enhanced plots, which applies an algorithm to enhance abrupt changes in value ("edges") to color-density slice maps. Table 7-1 summarizes the strengths and weaknesses of each of these display techniques. An additional display technique is a color composite of three different input grids, described in more detail in Chapters 10 and 11. Table 7-2 shows the sequence of programs that can be run in order to accomplish various display techniques on grids.

Table 7-1. Comparison of Display Techniques

Display Technique	Type of Map Features Enhanced, Not Affected, or Suppressed				Parameters Controlling Display Capabilities (in order of importance)
	Gradients	Local or Small Variations	Regional Variations	Linear Features	
Line-contour	Enhanced	Suppressed	Suppressed	Not Affected	Contour interval
Color-density slice	Not Affected	Suppressed	Enhanced	Not Affected	Density-slice interval or how data are mapped to color ranges, choice of colors
Graytone	Not Affected	Enhanced	Not Affected	Not Affected	How data are mapped to graytones
Gray shaded-relief	Enhanced	Enhanced	Suppressed	Enhanced in one direction, suppressed in normal direction	Direction of illumination, how data are mapped to gray ranges, height of illuminated relief
Color shaded-relief	Enhanced	Enhanced	Enhanced	Enhanced in one direction, suppressed in normal direction	Direction of illumination, density-slice interval or how data are mapped to color ranges, choice of colors, height of illuminated relief
Color edge-enhanced	Enhanced	Enhanced if variations are abrupt, suppressed if not	Enhanced	Not Affected	Density-slice interval, choice of colors, parameters of edge-enhancement algorithm

Table 7-2. Sequence of programs to follow for application of various display techniques to grids

Program Sequence	Page number of example, if applicable	Line-Contour	Color-Density Slice	Graytone	Gray Shaded-Relief	Color Shaded-Relief	Color Edge-Enhanced	Color Composite
CONTOUR	7-16	X						
DETOUR		X						
DETOURG		X						
GRAFEDIT		X						
GRDREM, HIST (optional), STRETCH (optional), DISPLAY	7-18			X				
GRDREM, HIST (optional), STRETCH (optional), DISPLAY (functions O, K)			X					
GRDREM on 3 input grids, DISPLAY (functions D, I, and M)	10-6							X
NORMAL, GRDREM on the 3 output grids, DISPLAY (functions D, I, and L)					X			
NORMAL, SHADE, GRDREM, DISPLAY (function B)					X			
HISTNORM (optional), RAINBOW, GRDREM on the 3 output grids, DISPLAY (functions D, I, and M)			X					
SHADE, HISTNORM (optional), RAINBOW, CSHADE, GRDREM on the 3 output grids, DISPLAY (functions D, I, and M)						X		
GRADIENT, HISTNORM (optional), RAINBOW, CEE, GRDREM on the 3 output grids, DISPLAY (functions D, I, and M)							X	

continued on next page

Table 7-2.--continued

Program Sequence	Page number of example, if applicable	Line-Contour	Color-Density Slice	Graytone	Gray Shaded-Relief	Color Shaded-Relief	Color Edge-Enhanced	Color Composite
GRD2IMG, IMVIS				X				
HISTNORM (optional), GRD2IMG, RAINPAL or ZEROPAL, ADDPAL, IMVIS	7-38		X					
NORMAL, SHADE, GRD2IMG, IMVIS					X			
CSR, IMVIS	CSR: 7-40					X		
CEDGE, IMVIS	CEDGE: 7-41						X	
GRDREM on 3 input grids, RSG3, REDUCE, IMVIS	11-1							X
GRD2IMG on 3 input grids, edit .LBL file, IMVIS, REDUCE, IMVIS	11-3							X

CONTOUR PLOTS

Four programs are provided for producing contour plots of data. The CONTOUR program is a general map production program that can produce contour maps from grids. DETOUR is a quick program to contour scattered data on the screen. DETOURG is a quick program to contour gridded data on the screen. GRAFEDIT is a graphical program for editing scattered data points; it can also be used to display contours of grids on the screen. We will start by looking at the extensive help file for CONTOUR.

CONTOUR PROGRAM HELP FILE

CONTOUR (originally named PCCONTUR) produces contour plots of two-dimensional data that are in standard USGS grid format. Scattered data must be transformed into a standard grid using a gridding program such as MINC. CONTOUR recognizes grid values in excess of 1.0E37 as uncontourable, and thus irregularly shaped data sets may be contoured. In addition to plotting contours, the program allows plotting of text, lines, symbols, labels, and geographic coordinate ticks.

Reference: Godson, R.E., Bracken, R.E., and Webring, M.W., 1988,
U.S. Geological Survey Open-File Report 88-593B

The original program was developed by Gerald I. Evenden on a Decsystem-10 computer in the early-mid 70's (Evenden,G.I., 1975, U.S. Geological Survey Open-File Report 75-317.)

Usage:

Create a namelist command file beginning with "$parms" or "&parms" and ending with "$" or "&". Run the program and respond with the name of the command file at the prompt. Essentially all parameters have standard default values, so usually only a small number of parameters need to be set by including them in the namelist file. It is also possible to run the program without a namelist file, in which case all parameters are set to their default values.

Example command file:

```
$parms dcval=2,fmtc='(f6.0)',fmtx='(f10.0)',fmty='(f10.0)',
gradi=60.,idashs=0,iplotr=4,neat=0,nsec=1,size=0.08,
sizex=0.08,sizey=0.08,sizel=.12,nchar=6,
title2='ANY TOWN  USA',xscale=0.,yscale=0.,lintx=15,
linty=15,title3='ANY TITLE',nsig=1,sigma=1.0,itpost=2,
baslat=43,30,00,cm=-104,00,00,iproj=2,pllx=1.0,plly=1.0,
latm=43,00,00,latx=44,00,00,longm=-103,00,00,longx=-105,00,00,
sizep=0.08,tint=15,unit=2.  $
```

Namelist Parameters:

Note: to list parameter values at runtime, set parameter IVERB=1. Otherwise IVERB defaults to 0.

Input grid

IFILE - the name of the gridded data file to be contoured. It must be enclosed in single quotes. Default is blanks, which means that the program will prompt for the name.

Contour_Levels

These parameters control the plotting of contours and their labels. Note that ACVAL and DCVAL are mutually exclusive and that NCVAL controls which is used.

To bypass contour plotting set NCVAL=1 & ACVAL=1.e37 or DCVAL=1.e37

ACVAL - An array of length NCVAL containing specific contour levels to be plotted. These may be arranged in any order. The ACVAL array may be specified in the fifth column of the ACFILE.

NCVAL - the number of values specified for ACVAL. Default is zero which means that contours will be plotted at a constant interval specified by DCVAL.

DCVAL - the contour interval. The value must be greater than zero if ACVAL is not used. Default is -1 for automatic setting. For this parameter to be effective, NCVAL must be set to 0.

CMIN - the lower limit of the contour values when DCVAL is used. If CMIN is less than the minimum value of the data, then the minimum data value is used to determine the first contour value. Default is zero.

CMAX - the upper limit of the contour values when DCVAL is used. If CMAX is greater than the maximum value of the data, then the maximum data value is used to determine the last contour value. Default is zero. If both CMIN and CMAX are zero, then the range of contouring is determined from the data.

NSEC - the interval of contour levels which are considered primary. This parameter is used when dcval is specified. Only primary contours are labeled. Default is 5.

FMTC - the format to be used for labeling the contour values (either F or E format). The parameter must be enclosed in single quotes, e.g., '(f5.0)'. A maximum number of 16 characters can be used. Default is blanks for automatic determinaion of a proper format.

NCHAR - the maximum number of characters to be used from the above format when labeling the contours. For example, with NCHAR equal to 4 and FMTC equal to '(f5.0)', four digits would be plotted without a trailing period. Contour labeling is performed for all specified contour levels (ACVAL) and for all primary incremental levels (NSEC). Default is -1 for automatic determination in connection with FMTC.

SIZE - the height in inches of labeled contour values. Default is 0.1.

DELB - the distance in map inches between contour line labels. Default is 7 inches.

IDASHS - determines line thickness and also which lines are to be dashed.
IDASHS = + or -(N + ITH * 8) where:
N = 0 = all contours plotted as solid lines
N = -1 to -6 secondary contour lines are plotted as dashed lines
N = 1 to 6 = primary contour lines are plotted as dashed lines
ITH = the additional thickness of the primary contours; e.g.
ITH = 1 produces primaries twice as wide, ITH = 2 produces primaries three times as wide, etc.

GRADI - the maximum gradient in contour lines per inch before the secondary contours in a grid cell are not plotted. Default is 30.

CONLIM - the minimum length, in map inches, required for any contour line to be plotted. Shorter contour lines, closed or unclosed, will not be plotted. Default is 0 which means no checking for contour length will be performed.

ACFILE - the name of an ASCII free format file containing parallel columns of the following arrays: ACVAL,ACDEL,ACGRAD,JCDASH,ACSIZE,ACMIN and ACMAX in that order. Each line in the file is like a miniature self-contained contouring package. That is, each line is independent of the other lines and will make its own set of contours according to the values on that line. The lines may be arranged in any order and on any given line the last few columns may be left blank. In this case, default values will be substituted. Blank columns may not be followed by non-blank columns. A single period (.) will be taken as a ditto mark and value of that column will be taken from the line above. Any non-numeric character on a line will signify the beginning of a comment, and everthing after will be ignored. Default for ACFILE is blanks and therefore any of the above variables to be used must be in a command file or input interactively. Following is an example of an ACFILE.

```
C  ACVAL    ACDEL    ACGRAD    JCDASH    ACSIZE    ACMIN    ACMAX
C  DESCRETE CONTOUR LEVELS
   1000      1000       50        16       .12  C THESE COLUMNS
      0         .        .         .         .  C DO NOT
   1000         .        .         .         .  C APPLY
```

```
C
C  GENERAL CONTOUR LEVELS
     0    -2500       50        8          .10     -12500    20000
     0     -500        .        8  C THESE COLUMNS WILL DEFAULT
     0     -100        .        0          .08      -2000     3000
     0      -20        .        0           0.       -300      500
     0       -4        .        3           .         -80       80
C  END OF ACFILE
```

ACDEL - an array of length NCVAL specifying the maximum allowable gradient in z-data units per contour line before the corresponding contour line in array ACVAL will not be plotted within a grid cell. If any element of ACDEL is negative, the corresponding ACVAL is ignored and a set of contour lines are plotted at exact multiples of ABS(ACDEL) from the lowest portion of the map to the highest (or from CMIN to CMAX if specified or from ACMIN to ACMAX if specified). In this case the maximum gradient per contour line for each contour level is equal to ABS(ACDEL) (i.e., negative ACDEL determines both the contour interval and the maximum gradient in Z-data units per contour line whereas positive ACDEL determines only the maximum gradient in Z-data units per contour line for the corresponding ACVAL element). If more than one ACDEL is negative, the largest absolute value takes precedence. Default is 0, which means no dropping of contour lines or if NCVAL is 0, gradient information will be taken from DCVAL.

ACGRAD - an array of length NCVAL specifying the maximum allowable gradient in contour lines per map inch. The contour line will not be plotted across grid cells with higher gradients (the gradient in Z-data units per map inch = (gradient in Z-data units per contour line(ACDEL) * gradient in contour lines per map inch(ACGRAD))). Default is 0, which means gradient information will be from GRADI.

ACMIN - an array of length NCVAL specifying the minimum contour level when the contour levels are determined by a negative ACDEL. Default is 0, which means that if ACMAX is 0 then all possible contour levels will be plotted.

ACMAX - an array of length NCVAL specifying the maximum contour level when the contour levels are determined by a negative ACDEL. Default is 0, which means that if ACMIN is 0 then all possible contour levels will be plotted.

ACSIZE - an array of length NCVAL containing the label size in map inches for each contour level specified by ACVAL. Default is equal to SIZE. To eliminate labels set ACSIZE to 0.

JCDASH - an array of NCVAL color/pen numbers corresponding to the NCVAL contour levels in array ACVAL. Color/pen numbers are specified as the sum of the value of IDASHS and 100 for color/pen 1, 200 for color/pen 2, etc.

MXHACH - the number of closed contours surrounding a low which will be hachured. Any negative number will result in maximum hachuring of contours around closed lows. Default is 0, which means no hachuring.

HACHSP - hachure tick spacing in map inches. Default is 0.15 inches.

HACHLN - hachure tick length in map inches. Default is 0.05 inches.

HACHGP - non-zero values allow hachuring of contour lines which partially surround a closed low, but intersect the map edge or an area with no data. The ratio of the direct distance between the endpoints of the contour line to the length of the contour line must be less than HACHGP for hachuring to occur. Default is 0.

HACHLM - all contours around closed lows having a circumference less than HACHLM will be hachured regardless of the value of MXHACH. Default is -1 which means HACHLM = 7 * HACHSP.

HACHVB - the maximum circumference of a closed high beyond which surrounding closed lows will be hachured. Adjustment of this parameter may produce deceptive results on the map.

LOWHI - plot H or L symbols at local maxima/minima on contour plot. Local is defined by search radius in grid units (i.e. the incremental sampling interval). Example, LOWHI=3 will plot H/L if a grid value is the max/min in the surrounding 7 x 7 window.

SIZEHI - the size of the LOWHI symbols in map inches. Default is 0.08.

DGRAD - a LOWHI symbol will not be plotted unless the local relief, within the search radius, is at least DGRAD z-data units. Default is 0 which means all LOWHI symbols will be plotted.

ICAPT - any non-zero value will allow capture of contour lines to a disk file. The primary output file is called contour.cor and contains segments for each contour line consisting of a header line containing the contour level and the number of points in the contour followed by lines containing the coordinates of the contour line in data units. A secondary file, contour.val, contains the values of the contour levels.

Smoothing

NSIG - Setting NSIG to any number other than zero invokes the B-spline option. Default is zero for no splining.

SIGMA - Adjusts the smoothness of a splined curve. It is the maximum allowable error (in thousandths of an inch) between the spline contour line and a perfectly smooth curve. The minimum grid cell that will be splined is: 8 *[.001*SIGMA/(PI-2)]**2 square map inches. Decreasing sigma will increase the number of points in each line, resulting in higher resolution at the expense of CPU time. Note: A given value of SIGMA will result in uniform smoothness for all map scales and grid cell sizes. Default is 7.3 mils which is sufficient for raster plots with pixel sizes of 0.01 inches or larger.

Axis_labeling

NEAT - a value that determines whether a rectangular border will be drawn around the contour plot. The default is zero, meaning a border line will be drawn. Any other number will suppress the border.

TITLE2 - 56 characters of identification to be plotted below the 56 characters obtained from the header record of the input gridded data file. This parameter must be enclosed in single quotes, e.g., 'scale 1:250,000'. Default is blanks.

TITLE3 - 56 characters of identification to be plotted below TITLE2. This parameter must also be enclosed in single quotes and the default is blanks.

SIZEL - the height in inches of the title lines. Default is zero, which means no title lines will be plotted.

ADELX & ADELY - the interval in data units along the x & y axes where a tick will be made. Default is zero which means that only the minimum and maximum values will be posted.

LINTX & LINTY - the interval of x & y axis ticks to be labeled. Default is 5.

FMTX & FMTY - the format to be used when labeling the x & y axes (either F or E format). This parameter must be enclosed in single quotes, e.g., '(f9.2)', and is limited to 16 characters. Default is blanks.

NCHARX & NCHARY - the maximum number of characters to be used from the above format when labeling the x & y axes. Default is zero for no labeling.

SIZEX & SIZEY - the height in inches of the labeled x & y axis values. Default 0.1.

PLLX & PLLY - offset in inches of the x & y axes from the lower-left corner of the plot edge. Default is zero. These variables are used to provide space for axis labeling and title information.

Plotter_type_and_scaling

IPLOTR - a number which determines which plotter device is to be used.
5 = Hewlett-Packard plotters
8 = CGA video mode
9 = EGA video mode(default)
10 = VGA video mode

XSCALE & YSCALE - the x & y axes data units per inch. For example, if the grid interval is in inches then a value such as 250000 is used. Default is zero. If both XSCALE and YSCALE are zero then they will both be set to the same value that will allow plotting on the chosen plot device or 10 by 8 inches, whichever is smaller. If one scale factor is zero and the other not, then the nonzero scale factor will be assigned to the zero scale factor.

MSCALE - scaling factor that can be used in lieu of XSCALE and YSCALE. It is given in map scale units such as 62500, 250000, etc. Default is zero.

UNIT - the units of the grid interval in the input gridded data set to be contoured. 0 = inches, 1 = meters and 2 = kilometers. Default is 2. This parameter must be specified if MSCALE is used.

Geographic_data

The following variables are to be used if plotting of latitude/longitude tick marks are desired. they are to be used only when the gridded data set coordinates have been calculated from a projection program where the central meridian, base latitude and type of projection are known. The longitude units can be either positive or negative. The 'unit' parameter explained above must be specified to use this option of the program.

BASLAT - a three unit aray containing the base latitude in degrees, minutes and seconds. Default is 999,0,0.

CM - a three unit array containing the central meridian in degrees, minutes and seconds. Default is 999,0,0.

IPROJ - a number referring to the type of projection to be used.
1 = American polyconic
2 = ellipsoidal transverse mercator
3 = mercator
4 = lambert (see variables PHI1 and PHI2)
5 = albers equal area for the conterminous U.S. (standard parallels of 29.5 and 45.5 degrees)
6 = albers equal area for Alaska (standard parallels of 55 and 65 degrees)
7 = albers equal area for Hawaii (standard parallels of 8 and 18 degrees)

9 = spherical transverse mercator
Default is 999 for no projection.

Note that if ETM (IPROJ=2) is chosen, the labeling and tic mark plotting for lines of longitude are limited to 3 degrees east and west of the central meridian. Therefore LONGM and LONGX should be specified within 3 degrees of CM.

PHI1 - lower standard parallel for a Lambert projection in degrees. Default is 33 degrees.

PHI2 - upper standard parallel for a Lambert projection in degrees. Default is 45 degrees.

LATM - a three unit array containing the minimum latitude in degrees, minutes and seconds. Default is 0,0,0.

LATX - a three unit array containing the maximum latitude in degrees, minutes and seconds. Default is 0,0,0.

LONGM - a three unit array containing the right longitude in degrees, minutes and seconds. Default is 0,0,0. If using ETM (IPROJ=2), see note under variable IPROJ above.

LONGX - a three unit array containing the left longitude in degrees, minutes and seconds. Default is 0,0,0. For longitudes east of Greenwich set LONGX less than LONGM. If using ETM (IPROJ=2), see note under variable IPROJ above.

If LONGX < LONGM then east longitude is assumed (lon increases to right)

TINT - the interval of tick marks in minutes. Default is 0 for automatic determination based on the range of the above arrays.

Fractional values of "TINT" are accepted, TINT=7.5, for example.

ITPOST - the tick mark interval where labeling will be performed. Default is 2.

SIZEP - the height in inches of the tick mark labels. Default is set at 0.1
inches.

SIZET - the height of the tick marks. Default is set at 0.1 inches.

Plotting of point data

IFILE2 - the name of the file containing the random data points. It must be enclosed in single quotes. Default is blanks.

ISPOST =0, no station post (default)
=1, vector plot- input records x,y,magnitude,inclination,declination
=2, station plot- input: x,y,z
negative values indicate post files, with the last digit determining the anomaly posted. (Post files are binary records: id,x,y,z1,z2,z3,...z6)
-1 to -6 z value posted
-11 to -16 station id posted
-21 to -26 z value and id posted

The order of anomalies in a .post file is FAA, CBA1, CBA2, ELEV (FEET), TC, OG

SZPOST - station symbol size in inches. Default is 0.1.

SZLAB - size of the symbol labels in map inches. Default is 0.08.

NID - The number of different station symbols (default = 0 , maximum = 19). To plot all stations with one symbol, let nid default to 0, and set ich equal to desired symbol.

CHID - Array of character strings (length <= 4) in the id field of the post file (IFILE2) for matching to symbols in ICH.

ICH - Array of symbol numbers associated with CHID. The default is 2. Summary of available symbols:

1	square
2	diamond
3	circle
4	x
5	x with small +
6	+, this is same symbol as lat-lon ticks
7	-
8	y
9	small square inside large x
10	hourglass
11	triangle point up
12	triangle point down
13	very small circle

Using these last three parms a different symbol can be plotted for various station ids. Example: NID=3,CHID="abc","xy","a", ICH=1,2,3,11 so that station abc001 is plotted with symbol 1; station abxx is plotted as symbol 3. The NID+1 ICH is a default symbol, any station which gets to the end of the list without being matched is plotted with this symbol (it can be left out and default to 2).

FMTV - format array of output z label, default "(f7.2)". Output label is a floating point number only (station id labels are internally formatted to a8).

NCHARV - number of chars in z label, default =0 ("ich" symbol marks sta. location)

IFMTV - format of input xyz file

VMAX - the maximum vector length in inches when ISPOST=1. Default is 1 inch.

VMIN - the minimum vector length in inches when ISPOST=1. Default is 0. The vectors are log scaled from VMAX to VMIN.

XXX - pair of numbers indicating the left and right coordinates of the random data file (IFILE2). See YYY

YYY - pair of numbers indicating the bottom and top coordinates of the random data file (IFILE2). See XXX. XXX and YYY are used when one wants to plot random data without providing a grid file. When these variables are used, the contouring option is bypassed but other options such as lat/lon tick marks, axis labeling, etc., are still available.

Plotting of line and text data

LXFILE - name of file containing ordered pairs representing line segments to be plotted. Each line segment must end with a 1.0e+37 in both x and y fields. Default is blanks.

LXFMT - format of the external line file. Default is blanks, which implies binary xy format. Any non-blank value will result in either xy or xyz data to be read in list format.

LXPROJ - Projection number for the line file data. If the line file data is projected, it must have the same projection as the grid file. Default is 999 which means unprojected data.

LXUNIT - the number representing the type of units in the LXFILE.
0 = inches (projected) or seconds (unprojected)
1 = meters, minutes
2 = kilometers, degrees(default)

LXTYPE - the number of the desired line type (see IDASHS) to be used for plotting the LXFILE data. If LXTYPE = 999, the first coordinate pair of each line segment in LXFILE is taken as the line type. In this case the first x and y of each segment must both equal the line type for the segment.

TXFILE - the name of a file containing ASCII information in list format to be used to plot text. Each line of this file must contain x-coordinate, y-coordinate, text to be plotted (in quotes), icode, size ofcharacters, rotation of characters, x-offset in plot units to the first character, and y-offset to the first character. Icode =

1 or 2 implies the coordinates are in data units. Icode = 3 implies the coordinates are in plot inches.

IBOUND - state boundaries.. For this option to work, the state boundary file must be available. State boundaries can be plotted by setting IBOUND=0 to 6 for the line style, 0=solid, 1 to 3=50%, 75%, 25%, 4 to 6= 1,2,3 short dashs (Not supported).

EXAMPLE - RUNNING CONTOUR

You will need to copy three files from diskette #2 of OF 93-560D to run this example (also see exercises on p.7-42). The command file 'gcon.cmd' (listed below) can be used to contour the gravity data grid 'gboug.grd' and display the gravity station locations from file 'gboug.pps'.

```
$parms
dcval=5, ispost=-2, iproj=2, cm=-117, baslat=0
$
```

CONTOUR will prompt for the file names:

```
C:>contour
     Welcome to Program PCCONTUR(Version 2.0)
     Note: set iverb=1 to list parameters
enter command filename : ggcon.cmd
enter grid filename : gboug.grd
enter station filename : gboug.pps
enter format, car ret if binary :
```

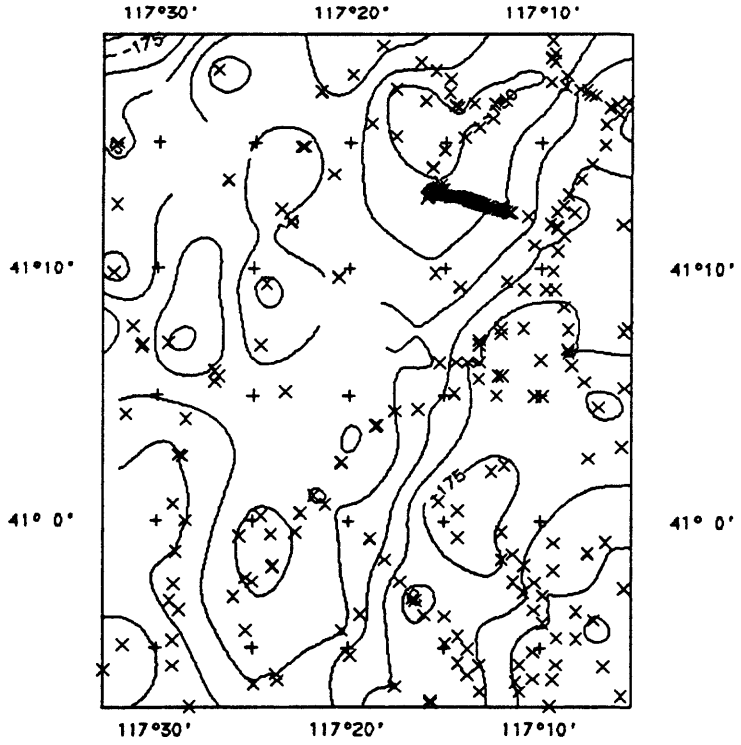

DETOUR AND DETOURG perform simple color contouring of xyz and post data (DETOUR) and gridded data (DETOURG) using Delaunay tessellation (Watson, 1982).

reference: Watson, D.F., 1982, Acord: Automatic contouring of raw data: Computers and Geosciences, v.8, no. 1, p.97-101.

GRAFEDIT is a grid-editing program utilizing interactive graphics. The current version allows expansion/contraction of contour plots, plotting station locations, deletion/restoration of data inside a movable box, and regridding & contouring of the displayed data. The program will track sequential data values generated by digitizing and change them to new values. Normally this function is not used and response to the querry "...track sequential values in the edit function..." should be no.

Input is a standard 2d grid and optionally a binary data set to be edited. Data files types are binary xyz or binary post. Post files may have variable length records; the program will print the number of channels found and the user selects the one to be used in the regridding operation.

The program is menu driven and menu items are selected by the mouse. Although the program has been tested with several popular brands of mice, mouse controllers, and mouse drivers, we cannot guarantee proper functioning with all brands.

Original code by M. Webring.

REMAPP DISPLAY PROGRAMS

REMAPP software uses a data format which is different from the USGS GRID standard. To use the **DISPLAY** program, GRID files must be converted (see the REMAPP-PC manual included with the software on Open-File 93-560C). The four programs below, **GRDREM, HIST, STRETCH,** and **DISPLAY** are used for this data conversion and for image enhancement.

GRDREM performs the data conversion. GRID real number data are converted to integer numeric data. The minimum and maximum grid values are assigned to the minimum and maximum REMAPP DNs (data numbers), with everything in between linearly interpolated. A linear equation is displayed which may be used to calculate GRID or REMAPP point values from the other format.

Generated images from GRID data usually are not yet contrast enhanced for visual study. Two ways of contrast enhancement are possible. The first is to read the image into **DISPLAY**, then use the <V> function for a quick contrast enhancement. The second way yields a more pleasing result. A histogram is generated by the program **HIST**, then the selected statistics are applied to the data using **STRETCH**. Display then can be used to view the image.

Basic REMAPP Programs - GRDREM, HIST, STRETCH, and DISPLAY

Image analysis of the USGS potential field data requires data conversion and image enhancement. Here is a simple approach to get you started. *Remember to run these programs from the DOS prompt, and NOT from* **PFMENU.** The following examples are used as part of the independent exercises at the end of this chapter, where more detail is explained. Files used are fully described in Chapter 12.

1) GRDREM - convert from GRID data format to REMAPP image format.

```
C:>grdrem
GRID FILENAME = gk.cgd
id,pgm,ncol,nrow,nw,xo,dxo,yo,dyo =
                                                    gdcnv                    194
        249    1    -46.000000    2.000000E-01    4525.000000
   2.000000E-01
DISKIO:ENTER OUTPUT FILENAME
gk.img
Minimum Values:  REMAPP DN = 1    GRID =   7.100961E-01
Maximum Values:  REMAPP DN = 255  GRID =   4.726213
Number of DVALs in Grid =      32237
REMAPP DN = INT (GRID Value *  63.245170 +  -43.910150 + .5)
         DISKIO(2): gk.img     [LINES  249PIXELS  194BYTESIZE 8]
Stop - Program terminated.
```

2) HIST - generate histogram and statistics for contrast enhancement.

```
C:>hist
Listing device (CON, PRN, OR diskfile)?
gk.hst
DISKIO:ENTER INPUT FILENAME
gk.img
ENTER 1ST SCANLINE, NO. SCANLINES, SKIPS:
0 0 0
ENTER 1ST PIXEL, NO. PIXELS, SKIPS:
0 0 0
        DISKIO(2): gk.img          [LINES   249PIXELS  194BYTESIZE  8]
enter TITLE for output (80 characters) or <return>
histogram and stats for image gk.img
enter MINIMUM and MAXIMUM DNs to test:   <return> for max range
  (DN permissible range: 0  to   255)
1 255
enter CLASS INTERVAL:   <return> for interval of  1
  CLASS INTERVAL permissible: 1  to   255)
1
Process another file ?  Yes or No  :  <Y> default
n
Stop - Program terminated.
```

To take a look at the histogram, type, print, or edit the file **gk.hst**.

3) STRETCH - apply statistics to raw image to generate contrast enhanced output image. (Mapping pairs and output pixel DN re-assignment are clarified in a later section.)

```
C:>stretch
DISKIO:ENTER INPUT FILENAME
gk.img
ENTER 1ST SCANLINE, NO. SCANLINES, SKIPS:
0 0 0
ENTER 1ST PIXEL, NO. PIXELS, SKIPS:
0 0 0
        DISKIO(2): gk.img          [LINES   249PIXELS  194BYTESIZE  8]
DISKIO:ENTER OUTPUT FILENAME
gks.img
HOW MANY MAPPING PAIRS ?  0=TEXT FILE /
3
INPUT MAPPING PAIRS, ONE PAIR PER LINE.
51 0
126 127
161 255
*** FAST STRETCH BEGINS ***
        DISKIO(2): gks.img        [LINES   249PIXELS  194BYTESIZE  8]
PROCESS ANOTHER FILE /
n
Stop - Program terminated.
```

NOTE: for color composites Red - Green - Blue (RGB), use images with mapping pairs:

```
 GK.IMG    GU.IMG     GT.IMG
 51   0    9   0      33   0
126 127   33 127      87 127
161 255   69 255     140 255
```

4) DISPLAY - display the enhanced image.

```
C:>display  (To quit, press <Esc>)
DISKIO:ENTER INPUT FILENAME
gks.img
ENTER 1ST SCANLINE, NO. SCANLINES, SKIPS:
0 0 0
ENTER 1ST PIXEL, NO. PIXELS, SKIPS:
0 0 0
```

DISPLAY contains several useful functions for image processing, such as a cursor, six image buffers, color composite, and graphics overlays. Each function is accessed by pressing its related key. A short help menu is called up by pressing <H>.

Once an image is displayed, any of the functions may be used. Each function is terminated by pressing the <Return> key. DISPLAY itself is terminated using the <Esc> key once all functions have been cleared.

Image buffers provide flexibility on image usage and storage. Any image appearing on the screen, may be stored in an image buffer. This allows image comparisons and enables several program functions. When an image is stored in a buffer, it may be recalled rapidly to the screen, updating the screen overwrites any previous screen image. Further information may be found in the REMAPP-PC manual included with the software on Open-File 93-560C as an ASCII text file.

DISPLAY functions are described on the next page.

DISPLAY Functions

Load or Save Image to Screen/Buffer:

<D> Display image from disk
<W> Window image from disk
<1 - 6> Display image buffer 1 - 6
<I> Save screen to buffers 1 - 6

<O> Change palette to pseudo-color

Graphics Overlays:

<G> Define graphics plane [0 - 10]
COLORS: <R Y G C B M D W>, DN: 0-255
<A> Add a graphic plane to screen
<S> Subtract a graphic plane
<R> Restore image without graphics

Image Manipulation and Utilities:

<V> Automatic Histogram Stretch
<M> Generate color composite image using buffers 1-3 (BGR)
<L> Generate shaded relief image using buffers 1-3 and 3 vector images
<C> Enable cursor
<Z> Zoom image by a factor of 2
<X> Scatter Plot;y-axis stored in buffer 1, x-axis in buffer 2
<P> Plot spectra from a band interleaved by line (BIL) file
<Y> Scale y-axis of spectra plot
<K> Reset display palette to color
<B> Reset display palette to black and white
<F> Generate a Frequency Histogram of all image buffers
<f> Generate a frequency Histogram of the screen image
<E> Temporary Exit to DOS (shell to DOS, return with the EXIT command)
(when sufficient memory is available)

<ESC> QUIT program to DOS {TERMINATE}
<H> Help

*Clarification of Mapping Pairs (**STRETCH**)*

Mapping pairs are used within STRETCH to reassign image pixel Data Numbers (DNs) to generate an enhanced output image. Each mapping pair is composed of an input pixel DN, followed by its corresponding output DN. Image input pixel DNs are re-mapped to corresponding output DNs. When a pixel input DN falls between two input mapping pairs, the pixel output DN is assigned through linear interpolation of the corresponding two output mapping pairs.

IMVIS PROGRAM INFORMATION

Program IMVIS is a simple-to-use image viewer which uses ASCII label files to describe binary image files. Program IMVIS can also do some limited image processing such as converting (with REDUCE) three images out of a set of N images to 24-bit color images or 8-bit color images with color palettes. Some boxcar filter applications are possible such as smoothing and relief shading. Color palette changes can be made in RGB space.

VIEWING A SINGLE IMAGE:

When you enter IMVIS you will see a list of label files of type '.LBL' in a window in the top right part of your screen in alphabetical order. These files are taken from the current directory. Label files from other directories may be included by entering the directory names on the IMVIS command line. For example,

```
imvis d:\imgdata\land\ d:\imgdata\water\
```

would allow label files from two additional directories to be used.

The window will display a maximum of 19 file names but up to 300 file names may be present. You can get to these other file names by scrolling (<arrow keys>, <PgDn>, <PgUp>, <Home> or <End>) or by typing the file name. When you select a file name by typing part or all of the name, you must press <Enter> twice -- once to terminate typing and again to display the selected file. You can also select a file by positioning the highlighted bar over the file name using the arrow keys and pressing <Enter>.

To exit the menu without choosing an image, press <Esc>. If you have given path options in the command line, the program will search other directories for label files. If you continue pressing <Esc>, you will eventually exit from the program.

If the label file you choose is for a single image (examples 1, 2, 4, 5, 6, and 7 below), you will leave text mode and go into image mode. The type of image mode is normally chosen automatically, but it can be forced by invoking IMVIS with a slash followed by a letter id. For example,

```
imvis /e
```

will force the program into EGA mode. The available modes are:

Id	Mode	Columns	Rows	Colors	Total Palette
E	EGA	640	350	16	64
V	VGA	640	480	16	262144
S	VGA	320	200	256	262144
Y	Extended VGA	640	400	256	262144
X	Extended VGA	640	480	256	262144

The program will try to boot the graphics board in the following order until it finds a mode which can be booted -- X,Y,S,E. The 'V' mode must be requested if you wish to use it. Many of the functions will not work in V and E mode, and none of them will work well in E mode. Although the program has been tested on many popular super-VGA graphics boards, we cannot guarantee that the program will correctly identify and boot all such boards.

The initial display of the image will include a 'zoom box'. This box can be moved 16 pixels at a time in any direction by using the arrow keys. To change the distance the box moves each time, use the <+> and <-> keys to double and halve this value respectively. The size (not the shape) of this box can be changed by pressing <L> for larger and <S> for smaller. Press <Enter> to zoom on the boxed portion of the image, or press <Esc> to exit without changing the display.

The resulting display of the image will include an option menu. You change the highlighted option by using the left or right arrow keys. If the menu option selected has a pull-down menu, you activate the pull-down menu by pressing the down arrow key. Within each pull-down menu, you select the highlighted option using the up or down arrow keys. To activate the highlighted option in a submenu, press <Enter>. The main menu options are as follows:

System : Zoom : Analyze : Plot : Quit

Selecting 'System' from the main menu by pressing the down arrow or <Enter> key produces a pull-down submenu. This System submenu contains three options: 'Color', 'Targa File', and 'Hide Menu'.

Selecting 'Color' from the System submenu presents several options that allow the user to change the color palette used to display the image. The modified version of the palette can be saved over the old one but one should save a copy of the old palette before using this option. The user should keep in mind the fact that one cannot write on a CD-ROM. The available options and descriptions for their use are as follows:

'change +/-,789,123':

This rather cryptic information refers to the <keypad+>, <keypad->, <Home>, <Up arrow>, <PgUp>, <End>, <Down arrow>, and <PgDn> keys which correspond to the <+>, <->, <7>, <8>, <9>, <1>, <2>, and <3> keys on the numeric keypad available on many keyboards. The <Home>, <Up arrow>, and

<PgUp> keys respectively increase the intensity of the red, green, and blue in the color palette. The <End>, <Down arrow>, and <PgDn> keys decrease the red, green, and blue intensities, respectively. Numlock must be off for these six keys to function. The <keypad+> key increases the intensity of all colors simultaneously. The <keypad-> key decreases the intensity of all colors simultaneously. This option affects the entire image.

'stretch RGB':

This option is only effective if the image data do not use the entire range of values from 0 to 255. If the data do not use the entire range, this option causes them to be linearly stretched to use the full range of red, green, and blue intensities.

'reset':

This option resets the color palette to the original values.

'change one color':

This option allows the user to move the cursor to a particular pixel, select that color by pressing <Enter>, and then change the color using the <Home>, <Up arrow>, <PgUp>, <End>, <Down arrow>, and <PgDn> keys to change the red, green, and blue intensities. The rate at which the cursor moves can be changed by the <-> or <+> keys to decrease or increase the rate. This option is particularly useful for changing the colors of the linework used in the various overlays. For example, the State boundaries might plot as a red color, and the user could choose to change that to a white color for greater visibility. In general, images use the range of values 1 to 240 for image data and 0 for areas of no data, and the overlays are plotted using colors assigned to numbers in the range 241 to 255.

'save new table':

This option allows the user to save the modified color palette. Because this option destroys the original palette, a copy of the original should be made first.

'exit color':

This returns you to the main menu.

NOTE: You can also exit from most options by pressing the <Esc> key.

Selecting 'Targa file' from the System submenu captures the screen as a 32-bit Targa file.

Selecting 'Hide Menu' from the System submenu hides all menus so the screen can be photographed or captured. Pressing any key will restore the main menu.

Selecting 'Zoom' from the main menu will clear the screen, restore the unzoomed image, and display a box which can be sized and positioned to select an area of the image which will be displayed as an enlarged image. This selection process is described above.

Selecting 'Analyze' from the main menu produces a pull-down menu which contains the following:

'pixel info':

This puts a cursor in the middle of the screen, which can be moved to get pixel information. The cursor is moved with the arrow or number pad (Num Lock = off), and the increment of movement is controlled with <+> and <->. The display at the bottom will change with available information but it will look something like this:

```
x=256 y=416  84  r: 57 g: 31 b: 26
3520  5120 lat =  47.76468 lon = -126.63266
```

Not all images will have all this information. Some will only give x and y locations. In this example the cursor on the screen is at pixel (256,416) which is pixel (3520,5120) in the image file. The value of the pixel on the screen is 84 while the value of the red, green, and blue pixels used to make the color image are 57, 31, and 26 respectively. These RGB values come directly from the files used to make the composite image and are not scaled in any way.

NOTE: This pixel information is NOT accurate unless the image is in a "zoomed" state.

'histogram':

This produces a histogram of the screen data. You must first choose the position of the histogram graph. This is done by positioning a box on the screen with the arrow keys. The part of the image covered by the interior of this box will not be regenerated until the next zoom operation. Use the following option keys to position the box:

```
(l)arger
(s)maller
(H)igher
(S)horter
(W)ider
(N)arrower
'+' move more
'-' move less
```

Next you must choose the region of the image to process. Use <Esc> to exit the option.

NOTE: The histogram option does not work on an unzoomed image. If you

are interested in looking at histograms of areas of the entire image, first execute the zoom option using a box which is larger than the image.

'shade':

Makes a shaded-relief version of the image with the light source to the right. This option currently does not work properly on a zoomed image.

'smooth':

Does a 3x3 average of the pixels. Use this before 'shade'.

'rescale image':

This image rescales the image using a graytone color palette. The effect is to convert a color image to a graytone image.

Selecting 'Plot' from the main menu produces a pull-down menu which enables you to plot vector or label information onto the displayed image. Menu options are 'boundary plot', 'Label.grf', and 'caption'.

Selecting 'boundary plot' from the Plot submenu produces a pop-up menu for plotting vector overlay files on the image. Examples of vector overlay files are:

'Geology':

This plots the geologic contacts for the test area. Symbols for the various geologic units can be plotted using the label plotting option described below. A brief description of these units can be viewed from the menu program under the discussion of the vector overlay files.

'Lat lon ticks':

This contains latitude longitude tick marks.

'Neat line':

This plots a line around the boundary of the test area.

'Scale bar':

This plots a kilometer scale bar below the test area. The bar may be labeled using the label plotting option described below.

'Faults':

This plots the faults from the digitized geology for the test area.

Selecting the 'Label .grf' option from the Plot submenu provides a pop-up menu from which you can select various sets of labels which can be plotted on the displayed image. The size of the labels is invariant, which means that some of the label files (particularly the geologic unit symbols) are only useful if the displayed image represents a small part of the total image. The available label files are:

'SCALE': These are the labels for the scale bar.

'GEOLOGY': These are the symbols for the geologic units.

'LATLON': These are latitude and longitude labels, which are only appropriate for the full images.

'DEPOSITS': These are the locations and types of mineral deposits.ames.

Selecting 'caption' from the Plot submenu plots the image caption near the bottom of the screen. Because of the way this has been implemented, the caption will write over the image if any part of it is displayed in the lower part of the screen.

Selecting 'Quit' from the main menu erases the image and returns to the label file menu.

VIEWING AN IMAGE SET:

If the selected label file is for a set of registered images (example 3 below), the initial menu will include the following options:

'display quick color':

Allows the user to select three images to be displayed as a combination of shades of red, green, and blue. The resulting image has 7 shades of red, 7 shades of green, and 5 shades of blue and is a reasonable approximation of the image that will be produced if the images are combined.

'make RGB composite file':

Combines three image files into a '.cmg' file for input to REDUCE. The '.cmg' file is simply a band-interleaved file, which is a format that facilitates the conversion to the 8-bit image, which looks very much like a 24-bit color image. REDUCE performs a statistical analysis of the images and assign colors to the pixels based upon the colors of the most abundant
pixels in the image.

'scan set -- full image':

Displays each image for 3 seconds with image name.

'scan set -- sub image'

Displays a portion of each image for 3 seconds with image name.

LABEL FILES:

The format of the label files is patterned after the Jet Propulsion Laboratory's (JPL's) Planetary Data System (PDS) ASCII label files. For program IMVIS the ASCII label and the binary image must be in separate files. The simplest label file possible is a file of type '.lbl' containing the rows, columns, and image data file name. For example,

```
IMAGE_LINES  = 2057
LINE_SAMPLES = 1435
IMAGE_POINTER= 'l:\coredata\PD356001.dat'
```

This label file tells IMVIS that the image PD356001.dat has 2057 lines, and each line contains 1435 pixels (picture elements). The image is assumed to be a gray scale image; each pixel will be one byte in size, and there is no header in the image file which is in directory \coredata on drive L.

The following are six examples of '.lbl' files in order of increasing complexity.

Example 1: Simple Gray Scale Image

```
FILE_TYPE    = IMAGE
IMAGE_LINES  =  400
LINE_SAMPLES =  640
HEADER_BYTES =    0
IMAGE_POINTER= 'canonbl.dat'
END
```

This is the simplest type of label file. Three of the lines are not needed but are included for clarity. The FILE_TYPE is not necessary but helps tell someone why this file is here. HEADER_BYTES in this case is zero, which is the default, but shows where to put this information if necessary. These bytes are skipped when the image is processed. An END is not required by IMVIS, but other programs which can read this type of file require it. IMAGE_LINES are the number of rows in the image file. LINE_SAMPLES are the number of columns in the image file. IMAGE_POINTER is the name of the image file. Path names can be entered on the IMVIS command line if necessary.

Example 2: Color Image

```
FILE_TYPE    = IMAGE
IMAGE_LINES  =  400
LINE_SAMPLES =  640
HEADER_BYTES =    0
IMAGE_POINTER= 'canonbl.dat'
PALETTE_POINTER    = 'canonbl.pal'
END
```

This file is identical to the first except a palette file name has been added. The palette file contains a list of red, green, and blue values that define up to 256 colors. The format of the palette file is four integers on a line -- color number, red, green, and blue. All numbers range from 0 to 255. Please note that the values 241 to 255 are used as colors for the vector overlay plots. For this reason it is generally desirable to restrict data images to the range of values from 0 to 240.

Example 3: Registered Image set

```
FILE_TYPE    = IMAGE
IMAGE_LINES  =  400
LINE_SAMPLES =  640
SET_POINTER  =    6
  canonbl.dat  40  70 100
  canonb2.dat  10  30  50
  canonb3.dat  10  37  65
  canonb4.dat   5  37  70
  canonb5.dat   0  65 130
  canonb7.dat   0  33  65
END
```

If you have a set of images of the same scene but with different information, they can be combined into an image set. All images must be of the same size, and each pixel must be of the same geographic location. In short, they must be registered. Currently you can have up to 20 images in a set. This can be extended to any reasonable number by changing the macro NUM_IMAGE in the source code for 'IMVIS.C' and recompiling.

"SET_POINTER = 6" in the above example means that the set contains 6 images. The names of the images are listed followed by optional scaling parameters. These indicate the image value to be plotted as 0, 127, and 255 in the output image. If there are no numbers the default is 0, 127, and 255, which means no change in the way the image is displayed. If only two numbers appear they are assumed to be the first and last parameter, and the middle is chosen to be their average. The "END" is for the file, not the image set.

Example 4: Composite image created by IMVIS

```
FILE_TYPE     = IMAGE
IMAGE_LINES   =  400
LINE_SAMPLES  =  640
IMAGE_POINTER= 'can421.dat'
PAL_POINTER   = 'can421.pal'
PALETTE_POINTER     = 'can421.pal'
SAMPLE_RATE = 1
CHANNEL_INPUT:
     RED    = canonb4.dat Range =  16  40  60
     GREEN  = canonb2.dat Range =  16  28  42
     BLUE   = canonbl.dat Range =  43  58  80
```

This label file was created by IMVIS and is for a color composite image from channels 4, 2, and 1. The ranges indicate that for the red channel, 0 on the screen is 16 (or less) in the file, 127 on the screen is 40 in the file, and 255 on the screen is 60 (or greater) in the file. The sample rate is 1, which means that every pixel was used. A sample rate of 2 would mean every second pixel, etc. The file names are given here so that IMVIS can read pixel data from them in 'pixel info' mode.

Example 5: Earth Located Image -- polynomial fit to projection

```
FILE_TYPE      = IMAGE
IMAGE_LINES    =  4583
LINE_SAMPLES   =  3132
IMAGE_POINTER = 'pac36.glo'
LATITUDE_COEF  = 6
 4.9993160e+001  -4.4824000e-004  -2.7323000e-011
 2.7988001e-005  -2.0332001e-009  -3.3854000e-010
LONGITUDE_COEF = 6
-1.2918469e+002   6.9518998e-004   4.0232001e-010
 4.3117001e-005  -4.0440001e-010  -6.1135998e-009
END
```

The addition of LATITUDE_COEF and LONGITUDE_COEF allow the program to convert X and Y in the image file to latitude and longitude. The upper left corner of the image is X=0 and Y=0 with X increasing to the right and Y increasing downward. Because north is up on many images, the order of the X and Y are reversed in the two equations.

```
Lat = A[0] + A[1]*Y + A[2]*X + A[3]*Y*Y + A[4]*X*X + A[5]*Y*X
Lon = B[0] + B[1]*X + B[2]*Y + B[3]*X*X + B[4]*Y*Y + B[5]*X*Y
```

This example uses 6 coefficient values for latitude and 6 for longitude, but any number from 2 to 6 can be used as long as the order shown above is

followed. If fewer than 6 are used, the unspecified higher order coefficients are assigned to zero.

Example 6: Earth Located Image -- Albers Equal Area Projection & Vector Data

```
FILE_TYPE     = IMAGE
IMAGE_LINES   = 1575
LINE_SAMPLES = 2627
IMAGE_POINTER= 'rad_shd.dat'
PAL_POINTER   = 'rad_shd.pal'
PALETTE_POINTER     = 'rad_shd.pal'
Projection = Albers equal area elliptical
    23.0  Lat0
    29.5  Lat1
    45.5  Lat2
   -96.0  Lon0
-2630000  X0
 3328046  Y0
    2000  PixelSize (meters)
 7  ellipsoid (Clark 1866) [0-10]
VECTOR_SETS = 6
  county = 1
     county 120.0 0.0 253
  coast  = 1
     coast  120.0 0.0 254
  state  = 1
     state  120.0 0.0 246
  rivers = 1
     rivers 120.0 0.0 251
  nation = 1
     nation 120.0 0.0 245
```

The addition of Projection allows the program to convert X and Y in the image file to latitude and longitude and back again. In the case of a projected image there are two sets of x/y coordinates -- one for the map and one for the image. The image is in pixels as before, but the map x/y is in meters from the map origin. At this time only Albers equal area elliptical and ellipsoidal transverse mercator projections can be processed, but others will be added as the need arises. The information for the Albers projection is as follows:

```
     Lat0 = base latitude of map
     Lat1 = 1st standard latitude
     Lat2 = 2nd standard latitude
     Lon0 = central longitude of map
       X0 = x map coordinate of pixel 0,0 (upper left corner)
       Y0 = y map coordinate of pixel 0,0
PixelSize = map coordinate size of a pixel in meters
ellipsoid = number of ellipsoid used in making map:
```

```
0  GRS 80          1980 6378137.0 6356752.3  Newly adopted
1  WGS 72          1972 6378135.0 6356750.5  NASA, DoD, oil Co.
2  Australian      1965 6378160.0 6356774.7  Australia
3  Krasovsky       1940 6378245.0 6356863.0  Soviet Union
4  International   1924 6378388.0 6356911.9  Remainder of the World
5  Hayford         1924 6378388.0 6356911.9  Remainder of the World
6  Clarke          1880 6378249.1 6356514.9  Most of Africa; France
7  Clarke          1866 6378206.4 6356583.8  North America;
                                              Philippines
8  Airy            1830 6377563.4 6356256.9  Great Britain
9  Everest         1830 6377276.3 6356075.4  India; Burma; Pak.;
                                              Afgan.; Thailand;etc.
```

Line work from program REORDER can be brought in by using the vector set option:

```
VECTOR_SETS = 6              [ There are to be 6 groups of lines.  ]
  county = 1                 [ Group 1 is 'country' and has 1 file ]
     county 120.0 0.0 253    [ to be plotted in color 253 for      ]
                             [ pixel size 120 to 0 kilometers.     ]
  coast  = 1
     coast  120.0 0.0 254
  state  = 1
     state  120.0 0.0 246
  rivers = 1
     rivers 120.0 0.0 251
  nation = 1
     nation 120.0 0.0 245
```

The colors can be any color in the palette by number. Refer to the documentation for program REORDER to obtain more information about creating a vector data set.

Example 7: Earth Located Image -- Ellipsoidal Transverse Mercator Projection & Vector Data

```
FILE_TYPE          = IMAGE
IMAGE_LINES        =  496
LINE_SAMPLES       =  387
IMAGE_POINTER      = 'grtpl.dat'
PAL_POINTER        = 'grtpl.pal'
PALETTE_POINTER    = 'grtpl.pal'
Projection = Ellipsoidal transverse mercator
     0.0  Lat0
  -117.0  Lon0
   .9996  k0
  -46050  X0
 4574550  Y0
     100  PixelSize (meters)
       7  ellipsoid (Clark 1866) [0-10]
```

```
VECTOR_SETS = 6
  Lat_lon_ticks = 1
     tics 120.0 0.0 245
  Neat_line = 1
     neat 120.0 0.0 245
  Scale_bar = 1
     scale 120.0 0.0 245
  Geology = 19
     geol1 120.0 0.0 244
     geol2 120.0 0.0 244
     geol3 120.0 0.0 244
     geol4 120.0 0.0 244
     geol5 120.0 0.0 244
     geol6 120.0 0.0 244
     geol7 120.0 0.0 244
     geol8 120.0 0.0 244
     geol9 120.0 0.0 244
     geol10 120.0 0.0 244
     geol11 120.0 0.0 244
     geol12 120.0 0.0 244
     geol13 120.0 0.0 244
     geol14 120.0 0.0 244
     geol15 120.0 0.0 244
     geol16 120.0 0.0 244
     geol17 120.0 0.0 244
     geol18 120.0 0.0 244
     geol19 120.0 0.0 244
  Faults = 1
     test 120.0 0.0 245
CAPTION = 3 LINES
TEXT_COLOR = 245
TEXT_SIZE = 2
___RTP AEROMAGNETIC MAP_____________________
____east illumination_______________________
____________________________________________
END
```

This has the same format as example 6, except that the information for the ellipsoidal transverse mercator projection is as follows:

```
     Lat0 = base latitude of map
     Lon0 = central longitude of map
       k0 = scale on the central meridian (0.9996 for the UTM projection)
       X0 = x map coordinate of pixel 0,0 (upper left corner)
       Y0 = y map coordinate of pixel 0,0
PixelSize = map coordinate size of a pixel in meters
ellipsoid = number of ellipsoid used in making map.
```

One or more lines of caption information can be plotted on the image using the caption option. The following lines are an example:

```
CAPTION = 2 LINES
TEXT_COLOR = 255
TEXT_SIZE = 1
POTASSIUM CONCENTRATIONS_____________
_____________________________________
```

The CAPTION line defines the number of lines of text to be printed as a caption. The TEXT_COLOR selects the color to be used for the caption from the current color palette. The TEXT_SIZE selects the text size -- 1 = maximum size, 2 = half of maximum size, 3 = one-third of maximum size, and 4 = one-fourth of maximum size. For most purposes either 1 or 2 are most appropriate. The text lines can
contain embedded blanks, and the underscore character is interpreted as a blank. Each line of text must be terminated by a carriage-return character. As shown in the above example, blank lines can be used to position the text vertically.

REDUCE PROGRAM INFORMATION

Program REDUCE produces an 8-bit image for display using IMVIS. An input file with the suffix '.cmg' containing interleaved scan lines from red, green, and blue images is required. A suitable input file can be produced by IMVIS. The output image consists of three files: a label file with the suffix '.lbl', an image file with the suffix '.dat', and a palette file with the suffix '.pal'. We recommend that REDUCE be invoked as follows:

```
reduce file_prefix /c 240 /m 10
```

where file_prefix is the prefix of the .cmg file, /c 240 means that the output image will have 240 colors, and /m 10 means that no color will occupy fewer than 10 pixels.

If you are processing a 'noisy' file, then a 'noise' modifier can be used:

```
reduce noise image1 /c 64 /m 10
```

REORDER PROGRAM INFORMATION

Adding vector data which can be used with IMVIS as an overlay file is relatively simple. The vector data need to be in the form of decimal degrees of latitude and longitude. Each distinct line must have an "attribute", which is an integer number but which does not have to be unique. The attribute number is entered as a single integer number on a line by itself. The latitude and longitude coordinates are then entered as coordinate pairs with an arbitrary number per line. The longitude of the last coordinate MUST be followed by the characters "//". These characters MUST be on the same line as the last coordinate. A sample of such a vector data file is given below.

```
    1
36.542213 -77.479012  36.550900 -77.849602  36.551899 -77.849503
36.543800 -78.248901  36.542801 -78.425400  36.542702 -78.577202
36.542999 -79.077301  36.542400 -79.231201  36.540600 -79.351700
36.545700 -79.842201  36.545300 -80.032600  36.544601 -80.194298
36.558998 -80.565201  36.563000 -80.685997  36.563000 -80.779800
36.568199 -81.161003  36.570801 -81.241402  36.574600 -81.332397//
    1
37.312099 -81.382698  37.314999 -81.373703  37.320702 -81.369102
37.309299 -81.345001  37.296902 -81.328102  37.287300 -81.315903
37.249802 -81.258202  37.241199 -81.244499  37.232601 -81.231903
37.262001 -81.169296  37.267799 -81.147797  37.273399 -81.127998
37.293301 -81.016701  37.296700 -81.002403  37.298698 -80.993599
37.290100 -80.973000  37.292099 -80.957603  37.297100 -80.941498
37.328701 -80.884697  37.335701 -80.875504  37.340500 -80.867203//
    1
37.425301 -80.865799  37.423698 -80.839699  37.417702 -80.833702
37.391300 -80.805397  37.391899 -80.797997  37.390099 -80.792099
37.373001 -80.765999  37.378399 -80.748802  37.382599 -80.738197
37.412201 -80.666000  37.418999 -80.652496  37.425701 -80.639603
37.447399 -80.597298  37.454300 -80.586601  37.464401 -80.571800
37.482101 -80.503502  37.472500 -80.499802  37.461800 -80.498299
37.433899 -80.485298  37.424801 -80.478996  37.424702 -80.474403
37.442501 -80.437401  37.448799 -80.427597  37.453400 -80.417397//
```

To convert the ASCII vector file to the binary form needed by IMVIS, you must first ensure that the file name is of the form FNAME.RAW where FNAME can be any desired name but the extension RAW is required. You then run the program REORDER which will produce files named FNAME.BIN, FNAME.HDR, FNAME.ATR. Program REORDER provides the following list of options :

```
c -- count segments in file (don't process)
R -- reorder file and make binary file without dupes

r -- reorder file and make binary file
```

p -- same as 'r' but not in order

To run the REORDER program type the following command:

REORDER FNAME [option]

where FNAME is required but specification of the option is optional. If it is not specified, the program will request an option. In general, the 'p' option is sufficient. 'R' is used with ARCINFO type files where duplicated lines are common. 'R' and 'r' reorder the files so that the lines will be drawn in order rather than randomly. After the binary files have been prepared, the "LBL" files associated with the images must be modified to include the new vector files. See examples 6 and 7 above.

GENERATING IMVIS IMAGES FROM GRID FILES

A grid file produced in the format which is compatible with the potential-field programs can be converted to an 8-bit image which can be viewed using the program IMVIS. Before you can do this, the potential-field software must be properly installed, and your execution path in DOS must be correct.

The first requirement in this process is to generate a grid file in the proper format. This can be done by writing a program to convert an existing grid format into either the binary USGS grid format described on page 6-3 or into the ASCII grid format supported by the program ASCII2SF (see the source code file ASCII2SF.FOR for details). You can also use the program MINC to calculate a binary grid from randomly located data. Documentation on the use of MINC is available through the potential-field software help facility PFHELP.

Once you have generated appropriate grid files, these can be converted to graytone, color shaded-relief, or color edge-enhanced images which can be viewed using the program IMVIS. DOS batch procedures have been provided in order to simplify the generation of the images.

HISTNORM is a program to stretch the values in a grid so that the resulting values follow a uniform distribution. It is used to prepare a grid for image display.

```
C:>histnorm
enter name of input grid file:gboug.grd
enter name of output grid file:gboug.hst
            mapping pairs          # in interval
        old              new
    -186.313300     -186.313300            0
    -172.043800     -181.666100        21290
    -167.779300     -177.019000        21211
    -164.827000     -172.371800        21166
    -162.366800     -167.724700        21578
    -160.234500     -163.077500        21901
    -158.430400     -158.430400        21278
    -156.626200     -153.783200        22560
    -154.165900     -149.136000        21367
    -145.473000     -144.488900        20941
Stop - Program terminated.
```

GRD2IMG is a procedure that produces a graytone image of the data. This procedure only requires the input grid file and produces the appropriate .DAT and .LBL files used by IMVIS. The .DAT file is simply an 8-bit image of the data and the .LBL file is an ASCII file which provides information to the IMVIS program. More details about the .LBL file are provided in the documentation for the IMVIS program.

USAGE: grd2img P1 P2

P1 = file name of input grid
P2 = output image name

```
C:>grd2img gboug.hst gboug
 ** Running GRDREM on the input grid **
 ** Running REM2DAT **
 ** Running MAKELBL **
 ** Deleting temporary files **
 ** Done:  gboug.lbl, gboug.dat created **
```

RAINPAL is a program to create a simple color palette file. A palette file is needed in order to display the graytone image created above in color.

```
C:>rainpal
Enter output file name:
rainbow.pal
Enter data range (eg. 1 240)
1 255
Stop - Program terminated.
```

ADDPAL is a program to add color to a graytone image by creating a new label (.LBL) file pointing to both the image (.DAT) file and the palette (.PAL) file.

```
C:>ADDPAL
enter graytone image name:
gboug
enter color image name:
gbougc
enter pallette file name:
rainbow.pal
Stop - Program terminated.
```

CSR is a procedure that produces a color shaded-relief image which can be viewed by IMVIS. This procedure requires a grid file to be used for the shading algorithm. The procedure also requires a second grid, which is used to determine the colors for the pixels of the output image. The same basic grid data can be used for both purposes.

USAGE: csr P1 P2 P3 P4 P5 P6 P7 P8 P9

P1 = file name prefix of input grid for shading
P2 = file name suffix of input grid for shading
P3 = desired average slope of the shading grid

A value of 10 seems to work well here.

P4 - complete file name of input grid for coloring
P5 - output image name
P6 - sun altitude in degrees above the horizon

The altitude of the sun can strongly affect the amount of shading in the image. Normally this parameter would have a value in the range of 30 to 60 degrees.

P7 - sun azimuth in degrees clockwise from north

This parameter is data dependent and emphasizes any linear features which are perpendicular to the selected angle while eliminating any which are parallel to it.

P8 - number of colors in the output image

This parameter should always be set to 240 unless you are sure that you understand the effects of another choice. The primary reason for this value is that IMVIS typically uses colors from 241 to 255 for plotting vector overlay data.

P9 - minimum number of pixels assigned to one color

This parameter should be based upon the size of the image. For small images (256 by 256), you might use a value of 1, but for large images (1000 by 1000), values of 5 or 7 are more appropriate.

```
C:>csr gboug grd 10 gboug.grd gbougcsr 60 -45 240 5
 ** Running NORMAL on the shading grid **
 ** Running SHADE on the normal vector grids **
 ** Running HISTNORM on the coloring grid **
 ** Running RAINBOW on the stretched coloring grid **
 ** Running CSHADE to combine color and shade grids **
 ** Running GRDREM on the red component **
 ** Running GRDREM on the green component **
 ** Running GRDREM on the blue component **
 ** Running RSG3 on the RGB image files **
 ** Running REDUCE to produce the composite image **
 ** Deleting temporary files **
 ** Done:  gbougcsr.lbl, gbougcsr.dat, gbougcsr.pal created **
```

CEDGE is a procedure which produces a color edge-enhanced image. This procedure also requires a grid with only valid data for shading and another grid for colors. The edge-enhancement algorithm emphasizes areas of steep gradients in the shading grid.

USAGE: cedge P1 P2 P3 P4 P5 P6 P7

P1 = file name prefix of input grid for shading
P2 = file name suffix of input grid for shading
P3 = complete file name of input grid for coloring
P4 = output image name
P5 = gradient level which appears black

The choice for this parameter is data dependent and may require some trial and error to get the desired effect.

P6 = number of colors in the output image

This parameter should always be set to 240 unless you are sure that you understand the effects of another choice. The primary reason for this value is that IMVIS typically uses colors from 241 to 255 for plotting vector overlay data.

P7 = minimum number of pixels assigned to one color

This parameter should be based upon the size of the image. For small images (256 by 256), you might use a value of 1, but for large images (1000 by 1000), values of 5 or 7 are more appropriate.

```
C:>cedge gboug hst gboug.hst gbougedg 100 240 5
 ** Running GRADIENT on the elevation grid **
 ** Running RAINBOW on the coloring grid **
 ** Running CEE to combine color and shade grids **
 ** Running GRDREM on the red component **
 ** Running GRDREM on the green component **
 ** Running GRDREM on the blue component **
 ** Running RSG3 on the RGB image files **
 ** Running REDUCE to produce the composite image **
 ** Deleting temporary files **
 ** Done:  gbougedg.lbl, gbougedg.dat, gbougedg.pal created **
```

INDEPENDENT PC EXERCISES II

1. Run **CONTOUR** and **DETOURG** on **gmagsub.grd,** the subset of the magnetic data that was created in #2 of Independent PC Exercises I. For CONTOUR, use the command file **gcon.cmd** (found on diskette #1 of 93-560D), or no command file at all (press ENTER when asked for the command file). Run **DETOUR** on **gboug.pps** (gravity post file on diskette #2) using a z-field of 2 (Bouguer gravity) and a contour interval of 5. DETOUR is designed to give a quick and dirty plot without having to make a grid first. How does the plot compare to the example shown on page 7-16 using CONTOUR on gridded Bouguer gravity? Note the difference in plot area.

2. Make sure you are in DOS. Copy **gk.cgd** (potassium data grid) from diskette #5 in 93-560D. Follow the recipe on pages 7-18 through 7-20 to create, stretch, and display a REMAPP image of the potassium data (some of these REMAPP programs are not available from **pfmenu).** Don't worry that the southern tip of the data is cut off; the area shown is a function of the original grid interval. Now while you're still displaying **gks.img**, type h to get a quick list of commands available. Note the command I for saving images to buffers. Hit any key to continue the list and also to get back to displaying the image. Type I and then the number 1 to save the image to buffer 1. Type D and then the file **gk.img** to display this as a new image. (In answer to the questions about Scanlines and Pixels, you can answer each with a return instead of three zeroes and get the same result.) Now store the display of **gk.img** to buffer 2. Toggle between the buffers by alternately pressing the numbers 1 and 2. Note the difference the stretching has made in the appearance of the image (gks.img in buffer 1) versus the unstretched image (gk.img in buffer 2). While displaying buffer 2, do an automatic stretch using the V command (no carriage return required). Store this new image to buffer 3 and toggle between 1 and 3. Any differences? The automatic stretch does a pretty good job for cursory looks at images.

3. Copy the files from diskettes #6, 7, and 8 of 93-560D to your test data set directory. These are image and overlay files of various Getchell data sets, for use with **IMVIS**. Run **IMVIS** and browse through the images available in the menu, listed with the suffix **.LBL** (see list of images in Chapter 12). Highlight a name and hit return to display the image. Hit return again and you have zoomed inside the default zoom box (you should see most of the area). There should now be a menu displayed across the top of the screen. Highlight the function you want and hit ENTER to see submenus. From the "boundary" submenu under the "PLOT" menu, plot geologic contacts, faults, scale bar, etc. (hit ENTER to choose the submenu function; highlight the desired file and hit ENTER to plot it). From the same "PLOT" menu, choose the "labels .grf" submenu to plot deposits.grf, scale.grf, whatever else you want. If you can't read the geology.grf labels, compare the geologic contacts instead to figure 5-2. Zoom in to look at features of interest. (You have to resize the zoom box from the original display each time you zoom. To resize, type the letter l for larger and s for smaller). To view pockmarks, take a look at the image GBOUG1.LBL. Plot GBOUG.GRF on top to see station locations. Note the sparse gravity coverage--not enough to do a good map interpretation at this scale.

4. One of the IMVIS images supplied in 93-560D is called **GMAGSE.LBL**. This is a color shaded-relief image of **gmagsub.grd**, illuminated from the E (90°). To look at the effect of a different illumination direction, run **CSR** on **gmagsub.grd** using an illumination direction *other* than east. Follow the example for program **CSR** (starting on page 7-39). **Pick a unique name for the image so you don't overwrite existing files.** For example, you could call it **gmagsN** if you are illuminating from the north (0°). After CSR has created the proper files, run **IMVIS** and compare your image to **GMAGSE.LBL**. Note that the **.LBL** file you created does not allow overlaying geology, deposits, etc. If you're feeling adventuresome, you can get such a .LBL file by the following steps (assuming you named your image **GMAGSN**).

```
C:> copy gmagse.lbl gmagsn.lbl
C:> edit gmagsn.lbl
```

Now change all the strings "gmagse" to "gmagsn". Go to the end of the file and change the title description. Save the new file, exit the editor and run IMVIS. You should now be able to overlay files from the PLOT submenus. Note that copying and editing the label file to get a new label file for gmagsn.lbl only works because both images come from grids that have the **exact same grid specifications**. To learn more about label files, start reading on page 7-28. Note that all the IMVIS images supplied to you have been made from grids having an interval of 0.1 km.

Chapter 8. Map Enhancement Techniques for Gravity and Magnetic Data

INTRODUCTION TO MAP ENHANCEMENT TECHNIQUES

Map enhancement techniques are designed to bring out certain features in the data at the expense of others or to transform the data into a form that is easier to interpret. The ultimate goal of the techniques are to view the data from every perspective so that nothing is overlooked. In mineral exploration, the details and subtle expressions in the geophysical data are normally the most important; we therefore concentrate on techniques that enhance these.

It is important to remember that many of the following techniques are based on certain assumptions about the physical properties or configuration of the subsurface. Commonly, these assumptions are unrealistic for parts of the study area. This should not prevent application of the technique as long as the areas that violate the assumptions are left out of consideration. More often, one does not know if the assumptions are met or not. In these cases, it may be helpful to ask oneself the following question about features of interest on an enhanced map: Is there evidence of the feature in the original data? If the answer is no even after experimentation with different display techniques or examination of the original ungridded data, the feature is probably an artifact. On the other hand, if the answer is yes, the next step is to make a checklist of potential misinterpretations of the feature that could arise from the assumptions of the enhancement technique. The checklist can then be evaluated using modeling techniques or inspection of other geophysical or geological data. For example, in many of the techniques, invalid assumptions lead to mislocations of the enhanced feature with respect to its causative source. Depending on the feature, this can be checked using other geophysical data, by modeling the data, or by inspection on the ground.

The largest variety of map enhancement techniques have been developed for gravity and magnetic data because of the unique mathematical properties of potential fields and the longevity of the methods. We touch on a few below. Some of these techniques can be applied successfully to other types of data, as we hope to show. We have not included analytical continution (see program FFTFIL later in this chapter); that is, continuation of potential-field data observed at one level to data that would have been observed on a different level. Although continuation can be used as a map enhancement technique, it is standardly used in modeling or merging of data sets.

Some creativity and experimentation in applying display and enhancement techniques in nontraditional ways may turn up new features in the data. After all, the point of these techniques is to garner as much information from the data as possible. However, what is concluded from such information should be treated with caution.

Reduction-to-Pole Transformation

Magnetic polarity effects occur where the measured magnetic field is not directed vertically. These effects are manifested by a shift of the main anomaly from the center of the magnetic source (the shift is southward in the northern hemisphere). The shifts can be removed through a mathematical transformation called "reduction-to-the-pole" or "reduction-to-pole". Reduction-to-pole recasts the data as though the magnetic field had been measured at the magnetic north pole, where the Earth's magnetic field is vertical. Reduced-to-pole data are normally computed by means of the fast Fourier transform (Hildenbrand, 1983).

Reduction-to-pole requires an assumption about the directions of magnetization of the magnetic sources. Generally, it is assumed that the total magnetizations of most rocks in the study area align parallel or anti-parallel to the Earth's main field (declination=16^{o}, inclination=66^{o} for the Getchell trend area). This is probably a good assumption for much of the study area, especially for the granodiorite pluton that produces the prominent, hour-glass shaped anomaly (Grauch and Bankey, 1991) in the north-central part of the area. The northern, elongate lobe of the anomaly is much more apparent on the reduced-to-pole data than on the total-field maps. However, magnetic anomalies in many parts of the extreme southern part of the study area are produced by volcanic rocks that may not have total magnetizations aligned with the Earth's field (V. J. S. Grauch, unpublished modelling, 1990). In these areas, the reduced-to-pole data are probably in error.

Reduced-to-pole magnetic data for the Getchell area are demonstrated for this workshop by an IMVIS image included diskettes accompanying this report, Open-File Report 93-XXD.

Pseudogravity Transformation

Gravity and magnetic fields are defined in similar ways mathematically, which permits transforming one field to the mathematical form of the other. The transformation of magnetic data to the form of gravity data is called the pseudogravity transformation (Baranov, 1957; Cordell and Taylor, 1971). Pseudogravity maps look like gravity maps, but reflect information solely about the *magnetic* properties of rocks, *not* density. Similarly, transformation of gravity data to the form of magnetic data is called the pseudomagnetic transformation, although this transformation is rarely used. Pseudogravity maps by themselves are useful in enhancing very regional features of the data. However, the pseudogravity transformation more often is used as an intermediate step in order to apply gravity interpretation methods to magnetic data. Pseudogravity data are normally computed by means of the fast Fourier transform (Hildenbrand, 1983).

Like reduction-to-pole, the pseudogravity transformation requires an assumption about the magnetization directions of the rocks in the area. The transformation also requires choice of a scaling factor that is input as a ratio of density to magnetization, but is normally somewhat arbitrary. Generally, it is assumed that the total magnetizations of most rocks in the area align parallel or anti-parallel to the Earth's main field (declination=16^{o}, inclination=66^{o} for the Getchell trend area). This is a good assumption for much of the Getchell study area except in the southern part, where total magnetizations of volcanic rocks probably differ significantly from the direction of the Earth's field. Pseudogravity transformations of the Getchell magnetic data are demonstrated for this workshop by means of the FFTFIL exercise on following pages.

Vertical Derivatives

Vertical derivatives, derivatives taken with respect to the *z* direction, are sometimes used to emphasis details of the data that may be masked by more regional features. This was a common practice in the past, when contour maps of second vertical derivatives, called "curvature" maps, were especially useful in bringing out details that were not well resolved with the original contour maps (Vacquier and others, 1951). Today, details can also easily be seen in the original data by displaying them as shaded-relief and graytone images. First and second vertical derivatives are normally computed by means of the fast Fourier transform (Hildenbrand, 1983).

The first vertical derivative is demonstrated on the Getchell reduced-to-pole magnetic data by the color figure on the following page.

References

Baranov, V., 1957, A new method for interpretation of aeromagnetic maps; Pseudo-gravimetric anomalies: Geophysics, v. 22, p. 359-383.

Cordell, Lindrith, and Taylor, P. T., 1971, Investigation of magnetization and density of a North Atlantic seamount using Poisson's thoerem: Geophysics, v. 36, no. 5, p. 919-937.

Grauch, V. J. S., and Bankey, Viki, 1991, Preliminary results of aeromagnetic studies of the Getchell disseminated gold deposit trend, Osgood Mountains, north-central Nevada, *in* Raines, G. L., Lisle, R. E., Schafer, R. W., and Wilkinson, W. H., eds., Geology and ore deposits of the Great Basin, symposium proceedings; Reno, Nev., Geological Society of Nevada, p. 781-792.

Hildenbrand, T. G., 1983, FFTFIL; A filtering program based on two-dimensional Fourier analysis: U. S. Geological Survey Open-File Report 83-237, 30 p.

Vacquier, V., Steenland, N. C., Henderson, R. G., and Zietz, Isidore, 1951, Interpretation of aeromagnetic maps: Geological Soc. of America Memoir 47, 155 p.

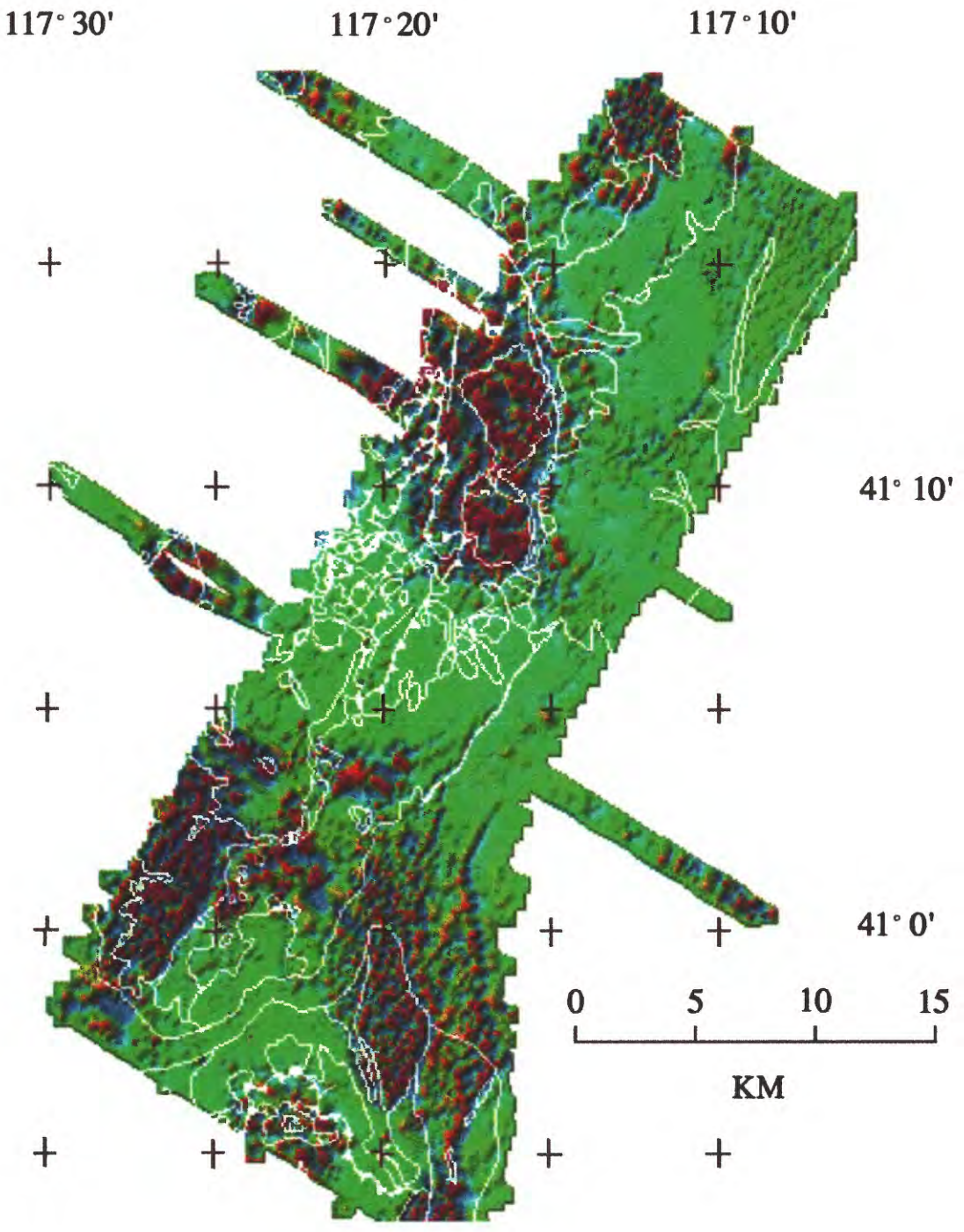

Figure 8-1.
Color-shaded relief image of the 1st-vertical derivative of the reduced-to-pole magnetic field data, illuminated from the northwest. The 1st-vertical derivative filter helps to resolve and accentuate shallow sources represented by short-wavelength anomalies. Geology is overlain in white. See Figure 5-2 for explanation of geologic contacts.

SPECTRAL ANALYSIS AND THE FFT

General Background

Just as sunlight can be reduced to a spectrum of colors based on the frequencies making up the different colors, we can examine the different frequency components of gravity and magnetic data. In this case, we are studying variations with respect to distance (variations in space rather than in time), so that "frequency" is a term describing the number of undulations of the data over a certain distance. The term "wavelength", the inverse of frequency, is the length of one undulation.

Potential-field geophysicists may refer to a "long-wavelength" (or "low-frequency") versus a "short-wavelength" (or "high-frequency") feature on a map in order to distinguish between an anomaly that covers a lot of ground versus one that covers little ground. In addition, anomalies are described in terms of their amplitude (high or low). Anomaly patterns may be described in similar terms. For example, a high-amplitude, short-wavelength anomaly pattern is an area that shows many very local anomalies having large amplitudes that may be described as a "busy" area of the map.

Because short-wavelength gravity or magnetic anomalies are associated with shallow sources and long-wavelength anomalies with deep sources, *as a rule of thumb* we assume that long-wavelength anomalies on a map are due to deep sources and short-wavelength anomalies are due to shallow sources. Using this assumption, we can separate the effects of the deep sources from the effects of the shallow sources where they are superimposed. However, this depth-wavelength correlation is not completely reliable because the wavelengths of anomalies are dependent on the shape of magnetic sources as well as depth. For example, shallow sources can produce long-wavelength anomalies if they are broad in shape. In addition, sources are normally continuous with depth, so that it is difficult to choose a cut-off wavelength separating the effects of deep sources from those of shallow sources. However, this analysis can be fruitful in some situations. To pursue this topic, advanced users should explore the program MFILT.

Gravity and magnetic data can be separated into different frequency (or wavelength) components through Fourier analysis, which involves a mathematical transformation, called a Fourier transform, that represents the data in terms of its different frequency components. Once in this form, certain frequency components can be enhanced or suppressed through bandpass filtering; that is, one band (or range) of frequencies is allowed to pass through the filter and the rest are eliminated. A lowpass (or high-gain) filter passes only low frequencies (long wavelengths); a highpass filter passes only high frequencies.

A second, perhaps more important, use of transforming gravity and magnetic data into frequency components is to facilitate complicated mathematical operations. The operations we have discussed earlier, namely pseudogravity transformation, reduction-to-pole, and vertical derivatives, are much easier to compute after Fourier transformation. Other common

operations are upward or downward continuation of the field to different observation levels. After the mathematical operations have been computed, the data are transformed back from frequency representation to space representation as an anomaly map.

For Fourier analysis of finite, digital data the theoretical Fourier transform is modified somewhat and organized efficiently for digital computation. This modified form is called the fast Fourier transform (FFT). Unfortunately, Fourier analysis is somewhat compromised by the use of digital data because of its digital nature and finite extent. The FFT requires some knowledge of what lies beyond the borders of the data area in order to properly construct the frequency components of the data, especially the low-frequency components. This can be overcome by making some good assumptions about the behavior of the data in these unknown areas, usually involving an extrapolation of the data beyond the data area and sometimes removal of a regional trend. In the FFTFIL program example we have suggested two ways to approach this extrapolation.

If the data have not been extrapolated properly before use of the FFT, the output anomaly map may contain artifacts called "ringing" or "edge effects". These are manifested in contour maps as rings around short-wavelength anomalies or stripes that parallel the edges of the data area, called edge effects.

References

Bhattacharyya, B. K., 1967, Some general properties of potential fields in space and frequency domain: A review: Geoexploration, v. 5, p. 127-143.

Bracewell, R. N., 1978, The Fourier transform and its applications: McGraw-Hill, Inc., New York, NY, 444 p.

Cordell, Lindrith, and Grauch, V. J. S., 1982, Reconciliation of the discrete and integral Fourier transforms: Geophysics, v. 47, no. 2, p. 237-243.

Dean, W. C., 1958, Frequency analysis for gravity and magnetic interpretation: Geophysics, v. 23, p. 97-127.

Hildenbrand, T. G., 1983, FFTFIL; A filtering program based on two-dimensional Fourier analysis: U. S. Geological Survey Open-File Report 83-237, 30 p.

Oppenheim, A. V., and Schafer, R. W., 1975, Digital signal processing: Prentice-Hall, Inc., Englewood Cliffs, New Jersey, 585 p.

Spector, Allan, and Grant, F. S., 1970, Statistical models for interpreting aeromagnetic data: Geophysics, v. 35, no. 2, p. 293-302.

FFTFIL PROGRAM HELP FILE

Program FFTFIL performs various two-dimensional filtering operations on standard grids using fast Fourier transforms (FFTs).

USAGE:

1. Create a command file with the following structure:

```
    line 1 : operator coded name (one of the following):
             --------  -----------
             psdmag    pseudomagnetic tranformation
             psdgrv    pseudogravity transformation
             redpol    reduction of total magnetic field intensity
                        to the north pole (see program F_RTP for
                        specialized filter for redution to pole at
                        low magnetic latitudes.
             upcont    upward continuation
             dncont    downward continuation
             1stver    1st-vertical derivative of the input field
             2ndver    2nd-vertical derivative of the input field
             banpas    bandpass filter
             strike    directional filtering
             vertot    change vertical-component data to total-field
             nofilt    no filtering
             (Note: If icoef=2, only Fourier coefficients are output;
                    any operator can be entered since it has no
                    effect)
    line 2 : input file name.ext
    line 3 : output file name.ext
    line 4 : title (cols. 1-56)
    line 5 : &parms
    line 6 : namelist parameters (see below)
    line 7 : &
```

Command file example:

```
strike
infile.grd
outfile.grd
FILTERED MAP
 &parms
 ioptl=-1,iopt2=1,thetl=15.,thet2=90.,
 &
```

Lines 1 through 4 can be left blank, in which case the program will prompt for the information.

2. Invoke the program by typing 'fftfil' and respond with the

command file name at the prompt.

Program FFTFIL cycles to the begining after each run. To exit from the program type 'ex' or carriage return.

The following queries are asked after each filter operation has been completed:

query 1 : additional filter to be applied? (y or n) - if 'y' the program asks queries 2 thru 6. if 'n' the program starts over by asking for the command file.
query 2 : new operator? Format same as in line 1 response.
query 3 : new datum level? Format same as in line 2 response.
query 4 : new output file name.ext?
query 5 : new title?
query 6 : parmameter change? (y or n) - If 'n' the filtering computations are started. If 'y' the user enters the parameters to be changed in a namelist (eg. &parms thetl=-90.,thet2=0.,&) (Note the following parameters cannot be changed: nadd,iopt2,idval,s,xo,yo).

Query 1 is then repeated for additional filter operations.

NAMELIST PARAMETERS

ioptl = 0 no printed output (default: ioptl=0)
6 output printed on terminal
-1 output printed on disk.
iopt2 = -1 no removal of mean from input array (default iopt2=-1)
0 remove mean using boundary values
1 remove mean and save grid, file name: CON.GRD.
nadd = no. of rows or columns added to each side of grid to reduce the effects of Gibbs phenomenon (default nadd=0).
wl,w2,w3,w4 - wavelengths used in bandpass filtering. Data are passed in the tetrahedral-shaped region starting at wl, ramping up to w2, and ramping down from w3 to w4. No data are passed with wavelengths less than wl or greater than w4. Data are passed unchanged between w2 and w3, and are increasingly suppressed from w2 toward wl and from w3 toward w4. wl<=w2<=w3<=w4. (default wl=w2=0, w3=w4=1.0e+30, i.e. all pass)
den - density contrast, gm/cc (default den=1.).
bmag - magnetization contrast, e.g. susceptibility * field strength for induced magnetization case (default bmag=1.).
dec, xinc - declination and inclination of earth's field,degrees. (default dec=0. xinc=90.)
bdec, binc - declination and inclination of magnetization vector. (default bdec=0. binc=90.)
idval = 0 no flagged grid points in input data (default idval=0)
1 flagged grid points in input data
-1 flagged values removed and locations in file FLAG.LOC.

Note: it may be best to plug the dval areas first, before running fftfil, in which case idval=0.

icoef = 2 output only Fourier coeff's of input grid in file FFTFIL.COF; no filter operation is performed (Note: location of flagged values are stored in file FLAG.LOC in users area.)

1 Save Fourier coefficients in file FFTFIL.COF for later use but perform designated filter operation. (Note: If data contains flagged values a file named FLAG.LOC containing their locations is also created in users disk area.) The saved fftfil.cof file has not been operated on by the disignated filter. Normally icoef=1 is associated with operation "nofilt".

0 Fourier coefficients not saved (default icoef=0).

-1 Fourier coefficients in file FFTFIL.COF are used as input. note that if flagged values are present in the data, file FLAG.LOC is required and 'idval' must be equal to -1. In addition, the parameter 'nadd' must be identical to its assigned value when the Fourier coefficients were saved.

z - continuation distance, in grid units. z > 0 for downward continuation and z < 0 for upward continuation (default z = 0).

thet1, thet2 - angles from geographic north that form a pie-slice filter for directional filtering (-90.ge.thet1 .le.+90.;thet2.gt.thet1). (default thet1=0. thet2=90, i.e., all pass)

istr = -1 reject trends between thet1 and thet2.

+1 pass (default istr=1).

The following parameters can be used if the spacing and origin of the output grid is to differ from that of the input grid.

ddx - new grid spacing in the x direction, in grid units.
ddy - new grid spacing in the y direction, in grid units.
xo - new origin of rows, in grid units.
yo - new origin of columns, in grid units.

REFERENCE

Hildenbrand, T.G., 1983, FFTFIL: A filtering program based on two dimensional Fourier analysis: U.S. Geological Survey Open-File Report 83-237, 31 p.

FFTFIL PROGRAM DEMONSTRATION AND EXERCISE

We begin by loading the magnetic anomaly grid file GMAG.TRM from data diskette #1 of OF 93-560D (also see exercise #1 on p.8-16). For this exercise we will need a decimated version of GMAG.TRM to be called GMAG.CGD. The program REGRID can be used to create this coarse grid as follows:

```
C:>regrid
file to be interpolated :  gmag.trm
Residual mag, Getchell DIGHEM survey, UTM 0 117          pgm:gdcnv
ncol=  341 nrow=  495
xo,yo=    -41.800        4525.0       dx,dy=     .10000      .10000
output file :  gmag.cgd
title :  Residual mag at 0.2 km grid spacing
new dx,dy :  .2 .2
change location or areal coverage ?  y
enter new  x origin, y origin, ncol, nrow : -46 4525 194 249
Stop - Program terminated.
```

Because FFTFIL requires that the first row of the input grid contain at least one valid data value, we must trim empty rows from GMAG.CGD using the program TRIMGRD:

```
C:>trimgrd
This program trims off rows and columns around the edges of the grid
that are entirely dvals
Enter input file name gmag.cgd
Enter output file name gmag.tgd
 writing output file...
Stop - Program terminated.
```

The following command file (GFFTDV.CMD) will perform a pseudogravity transformation on the grid GMAG.TGD, filling in no-data areas (DVALs), and extending the grid 15 or more rows and columns (As as rule of thumb we usually try to extend the grid about 10% or at least 10 rows and columns in order to reduce edge effects):

```
psdgrv
gmag.tgd
gpgl.tgd

$parms bdec=16,dec=16,xinc=66,binc=66,bmag=100,den=1,nadd=15,idval=1 $
```

This is what the output looks like:

```
C:>fftfil
Enter command file name (car ret to exit):  gfftdv.cmd
enter title:  pseudogravity, using fftfil to plug and extend grid
blocking rows =  9
transformation   of   total   magnetic   intensity   field   to
```

```
pseudo-gravitational field,
by means of the fast fourier transform and the poisson equation.

title: pseudogravity, using fftfil to plug and extend grid
parameters: density=  1.000     datum level z=   .000
            intensity of magnetization=  100.000
            inclination & declination of geomagnetic field=  66.000
 16.000
            inclination & declination of magnetization vector=
66.000   16.000
            thetl=     .000     thet2=   90.000     istr= 1
            wl,w2,w3&w4= .0000E+00 .0000E+00 .1000E+31 .1000E+31

            dx & dy=   .200000E+00   .200000E+00
            origin of grid(xo & yo)=   .452540E+04  -.418000E+02
            no. of columns & rows=  168  245
            nadd=   15  extended columns & rows=  198  288
            input file name: gmag.tgd

            output file name: gpgl.tgd


forward transform completed
completed applying filter to coefficients
inverse transform completed
additional filtering to original grid?(y or n)  n
Enter command file name (car ret to exit):
end of job
Stop - Program terminated.
```

PRACTICAL USAGE

FFTFIL contains options to extend grids to reduce edge effects (NADD) and plug holes in grids (IDVAL = 1) (and it will also automatically extend grids to improve fast Fourier transform (FFT) performance); however, the algorithm used to extend and plug grids is rather crude and there is no provision for output or display of plugged/extended grids. As an alternative, a series of programs has been developed to perform these steps outside of FFTFIL:

MEGAPLUG, MEDIPLUG, or SKIM can be used to plug holes in a grid.

CK_DIMS can be used to check the dimensions of a grid and recommend new dimensions for efficient use of the FFT algorithm.

PREP will extend a grid to specified dimensions (as recommended by CK_DIMS) prior to running FFTFIL; it will also remove a mean and a planar surface from the data to improve FFTFIL results.

DE_PREP will restore a grid to its initial dimensions following FFTFIL filtering; it will optionally add back the planar surface removed by PREP.

ADDGRD can be used to restore holes in the filtered grid.

EXERCISE - PSEUDOGRAVITY TRANSFORMATION

1. Use MEGAPLUG to fill holes in the aeromagnetic data grid, GMAG.TGD, which was created during the preceeding demonstration:

```
C:>megaplug
enter grid filename: gmag.tgd
enter output filename :  gmag.plg
number of minimum curvature iterations to use :  20
enter 1 to completely fill
    or 2 generate hulls around contiguous data 1
   1.701412E+38          10          11
        168         245          20       50000       50001
Stop - Program terminated.
```

2. Use CK_DIMS to get recommended dimensions for the extended grid.

```
C:>ck_dims
Enter input grid name (NO DVALS !): gmag.plg
* ncol =   168 nrow =   245
Suggested new values:
 ncol =   176  192  208  224
 nrow =   256  288  320  352
Stop - Program terminated.
```

3. Use PREP to extend the plugged grid. Call the output grid 'GMAG.PRP'.

```
C:>prep
Enter input grid name (NO DVALS !): gmag.plg
* Enter (new) ncol and nrow: 192 288
* blocking rows =  9
 alpha =   -3.041139E-01, beta =    2.081435E-01
Enter output grid name: gmag.prp
*
Stop - Program terminated.
```

4. Use IGRFPT to determine the magnetic inclination and declination at the location and time of the original magnetic survey.

```
C:>igrfpt
 DIGRF model calculation
 enter year and day [ eg.       1980          1  ] 1989 300
 enter lat (deg), long (deg positive EAST )  [ eg.      40.000000
    -105.000000 ] 41 -117
 enter altitude in meters asl  [ eg.    1500.000000 ] 1480
 input=    1989300       41.000000     -117.000000     1480.000000

   total field       inclination      declination
      53577.86          65.60           15.96

 components: North        East         Vertical
      21276.44        6085.95       48794.06

 another ? [y] n
Stop - Program terminated.
```

5. Use the editor EDIT to create a command file called GFFT.CMD as follows:

```
psdgrv
gmag.prp
gpg2.prp
Pseudogravity, prepped grid
$parms bdec=16,dec=16,xinc=66,binc=66,bmag=100,den=1,nadd=0 $
```

6. Run FFTFIL. Respond to the prompt with the name of the command file.

```
C:>fftfil

Enter command file name (car ret to exit):  gfft.cmd
blocking rows =  9
transformation   of   total   magnetic   intensity   field   to
pseudo-gravitational field,
by means of the fast fourier transform and the poisson equation.

title: Pseudogravity, prepped grid
parameters: density=  1.000     datum level z=    .000
            intensity of magnetization=  100.000
            inclination & declination of geomagnetic field=   66.000
 16.000
            inclination & declination of magnetization vector=
66.000   16.000
            thet1=      .000     thet2=   90.000     istr= 1
            w1,w2,w3&w4=  .0000E+00  .0000E+00  .1000E+31  .1000E+31

            dx & dy=    .200000E+00   .200000E+00
            origin of grid(xo & yo)=    .452540E+04  -.418000E+02
            no. of columns & rows=  192  288
            nadd=    0  extended columns & rows=  192  288
            input file name: gmag.prp

            output file name: gpg2.prp


forward transform completed
completed applying filter to coefficients
inverse transform completed
additional filtering to original grid?(y or n)  n
Enter command file name (car ret to exit):
end of job
Stop - Program terminated.
```

7. Run DE_PREP on the output grid 'GPG2.PRP'. Do not restore the surface.

```
C:>de_prep
Enter name of grid to be de-prepped:
* gpg2.prp
Enter output grid name:
* gpg2.plg
Enter id:
* de_prepped pseudogravity
Enter mode: 1 to add back linear trend, or 2 not to add
back linear trend:
* 2
Stop - Program terminated.
```

8.Run ADDGRD using the 'm' (mask) operator to restore holes in the grid. Note: the second input file is used as a mask or template to restore DVAL's where they existed in the original grid.

```
C:> addgrd
 first input file : gpg2.plg
title=plugged pseudogravity
 nc X nr          =        168          245
 xo, yo, dx, dy =      -41.800000      4525.400000     2.000000E-01
   2.000000E-01
 operator  h(elp), + - * / m %    : m
 second input file [constant] : gmag.tgd
 output file : gpg2.tgd
 output title [ same as file 1 ] pseudogravity using prepped grid
Stop - Program terminated.
```

9. Now compare the two grids GPG1.TGD and GPG2.TGD in two ways. First use the program ADDGRD to take the difference of the two grids (see the demonstration of ADDGRD in chapter 9 if in doubt), and use DETOURG to contour the difference. Then use GRDREM to convert the two grids into REMAPP images; load the images into buffers of program DISPLAY (I option), stretching them first (V option); then toggle between the memory channels to see the differences.

This exercise has demonstrated the use of FFTFIL on grids containing DVALS. The differences between GPG1.GRD and GPG2.GRD result from the two methods used to extrapolate data away from the observed data values. It is important to remember that the methods and parameters used in preparation of data grids for fourier transform operations can affect the resulting filtered grids.

INDEPENDENT PC EXERCISES III

1. Follow the demonstration of **FFTFIL** starting on page 8-10 to create and compare the pseudogravity created in two different ways from the magnetic data. (No need to create the command files **gfftdv.cmd** and **gfft.cmd**; they are available on diskette #1 on 93-560D.) The two ways to create the pseudogravity involve different extrapolations of the data before pseudogravity transformation. The first way allows **FFTFIL** to extrapolate the data internally. The second way uses **MEGAPLUG, CK_DIMS,** and **PREP** to prepare the grid for **FFTFIL**, and **DE_PREP** and **ADDGRD** to remove the extrapolated data afterwards. As suggested at the end of the demonstration, compare the differences between the two results by subtracting the grids and looking at the difference. Alternatively, you can compare the two pseudogravity grids in program **DISPLAY** as follows. Using **GRDREM**, create images of the two pseudogravity grids, **gpg1.img** and **gpg2.img**. As described in #2 of the Independent PC Exercises II, run **DISPLAY** to display and store these images in buffers 1 and 2. Now toggle between buffers 1 and 2. The differences stress the importance of careful consideration of the data preparation before using the FFT.

2. Copy **grtp*.*** from diskette #2 of 93-560D (this should copy 5 files). From #1 above, you should have **gmag.cgd** and **gpg2.img**. Using **GRDREM**, create **gmag.img** from **gmag.cgd**. Using **DISPLAY**, put the following images into buffers 1-3, respectively: **gmag.img, grtp.img, gpg2.img** (magnetic, reduced-to-pole (RTP) magnetic, and pseudogravity data). Toggle between these buffers. *(The pseudogravity image will be slightly shifted in location)*. Note the shift in anomaly locations between the RTP and magnetic images. Note how the pseudogravity enhances the most regional features.

3. Copy **g1ver.img** from diskette #2 of 93-560D to your test data directory. From #2 above, you should already have copied **grtp.img, grtplo.img, grtpmid.img,** and **grtphi.img.** Using program **DISPLAY**, input and store **grtp.img, grtplo.img, grtpmid.img, grtphi.img** and **g1ver.img** to buffers 1-5, respectively. These are the reduced-to-pole (RTP) magnetic data, lowpassed RTP magnetic data, mid-range bandpassed RTP magnetic data, highpassed RTP magnetic data, and first vertical derivative of the RTP magnetic data, respectively. The bandpassed data were actually constructed using program **MFILT** (for very advanced users only), where one can choose the cut-off wavelengths for bandpass filtering based on looking at the spectrum of the data. Toggle between the various bandpassed data to see the variation in frequency content. Note the similarity between the low-passed RTP magnetic data and the original RTP data, showing the dominance of long wavelengths in the original. Then toggle between the highpassed, mid-range bandpassed, and the first vertical derivative images and compare.

4. Using program **IMVIS**, compare the original magnetic data (GMAG1.LBL) to the reduced-to-pole magnetic data (GRTP1.LBL). Compare either magnetic image to the color figure of the first vertical derivative (figure 8-1). Which features are enhanced? Which are subdued? Note that beading due to the wide line spacing (the blotchy character) is very noticeable in the first vertical derivative.

HORIZONTAL-GRADIENT METHOD

Applied to Gravity Data

The horizontal-gradient method for gravity (Cordell, 1979) is a boundary finder, which helps objectively locate the edges of gravity sources from gravity anomalies that have unclear edges. The method is based on the behavior of gravity anomalies over simple vertical boundaries. Figure 8-2 shows a plot of the gravity field over a simple near-vertical boundary between homogeneous materials having contrasting densities. The steepest part of the slope of the gravity curve (also, the inflection point) is directly over the top edge of the boundary. The steepness of the slope can be computed by calculating the magnitude of the first derivative in the horizontal direction. This calculation will produce peaks over places where the gravity curve is steepest, i.e., over the contacts.

In map form, the derivative takes the form of the two-dimensional horizontal gradient. Analogous to the one-dimensional case in figure 8-2, the horizontal-gradient magnitude (HGM) has local maxima along ridges of a HGM map. These maxima can be located automatically by computer (Blakely and Simpson, 1986) and plotted as symbols. The sizes of the symbols can be varied to indicate the sizes of the HGM, which in turn is related to the amount of contrast in physical properties across the boundaries, thickness of the rock masses, and depth of burial. On the other hand, it may be informative to examine the HGM data as an image rather than as plotted symbols. Before displaying the HGM data, it may be useful to take the logarithm of the data before displaying in color or to stretch the histogram of the data before imaging.

Many HGM maxima locate density boundaries in the subsurface, which are commonly associated with faults and lithologic contacts that juxtapose rocks of differing densities. The accuracies of the locations of HGM maxima over density boundaries are determined primarily by how well the boundaries approximate steeply dipping planes, terrain effects, data control, interference from neighboring anomalies, and boundary dip (Grauch and Cordell, 1987).

Applied to Magnetic Data

The horizontal-gradient method can be applied to magnetic data by first transforming the data to pseudogravity (Cordell and Grauch, 1985), in which case the HGM maxima generally locate near-vertical boundaries between rocks of contrasting magnetization rather than density. As with gravity data, the accuracies of the locations of HGM maxima over magnetization boundaries are determined primarily by how well the boundaries approximate steeply dipping planes, terrain effects, data control, interference from neighboring anomalies, and boundary dip (Grauch and Cordell, 1987). In addition, the accuracy is compromised by inappropriate choice of magnetization direction during pseudogravity transformation.

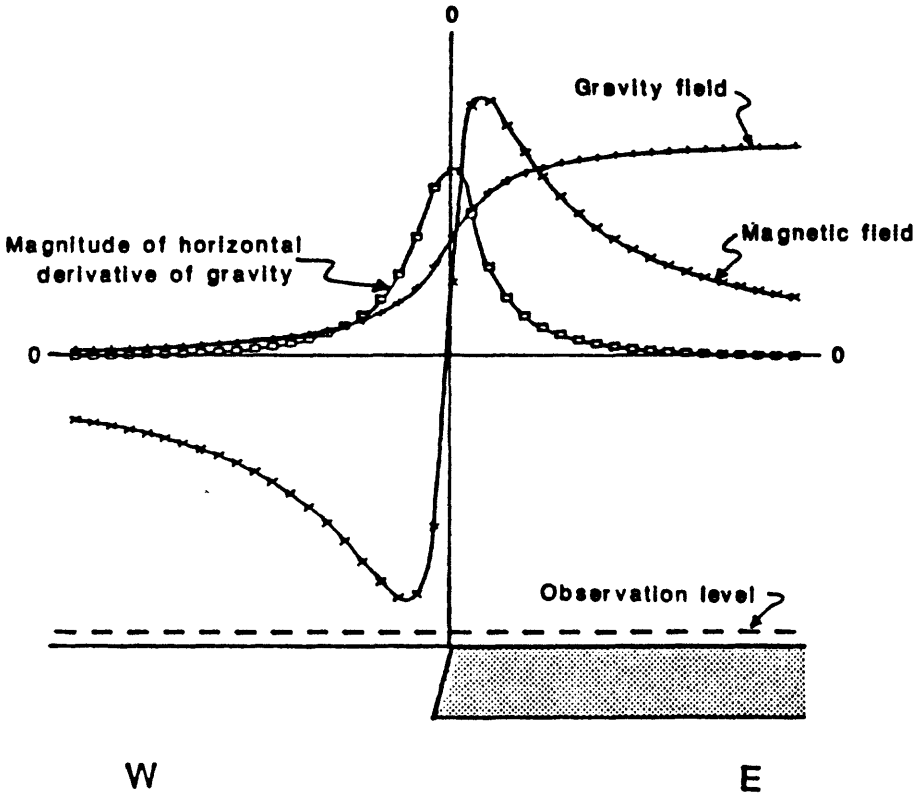

Figure 8-2. Various fields over a dense/magnetic body with a near-vertical edge, demonstrating the horizontal-gradient method.

In some cases, strong gradients associated with regional magnetic anomalies overwhelm more subtle gradients in the vicinity of the anomaly (this occurs in the north-central part of the Getchell area near the large anomaly associated with a highly magnetic pluton). The problem is exacerbated by pseudogravity transformation, which emphasizes regional features over local ones. In such cases, the horizontal-gradient method can be applied to the reduced-to-pole magnetic data instead of pseudogravity *if* one considers some added limitations. This practice has recently become popular with some workers. Because it is not discussed in the literature, a more detailed discussion is required here.

Figure 8-3 shows magnetic-anomaly profiles over two hypothetical, prism-shaped, magnetic sources at the North Pole. The depth extent of one prism is much less than its lateral extent (thin prism) whereas the depth extent of the other is much greater than its lateral extent (thick prism). Inspection of the profile over the thick prism suggests that, like the gravity field, the steepest slopes (and also, the inflection points of the curves) occur directly over the two edges of the prism. On the other hand, there are three inflection points associated with each prism edge in the profile over the thin prism, with only one directly over an edge (albeit the one associated with the largest gradient). This suggests that the horizontal-gradient method applied to reduced-to-pole magnetic data can be very useful in areas where magnetic sources are generally deeper than they are wide, such as plutons or near-vertical faults with large throw. On the other hand, in areas where magnetic sources are likely to be thin, such as areas of basalt flows, the method may produce many artifacts. Comparison of applying the method to reduced-to-pole magnetic data versus pseudogravity is demonstrated in map view by figure 8-4.

Other than the added problem of multiple HGM maxima associated with one boundary, the limitations to the horizontal-gradient method applied to reduced-to-pole magnetic data are the same as when applied to pseudogravity. The most severe problem is interference from neighboring or overlying magnetic sources. Inappropriate choice of magnetization for the rocks in the area will offset the location of HGM maxima from their causative magnetization boundaries.

The HGM of Getchell pseudogravity data are shown on figure 8-5 and HGM from the Getchell reduced-to-pole magnetic data are included as an IMVIS image in the diskettes accompanying this report, Open-File Report 93-560D. The following demonstration of program BOUNDARY also suggests ways to compare the two results.

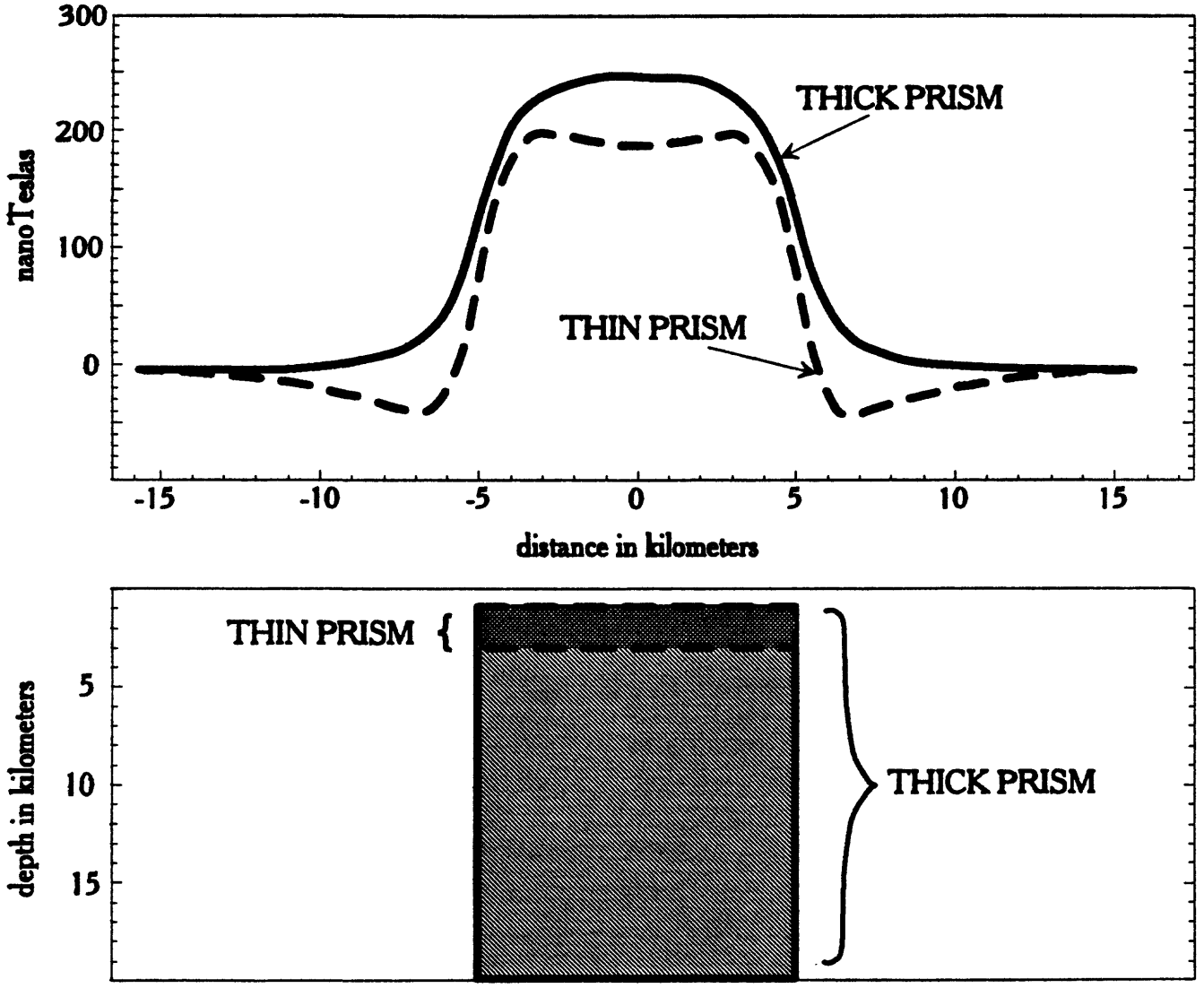

Figure 8-3. Magnetic profiles over hypothetical thick and thin prisms, computed at the North Pole. Magnetic susceptibility of the thin prism is twice that of the thick prism for convenience of scale.

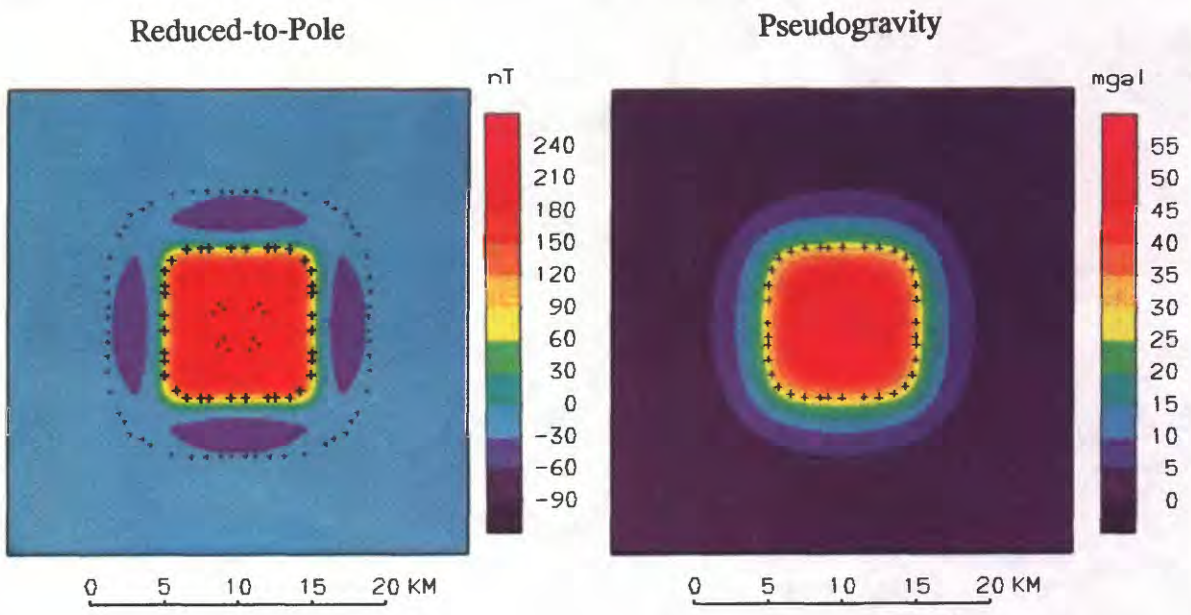

Figure 8-4. Comparison of horizontal-gradient method applied to reduced-to-pole magnetic data versus pseudogravity for the thin versus thick prisms of Figure 8-3. The plus symbols indicate the locations of HGM maxima; their sizes are proportional to relative magnitude. Depth to the tops of both prisms is 1 km; depth extent for the thin prism is 2 km and 20 km for the thick prism.

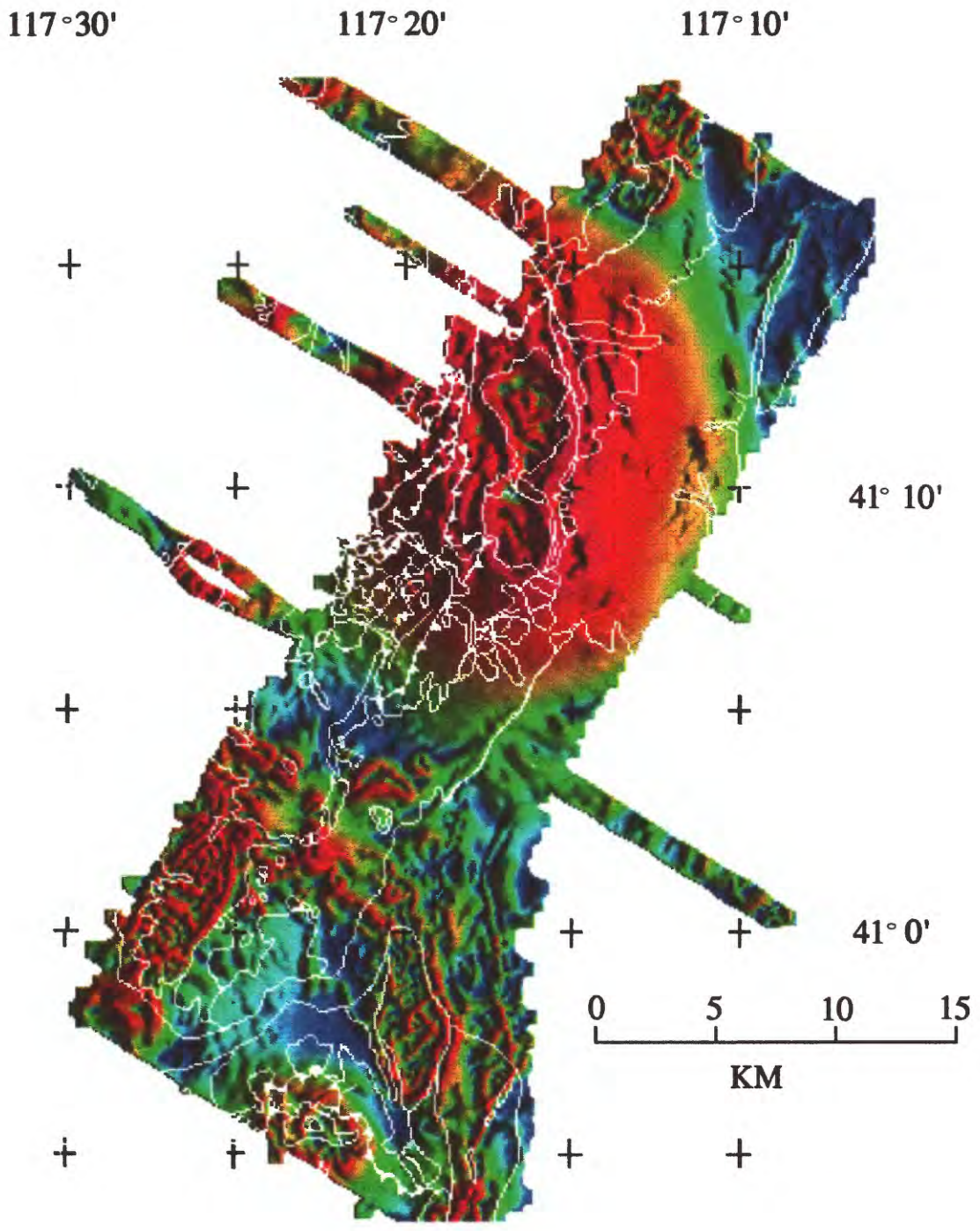

Figure 8-5

Color-shaded relief image of horizontal-gradient magnitudes of pseudogravity, illuminated from the east. The ridges mark the steepest slopes in the pseudogravity field and in many cases locate abrupt boundaries between rocks with different magnetic properties, such as faults. See Figure 5-2 for explanation of geologic contacts (white lines).

References

Blakely, R. J., and Simpson, R. W., 1986, Locating edges of source bodies from magnetic or gravity anomalies: Geophysics, v. 51, p. 1494-1498.

Cordell, Lindrith, 1979, Gravimetric expression of graben faulting in Santa Fe country and the Espanola Basin, New Mexico: New Mexico Geol. Soc. Guidebook, 30th Field Conference, Santa Fe Country, p. 59-64.

Cordell, Lindrith, and Grauch, V. J. S., 1985, Mapping basement magnetization zones from aeromagnetic data in the San Juan Basin, New Mexico *in* Hinze, W. J., ed., The utility of regional gravity and magnetic anomaly maps: Society of Exploration Geophysicists, Tulsa, Oklahoma, p. 181-197.

Grauch, V. J. S., and Cordell, Lindrith, 1987, Limitations of determining density or magnetic boundaries from the horizontal gradient of gravity or pseudogravity data: Geophysics, V. 52, no. 1, p. 118-121.

BOUNDARY PROGRAM DEMONSTRATION AND EXERCISE

This is a demonstration and explanation of the program **BOUNDARY**, which implements the horizontal-gradient method. The program has several options, including the pseudogravity transformation if desired. However, the pseudogravity option is limited to very small grids. One can transform magnetic data to the pseudogravity beforehand by using program **FFTFIL** instead. We will begin with pseudogravity grid **gpg2.tgd** that was created in the **FFTFIL** demonstration earlier in this chapter.

```
C:>boundary

BOUNDARY - VERSION 1.01


See file BOUNDARY.HLP for information


Operation [0-4]:

    0.  Information
    1.  Transform grid to pseudogravity
    2.  Calculate horizontal gradient magnitude
    3.  Locate maxima in grid
    4.  Stop

 = ?   2

HORIZONTAL GRADIENT CALCULATION


Filename of input grid = ?    gpg2.tgd
Filename of output grid = ?   gpgg.tgd
pg of Getchell DIGHEM, dec=16,inc=66,mag/den=100
regrid
 ncol=         168      nrow=         245
 xo=       -41.800000      yo=       4525.400000
 dx=     2.000000E-01      dy=     2.000000E-01

New ID (56 characters or less) = ?  HGM of Getchell pseudogravity
```

The horizontal-gradient magnitudes (HGM's) have now been computed and the program cycles back to asking for the input operation number. At this point you can either (1) exit from the program and create a color or color shaded-relief image (making sure the image is stretched using **HISTNORM** in the process) for viewing with **IMVIS**, (2) exit from the program and take the logarithm of the HGM grid before creating a color-contour or color shaded-relief image with **IMVIS** (in which case stretching may not be necessary), or (3) continue with the program and create points indicating the locations of HGM maxima in the grid. For this demonstration, we will continue with the program and compute maxima points, affectionately called "maxspots".

```
Operation [0-4]:

    0.  Information
    1.  Transform grid to pseudogravity
    2.  Calculate horizontal gradient magnitude
    3.  Locate maxima in grid
    4.  Stop

 = ?   3

LOCATION OF MAXIMA WITHIN A GRID


Filename of input grid = ?   gpgg.tgd                    <<Input the HGM grid
Output is a binary xyz file.

x and y in cartesian or geodetic coordinates [g/c] ?   c
```

(Cartesian coordinates are in distance units, such as km; geodetic coordinates are latitude/longitude in decimal degrees).

```
1.  Significance levels = 1,2,3, and 4
2.        "          "    = 1
3.        "          "    = 2,3, and 4
4.        "          "    = 2
5.        "          "    = 3 and 4
6.        "          "    = 3
7.        "          "    = 4
```

These options require some explanation. The figure below shows the location of grid intersections used to test for a maximum near the grid point (*i,j*). The program tests each of the four directions to see if (*i,j*) is the maximum of the three points tested. A value of 1 is added to a counter *N* for each direction that (*i,j*) is found to be maximum. *N* is called the significance level of the maximum, and can have a value from 0 to 4. The options above allow the user to determine which significance levels are acceptable for a given maximum. For instance, option 1 accepts (*i,j*) as a maximum if it is found to be maximum in one or more of the four directions (*N* can range from 1-4). Option 5 accepts only maxima that are maximum in three or four directions (*N*=3 or 4). The choice of option is usually empirical, depending on the features that each trial brings out. A good starting place is option 3.

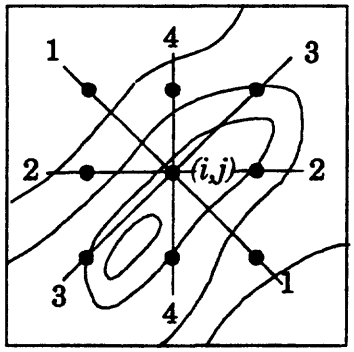

```
Pick one (1 through 7) ?   3
The total set of maxima from this grid have the following
statistics:

Number =     2427
Average =    9.678
Standard deviation =    9.071
Maximum =    51.08
Minimum =    .2883


Specify range of maxima to be output...
```

Here's another place where trial and error can help determine which values of HGM you wish to keep. The lowest values can bring out very subtle features, but they also can arise from insignificant variations in the data. In this example, we'll keep all the "maxspots".

```
Lower limit = ?   0
Upper limit = ?    52
Filename for output list = ?   gpgg3.spt          <<The output binary xyz file
     2427 records written

Another output file with a new range (y/n) ?   n
```

Alternatively, you could output various ranges of values at this point for later comparison.

```
Operation [0-4]:

    0.  Information
    1.  Transform grid to pseudogravity
    2.  Calculate horizontal gradient magnitude
    3.  Locate maxima in grid
    4.  Stop

 = ?   4
Stop - Program terminated.
```

Now you can quickly view the spots using program **CONTOUR**, described earlier. Use the command file **gconxyz.cmd** (diskette #1 of 93-560D) that looks like this:

```
 $parms
 ispost=2, iproj=2, cm=-117, baslat=0, szpost=.015
 $
```

This command file will ask for an input grid to contour (use either **gpg2.tgd** or **gmag.tgd**) and a station file. The station file is the maxspot file you just created, **gpgg3.spt**. (Note that this file *must* have projected distance coordinates that match the projection of the grid.) The format of the xyz file is binary, so press ENTER after the next question about format.

A more satisfying way to look at the maxspots is to create an overlay of them for viewing over **IMVIS** images. The following example shows how to create a **.grf** file for this purpose. Note that the **.grf** *must* have unprojected latitude/longitude coordinates. If the

0^{o}). Alternatively, we could have output the maxspots in latitude/longitude coordinates (geodetic coordinates) in program **BOUNDARY**.

```
C:>genproj
GENERAL PROJECTION PROGRAM WEST LONGTITUDES AND CENTRAL MERIDIAN MUST BE
NEGATIVE
ENTER INPUT FILE NAME:  gpgg3.spt
ENTER OUTPUT FILE NAME:  gpgg3.xyz
is input file xyz or pos? xyz
enter cm,baslat,proj no. & 1(forw) or 2(inv)
-117 0 2 2
Stop - Program terminated.

C:>xyz2grf
enter input xyz file:
gpgg3.xyz
enter output grf file:
gpgg3.grf
enter symbol (4 characters max):
+
```

(A period or other very small character works best on the plot)

```
enter symbol color (1=241,2=242,...15=255):
5
```

(The 241, 242, etc. numbers refer to the color number in the **IMVIS .pal** file. In this particular case, entering a 5 designates color number 245 in the **.pal** files used for the Getchell images, the color used by the tick marks.)

```
enter symbol size (1=large, 2=medium, 3=small):
3
Stop - Program terminated.
```

Now when you invoke **IMVIS** and use the .GRF option in the PLOT menu, you should see GPGG3.GRF displayed as a choice for overlays.

TERRACE METHOD

General Background

The terrace method (Cordell and McCafferty, 1989) is a data processing technique that transforms gridded aeromagnetic or gravity data into inferred physical-property (magnetization or density) maps. The results are maps that emphasize large, sharply bounded domains of magnetization (in the case of magnetic data) or density (for gravity data). Like the horizontal gradient method, we assume the edges of the domains are vertical-sided or very steeply dipping. The domains and their edges often delineate known geologic features such as faults, contacts, or intrusive igneous bodies. One could think of a terrace map as crudely analogous to a geologic map of the magnetic sources or density sources.

To scale the terrace grids to values of magnetization (cgs units; emu/cm^3) or density (cgs units; g/cm^3), involves taking a few more data processing steps and, like any other modeling process, requires having some geologic knowledge on the three-dimensional geometry (depth and thickness) of the magnetic or density sources. This procedure is called a forward calculation. Many times, it is unrealistic to attempt to calculate physical property values within domains because the geometry of the sources is too complicated or there is too little information available. However, even without a forward calculation, the terrace maps are still very useful as a way to qualitatively outline magnetization and density sources.

Demonstration I - Terrace Operation on Getchell Pseudogravity

The first demonstration illustrates the terrace method on the Getchell data using the grid **gpg2.tgd** created previously in the FFTFIL demonstration (see #2 on p. 8-38 for more instruction). There is no attempt to scale the terrace map to units of magnetization.

In general, the first step in the terrace process usually involves the removal of a regional field from the potential-field data in order to enhance the short-wavelength features. The regional field can be removed from the gravity, magnetic, or pseudogravity anomaly data. There are many approaches to remove a regional field (see FFTFIL, MFILT, SURFIT).

In the Getchell data, the long-wavelength magnetic anomaly associated with the pluton masks many of the shorter wavelength features. When the magnetic data are transformed to pseudogravity anomalies, the problem becomes worse. The pseudogravity anomaly associated with the pluton 'swamps' the signal from the shorter wavelength features. The program SURFIT is used to calculate and remove a regional field from the Getchell pseudogravity grid. SURFIT provides a computationally quick method to calculate and output regional and residual fields for polynomial surfaces of order 1 through n. It's a good idea to display and compare the residual field grids to determine which residual grid suits the purpose of your study. There is no set answer on which

residual field to use. The choice depends on what features in the data set are to be enhanced.

For this demonstration, calculate four regional and residual grids using SURFIT:

```
C:>surfit
enter grid filename : gpg2.tgd
start, end, increment of orders, [e.g., 2,5,1] 1 4 1
```

This tells the program that the first polynomial order we want to fit is the 1st order, the last is the 4th order, and to increment the orders by 1 each time; that is, the desired orders are 1, 2, 3, and 4.

```
Want grids of residuals? [0=no, 1=yes] 1
start, end, increment :  1 4 1
least_square coefficients completed
order  1 finished
order  2 finished
order  3 finished
order  4 finished
Stop - Program terminated.

C:> dir gpg2.*
 Volume in drive C has no label
 Directory of C:\WORKSHOP

GPG2     S01     168656 05-18-93  11:36a
GPG2     R01     168656 05-17-93   3:27p
GPG2     S02     168656 05-18-93  11:36a
GPG2     R02     168656 05-17-93   3:27p
GPG2     S03     168656 05-18-93  11:36a
GPG2     R03     168656 05-17-93   3:27p
GPG2     S04     168656 05-18-93  11:37a
GPG2     R04     168656 05-17-93   3:27p
GPG2     TGD     168668 05-05-93   9:56a
        9 file(s)     1517916 bytes
```

A suffix beginning with S means the grid is the surface that was fit to the data, one beginning with R means the grid is a residual (the original minus the surface). The 01, 02, etc. indicate the order of the surface that was fit. You can examine the differences in the residuals by using **GRDREM** to change them to REMAPP image files and **DISPLAY** to display them (store them in buffers 1-4 so that you can toggle between them). In this demonstration, the 4th-order pseudogravity grid was chosen to be the input to TERRACE (**gpg2.r04**). TERRACE is actually a batch file that runs several different programs. The two input parameters for this batch file are the file name of the input grid and the number of iterations for the terrace operation. From experience, defining the number of iterations to be between 10 and 20 is sufficient for potential-field data.

```
C:>terrace gpg2 r04 10
..
**Running the gradient program**
**Running the stdbndy program**
**Running the combgrd program**
**Running the terrace4 program**
.
Enter input file name:
*Enter output file name:
*Enter number of iterations:
Enter output-file id:
*Iteration=1 Percent of flat slopes=67.42712
Iteration=2 Percent of flat slopes=75.32556
Iteration=3 Percent of flat slopes=80.77988
Iteration=4 Percent of flat slopes=84.30029
Iteration=5 Percent of flat slopes=87.09184
Iteration=6 Percent of flat slopes=88.86784
Iteration=7 Percent of flat slopes=90.34499
Iteration=8 Percent of flat slopes=91.43100
Iteration=9 Percent of flat slopes=92.35909
Iteration=10 Percent of flat slopes=93.07337
Stop-Program terminated.

**Running the transpos program**
**Running the fixter program**
**Running the transpos program**
**Running the fixter program**
**Running the mediplg1 program**
**Running the medifilt program**
**Deleting the temporary files
.
**Done:  gpg2.ter,gpg2.fil created**
```

The output terrace-magnetization grid is **gpg2.fil** and is shown on figure 8-6.

Demonstration II - Terrace Operation with Density Scaling

The second demonstration documents the steps taken to calculate a terrace-density map with actual values of density contrast (in g/cm^3) by referring the terrace grid to a slab model. The logic behind how this model was defined is given in McCafferty and Cordell (1992). Physical property units are output in cgs.

The grid **grav.grd**, *used in this demonstration, is not provided to you as part of this open-file report.* This demonstration is presented to illustrate how one could scale a terrace grid to values of density contrast.

The same procedure can be followed with magnetic data (the result being a terrace-magnetization map in units of emu/cm^3) if the data are first transformed to pseudogravity anomalies (see the program BOUNDARY or FFTFIL). Additionally, one would substitute the program F_MAG for F_GRAV (described below).

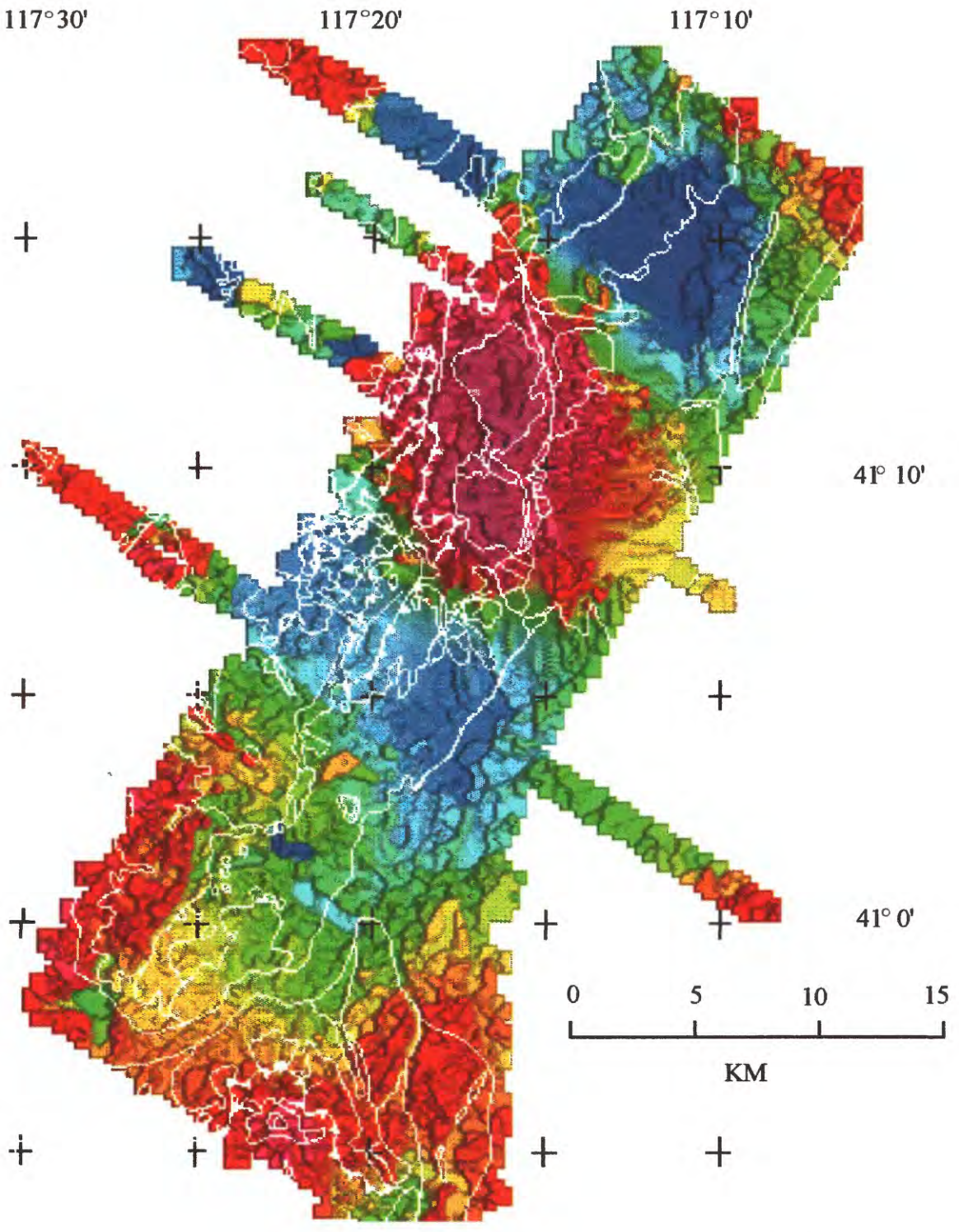

Figure 8-6. TERRACE-magnetization map of pseudogravity residual displayed with vertical illumination (an edge-enhancing technique). A 4th-order regional surface was calculated and removed from the pseudogravity data before terracing. The colors indicate variations in magnetization *and* depth to magnetic sources. Geologic contacts (see Figure 5-2) are overlain in white.

The initial step involves removal of a regional field to 'sharpen up' and better define the shorter wavelength anomalies. In this example, a second-order regional field was calculated and removed from the data using the program SURFIT.

```
C:>surfit
enter grid filename:  grav.grd
start, end, increment of orders, [e.g., 2,5,1] 1 2 1
Want grids of residuals? [0=no, 1=yes] 1
start, end, increment:  1  2  1
least_square coefficients completed
order 1 finished
order 2 finished
Stop- Program terminated.
```

SURFIT outputs both the regional surface (*.s0*-grids) and the residual gravity grids (*.r0*).

```
C:>dir grav.*
Volume in drive C has no label
Directory of C:\WORKSHOP

GRAV.GRD    68730 04-06-93 12:29p
GRAV.S01    68730 04-06-93 12:36p
GRAV.R01    68730 04-06-93 12:36p
GRAV.R02    68730 04-06-93 12:36p
GRAV.S01    68730 04-06-93 12:36p
   5 file(s)   343650 bytes
```

The second-order residual gravity data (**grav.r02**) can now be 'terraced'. The smoothly varying gravity field is transformed into a step-function via a modification of the terrace algorithm (Phillips, 1990). The program iterates on the data until the data set has either horizontal or vertical segments only. The vertical segments pass through the maxima of the horizontal gradient (equivalent to the steepest part of the slope). From experience and practice, defining the number of iterations to be between 10 and 30 should be sufficient so that 'percent of flat slopes' will be near 100%. Be careful not to over-iterate. If you find that you can't reach more than 90% flat slopes (using approximately 30 iterations), try regridding your data to a coarser interval and then run the TERRACE program again. Over-iterating will cause artifacts in the terrace map that resemble ringing or that look like combs.

```
C:>terrace grav r02 15
..
**Running the gradient program**
**Running the stdbndy program**
**Running the combgrd program**
**Running the terrace4 program**
.
Enter input file name:
*Enter output file name:
*Enter number of iterations:
Enter output-file id:
*Iteration=1 Percent of flat slopes=43.60897
Iteration=2 Percent of flat slopes=61.25474
Iteration=3 Percent of flat slopes=74.27666
Iteration=4 Percent of flat slopes=82.09853
Iteration=5 Percent of flat slopes=86.92014
Iteration=6 Percent of flat slopes=90.06545
Iteration=7 Percent of flat slopes=92.09785
Iteration=8 Percent of flat slopes=93.51286
Iteration=9 Percent of flat slopes=94.45243
Iteration=10 Percent of flat slopes=95.16345
Iteration=11 Percent of flat slopes=95.48760
Iteration=12 Percent of flat slopes=95.73250
Iteration=13 Percent of flat slopes=96.06675
Iteration=14 Percent of flat slopes=96.25611
Iteration=15 Percent of flat slopes=96.52081
Stop-Program terminated.

**Running the transpos program**
**Running the fixter program**
**Running the transpos program**
**Running the fixter program**
**Running the mediplg1 program**
**Running the medifilt program**
**Deleting the temporary files
.
**Done:  grav.ter,grav.fil created**
```

The terrace grid is called **grav.fil**. *At this point, the range of values within this grid is the same as the range of values of the second-order residual gravity grid* (**grav.r02**). The following steps described below, go through the programs necessary for a forward calculation by referring the terrace grid to a 1-km thick slab model with a flat top and bottom. Again, the reasoning behind these assumptions for this particular gravity data set and study area is given in McCafferty and Cordell, 1992.

FFTFIL is used to calculate the Fourier coefficients of the unscaled terrace grid (**grav.fil**). The command file is given below:

```
C:>type fftfil.cmd
nofilt
grav.fil
junk.grd
No Filtering, just calculate fft coef's
&Parms
 nadd=10,icoef=1,idval=1
&end
```

```
C:>fftfil
Enter command file name (car ret to exit):  fftfil.cmd
blocking rows = 9
no filter operation performed:  only fourier coef.s are outputed in
fftfil.cof

title:  No Filtering, just calculate fft coef's
parameters:  density=  1.000  datum level z=    .000
      intensity of magnetization=  1.000
      inclination & declination of geomagnetic field=  90.000    .000
      inclination & declination of magnetization vector=  90.000  .000
      thetl=    .000   the2=    .000   istr= 1
      w1,w2,w3,&w4= .000E+00  .000E+00 .100E+31 .100E+31
      dy & dx =  .100E+31 .100E+31
      origin of the grid(x0 & y0)=.105375E+3 -.979417E+02
      no. of columns & rows= 156 144
      input file name:  grav.fil
      output file name:  junk.grd
Enter command file name (car ret to exit): <CR>
end of job
Stop - Program terminated.
```

The coefficient file is called **fftfil.cof**. This file is input into the next program to calculate the coefficients of the gravity field over the slab. The selection of slab thickness is chosen by trial and error. The top of the slab is usually controlled by drill hole information or some other geologic knowledge of the depth to the top of the gravity source(s). The slab, with a thickness that yields the best forward calculated field (described below), is chosen for the final model. For this study, a slab thickness of 1-km yielded the best fit between the second-order residual gravity and the forward calculated gravity.

```
C:>f_grav
Enter grid from which Fourier coeff.s created: grav.fil
* Enter no. or rows and cols added to grid(nadd): 10
* blocking rows = 9
Enter z1,z2: 1.2
* Output in file FFTFIL.NCF
Don't forget to rename this FFTFIL.COF before rerunning
fftfil.
Stop - Program terminated.
```

The coefficients (**fftfil.ncf**) are renamed, input into FFTFIL, and output as a gravity field grid. Make sure to set the 'icoef' and 'idval' parameters to '-1' in the **fftfil.cmd** file.

```
C:> rename fftfil.ncf fftfil.cof
```

Create a new fftfil command file (fft_fc.cmd) with 'idval=-1' and 'icoef=-1'.

```
C:> type fft_fc.cmd
nofilt
grav.fil
grav_fc.grd
Forward calc gravity, calc from f_grav coef's
&parms
 nadd=10, icoef=-1,idval=-1
&end

C:>fftfil
Enter command file name (car ret to exit):  fft_fc.cmd
blocking rows = 9
no filter operation performed:  only fourier coef.s are inputted and
inverse transformed

title:  Forward calc gravity from f_grav coef's
parameters:  density=  1.000  datum level z=   .000
      intensity of magnetization=  1.000
      inclination & declination of geomagnetic field=  90.000   .000
      inclination & declination of magnetization vector=  90.000  .000
      thet1=   .000   the2=   .000   istr= 1
      w1,w2,w3,&w4= .000E+00  .000E+00 .100E+31 .100E+31
      dy & dx =  .100E+31 .100E+31
      origin of the grid(x0 & y0)=.105375E+3 -.979417E+02
      no. of columns & rows= 156 144
      input file name:  grav.fil
      output file name:  junk.grd
Enter command file name (car ret to exit): <CR>
end of job
Stop - Program terminated.
```

The output gravity field calculated from the terrace grid referred to the slab model, (**grav_fc.grd**) is similar to the input gravity grid (**grav.r02**) except for a multiplication factor and a constant. This scaling factor is calculated (using the program SCALE) and multiplied to the forward calculated gravity grid *and* to the terrace grid (**grav.fil**) (using the program ADDGRD, which is demonstrated in more detail in Chapter 9).

```
C:> scale
To find s,c| sum[sF+c-G)**2]=min
* Enter grid F name: grav_fc.grd
* Enter grid G name: grav.r02
* s= .27493E-01 c=-.196000E+00 % =100.0
Stop - Program terminated.

C:>addgrd
first input file:  grav_fc.grd
title=Forward calc gravity from f_grav coef's
nc X nr   =   136   123
xo,yo,dx,dy = -97.941700   105.374800   1.000000  1.000000
operator h(elp),+-*/m%  :  *
second input file [constant] <CR>
the 2nd grid will be replaced by a constant value
enter constant:  0.027493
output file:  grav_fc.r02
output title [same as file 1] Forward calc gravity from terrace model
Stop - Program terminated.
```

```
C:> addgrd
first input file : grav.fil
title= Unscaled terrace-density map
nc X nr    =    136    123
xo,yo,dx,dy = -97.941700    105.374800    1.000000  1.000000
operator h(elp),+-*/m%   :  *
second input file [constant] <CR>
the 2nd grid will be replaced by a constant value
enter constant:  0.027493
output file:  ter_dens.grd
output title [same as file 1] Terrace density map g/cm3
Stop - Program terminated.

C:> ghist
Enter input file: ter_dens.grd
minimum=-.2466510        maximum= .4086909
mean=-.2005588E-02       max-min=.6553419
    16728 valid points,   100.00% of grid

Want to see histogram, standard dev., both, or none [h,s,b,b]?n
Stop - Program terminated.
```

The final result is a terrace-density map with range of values given in the histogram. This map can be used to infer rock type based on ranges of density contrast.

References

Cordell, Lindrith, and McCafferty, A.E., 1989 A terracing operator for physical property mapping with potential field data: Geophysics, v.54, no. 5, p. 621-634.

McCafferty, A.E., and Cordell, Lindrith, 1992, Geophysically inferred structural and lithologic map of the Precambrian basement in the Joplin 1o x 2o quadrangle, Kansas and Missouri: U.S. Geological Survey Miscellaneous Field Studies Map MF-2125-D, 17 p., scale 1:500,000.

Phillips, J.D., 1990, TERRACE--a terracing procedure for gridded data, with FORTRAN programs and VAX command procedure and Unix C-shell implementations: U.S. Geological Survey Open-File Report 92-5 A-B, 18 p.

INDEPENDENT PC EXERCISES IV

1. Using the pseudogravity grid **gpg2.tgd** created in #1 of Independent PC Exercises III, create HGM's following the program **BOUNDARY** demonstration from page 8-24 through page 8-27. Create and view "maxspots" using program **IMVIS**. (IMVIS images of the horizontal gradient magnitudes, listed below, should have been copied as part of #3 of Independent PC Exercises II.) Overlay the maxspots you've made (**gpgg3.grf**, now available in the "labels .grf" submenu of the "PLOT" menu) on the following images:

   (a) GPGG1.LBL (HGM of pseudogravity). The maxspots should be located on top of the ridges (boundaries between rocks of different magnetizations). Some apparent offset in locations of spots may be a function of the shading of the HGM plot. Can you see some ridges in the HGM data that are not represented by maxspots, and some spurious maxspots that are unrelated to ridges?

   (b) GRTP1.LBL (reduced-to-pole aeromagnetic data). Note how the maxspots define the edges of the pluton, for example, that would have been hard to derive from the magnetic anomaly alone.

   (c) G1VER1.LBL (first vertical derivative of reduced-to-pole magnetics). Note how the maxspots commonly follow the edges of the first vertical derivative features. The first vertical derivative still is an indirect (field value) representation of changes in magnetization whereas the maxspots actually map the magnetization changes (where the assumptions are valid).

   (d) GRES9G1.LBL (HGM of log of 900 Hz apparent resistivity). The ridges in this image indicate resistivity boundaries. It is remarkable how many of the maxspots, which represent magnetization boundaries (an unrelated physical property), are coincidental or nearly coincidental with these ridges. The coincident boundaries must be produced by the same geologic contact. The nearly coincidental ones are produced by related geologic contacts. For example, the eastern edge of the pluton is indicated by the magnetization boundary, whereas the resistivity boundary reflects the alteration in the Getchell fault (see figure 5-2 and/or overlay the geology in IMVIS), a range-bounding fault partly controlling the edge of the pluton.

   (e) GRTPG1.LBL (HGM of reduced-to-pole aeromagnetic data). Note that much more detail is apparent in the reduced-to-pole HGM image than in the maxspots, which were computed from the HGM of the pseudogravity, especially in the vicinity of the pluton. You may want to compare the HGM of pseudogravity (GPGG1.LBL) again to see the difference. Look especially at the boundary in the northeastern part of the area that trends northeasterly toward the pluton near the center of the area (the Rabbit Creek fault). Which HGM image represents the original magnetic feature (GMAG1.LBL) the best? Can you see candidates for artifacts in the HGM of the reduced-to-pole magnetics? (Look for parallel ridges that are close together in the area where a lot of volcanic flows have been mapped.)

2. Follow the demonstration of **TERRACE** starting on page 8-28 to make a terrace map from the pseudogravity data for Getchell, using the grid **gpg2.tgd** (constructed in #1 of Independent PC Exercises III). **STOP** at the end of Demonstration I (page 8-30). Special treatment is required for the Getchell area in order to scale the terraced values to magnetization values because the top to magnetic sources is quite variable. The scaling part of the demonstration is there for reference if you can use it in a different area. Use **GRDREM** and **DISPLAY** to display your results. Try adding color with the O command. Compare your results to figure 8-6. Note that the terraced map reflects variations in magnetization *and* depth of magnetic sources.

CHAPTER 9. MAP ENHANCEMENT TECHNIQUES FOR RESISTIVITY DATA

HORIZONTAL-GRADIENT METHOD

Abrupt changes in resistivity give rise to very steep gradients in apparent resistivity maps. Thus, the horizontal-gradient method, which responds to steep gradients, or slopes, can be used as a boundary finder for resistivity data as well as potential-field data. The technique helps enhance changes in resisitivity that may be missed upon original inspection of the data. Figure 9-1 shows a color-shaded relief image of the horizontal gradient magnitude (HGM) for the 900 Hz apparent resistivity data. Because the original 900 Hz resistivity data were viewed as logarithms, the HGM's reflect logarithm values per kilometer.

RESISTIVITY RATIO DATA

In a preliminary assessment of the apparent resistivity maps for the Getchell trend area, Hoover and others (1991) observed that all the exposed gold deposits are associated with linear conductive zones. Because EM surveys can map subsurface resistivities, apparent resistivity maps thus can be an important guide to locating *buried* conductive zones, which in turn may be associated with buried gold deposits.

Unfortunately, the geophysical signature of buried conductive material is commonly masked by the effect of overlying or neighboring rocks, making identification on apparent resistivity maps difficult. A step towards isolating this signature is to take the ratio of apparent resistivities calculated for two different frequencies. As shown by Pierce and Hoover (1991) for the Getchell area, the logarithm of the ratio of 7200-Hz apparent resistivity divided by 900-Hz apparent resistivity gives information about how resistivity changes with depth. The logarithms of these ratios are also shown on Figure 9-2. Where the ratio is greater than one (the logarithm is positive), resisitivity generally decreases with depth. Where it is less than one (the logarithm is negative), resistivity generally increases with depth.

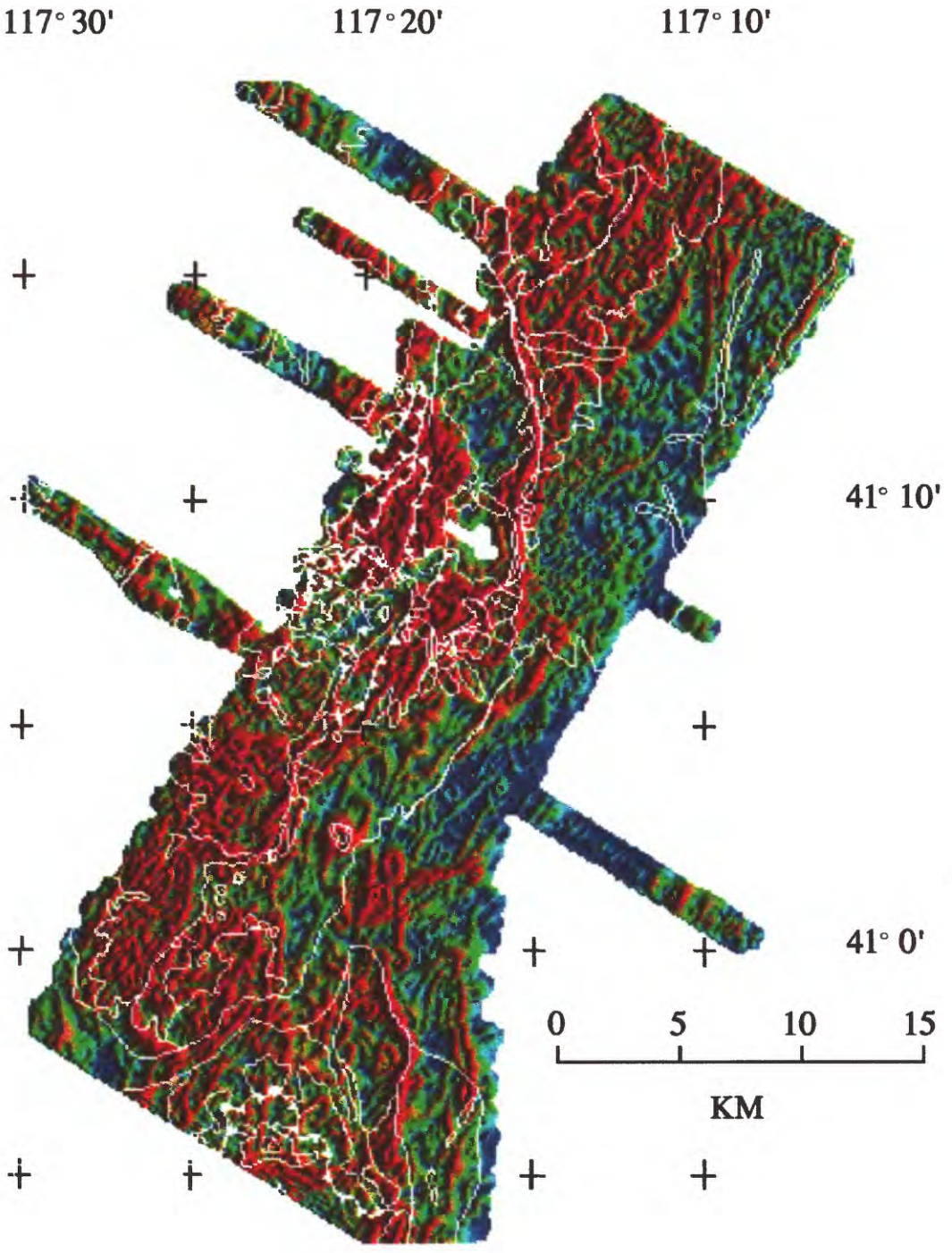

Figure 9-1.

Color-shaded-relief image of the horizontal-gradient magnitude of the log of the 900-Hz apparent resistivity. The ridges emphasize abrupt lateral changes in resistivity. Geologic contacts are overlain in white.

See Figure 5-2 for explanation of geologic contacts.

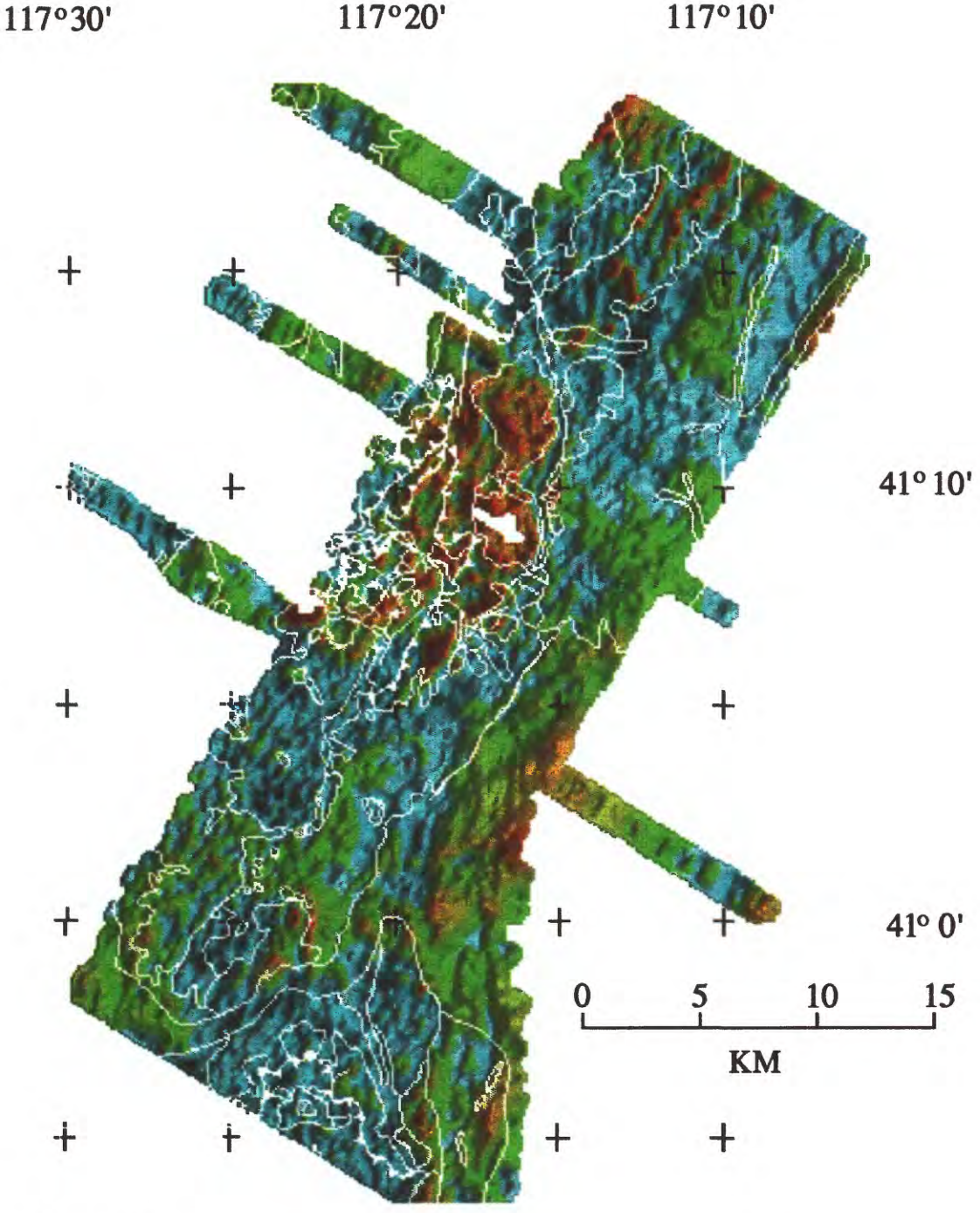

Figure 9-2.

Color shaded-relief image of log10 of the ratio of 7200-Hz apparent resistivity to 900-Hz apparent resistivity. This enhancement is designed to distinguish areas where resistivity is decreasing or increasing with depth. Negative values (resistivity increasing with depth) are shown in the cyan colors. Positive values (resistivity decreasing with depth) are shown in greens, yellows, and browns. Geologic contacts are overlain in white. See Figure 5-2 for explanation of geologic contacts.

BURIED-CONDUCTOR ENHANCEMENT

Buried conductive material, which we define as rocks with very low resistivity underlying rocks with moderate to high resistivity, will be represented by areas on the ratio map indicating resistivity decreasing with depth. However, areas where highly resistive rocks overlie moderately resistive rocks also express decreasing resistivity and yet are areas of no interest. Thus, a better approach enhances areas where resistivity is decreasing with depth *and* the apparent resistivity is low. We call such an operation a buried-conductor enhancement.

For the buried-conductor enhancement, the logarithm of the resistivity ratio is multiplied by the logarithm of the 900 Hz apparent conductivity (the inverse of apparent resisitivity) after adding a constant to ensure only positive logarithms for the conductivity. The conductivity for the 900 Hz frequency is used because it represents the deepest looking frequency. In equation form, the results of the enhancement E can be written for each grid point as

$$E = \left\{ \log\left(\frac{1}{\rho_{900}}\right) + k \right\} \cdot \log\left(\frac{\rho_{7200}}{\rho_{900}}\right), \qquad (9\text{-}1)$$

where

ρ_{900} = 900 Hz apparent resistivity (ohm-meters)
ρ_{7200} = 7200 Hz apparent resistivity (ohm-meters), and
k = a constant that ensures the left-hand side of the product will be positive for all grid points.

Note that k is usually chosen by inspection of the minimum value of $\log\left(\frac{1}{\rho_{900}}\right)$ for all grid points.

Because the negative values of E represent the uninteresting case where the resisitivities are increasing with depth, these values are neglected. Thus, the final plot of E has high values where the *product* of the 900 Hz apparent conductivity and the amount of decrease in resistivity with depth is great. The highest E values represent places where there is a large, probably abrupt, decrease in resistivity at depth. Moreover, the change in resistivity must occur at fairly shallow depths because the depth of exploration is diminished by the presence of the low resistivities in the subsurface.

The result of applying the above buried-conductor enhancement to apparent resisitivity data for the Getchell trend area are described in Grauch and Hoover (1993) and shown on Figure 9-3. It has a similar appearance to the ratio map except that the pluton area has been subdued and some linear features are more enhanced.

REFERENCES

Grauch, V. J. S., and Hoover, D. B., 1993, Locating buried conductive material along the Getchell trend, Osgood Mountains, Nevada: Implications for gold exploration and the carbon-gold association(?): U. S. Geological Survey Bulletin 2039, p. 237-244.

Hoover, D. B., Grauch, V. J. S., Pitkin, J. A., Krohn, M. D., and Pierce, H. A., 1991, An integrated airborne geophysical study along the Getchell trend of gold deposits, north-central Nevada, *in* Raines, G. L., Lisle, R. E., Schafer, R. W., and Wilkinson, W. H., ed., Geology and Ore Deposits of the Great Basin, Symposium Proceedings: Reno, NV, Geological Society of Nevada, p. 739-758.

Pierce, H. A., and Hoover, D. B., 1991, Airborne electromagnetic applications--mapping structure and electrical boundaries beneath cover along the Getchell Trend, Nevada *in* Raines, G. L., Lisle, R. E., Schafer, R. W., and Wilkinson, W. H., Eds., Geology and Ore Deposits of the Great Basin, Symposium Proceedings: Geological Society of Nevada, Reno, Nevada, p. 771-780.

Wojniak, W. S., Hoover, D. B., and Grauch, V. J. S., in press, Electromagnetic survey maps showing apparent resistivities of the Getchell gold trend, Osgood Mountains, north-central Nevada: U. S. Geological Survey Geophysical Map GP-1003-A, 3 plates, scale 1:100,000.

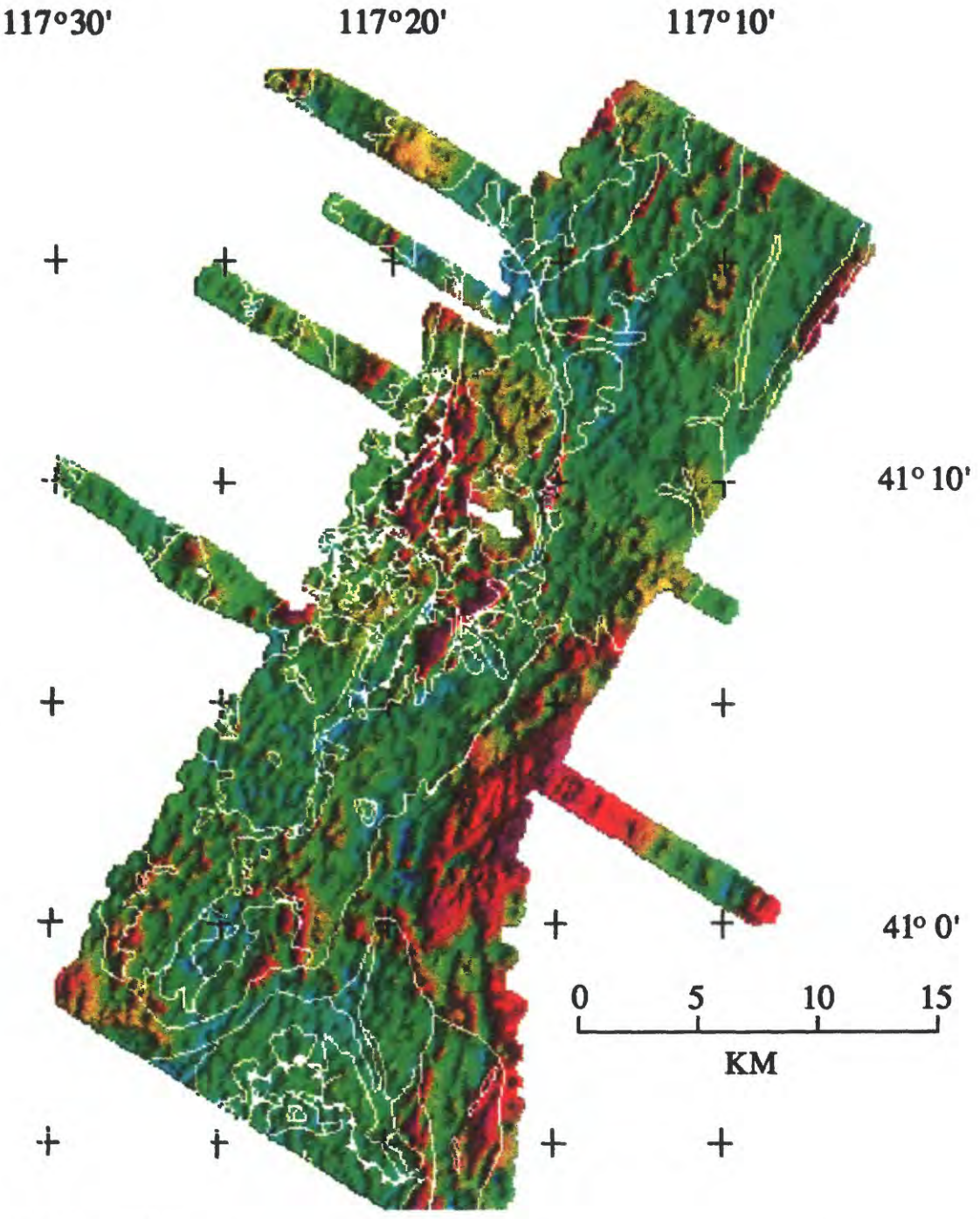

Figure 9-3.

Color shaded-relief image of a data combination to enhance buried conductive material. The resistivity data were combined as follows: (-log10 (900-Hz apparent resistivity) + 3.5) multiplied by log10 of the ratio of 7200-Hz apparent resistivity over 900-Hz apparent resistivity. This is designed to locate areas where resistivity is decreasing with depth *and* resistivity is low (or conductivity is high). Geologic contacts are overlain in white. See Figure 5-2 for explanation of geologic contacts.

ADDGRD PROGRAM DEMONSTRATION

The buried conductive material enhancement for the Getchell resistivity data is designed to enhance areas where the log of the ratio between 7200 Hz and 900 Hz apparent resistivities is positive (resistivitity decreasing with depth) *and* the 900 Hz resistivity is low. The operation is

$$(\log_{10}(\frac{1}{900\text{ Hz res}}) + 3.5) \cdot \log_{10}(\frac{7200\text{ Hz res}}{900\text{ Hz res}}).$$

Note that conductivity is the inverse of resistivity. The constant of 3.5 added to the log of the 900 Hz conductivity ensures that all the values in the lefthand term are positive before multiplication. In practice, the grids of resistivity data were already in log form, so the operation took the form:

$$(- \log_{10}(900\text{ Hz res}) + 3.5) \cdot (\log_{10}(7200\text{ Hz res}) - \log_{10}(900\text{ Hz res}))$$

This operation was performed using program **ADDGRD**, assuming that the righthand term has already been constructed as the grid **g72_9.cgd**. The log of the 900 Hz resistivity data are in grid **gres9.cgd**.

```
C:>addgrd
 first input file :
 gres9.cgd
title=Getchell log10 of 900 Hz resistivity, decorrugated
 nc X nr        =        194         249
 xo, yo, dx, dy =     -46.000000     4525.000000    2.000000E-01
  2.000000E-01
 operator  h(elp), + - * / m %   :
 *
 second input file [constant] :
 <CR>
 the 2nd grid will be replaced by a constant value
 enter constant:
 -1
 output file :
 gcond9.cgd
 output title [ same as file 1 ]
 Getchell log10 900 hz conductivity (log of resist. inverse)
Stop - Program terminated.
```

First let's take a quick look at the range of values in the new conductivity file:

```
C:>ghist
Enter input file:
 gcond9.cgd
minimum= -3.269111              maximum=  .3578272E-02
mean= -1.877310               max - min =  3.272690
       19320 valid points,    40.00% of grid
Want to see histogram, standard dev., both, or none [h,s,b,n]? n
Stop - Program terminated.
```

We want to enhance the positive part of the log(7200/900 Hz ratio), because that is where resistivity is decreasing with depth, so for these values to remain positive, we need to make the 900 Hz conductivity positive. To do this, we simply add a constant:

```
C:>addgrd
 first input file :
 gcond9.cgd
title=getchell log10 900 hz conductivity (log of resist. inver
 nc X nr         =        194         249
 xo, yo, dx, dy =     -46.000000     4525.000000    2.000000E-01
  2.000000E-01
 operator  h(elp), + - * / m %   :
 +
 second input file [constant] :
 <CR>
 the 2nd grid will be replaced by a constant value
 enter constant:
 3.5
 output file :
 gcond9b.cgd
 output title [ same as file 1 ]
 Getchell log10 900 hz conductivity + 3.5
Stop - Program terminated.
```

Now for the final multiplication:

```
C:>addgrd
 first input file :
 gcond9b.cgd
title=Getchell log10 900 hz conductivity + 3.5
 nc X nr         =        194         249
 xo, yo, dx, dy =     -46.000000     4525.000000    2.000000E-01
  2.000000E-01
 operator  h(elp), + - * / m %   :
 *
 second input file [constant] :
 g72_9.cgd
 output file :
 gburcond.cgd
 output title [ same as file 1 ]
 buried conductive material enhancement, getchell 7200,900 hz
Stop - Program terminated.
```

```
Stop - Program terminated.
```

The program **RAINZERO** was used in conjunction with **CSR** (minus **HISTNORM**, the histogram stretching) to make an image to view with **IMVIS**. The image can be viewed from **IMVIS** by choosing **GCOND.LBL** from Open-File 93-560D.

Chapter 10. Map Enhancement Techniques for Radioactivity Data

Aerial gamma-ray spectrometry data are presented as contour maps of the surface distribution of K in percent, and U and Th in parts per million. Color contour maps of the Getchell gold trend are included as Figure 10-1 for K, Figure 10-2 for U, and Figure 10-3 for Th. The reader/user may use these maps as a basis of comparison with the color composite image available as an IMVIS image on the accompanying diskette in Open-File 93-560-D.

A major problem with examination and interpretation of radioelement maps generated from aerial surveys is the difficulty of using three maps simultaneously with other data also in map form for the area of interest. The color compositing technique solves this problem by enabling the combining of three parameters (K, U, Th) in one map.

INTRODUCTION TO COLOR COMPOSITES

Composite images are formed by combining three separate gray tone images as red, green, and blue components of a single color image. Color Landsat images provide an example of composite images. Each of the three color planes is formed from a different bandpass channel of the Landsat data. Composite gamma-ray images are another example. Here red, green, and blue image planes correspond to the uranium, potassium, and thorium gamma-ray channels.

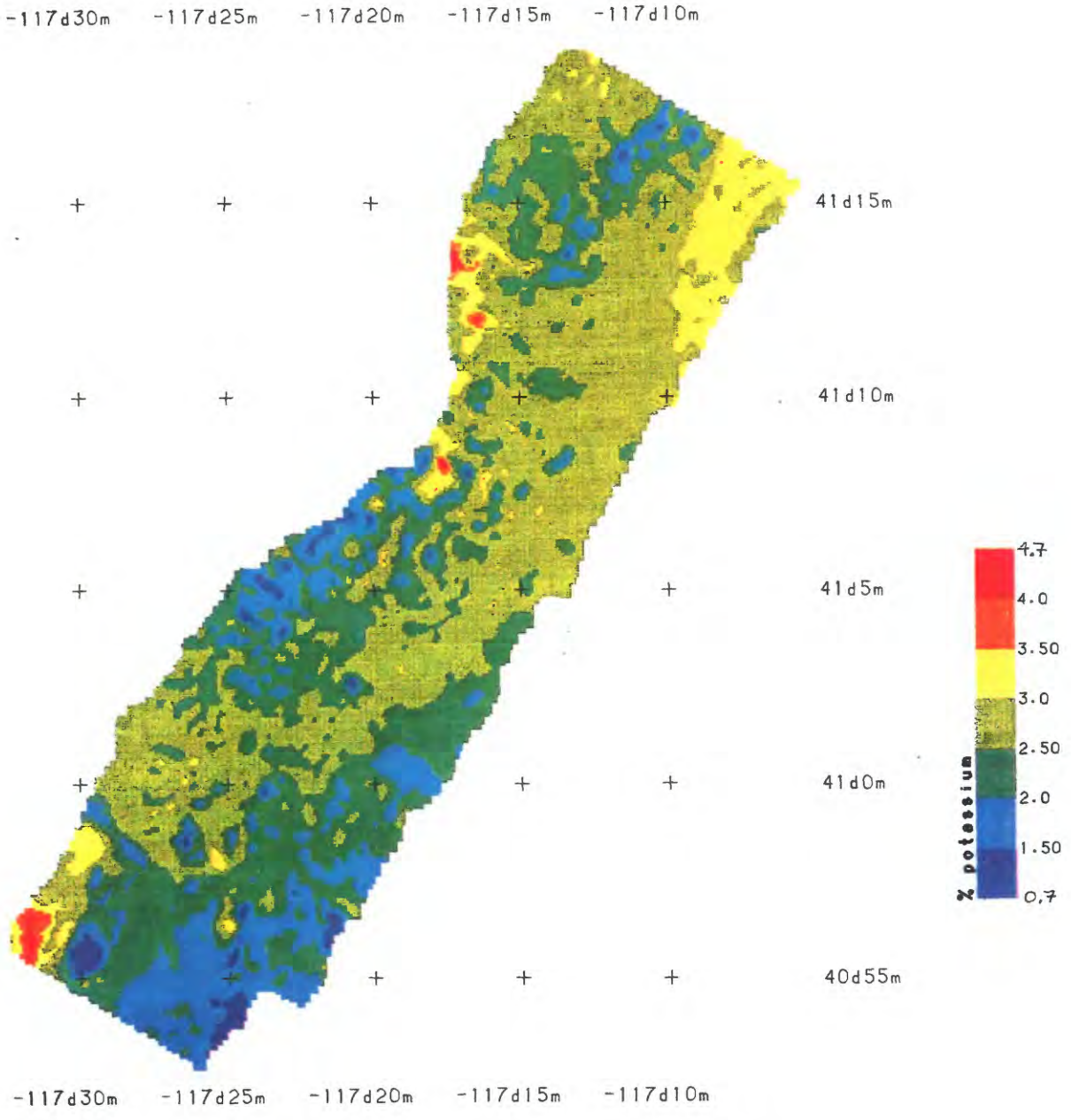

Figure 10-1. **Potassium contour map, Getchell trend**

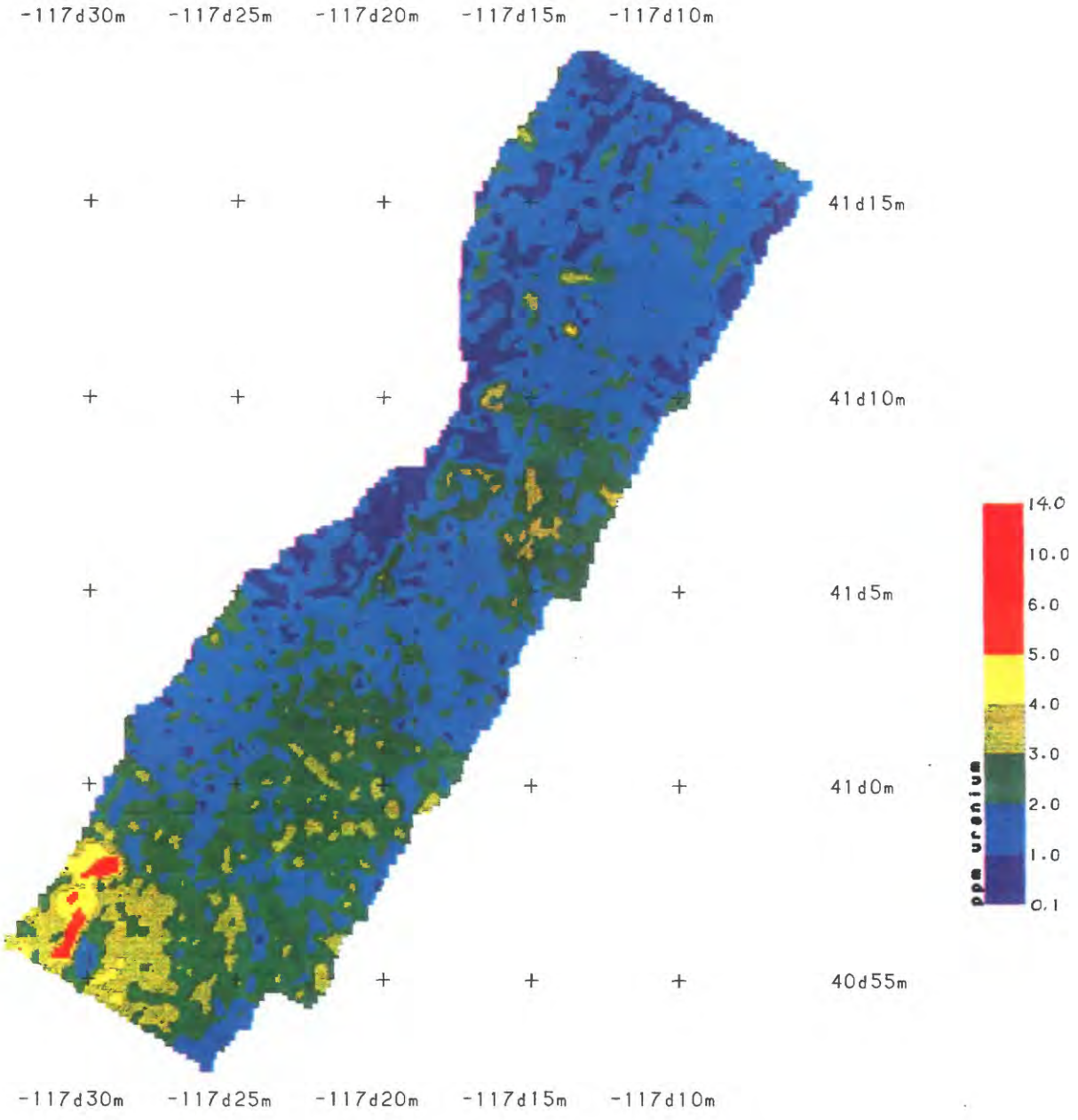

Figure 10-2. **Uranium contour map, Getchell trend**

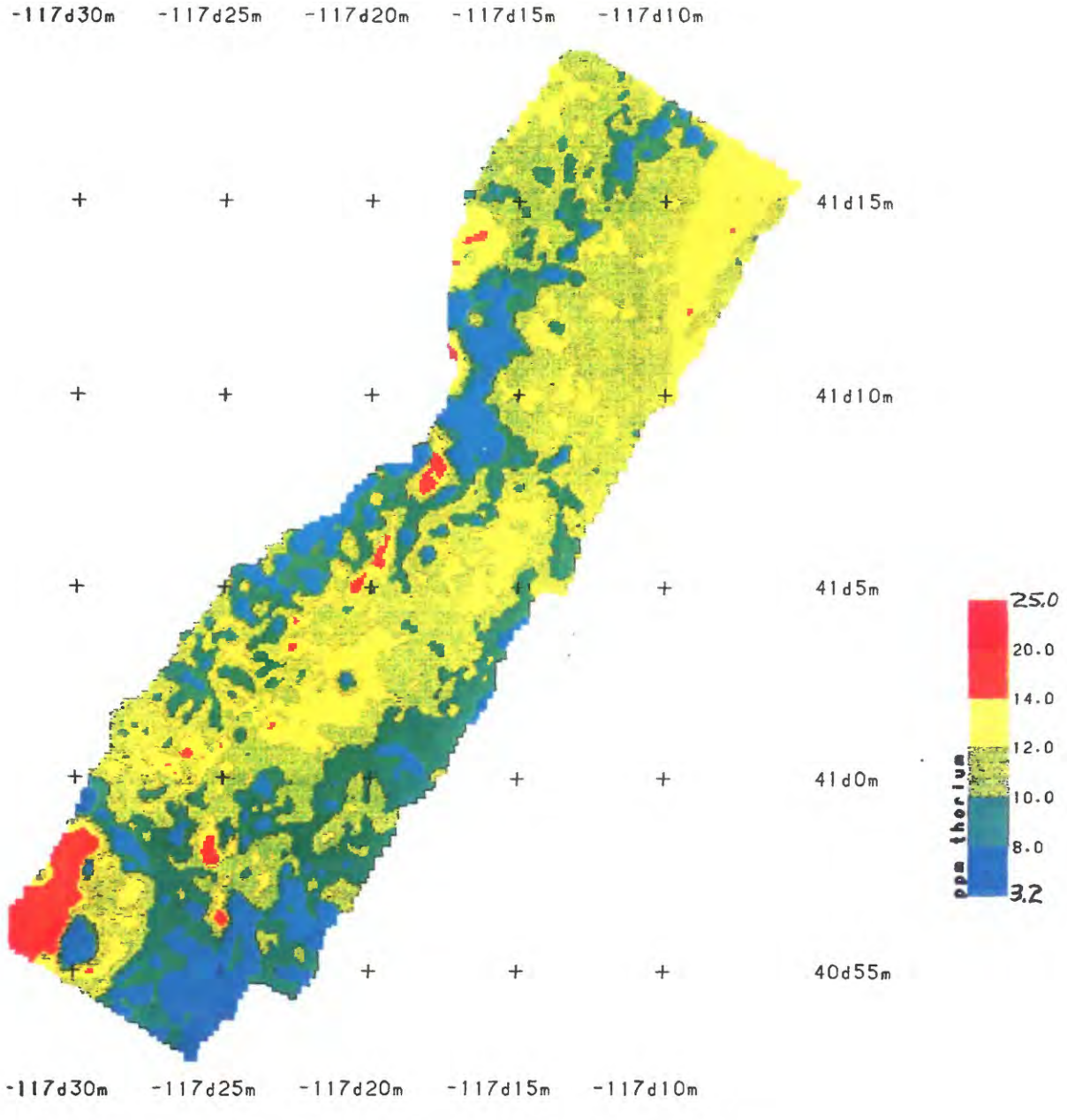

Figure 10-3. **Thorium contour map, Getchell trend**

To interpret color composite images, you must understand how the composite colors relate to the input shades of red, green, and blue. The following table shows the colors resulting from various combinations of red, green, and blue intensity levels.

composite color	% red	% green	% blue
black	0	0	0
dark blue	0	0	50
blue	0	0	100
dark green	0	50	0
dark cyan	0	50	50
green	0	100	0
cyan	0	100	100
dark red	50	0	0
dark magenta	50	0	50
brown	50	50	0
gray	50	50	50
red	100	0	0
magenta	100	0	100
yellow	100	100	0
white	100	100	100

For example, a red pixel on a composite image indicates a location where the red component (such as the uranium anomaly) is high and the other components (such as potassium and thorium anomalies) are low. A white pixel indicates a location where all components are high, and a black pixel indicates a location where all components are low.

DEMONSTRATION OF DISPLAY TO MAKE GETCHELL RADIOELEMENT COMPOSITES

The quickest way to make a color composite is with the REMAPP program **DISPLAY**. A more time-consuming method, which gives a result that is easier to examine in detail, is demonstrated at the beginning of Chapter 11 using IMVIS. The following demonstration is also included as an exercise at the end of Chapter 11.

Construction of REMAPP Image Files

First copy the files **gu.cgd, gt.cgd, and gk.cgd** (U, Th, and K, respectively) off of the diskettes of the accompanying Open-File Report 93-560D diskettes onto your hard drive.

Using the program **GRDREM**, create REMAPP image files of these grids, as demonstrated under Basic REMAPP Programs in Chapter 7, calling them **gu.img, gt.img, and gk.img**.

U, K, Th Color Composite

```
DISPLAY

DISKIO:ENTER INPUT FILENAME =  gt.img                    <<input the Th image

Enter 1st Scanline, No.Scanlines,Skips: 0 0 1
```

skip=1 allows the entire data set to be displayed; skip = 0 results in the southern tip not being displayed.

```
Enter 1st Pixel,Number of Pixels,Skips: 0 0 1
```

At this point DISPLAY will go into graphics mode. To continue with the color composite, type the following commands while still in graphics mode. Many of the commands do *not* require a carriage return afterwards, noted by `[no <CR>]`.

`v`	`[no <CR>]`	<<applies an automatic stretch to the grid
`i 1`		<<stores the Th image in buffer 1; there are 6 buffers
`h`	`[no <CR>]`	<<help option, in case you aren't familiar with the options

```
d gk.img                <<display another image, this time K
0 0 1
0 0 1
y       [no <CR>]
i 2                     <<store the K image in buffer 2
d gu.img                <<display another image, this time U
0 0 1
0 0 1
y       [no <CR>]
i 3                     <<store the U image in buffer 3
m       [no <CR>]       <<the m command generates a color composite image using
                          the images stored in buffers 1 (coded as blue), 2 (green),
                          and 3 (red)
i 4                     <<store the composite image in buffer 4
```

toggle among the buffers;
1 = thorium
2 = potassium
3 = uranium
4 = radioelements color composite

ESC to leave display; BE CAREFUL, buffer contents are not retained!

Individual Element Color Composites

You can also make individual element color composite images. These images consist of an element and its two ratios to the other two elements.

U color composite: U,U:K,U:T
K color composite: K,K:U,K:T
T color composite: T,T:U,T:K

Ratios can either be constructed from the grids, using **ADDGRD** and the / function, or from REMAPP images with program **ARITH** in the REMAPP package (see help file on the diskettes in Open-File 93-560C or the REMAPP documentation text Open-File Report 90-88A). For present purposes, it is easiest to use **ADDGRD.** It is often wise to examine the distribution of the values in each grid before dividing grid values, because the division will tend to eccentuate spurious values if the spurious values occur in the denominator. To examine the

values, use program **GHIST** (demonstrated under basic grid utilities in Chapter 6) to look at each of the three grids, **gu.cgd, gt.cgd, and gk.cgd.** Note that **gu.cgd** has a skewed distribution:

```
C:> ghist
Enter input file:
gu.cgd
minimum=  .1000000E-02          maximum=  14.43086
mean=  1.913466              max - min =  14.42986
    16069 valid points,    33.27% of grid
Want to see histogram, standard dev., both, or none [h,s,b,n]?  h
I found histogram interval of   .7600000    , giving  18 histogram classes
Want to redefine interval ?  y
Enter new interval:  1
Interval of   1.000000     gives  14 histogram classes
Want to see percent or count of values [p or c]?  c

Standard Deviation =   .8595989

midpoint (interval=     1.000    )   HISTOGRAM

 .1000E-02  |XX   413
 1.001      |XXXXXXXXXXXXXXXXXXXXXXXXXXXXXX   4746
 2.001      |XXXXXXXXXXXXXXXXXXXXXXXXXXXXXXXXXXXXXXXXXXXXXXXXXXX   7540
 3.001      |XXXXXXXXXXXXXXXXX   2767
 4.001      |XXX   466
 5.001      |     92
 6.001      |     22
 7.001      |     10
 8.001      |     2
 9.001      |     2
 10.00      |     3
 11.00      |     1
 12.00      |     2
 13.00      |     1
 14.00      |     2

REPRINT info, CHANGE histogram, or STOP [r, c, or s]? s

Stop - Program terminated.
```

This will probably give useless K/U and Th/U ratios (because the extreme values will be in the demominator). To get a better ratio, one can use the program **SKIM** on gu.cgd beforehand to get rid of the high values (this also facilitates making contour plots of the grid). In this case, examination of the above histogram shows that most data values lie below 5.0, so we'll make all values greater than 5.0 equal to 5.0 and output the values in **gu.skm**. (Choice of this value is somewhat arbitrary but allows quick and dirty examination of the radioelement ratios. Alternatively, one could use the program **HISTNORM** in the REMAPP package (see REMAPP help file) to redistribute the U data.)

```
C:> skim
Enter input file name:
*gu.cgd
Enter output file name:
*gu.skm
Enter new id:
*Getchell U data, skimmed off at 5.0
Enter min, max data bounds:
*0 5
Enter dval option;
      1: Dvals unchanged.
      2: Dvals set equal to min.
      3: Dvals set equal to max.
*1

Stop - Program terminated.
```

To construct the various ratios, follow the demonstration of multiplication in **ADDGRD** (p. 9-8) using the division operator / instead of the multiplication operator, and making the following substitutions for first and second input file:

RATIO	FIRST FILE	SECOND FILE	OUTPUT FILE
U:K	gu.skm	gk.cgd	guk.cgd
U:T	gu.skm	gt.cgd	gut.cgd
K:U	gk.cgd	gu.skm	gku.cgd
K:T	gk.cgd	gt.cgd	gkt.cgd
T:U	gt.cgd	gu.skm	gtu.cgd
T:K	gt.cgd	gk.cgd	gtk.cgd

Using **GRDREM**, convert each the output grids to REMAPP images with the suffix of **.img**.

The various individual element composites can be created using program **DISPLAY** in the same way as demonstrated earlier, putting the following image files into the 1, 2, and 3 (blue, green, red) buffers **(on next page)**:

put gut.img in buffer 1,
guk.img in buffer 2
gu.img in buffer 3
v for stretching all black&white images
m to compute the U and its ratios composite image
store in buffer 4
toggle through 1, 2, 3, 4

put gkt.img in buffer 1
gku.img in buffer 2
gk.img in buffer 3
v for stretching the images
m to compute the K and its ratios composite image
store in buffer 5
toggle as you want to

put gtk.img in buffer 1
gtu.img in buffer 2
gt.img in buffer 3
v for stretching the images
m to compute the T and its ratios composite image
store in buffer 6

compare the U image in buffer 4
K image in buffer 5
T image in buffer 6

Chapter 11. Data Integration

INTEGRATING DATA SETS USING COMPOSITE IMAGES

Introduction

Color composite techniques (introduced in the previous chapter) can be used to combine any three registered data grids into a single image. For example the three Getchell resistivity grids, representing shallow, intermediate, and deeper sources, could be combined as red, green, and blue components of a composite image. Three bandpass filters could be applied to a single grid, such as the magnetic data grid, and the three resulting grids (highpass, intermediate bandpass, and lowpass) could be displayed as red, green, and blue components of a composite image emphasizing the frequency content of the data rather than the amplitude content (Phillips, 1990). Completely different data sets can also be combined as composite images. Phillips (1990) combines magnetics, gravity, and the ratio of magnetics to gravity as red, green, and blue components of a composite image to help separate felsic and mafic units.

Reference

Phillips, J.D., 1990, Integration of potential-field and digital geologic data for two North American geoscience transects: Journal of Geologic Education, v.38, pp.330-338.

Constructing IMVIS Color Composites

In the previous chapter, we saw how the program DISPLAY can be used to construct composite images from REMAPP image files. The potential-field software package contains programs that can be used to construct composite images from three registered grids representing the red, green, and blue image components. These composite images, which are displayed using IMVIS, can be constructed in two ways. The first approach is used in an exercise at the end of this chapter.

In this first approach, the program GRDREM is run three times to convert the three grids into three REMAPP images. The three REMAPP images are used as input to the program RSG3 which produces an output file of the type 'image'.CMG, where 'image' will be the name of the resulting IMVIS image. Note that RSG3 asks for the number of pixels (columns) and scan lines (rows) in the image. These can be read from the output of GRDREM or determined from the input grids using the program ID to display the ncol and nrow values. The 'image'.CMG file is used as input to the program REDUCE, which produces the final IMVIS image. The approach is illustrated by the following sequence of commands and responses:

```
C:>grdrem
GRID FILENAME - red.grd
id,pgm,ncol,nrow,nw,xo,dxo,yo,dyo -
                de_prep          128
  128           1       -31.000000     1.000000E-01     4551.000000
   1.000000E-01
DISKIO:ENTER OUTPUT FILENAME red.rem
Minimum Values:  REMAPP DN - 1    Grid -       -49.318440
Maximum Values:  REMAPP DN - 255  Grid -        78.271760
Number of DVALs in Grid -            0
REMAPP DN - INT (GRID Value *         1.990749 +        99.180610 +
.5)
  DISKIO(2): RED.REM         [LINES   128PIXELS  128BYTESIZE  8]
Stop - Program terminated.

C:>grdrem
GRID FILENAME - green.grd
id,pgm,ncol,nrow,nw,xo,dxo,yo,dyo -
                de_prep          128
  128           1       -31.000000     1.000000E-01     4551.000000
   1.000000E-01
DISKIO:ENTER OUTPUT FILENAME green.rem
Minimum Values:  REMAPP DN - 1    Grid -       -49.318440
Maximum Values:  REMAPP DN - 255  Grid -        78.271760
Number of DVALs in Grid -            0
REMAPP DN - INT (GRID Value *         1.990749 +        99.180610 +
.5)
  DISKIO(2): GREEN.REM         [LINES   128PIXELS  128BYTESIZE  8]
Stop - Program terminated.

C:>grdrem
GRID FILENAME - blue.grd
id,pgm,ncol,nrow,nw,xo,dxo,yo,dyo -
                de_prep          128
  128           1       -31.000000     1.000000E-01     4551.000000
   1.000000E-01
DISKIO:ENTER OUTPUT FILENAME blue.rem
Minimum Values:  REMAPP DN - 1    Grid -       -49.318440
Maximum Values:  REMAPP DN - 255  Grid -        78.271760
Number of DVALs in Grid -            0
REMAPP DN - INT (GRID Value *         1.990749 +        99.180610 +
.5)
  DISKIO(2): BLUE.REM         [LINES   128PIXELS  128BYTESIZE  8]
Stop - Program terminated.


C:>id
Enter input file name:
*  red.grd
de_prep
ncol -  128      nrow -  128      nz -  1
```

```
x0 = -31.00000      dx =  .1000000      y0 =  4551.000      dy =
.1000000
Stop - Program terminated.


C:>rsg3
Enter red file name: red.rem
Enter green file name: green.rem
Enter blue file name: blue.rem
Enter output file name: composite.cmg
Enter number of pixels: 128
Enter number of scan lines: 128

C:>reduce composite /c 240 /m 5
```

The parameters used in this last command specify that the output image will have no more than 240 colors and no color will occupy fewer than 5 pixels.

To view the composite image (called 'composite' in the example), use IMVIS. To add projection, vector and title information to the image, edit the label file ('composite.lbl' in the example).

The second approach to producing composite images from three registered grid files involves first converting the grids into graytone IMVIS images using the program GRD2IMG. Next one of the label files for the graytone images is copied to a label file with a new name, and this new label file is edited so as to become an image_set label file. The program IMVIS is used to access the image_set label file; stretch the red, green, and blue images as desired; and create a .CMG file for input to REDUCE. REDUCE is then used to produce the composite image. For example:

```
C:>grd2img red.grd red
C:>grd2img green.grd green
C:>grd2img blue.grd blue
C:>copy blue.lbl rgb.lbl
C:>edit rgb.lbl
```

The edited image_set label file should resemble this:

```
FILE_TYPE          = IMAGE
IMAGE_LINES        =    240
LINE_SAMPLES       =    127
SET_POINTER        =      3
      red.dat
      green.dat
      blue.dat
END
```

C:>imvis

First display the red, green, and blue images ('red.lbl', 'green.lbl', and 'blue.lbl' in the example) in order to check them and to create any internal files that may be needed for the image stretch.

Next select the label file for the image set ('rgb.lbl' in the example). A menu will appear with various options. Use the 'display quick color' option to select the desired red, green, and blue channels. A crude composite image will be displayed. Use the <Enter> key to return to the menu. Repeat this option until the choice of red, green, and blue channels has been determined.

Next select the 'make RGB composite file' menu option. After you again choose the red, green, and blue channels, a new menu will appear. Select the 'Histogram from full image files' option to generate preliminary stretch parameters for the three input images. A new menu will appear.

For default results, select the 'Use as is' option form this new menu. For more controllable results, select the 'Change image' menu option. This will display the three images and a table of stretch parameters. The three parameters for the red image will be enclosed in a box. The left number in the box is the pixel value that will become the zero level in the stretched red image; the center number is the pixel value that will become 127 in the stretched image; and the right number is the pixel value that will become 255 in the stretched image. By using the numeric keypad keys, (<7> <8> <9> to raise the numbers, <1> <2> <3> to lower the numbers) the three numbers in the box can be changed until the red image appears to have a satisfactory stretch. The <Enter> key is used select the parameters for the green or blue image, and the numeric keypad keys are again used to modify the stretch. When the stretch parameters have all been set, the <Esc> key will return to the previous menu.

Select the 'Use Current Parameters' menu option to create

the .CMG file. You will be prompted for the name of the image. This name will also be used for the .CMG file. In this example we use the name 'composite'.

```
C:>reduce composite /c 240 /m 5
```

As in the other approach, use IMVIS to view the composite image (called 'composite' in the example). To add projection, vector and title information to the image, edit the label file ('composite.lbl' in the example).

INTEGRATING DATA SETS THROUGH MULTIPLICATION

The information from two different data sets can be integrated into one data set by multiplying their values together at each grid point. This combines the information into one map for inspection rather than two. This may be advantageous for two main reasons. First, multiplying two data sets together will enhance features that are common to both data sets. Second, two features that are indistinguishable in one data set and very distinguishable in the second data set will also become distinguishable in the combined data set. On the other hand, it simply may be more convenient to have features of both data sets apparent on one map rather than two.

For the Getchell area, trial-and-error found two combinations of various products from the magnetic and 900 Hz resistivity data that successfully combined certain aspects of the data sets. First, we observed that many of the boundaries enhanced by the horizontal-gradient method in both the reduced-to-pole magnetic data and the 900 Hz resistivity data were coincidental. To further enhance these particular boundaries, we multiplied the HGM's of the two data sets together (figure 11-1). In order to better match the range of values before multiplication, the logarithms (base 10) of the HGM's of the reduced-to-pole magnetic data were computed prior to multiplication. Second, the 900 Hz resistivity data are high in value over both the granodiorite pluton and Cambrian quartzite in the central to southern part of the Osgood Mountains (Figure 5-2). However, the magnetic data are very high over the granodiorite and near zero over the most of the quartzite. Thus, the granodiorite and quartzite are indistinguishable on the resistivity map, and easily distinguishable on the magnetic map. Once again, by trial-and-error, we found that multiplication of the logarithms of the HGM of the reduced-to-pole magnetic data to the 900 Hz resistivity data (already in logarithm form) best distinguished the geophysical character of these two lithologies *and* enhanced some of the boundaries common to both data sets (Figure 11-2).

Trial-and-error is important in determining how to multiply data sets together. The biggest problem is matching the range of values of one data set to that of the other, especially when multiplying such diverse data values, such as resisitivity (a physical property) and total-field intensity (a field value). One may wish to normalize each data set beforehand by other means than taking the logarithm, such as division by the mean value or some other empirically determined constant.

Multiplication of two grids can be accomplished using the program ADDGRD. This program is demonstrated in Chapter 9.

REFERENCE

Wojniak, W. S., Hoover, D. B., and Grauch, V. J. S., in press, Electromagnetic survey maps showing apparent resistivities of the Getchell gold trend, Osgood Mountains, north-central Nevada: U. S. Geological Survey Geophysical Map GP-1003-A, 3 plates, scale 1:100,000.

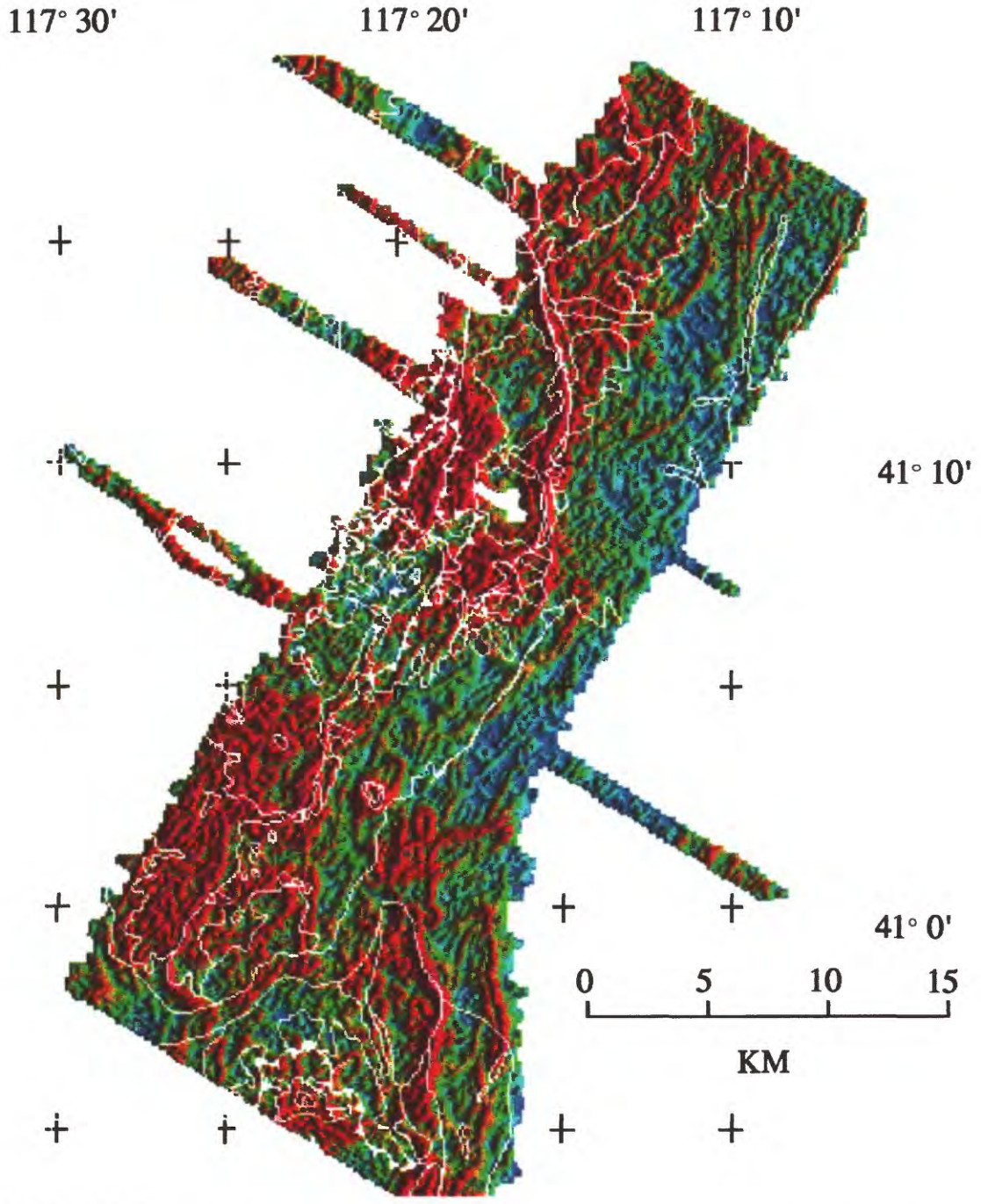

Figure 11-1.

Color shaded-relief image of a data combination to enhance physical-property boundaries: log of the horizontal-gradient magnitudes of reduced-to-pole magnetic data multiplied by horizontal-gradient magnitudes of log values of 900-Hz apparent resistivity. Illumination direction is from the east. Geologic contacts are overlain in white. See Figure 5-2 for explanation of geologic contacts.

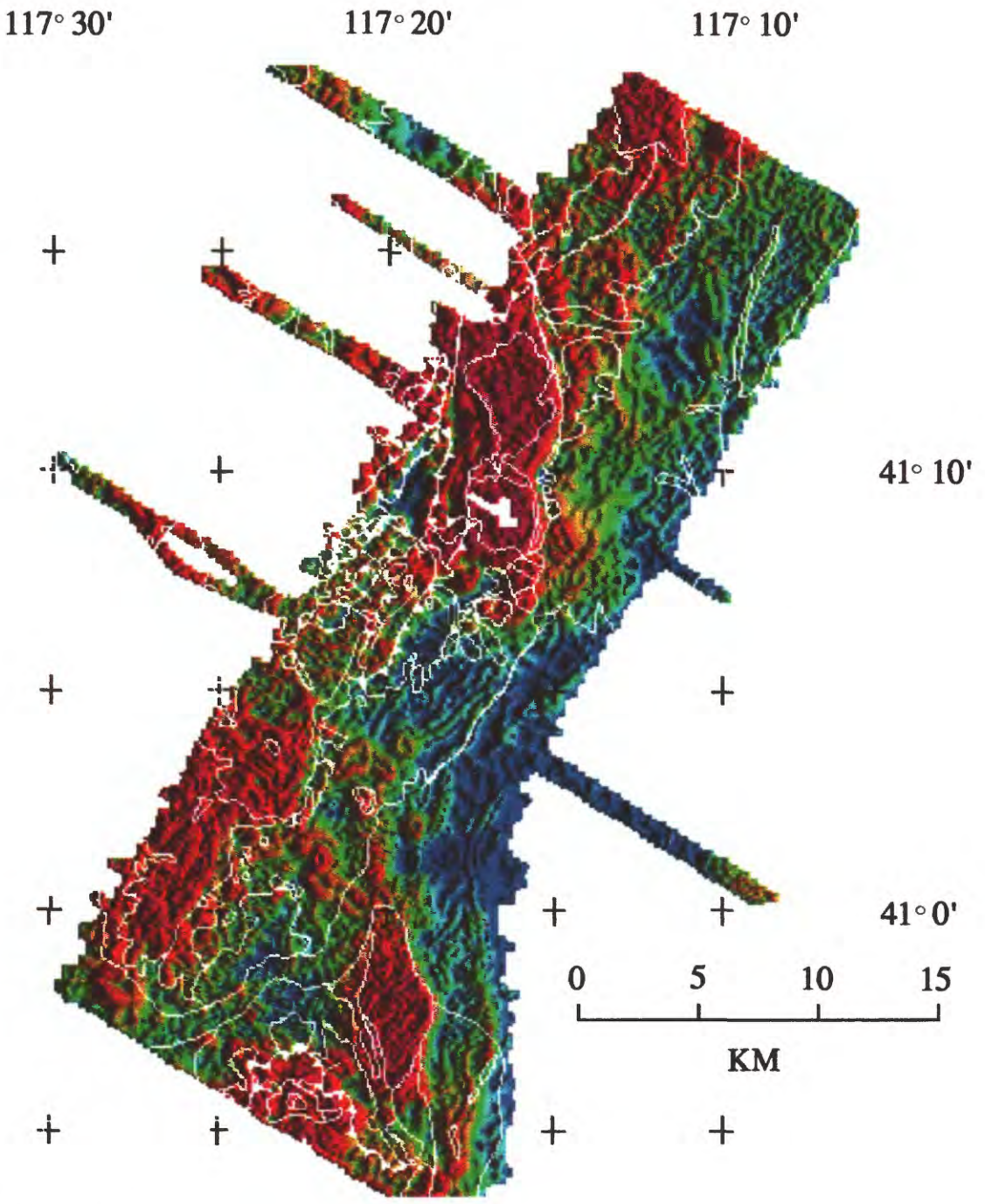

Figure 11-2.

Color shaded-relief image of a data combination to enhance lithologic variations : the log of the horizontal-gradient magnitudes of reduced-to-pole magnetics were multiplied by the log values of 900-Hz apparent resistivity. Illumination is from the east. Geologic contacts are overlain in white. See Figure 5-2 for explanation of geologic contacts.

INDEPENDENT PC EXERCISES V

1. Follow the demonstration starting on page 10-6 to make various composite images of the radioelements and their ratios using **DISPLAY**. (You may have already constructed gk.img in previous exercises--no need to redo it).

2. Browse through the grids available for the Getchell area on the diskettes of Open-File 93-560D (Table 12-2). Using **GRDREM** (if necessary) and **DISPLAY**, create color composite images of three of these grids, analogous to the procedure in #1. Before you use GRDREM, make sure the specifications of the three grids match (see demonstration of basic grid utility programs starting on page 6-15). If necessary, use program **UTILITY** or **REGRID** to make the grids match, otherwise the images won't register to each other. A couple of suggestions for composite combinations:

   The three resistivity grids, 900 Hz, 7200 Hz, and 56,000 Hz resistivities: **gres9.trm, gres72.trm,** and **gres56.trm**. (Skip every other scanline and every other pixel to get the image to mostly fit on the screen.)

   RTP magnetics, thorium, and 900 Hz resistivity: **grtp.cgd, gt.cgd, gres9.trm** (you'll have to create **gres9.cgd** from **gres9.trm** first).

   Experiment with which data set to make red, which blue, etc. (buffer 1=blue; buffer 2=green; buffer 3=red).

3. From your experiments in #2, pick the three data sets that make the most interesting composite. Follow the demonstration on making composite images in IMVIS to make a composite image for **IMVIS** (use the first approach, starting p. 11-1). Remember the grid specifications *must* match. Note that the most aesthetic images come from the 0.1 km-interval grids. (You can always use program **REGRID** to get the interval you want.)

4. Take a look at the IMVIS images called GBNDCMB.LBL and GLITHCMB.LBL. These are the combinations to enhance boundaries and lithologic differences (figures 11-1 and 11-2), respectively. On top of GBNDCMB.LBL, overlay **gpgg3.grf** (from #1 in Independent PC Exercises IV) from the "labels .grf" submenu of the "PLOT" menu to compare the magnetization boundaries. Overlay the geology on GLITHCMB.LBL to see how the quartzite and granodiorite are distinguished. Compare this to the 900 Hz resistivity image GRES91.LBL.

INDEPENDENT PC EXERCISES V - CONTINUED

5. To get practice with multiplication, do the following steps to create the lithologic enhancement combination:

   a. Use the program **BOUNDARY** to create **grtpg.cgd** (HGM's) from **grtp.cgd** (reduced-to-pole magnetic data, copied in #2 of Independent PC Exercises III). For help on BOUNDARY, see the demonstration starting on p. 8-24.

   b. Because the HGM is always positive by definition, we can take the logarithm of **grtpg.cgd** without any worry. Use program **LOG** to do this (it's self-explanatory), resulting in **grtpgl.cgd**.

   c. Use **ADDGRD** to multiply (the * operator) **grtpgl.cgd** by **gres9.cgd**. (If you didn't make gres9.cgd from gres9.trm using **REGRID** in #2 above, you'll have to do it now before you can run **ADDGRD.**) If you need help on **ADDGRD**, see the demonstration in Chapter 9. The output you can name something like **glith.cgd**. Run **CSR** using a sun azimuth of 90^{o} and sun altitude of 45^{o} to look at the result (see explanation of **CSR** starting on p. 7-39). Now compare your result to figure 11-2. Note that your image was made from a 0.2 km grid so that it doesn't have as much resolution as figure 11-2 nor the IMVIS image GLITHCMB.LBL. It also means that you *won't* be able to fix your .LBL file to allow for overlays by copying other label files as was done earlier.

Chapter 12. Sources of Information

GRAVITY AND MAGNETIC DATA SOURCES

General Information on Availability (Start Here)

Pat Hill
Branch of Geophysics
U. S. Geological Survey
Denver, Colorado
(303) 236-1343

Digital Gravity and Seismic Data

Dave Dater
National Geophysical Data Center (NGDC)
NOAA
Boulder, Colorado
(303) 497-6128

Digital Airborne Magnetic Data

Ron Buhmann
National Geophysical Data Center (NGDC)
NOAA
Boulder, Colorado
(303) 497-6128

Information on the Geomagnetic Field

Jill Caldwell
Branch of Global Seismology and Geomagnetism
U. S. Geological Survey
Golden, Colorado
(303) 273-8486

AIRBORNE GEOPHYSICS CONTRACTORS

Aeromagnetic Surveys

Airmag Surveys, Inc.
Northeast Philadelphia Airport
P.O. Box 16157
Philadelphia, PA 19114
Attn: John M. Schmunk
(215) 673-2012

Applied Geophysics, Inc.
675 South
400 East
Salt Lake City, Utah 84111-3997
(801) 328-8541

Geonex Aero Service
3300 South Gessner, Suite 261
Houston, TX 77063
(713) 708-1188

Sander Geophysics Limited
303 Legget Drive
Kanata, Ontario
Canada, K2K 2B1
Attn: George Sander

Aeromagnetic and Gravity Surveys

Carson Services, Inc.
32-H Blooming Glen Road
Perkasie, Pennsylvania 18944
(215) 249-3535

Helicopter Aeromagnetic and Electromagnetic Surveys

Dighem Surveys and Processing, Inc.
228 Matheson Blvd. East
Mississauga, Ontario
Canada L4Z 1X1
(416) 518-7744

Geonex Aerodat, Inc.
3883 Nashua Drive
Mississauga, Ontario
Canada L4V 1R3
(416) 671-2446

Geophex, Ltd.
605 Mercury St.
Raleigh, North Carolina 27603-2343
(919) 839-8515

Aeromagnetic and Input Electromagnetic Surveys

Geoterrex Ltd.
2060 Walkley Road
Ottawa, Ontario
Canada K1G 3P5
(613) 731-9571

BGM Airborne Surveys, Inc.
West Houston Airport
Box 219357
Houston, Texas 77218-9998
(713) 647-9025

Geonex Aero Service
3300 South Gessner, Suite 261
Houston, TX 77063
(713) 708-1188

Sander Geophysics Limited
303 Legget Drive
Kanata, Ontario
Canada, K2K 2B1
Attn: George Sander

Carson Services, Inc.
32-H Blooming Glen Road
Perkasie, Pennsylvania 18944
(215) 249-3535

Dighem Surveys and Processing, Inc.
228 Matheson Blvd. East
Mississauga, Ontario
Canada L4Z 1X1
(416) 518-7744

Geonex Aerodat, Inc.
3883 Nashua Drive
Mississauga, Ontario
Canada L4V 1R3
(416) 671-2446

Geoterrex Ltd.
2060 Walkley Road
Ottawa, Ontario
Canada K1G 3P5
(613) 731-9571

BGM Airborne Surveys, Inc.
West Houston Airport
Box 219357
Houston, Texas 77218-9998
(713) 647-9025

Getchell Trend Data

SE-0103 02/91

The Getchell Trend, located along the eastern flank of the Osgood Mountains, north-central Nevada, is a geological trend with gold and other significant mineral deposits. During 1988, the U.S. Geological Survey (USGS) conducted an Integrated Airborne Geophysical Demonstration Project over this area. In 1989 and 1990, derived, gridded and observed data from this program were transferred to NGDC for public distribution.

Digital data from several sources including USGS contractors, private exploration companies, and various government groups have been integrated into the Getchell Trend digital data collection. A major portion of this collection, approximately 1,150 line miles of airborne magnetic and electromagnetic (EM) data, was collected by a USGS contractor, Dighem, Inc. Characteristics of this data set are 1/4 mile flight-line separation, draped terrain clearance of 100 feet, and NW-SE flight direction.

The Getchell Trend files include multi-spectral electromagnetic radiation measurements, airborne magnetics, electromagnetic resistivity, and terrain clearance data. Thermal imagery and gamma radiation data are also included but originated as separate geophysical surveys collected under different USGS specifications.

The original purpose of the Getchell Trend Demonstration Project was to illustrate the advantages of using multi-disciplinary data for resource assessment or exploration of covered deposits. Analyses from this program are applicable to other geological and geophysical studies as well.

Available Data

Airborne geophysical data are available on magnetic tape. Nine grid files are included: resistivity (3 channels), VLF (total-field, quadrature, and filtered), radiometrics (K, Th, U), terrain clearance, and magnetics. The data are available in digital helicopter electromagnetic (DIGHEM) grid format (product number 990-A07-002) or in standard USGS grid format (990-A07-008).

Complementary gridded magnetic data are available on tape in DIGHEM grid format (990-A07-001) or in standard USGS grid format (990-A07-009). The tape contains two files: CONOCO.GRD, which the USGS digitized and derived from a Conoco contour map of data from a 1973 airborne magnetics survey, and GETMAGRES.GRD, Getchell magnetic residual value grid.

Original profile data from the Dighem, Inc., helicopter flight-lines (36 parameters) are also available on magnetic tape (990-A07-010). Digital geological map units of the Getchell Mining District are available on diskette (990-B25-001).

The Thermal Infrared Multi-Spectral scanner (TIMS) data for the Getchell Trend consist of six channels of daytime thermal imagery which can be related to silicate mineralogy (990-A07-003). The Geophysical Environmental Research (GER) data are imaging spectrometer data (64 channels) on four magnetic tapes (990-A07-011).

Magnetic tape data are provided on 9-track, 6250 bpi magnetic tapes. (Data may also be requested on 1600 bpi; please write or phone ahead for alternative pricing). Please refer to the product number when ordering.

Product Number	Description
990-A07-001	East and West gridded magnetic data (2 files) in DIGHEM grid format; magnetic tape output
990-A07-009	Data (2 files) in USGS standard grid format; magnetic tape output
990-A07-002	Airborne geophysical data (8 files) in DIGHEM grid format; magnetic tape output
990-A07-008	Data (9 files) in USGS standard grid format; magnetic tape output
990-A07-010	Flight-line profile data from a Dighem helicopter; magnetic tape output
990-C25-001	Digital geological map units of the Getchell Mining District. Output is one high density, IBM-PC compatible diskette in binary *and* ASCII format. Please specify 5.25" or 3.5".
990-A07-003	TIMS data for the Getchell Trend; binary format; magnetic tape output
990-A07-011	GER data for the Getchell Trend; binary format; four magnetic tapes

Note: The USGS has compiled a folio of 25 colored geophysical maps and overlays at a scale of 1:100,000 for the Getchell Trend Demonstration Project. These folios are available for review only at several USGS offices. Call 303-497-6128 for more information.

Data contributors and academic researchers should call 303-497-6128 for information about obtaining data by special arrangement.

U.S. DEPARTMENT OF COMMERCE REGULATIONS REQUIRE PREPAYMENT ON ALL NON-FEDERAL ORDERS. Please make checks and money orders payable to COMMERCE/NOAA/NGDC. All foreign orders must be in U.S. Dollars drawn on a U.S.A. bank. Do not send cash. Orders may be charged to American Express, MasterCard, or VISA by telephone, letter, fax, or Order Form. Please include the credit card account number, expiration date, telephone number, and your signature with the order.

A ten-dollar ($10) handling fee is required for non-U.S.A. orders. Overnight delivery is available at an additional cost; please call for details.

Please direct telephone inquiries about these data to (303) 497-6128 (fax: 303-497-6513; telex: 592811 NOAA MASC BDR; email: info@ngdc1.colorado.edu). Inquiries, orders, and payment should be addressed to National Geophysical Data Center, NOAA, Code E/GC1, 325 Broadway, Boulder, CO, 80303.

Due to recent legislation, prices are subject to change without notice. Please call for price verification.	Mention of a commercial company or product does not imply endorsement by NOAA or the United States Department of Commerce.

DESCRIPTION OF DATA FILES CONTAINED IN 93-560D

Common Parameters for Getchell Data

All horizontal distance units are measured in kilometers and were projected using Universal Transverse Mercatur (UTM) projection (iproj = 2), although without false easting or false northing. Base latitude and central meridian: 0^{o}, 117^{o}W (by convention 0, -117).

The geomagnetic field in the Getchell area has declination of 16 degrees east, inclination of 66 degrees down from horizontal (by convention, 16, 66).

Explanation Of File Extensions for Getchell Data

Extension	Explanation
.grd	binary grid, grid interval 0.1 km
.trm	binary grid, grid interval 0.1 km, trimmed of excess rows and (or) columns where there are no data
.cgd	coarse grid, grid interval 0.2 km
.pps	projected USGS post file (binary)
.cmd	command file used in demonstrations
.img	REMAPP image file made from 0.2 km grid

TABLE 12-1 - Diskette Index And Specification of Grid Files
(in order by diskette)

File	Diskette	xo	yo	nc	nr	dx & dy
gmag.trm	1	-41.8	4525	341	495	0.1
gmagalt.trm	1	-41.8	4525	341	495	0.1
gcon.cmd	1	N/A--command file for CONTOUR				
gfft.cmd	1	N/A--command file for FFTFIL				
gfftdv.cmd	1	N/A--command file for FFTFIL				
gconxyz.cmd	1	N/A--command file for CONTOUR				
gboug.grd	2	-46.0	4525	387	496	0.1
gboug.pps	2	N/A--USGS gravity post file (Chapter 6)				
grtp.cgd	2	-46.0	4525	194	249	0.2
grtp.img	2	N/A--REMAPP image file				
grtplo.img	2	N/A--REMAPP image file				
grtpmid.img	2	N/A--REMAPP image file				
grtphi.img	2	N/A--REMAPP image file				
g1ver.img	2	N/A--REMAPP image file				
ggcon.cmd	2	N/A--command file for CONTOUR				
gres9.trm	3	-41.8	4525	341	495	0.1
gres72.trm	3	-41.8	4525	341	495	0.1
gres56.trm	4	-41.8	4525	341	495	0.1
gemalt.trm	4	-41.8	4525	341	495	0.1
gtopo.grd	5	-46.0	4525	387	496	0.1
gu.cgd	5	-46.0	4525	194	249	0.2
gt.cgd	5	-46.0	4525	194	249	0.2
gk.cgd	5	-46.0	4525	194	249	0.2

TABLE 12-2 -- Description Of Data Files

Filename	Description
gmag.trm	Residual total-magnetic-field intensity (nT) [DIGHEM survey]
gmagalt.trm	Terrain clearance (ft) of magnetometer [DIGHEM survey]
gboug.grd	Bouguer gravity grid for reduction density of 2.67 g/cm^3
gboug.pps	Reduced gravity-station data (in projected, binary, USGS post-file format) containing: ID (2 words of identification), x (projected km from central meridian), y (projected km from base latitude), FA (free-air anomaly, mGal), CBA (complete Bouguer anomaly, mGal), Elevation (ft above sea level), ITC (inner-zone terrain correction, mGal), OTC, (outer-zone terrain correction, mGal), OG (observed gravity minus 980,000 mGal)
grtp.cgd	Reduced-to-pole magnetic data using declination= 16 degrees E of N, inclination 66 degrees down from horizontal. Derived from program FFTFIL and regridded to 0.2 km grid interval
grtp.img	REMAPP image file made from grtp.cgd
grtplo.img	REMAPP image file made from the lowpassed reduced-to-pole magnetic data (from program MFILT)
grtpmid.img	REMAPP image file made from the mid-range bandpassed reduced-to-pole magnetic data (from program MFILT)
grtphi.img	REMAPP image file made from the highpassed reduced-to-pole magnetic data (from program MFILT)
g1ver.img	REMAPP image file made from the first vertical derivative of the reduced-to-pole magnetic data
gres9.trm	Log10 apparent resistivity for airborne EM data at 900 Hz
gres72.trm	Log10 apparent resistivity for airborne EM data at 7,200 Hz
gres56.trm	Log10 apparent resistivity for airborne EM data at 56,000 Hz

TABLE 12-2 -- Description Of Data Files - CONT'D

Filename	Description
gemalt.trm	Terrain clearance (ft) of EM sensor
gtopo.grd	Topographic data (ft above-sea-level) from 3-arc-second digital elevation model
gu.cgd	Uranium surface concentration (ppm) from airborne radioactivity survey
gt.cgd	Thorium surface concentration (ppm) from airborne radioactivity survey
gk.cgd	Potassium surface concentration (percent) from airborne radioactivity survey

DESCRIPTION OF IMAGES CONTAINED IN 93-560D

The image files on disks 6 through 8 of 93-560D are to be used with the image viewing system IMVIS as provided by 93-560B and described by Phillips and others (1993). After these files are copied to hard disk, the user can choose to view one of 16 different images when IMVIS is invoked. In addition, boundary and label/point files (files with extension .grf) are available as overlay plots. The names of these files are explained below.

The geologic information for image overlays was digitized and compiled from Hotz and Willden (1964) and Willden (1964).

Hotz, P. E., and Willden, R., 1964, Geology and mineral deposits of the Osgood Mountains quadrangle, Humboldt County, Nevada: U. S. Geological Survey Professional Paper 431, 128 p.

Phillips, J. D., Duval, J. S., and Ambroziak, R. A., 1993, National Geophysical Data Grids: Gamma-ray, gravity, magnetic, and topographic data for the conterminous United States: U. S. Geological Survey Digital Data Series DDS-9 (CD-ROM).

Willden, Ronald, 1964, Geology and mineral deposits of Humboldt County, Nevada: Nevada Bureau of Mines and Geology Bulletin 59, 154 p.

Table 12-3. Diskette Index and Image File Descriptions (.LBL Files) in alphabetical order

Filename	Diskette	Brief Description
G1VER1.LBL	7	First vertical derivative of reduced-to-pole magnetic data
GBNDCMB.LBL	8	Combination of magnetic and resistivity data to enhance physical-property boundaries.
GBOUG1.LBL	7	Bouguer gravity.
GCOND.LBL	6	Buried conductive material enhancement derived from the resistivity ratio data (described below under GRATIO.LBL) and 900-Hz apparent resistivity data as follows: (-log10(900-Hz res.) + 3.5)*ratio.
GLITHCMB.LBL	8	Combination of magnetic and resistivity data to enhance lithologic variations.
GMAG1.LBL	6	Aeromagnetic data from the DIGHEM survey.
GMAGSE.LBL	8	Subset of magnetic data over pluton, illuminated from the east
GRATIO.LBL	6	Log10 of ratio 7200-Hz apparent resistivity over 900-Hz apparent resistivity.
GRES91.LBL	6	Log10 apparent resistivity for airborne EM data at 900 Hz.
GRES9G1.LBL	7	Horizontal-gradient magnitude (HGM) of log10 900 Hz apparent resistivity.
GRTP1.LBL	8	Reduced-to-pole magnetic data
GRTPG1.LBL	8	Horizontal-gradient magnitude (HGM) of reduced-to-pole magnetic data
GPG1.LBL	7	Pseudogravity of magnetic data
GPGG1.LBL	7	Horizontal-gradient magnitude (HGM) of pseudogravity
GTOPO1.LBL	7	3-arc-second digital elevation model
GUKTHRGB.LBL	6	Composite, red-green-blue image of uranium, potassium, and thorium from the aerial gamma-ray survey.

Table 12-4 PLOT Menu Overlay File Descriptions
(all files on diskette 6)

Name	Brief Description
------boundary SUBMENU-------	
Lat lon ticks	Latitude/longitude tick marks
Neat line	Neat line around whole data area
Scale bar	Scale bar
Geology	Geologic contacts
Faults	Faults, teeth on upthrown side of thrust faults
-----labels .grf SUBMENU------	
DEPOSITS.GRF	Locations of Au, Ag, Ba, and W deposits
GBOUG.GRF	Station locations of gravity data
GEOLOGY.GRF	Labels for geologic units
LATLON.GRF	Labels for latitude/longitude ticks
SCALE.GRF	Labels for scale bar
TICS.GRF	Latitude/longitude tick marks

PC SOFTWARE

Background

The software provided to the workshop participants and contained in the companion Open-File Reports 93-560B and C represent version 2.11 of the PC potential-field programs, and version 1.03 of the REMAPP PC software. Version 2.11 of the potential-field software is intermediate between version 2.1 (Phillips and others, 1992) and version 2.2, in preparation. The 2.11 diskettes provided in 93-560B require prior installation of version 2.0 (Cordell and others, 1992) or 2.1.

Version 1.03 of REMAPP PC software is an update to version 1.00 (Livo, 1990). This update incorporates the modified functions of version 3.00 (in preparation) and is compatible with the data formats supported by the PC potential-field software, whereas the data format of version 2.00 (Livo and Gallagher, 1991) is not compatible. Open-file 93-560C does not require any previous installation of the REMAPP software. However, the update contains the documentation text only as an ASCII file on the diskette and does not provide test data sets. Documentation is provided by Open-File Report 90-88A (version 1.00) and test data sets are contained on two diskettes, 90-88D and E.

These PC software packages are derived from software developed over many years by the Branch of Geophysics on various mainframe computers. Information on the original potential-field software is contained in Bankey and Anderson (1989) and U. S. Geological Survey (1989). The original REMAPP software is described by Sawatzky (1985).

References

Bankey, Viki, and Anderson, W. L., 1989, Some geophysical programs, data bases, and maps from the U. S. Geological Survey, 1971-1989: U. S. Geological Survey Open-File Report 89-659, 18 p.

Cordell, Lindrith, Phillips, J. D., and Godson, R. H., 1992, U. S. Geological Survey potential-field geophysical software, version 2.0: U. S. Geological Survey Open-File Report 92-18. 92-18A is 16 p. of documentation; 92-18B through G are six diskettes containing software and test data sets.

Livo, K. E., 1990, REMAPP - PC: Remote sensing image processing software for MS-DOS personal computers, version 1.00: U. S. Geological Survey Open-File Report 90-88. 90-88A is 62 p. of documentation; 90-88B through E are four diskettes containing software and test data sets.

Livo, K. E., and Gallagher, A. J., 1991, REMAPP - PC: Remote sensing image processing software for MS-DOS personal computers, version 2.00: U. S. Geological Survey Open-File Report 91-449. 91-449A is 83 p. of documentation; 91-449B through G are six diskettes containing software and test data sets.

Phillips, J. D., Duval, J. S., and Ambroziak, R. A., 1993, National geophysical data grids: gamma-ray, gravity, magnetic, and topographic data for the conterminous United States: U. S. Geological Survey Digital Data Series DDS-9. CD-ROM containing data sets and PC software.

Sawatzky, D. L., 1985, Programmer's guide to REMAPP, REMote sensing Array Processing Procedures: U. S. Geological Survey Open-File Report 85-231, 21 p.

U. S. Geological Survey, 1989, Potential field geophysical programs for VAX 7xx computers: U. S. Geological Survey Open-File Report 89-115. 89-115A is 21 p. of documentation; 89-115B through D are three diskettes of source code.